BERGISCHE
UNIVERSITÄT
WUPPERTAL

Schumpeter School
of Business and Economics

A New Assortativity Coefficient for Weighted and Directed Networks and its Application to the Cryptocurrency Market

Inauguraldissertation zur Erlangung des akademischen Grades eines
Doktors der Wirtschaftswissenschaft (doctor rerum oeconomicarum)
an der Fakultät für Wirtschaftswissenschaft
– Schumpeter School of Business and Economics –
der Bergischen Universität Wuppertal

vorgelegt von
Marc Sabek, M. Sc.
aus Solingen

Solingen, August 22, 2022

Für Sarah und Nora

Contents

List of Figures

List of Tables

1 Introduction

Network theory, which is the study of graphs as a representation of the relations between the objects of a complex system, has gained importance in many research areas in recent years. The reason for this is that many real world problems are basically problems of complex systems. Examples of such systems from different research areas, in particular the networks formed by the interacting of their objects, are, for example, technological networks (e.g., the internet), infrastructure networks (e.g., power grids, airports, or roads), social networks (e.g., Facebook, Twitter, or Instagram), biological networks (e.g., metabolic or brain networks), and financial networks.

Since the financial crisis of 2008, when network effects led to one of the worst global economic crises to date, the techniques provided by network theory have also become an integral part of economic research. In financial networks the focus is mainly on the contribution that network analysis can make in order to assess, manage, or monitor (systemic) risk in financial systems. An attempt is made to examine these systems and their underlying network structures with regard to their *stability* or *robustness*.[1] Financial systems that are frequently examined are, for example, banking markets, (global) stock markets, or the cryptocurrency market. Analysing the systemic risk of such markets is very important from both an investor and a policymaker perspective, since major fluctuations can affect both investment decisions and regulatory actions, respectively.

A particular network measure that is often associated with the robustness of a network against exogenous shocks is *assortative mixing* or simply *assortativity*, cf. Newman (2002). Assortativity is the tendency of one node to form a connection with another that has a similar number of connections as itself. The most popular assortativity measure is the assortativity coefficient, which has been originally proposed by Newman (2002, 2003) first for unweighted and undirected networks, then for unweighted directed networks. Piraveenan, Prokopenko, and Zomaya (2012) have refined the measure of Newman (2003) so that a further differentiation of the assortativity structure in directed networks is possible.

Assortativity is closely related to the *epidemic threshold*, which is a key figure in mathematical epidemiology, indicating when an epidemic will persist, and when it will become extinct, cf. Peng, Jin, and Shi (2010). The epidemic threshold is the critical ratio of the infection to cure rate beyond which epidemics emerge. When mod-

[1] Sometimes also referred to as *resilience*.

elling epidemics using networks it can be shown that the epidemic threshold is inversely proportional to the largest eigenvalue of the adjacency matrix of the network (i.e., a matrix that completely defines the network), see Boguñá and Pastor-Satorras (2002), Yang Wang, Chakrabarti, Chenxi Wang, and Faloutsos (2003) and Chakrabarti, Wang, Wang, Leskovec, and Faloutsos (2008). The influence of the assortativity of a network on the largest eigenvalue of its adjacency matrix or the epidemic threshold is studied by Brede and Sinha (2005) and Scala and D'Agostino (2013). They find that networks, which exhibit a high assortativity tend to have a lower epidemic threshold, and thus, are less robust than networks, for which the assortativity is low (i.e., disassortative networks).

In this context, it is also interesting to know which of the nodes (or vertices) or connections (or edges) of a network are the most endangering on the one hand, and which are the most protective ones on the other hand. This can help with developing efficient strategies for both breaking up a network (e.g., with vaccination in disease spreading social networks) and protecting particularly vulnerable networks (e.g., financial networks or technological networks, such as the Internet), cf. Newman (2002).

The assortativity coefficient, being a global measure, however, cannot provide answers to those kinds of questions. There is a need for a local assortativity measure that can either be *vertex based* or *edge based*, and thus, identify those vertices or edges that contribute most to the global assortativity structure of a network, respectively. Local assortativity in undirected and directed yet unweighted networks has been studied for example by Piraveenan, Prokopenko, and Zomaya (2008, 2009, 2010); Piraveenan et al. (2012), Zhang, Cheng, and Zhang (2012) and Thedchanamoorthy, Piraveenan, Kasthuriratna, and Senanayake (2014).

So far, as already pointed out by Noldus and van Mieghem (2015), assortativity in weighted networks has been insufficiently studied, which is surprising as many real-world networks exhibit weighted edges. Basically, every (interesting) financial network that we are aware of is a weighted network, e.g., the above-mentioned banking or cryptocurrency networks. Moreover, financial networks may be complete networks, by construction, for which the unweighted assortativity coefficient cannot even be computed. That implies that, so far, there is no straightforward way of analysing the robustness of (complete) financial networks in terms of assortativity. There have been several attempts at generalizing (global) assortativity for weighted networks, though, claiming the superiority of one measure over the other. However, none of the measures has established itself as a standard for weighted networks. We aim therefore at introducing a *generalized assortativity coefficient* that unifies previous definitions by nesting them as special cases, and that is also applicable to complete networks, e.g., the financial networks just mentioned.

Although local assortativity has been widely studied, to the best of our knowledge, there exists no definition of local assortativity for weighted networks at all, so far.

We aim therefore at also closing this gap by introducing a *generalized local assortativity coefficient*, which is flexible in the sense that it can be either vertex based or edge based. After generalizing global and local assortativity, we then test our new coefficients and demonstrate their usefulness by analysing the network underlying the cryptocurrency market in terms of its robustness in order to assess its systemic risk.

In 2008, by publishing the white paper *"Bitcoin: A Peer-to-Peer Electronic Cash System"* under the pseudonym Satoshi Nakamoto, an individual or group laid the foundation of today's cryptocurrency market, see Nakamoto (2008). By proposing a system for electronic transactions that does not rely on trust, they introduced the first cryptocurrency now known as Bitcoin. Moreover, they en passant popularized a technology referred to as blockchain, on which also many of the newer cryptocurrencies are based on. Already well before the Bitcoin price reached its all-time high above $\$67,500$ in November 2021 cryptocurrencies have attracted the attention of mainstream media and their popularity has increased ever since.

As far back as 2018, it has been considered likely that Bitcoin and alternative blockchain-based tokens emerge as their own asset class that may become an interesting investment alternative and diversification instrument, cf. Berentsen and Schar (2018). Back then, others have also studied the technology of blockchain and identified its potential for *financial inclusion*, cf. Ohnesorge (2018). The term financial inclusion refers to individuals and businesses having access to financial products and services (e.g., transactions, payments, savings), cf. The World Bank Group (2022).

Meanwhile, in 2022, *Forbes Advisor* presents for the venturesome investors overviews of the top cryptocurrencies together with guides on how to buy them on a regular basis, see, e.g., Tretina (2022a, 2022b). Moreover, Bitcoin has been adopted as an official currency in El Salvador and the Central African Republic, in 2021 and 2022, respectively, cf. Aswad (2021) and Reuters (2022). The market of cryptocurrencies is a \$932B market that comprises approximately $10,000$ active cryptocurrency projects.[2] Thus, cryptocurrencies appear to be more than a fad, and one can no longer deny the market's increasing importance for the global economy. In this context, great interest is taken in assessing the stability of the market, i.e., its systemic risk, as cryptocurrencies are well known for their high volatility. We expect that the results of analysing the cryptocurrency network will also be of relevance for other (financial) networks.

This work is structured therefore as follows: Chapter 2 briefly reviews essential network foundations to facilitate the understanding of the subsequent derivations and explanations. The reader who is already familiar with the basics of network theory may skip this chapter and proceed directly to Chapter 3, where we propose a generalization of the concept of assortativity by introducing our generalized assortativity coefficient. We also provide procedures that allow for both precisely assessing and interpreting the

[2] Information sourced from `coinmarketcap.com`, current as of June 30, 2022.

assortativity of weighted networks as well as its statistical significance. Finally, we demonstrate the usefulness of our proposed generalized assortativity coefficient by in-depth analysing the assortativity structure of several weighted real-world networks. An abridged version of this chapter has already been published in *Physica A: Statistical Mechanics and its Applications*, cf. U. Pigorsch and M. Sabek (2022).

In Chapter 4, we present an extension of local assortativity for weighted networks. By unifying two approaches used in the literature, we are able to derive distinct measures that allow us to determine the assortativeness of individual edges and vertices as well as of entire components of a weighted network. We demonstrate the usefulness of these measures by applying them to various theoretical and real-world networks. Along the way, we also explain how to compute local assortativity profiles, which are informative about the pattern of local assortativity either with respect to edge weight or vertex strength.

Building on this foundation the robustness of the network structure of the cryptocurrency market is analysed in Chapter 5 by means of the previously extended global and local assortativity measures. We first present in detail the method we have chosen to estimate the underlying network structure based on cryptocurrency price data. After analysing the robustness of the network, we present a method to determine its community structure, as this provides additional information for risk assessment and management.

Chapter 6 provides a summary of this work and points out interesting questions for further research. An important empirical finding of this work is that the systemic risk of the cryptocurrency market appears to be inversely related to the generalized assortativity structure of its underlying network. This allows statements to be made on the significance and severity of a potential crisis. Previously, this has not been possible with the methods existing so far.

2 Basic Concepts of Network Analysis

The term network refers to *"... any real system that can be described by means of a mathematical object called a graph."* Caldarelli (2007, p. 10). This chapter provides an introduction into the foundations of network theory with focus on those concepts that are most relevant for the understanding of the remainder of this thesis. Thus, in Section 2.1 we present the very basics of graph theory. Important terms such as, e.g., graphs, vertices, and edges are introduced and their notation defined. Further, we give an example of a simple graph representation, such as the adjacency matrix, which can be used to implement and analyse networks. Some properties of networks are introduced, such as, e.g., paths, cycles and components, that help with characterizing their structural features. In addition, a brief overview of some special networks, such as, e.g., trees, stars, and complete networks is given. Finally, we introduce the concept of degree and degree centrality as this is the basis for the assortativity measures discussed in the subsequent chapters. Section 2.2 introduces two basic random graph models, as extensions thereof will be analysed in Chapter 4.

2.1 Graph Representation of Networks

The following introduction to the terminology of graph theory and its notation is a synthesis of the following resources: Gibbons and Gibbons (1999), Bollobás (2008) and Diestel (2018) are excellent textbooks on (algorithmic) graph theory. Moreover, Harary, Norman, and Cartwright (1966) and Wasserman and Faust (1994) are classics of social network analysis, whereas Jackson (2011), Barabási (2016) and Newman (2018) give a more modern, state of the art, view into the field of network science.

2.1.1 Graphs, Vertices, and Edges

A *graph* $G = (V, E)$ is an ordered pair, where $V = \{v_1, v_2, \ldots, v_n\}$ is a finite set of elements, and $E = \{e_1, e_2, \ldots, e_m\}$ is a set of 2−subsets of V. The graph $G = (V, E)$ is then said to be a graph on the *vertex set* V with the *edge set* E. In order to refer to the vertex set or edge set of a graph, $V(G)$ and $E(G)$ are used, respectively. For example, the vertex set $V(H)$ of a graph $H = (W, F)$ is W and its edge set $E(H)$ is F. For convenience, the distinction between a graph and its vertex set or edge set will not be very strict, likewise, it may be appropriate to state that a vertex $v \in G$ or an edge $e \in G$ instead of $v \in V(G)$ or $e \in E(G)$, respectively.

The cardinality of the vertex set $|V(G)|$ determines the number of vertices of a graph which is called *order* of a graph. The order of a graph is often denoted by n. The cardinality of the edge set $|E(G)|$ determines the number of edges in a graph which is called *size* of a graph. The size of a graph is often denoted by m. For example, the graph shown in Figure 2.1a has order $n = 7$ and its size is $m = 5$. An arbitrary graph of order n and size m is denoted by $G(n, m)$.

Sometimes, vertices have *labels*, so they can be distinguished. Typically, integer labels $1, \ldots, n$ as in Figure 2.1a are used. In minimal examples sometimes character labels are used, e.g., upper case or lower case letters. The labelling is arbitrary but unique, thus, it does not matter which vertex gets which label as long as the label can be used to unambiguously refer to a specific vertex.

Let u, v be vertices, the edge $e = \{u, v\}$ that joins these vertices is sometimes, more conveniently, denoted by uv. The vertices u and v are *end vertices* or *ends* of the edge e, moreover, u and v are said to be *incident* with e. Furthermore, u and v are *adjacent*, or *neighbouring*, vertices of a graph. Let w be another vertex, if $e_1 = uv$ and $e_2 = uw$, then e_1 and e_2 are adjacent edges of a graph, because they share a common end, i.e., vertex u.

If each edge has a direction associated to it, i.e., the ordering of its end vertices becomes relevant, the graph is called a *directed graph*. To distinguish directed from undirected edges parentheses are used rather than braces, thus, $e = (u, v)$ is an edge pointing from u to v. In undirected graphs, uv and vu denote the same edge, whereas in directed graphs these edges are distinct, i.e., $uv \neq vu$.

Usually, a graph is depicted by drawing points for the vertices and connecting them with lines, if they form an edge. Figure 2.1a shows an example of a graph on seven vertices with five edges. Similarly to an undirected graph, a directed graph is depicted by drawing points for the vertices, but instead of connecting the vertices with lines they are connected by arrows, if they form an edge. Figure 2.1b shows an example of a directed graph on seven vertices and with six directed edges. The arrows indicate the direction for which a traversal of the edges is possible. For example, vertex 1 can be reached from 5 by using the edge $(5, 1)$, but starting from 1 vertex 5 cannot be reached.

An edge leading from a vertex to itself is called a *self-edge* or *self-loop* or simply a *loop*. If there is more than one edge running between two vertices, and thus, an edge cannot be unambiguously identified by only specifying its end vertices, then, those edges are collectively referred to as *parallel edges* or *multiedges*. Graphs that neither contain loops nor multiedges are called *simple graphs*, whereas graphs that contain multiedges are called *multigraphs*. However, no particular term is assigned to graphs that contain loops. In the following we focus on simple graphs.

In a simple graph $G(n, m)$, each of the n vertices can be joined to at most $(n - 1)$ other vertices by an edge, resulting in a maximum size of $m_{\max} = \frac{n!}{(n-2)!} = n(n - 1)$,

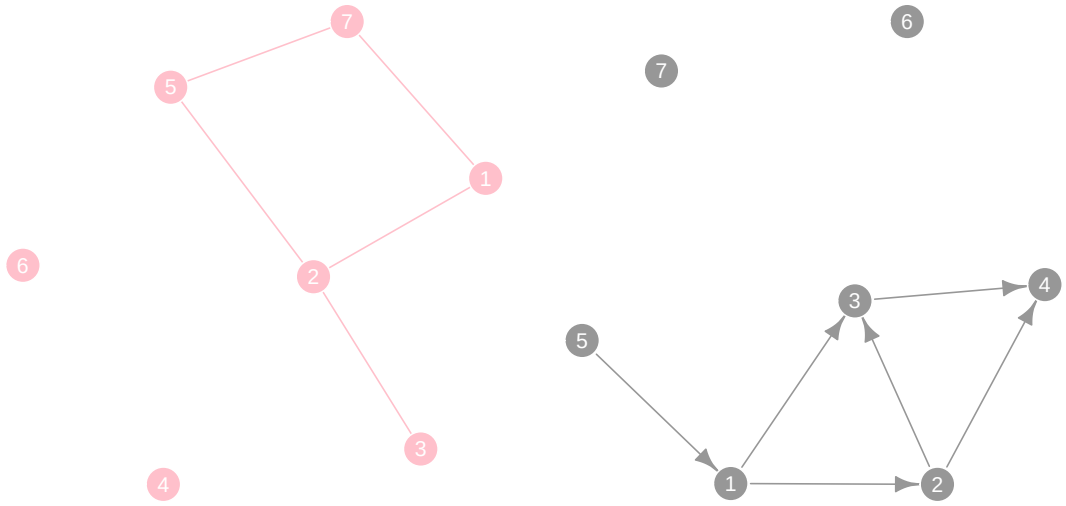

(a) Undirected graph. **(b)** Directed graph.

Figure 2.1. Undirected and directed graphs. Both graphs have the same set of vertices $V = \{1, \ldots, 7\}$. The edge set of the undirected graph is given by $E = \{\{1,2\},\{1,7\},\{2,3\},\{2,5\},\{5,7\}\}$, whereas for the directed graph it is given by $E = \{(1,2),(1,3),(2,3),(2,4),(3,4),(5,1)\}$.

if G is directed. For undirected graphs, the number of possible edges halves, since uv and vu denote the same edge between vertices u and v, and thus $m_{\max} = \binom{n}{2} = \frac{n(n-1)}{2}$. The proportion of actual number of edges present to the maximum number of edges possible is called *density* of a graph. If this proportion is high, the graph is called *dense*, whereas, if it is low, i.e., most of the edges that could exist, are not present, the graph is referred to as *sparse*.

The pair (G, f) is called *weighted graph*, where $G = (V, E)$ is a graph, and the function $f : E(G) \to \mathbb{R}$ is a weight function, that assigns a weight to each edge of the graph. Depending on the application, the edge weights can have a different meaning, and may refer to either distances, costs, or throughputs or the like. For example, Figure 2.2 shows a weighted graph constructed from network data on online discussion groups collected by Beck et al. (2003). In this network the eight vertices $a, b, \ldots, h$ represent members of a group, and the edges indicate communication between group members. The total number of messages sent and received between group members is represented by the edge weights, cf. Boyd, Fitzgerald, and Beck (2006).

There are several types of data structures available which can be used to represent graphs. A simple representation of a graph G is given by a $(n \times n)$ matrix $\boldsymbol{A}$, which

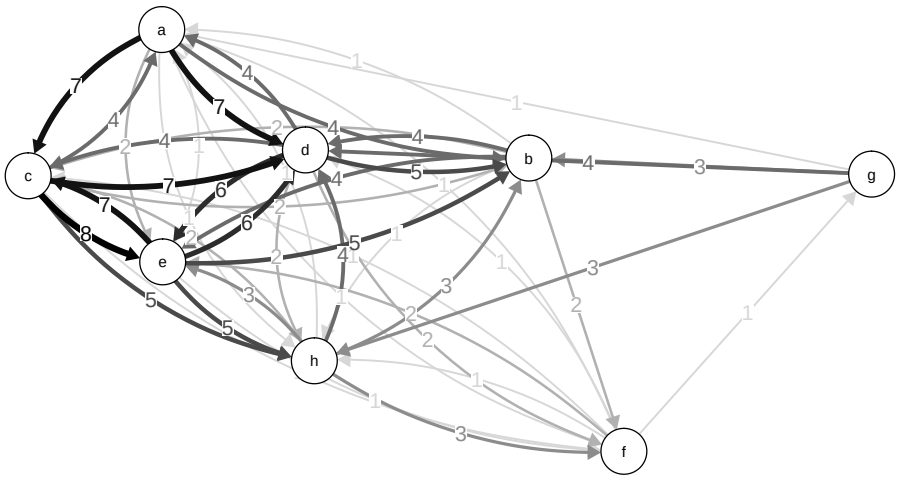

Figure 2.2. Weighted graph. The data has been collected by Beck et al. (2003, group 1). Vertices with labels $a, b, \ldots, h$ in the graph correspond to members of the group, and edges indicate communication between group members, where darker edges indicate a higher rate of communication. The edge labels correspond to the total number of messages sent and received between group members.

is called *adjacency matrix*, and of which its elements $a_{ij} = 1$ if vertices i and j are connected, and $a_{ij} = 0$ otherwise, and thus, the adjacency matrix is defined as:

$$\boldsymbol{A} = \begin{pmatrix} a_{11} & a_{12} & \ldots & a_{1n} \\ a_{21} & a_{22} & & \\ \vdots & & \ddots & \vdots \\ a_{n1} & & \ldots & a_{nn} \end{pmatrix}, \quad \text{where } a_{ij} = \begin{cases} 1 \text{ if } (ij) \in E(G), \forall\, i, j \in V(G) \\ 0 \text{ otherwise.} \end{cases}$$

If the graph is simple, then there are no loops and the diagonal elements of the adjacency matrix of G are zero. If the graph is undirected, then $\boldsymbol{A}$ is a symmetric matrix, i.e., $a_{ij} = a_{ji}$. For weighted graphs it is possible to give a *weighted adjacency matrix*. The entries of the $(n \times n)$ matrix $\boldsymbol{W}$ correspond to the weights of the edges, i.e., $w_{ij} = f(ij)$, if there is an edge between vertex i and j, and $w_{ij} = 0$ if there is no edge, therefore, the weighted adjacency matrix is defined as:

$$\boldsymbol{W} = \begin{pmatrix} w_{11} & w_{12} & \ldots & w_{1n} \\ w_{21} & w_{22} & & \\ \vdots & & \ddots & \vdots \\ w_{n1} & & \ldots & w_{nn} \end{pmatrix}, \quad \text{where } w_{ij} = \begin{cases} f(ij) \text{ if } (ij) \in E(G), \forall\, i, j \in V(G) \\ 0 \text{ otherwise.} \end{cases}$$

Similar to $\boldsymbol{A}$, the diagonal elements of $\boldsymbol{W}$ are zero, if the weighted graph is simple, and $\boldsymbol{W}$ is symmetric for undirected weighted graphs, i.e., $w_{ij} = w_{ji}$. For example, for the graph in Figure 2.2, its adjacency matrix $\boldsymbol{A}$ as well as its weighted adjacency matrix $\boldsymbol{W}$ are given by the following two matrices:

$$\boldsymbol{A} = \begin{pmatrix} 0 & 1 & 1 & 1 & 1 & 1 & 0 & 1 \\ 1 & 0 & 1 & 1 & 1 & 1 & 0 & 1 \\ 1 & 1 & 0 & 1 & 1 & 1 & 0 & 1 \\ 1 & 1 & 1 & 0 & 1 & 1 & 0 & 1 \\ 1 & 1 & 1 & 1 & 0 & 1 & 0 & 1 \\ 1 & 0 & 1 & 1 & 1 & 0 & 1 & 1 \\ 1 & 1 & 0 & 1 & 0 & 0 & 0 & 1 \\ 1 & 1 & 1 & 1 & 1 & 1 & 0 & 0 \end{pmatrix}, \qquad \boldsymbol{W} = \begin{pmatrix} 0 & 4 & 7 & 7 & 2 & 1 & 0 & 1 \\ 1 & 0 & 2 & 4 & 4 & 2 & 0 & 1 \\ 4 & 2 & 0 & 7 & 8 & 1 & 0 & 5 \\ 4 & 5 & 4 & 0 & 6 & 2 & 0 & 2 \\ 1 & 5 & 7 & 6 & 0 & 1 & 0 & 5 \\ 1 & 0 & 1 & 1 & 2 & 0 & 1 & 1 \\ 1 & 3 & 0 & 4 & 0 & 0 & 0 & 3 \\ 1 & 3 & 2 & 4 & 3 & 3 & 0 & 0 \end{pmatrix}.$$

When choosing a graph representation, there exist a trade-off between the *time complexity* and the *space complexity* of a particular representation. Time complexity refers to the mapping of the input size n to the number of elementary steps needed by an algorithm to compute a result. In contrast, space complexity refers to the mapping of the input size to the number of storage locations. For adjacency matrices, some operations require only constant time (e.g., adding or deleting an edge) by accessing the respective matrix element. However, since the matrix has n^2 elements, its space complexity is quadratic. For trading off *time complexity* against *space complexity*, when solving algorithmic problems on graphs, other more space-efficient graph representations are available, e.g., adjacency lists, cf. Magnani and Marzolla (2014).

2.1.2 Directed Paths and Cycles

A *path* P_n is a graph of order n, of which vertices can be arranged in a sequence $v_1, \ldots, v_n$ such that the edge set is $E = \{v_i v_{i+1} \,|\, i = 1, \ldots, n-1\}$. A path starts at its initial vertex and ends at its terminal vertex, where the length of a path is the number of edges it consists of. A path from vertex u to v it is called a uv-path. Paths may also be denoted in terms of their lengths, hence a path from vertex u to v of length k is denoted by $u \xrightarrow{k} v$, whereas a path of unknown length between the two vertices is denoted by $u \xrightarrow{*} v$.

A *cycle* C_n is a graph of order n, of which vertices can be arranged in a cyclic sequence $(v_1, v_2, v_3, \ldots, v_n)$ such that the edge set is $E = \{v_i v_{i+1} \,|\, i = 1, \ldots, n-1\} \cup \{v_1 v_n\}$. Thus, a cycle is a path, of which initial and terminal vertices are identified. For the order of a cycle it holds that $n \geq 3$, otherwise if $n = 1$ the cycle is a loop and if $n = 2$ it is a multiedge both of which are not allowed in simple graphs. Moreover, a cycle of order $n = 3$ is called *triangle*.

2.1.3 Components and Connected Subgraphs

A graph G' is a *subgraph* of a graph G if the vertex set of G' is contained in the vertex set of G, i.e., $V(G') \subseteq V(G)$, and if the edge set of G' is contained in the edge set of G, i.e., $E(G') \subseteq E(G)$. Moreover, if $G' \neq G$, then F is a *proper subgraph* of G. In other words, a proper subgraph of G is obtained by removing both or either a vertex (or set of vertices) or an edge (or set of edges) from G. If G' is a subgraph of G, then this is denoted by $G' \subseteq G$ and G' is said to be contained in G, or simply, G contains G'. A subgraph G' of G is called a *spanning subgraph* if the vertex sets of the two graphs are equal, i.e., $V(G') = V(G)$. Thus, a spanning subgraph G' is obtained from G by performing only edge deletions. A subgraph G' of G is called induced by a vertex set $V(G')$ if its edge set contains all the edges with both end vertices in $V(G')$ and is denoted by $G' := G[V(G')]$. An *induced subgraph* G' is obtained by removing vertices from G together with their incident edges.

The removal of a set of edges F from a graph G is denoted by $G - F := (V, E \setminus F)$, whereas adding the edges in F is denoted by $G + F := (V, E \cup F)$. If the set $F = \{e\}$ consists of a single edge then, for simplicity, removing or adding this edge is denoted by $G - e$ or $G + e$ rather than $G - \{e\}$ or $G + \{e\}$, respectively. Similarly, the removal of a set of vertices U from a graph G is denoted by $G - U := G[V \setminus U]$. As before, removing or adding a single vertex v from G is denoted by $G - v$ or $G + v$ rather than $G - \{v\}$ or $G + \{v\}$, respectively.

The *shortest path* from vertex u to v in a graph G denotes the *distance* between the two vertices, i.e., $\mathrm{dist}_G(u, v) = \min(k \mid u \xrightarrow{k} v)$. When there is no path $u \xrightarrow{*} w$ then, by convention, the distance between two vertices u and w is $\mathrm{dist}_G(u, w) = \infty$. In directed graphs distances are not necessarily symmetrical since the ordering of the vertex pairs is significant, therefore $\mathrm{dist}_G(u, v)$ might differ from $\mathrm{dist}_G(v, u)$. For example, consider vertices 5 and 4 in Figure 2.1b, then $\mathrm{dist}_G(5, 4) = 3$ but $\mathrm{dist}_G(4, 5) = \infty$. In case of a weighted graph, If there is an edge $uv \in E(G)$, then $f(uv)$ denotes the length of uv, moreover, for any subgraph $H \subseteq G$ the weight of H is the sum of the weights of its edges, i.e., $f(H) = \sum_{e \in E(G)} f(e)$. Let $P \subseteq G$ be a path, then $f(P)$ is its length, hence, $\mathrm{dist}_{G,f}(u, v) = \min\{f(P) \mid P : u \xrightarrow{*} v\}$ is the length of the *shortest weighted path* between vertices u and v.

An undirected graph G is *connected* if $\mathrm{dist}_G(u, v) < \infty$ for all $u, v \in G$ and *disconnected* otherwise, i.e., starting from any vertex u every other vertex v is reachable via a path. The maximal connected subgraphs of a graph G are its *connected components*. In this case maximal connected means that a subgraph $H \subseteq G$ is a connected subgraph and for any vertex $v \in V(G)$ but $v \notin H$ the graph $G[V(H) \cup \{v\}]$ is disconnected. The number of connected components of a graph G are denoted by $c(G)$. Clearly, if $c(G) = 1$ then G is connected.

2.1.4 Trees, Stars, Circles and Complete Networks

A graph on n vertices, for which every possible edge is present, i.e., there is an edge between every pair of vertices, is called *complete graph* and is denoted by K_n. Figure 2.3 shows examples of complete graphs on up to seven vertices. A graph that has no edges is called *empty graph*. The empty graph has no dedicated symbol and is rather denoted in terms of the *complement* of a complete graph, i.e., $\overline{K}_n$.

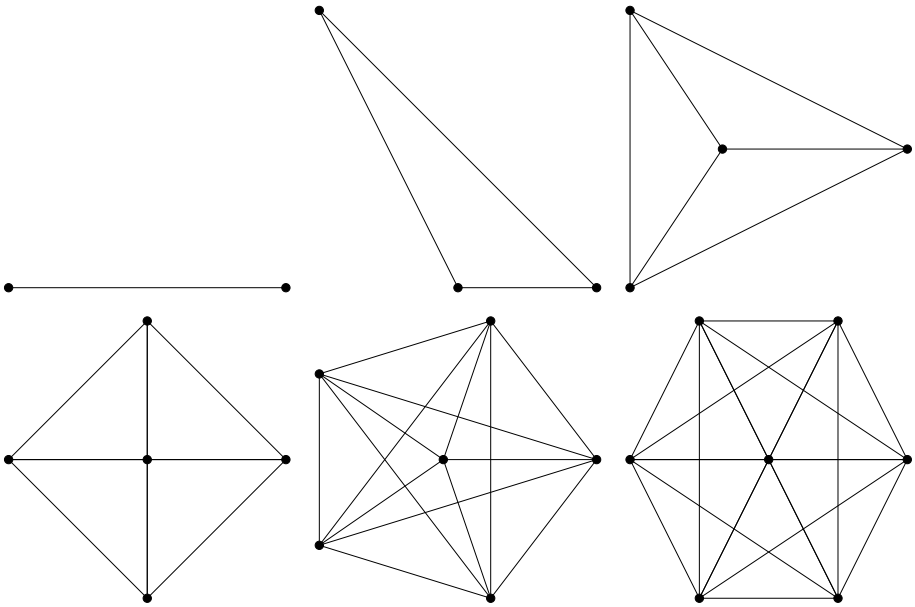

Figure 2.3. Complete graphs.

In general, the complement of a graph $G = (V, E)$ is the graph where all the adjacencies and non-adjacencies are inverted. This means that two vertices that are adjacent in G are not adjacent in $\overline{G}$ and two vertices that are not adjacent in G are adjacent in $\overline{G}$, thus $\overline{G} = (V, V^{(2)} \setminus E(G))$ where $V^{(2)}$ denotes the set of vertex pairs. Thus, to construct the complement of a graph G one simply deletes the edges in $E(G)$ from a complete graph of equal order.

If there exists a one-to-one correspondence $\theta : V(G) \to V(H)$ between two graphs G and H such that θ preserves all the adjacencies and non-adjacencies, i.e., $uv \in E(G)$ if and only if $\theta(u)\theta(v) \in E(H)$, or in other words, the number of edges joining any two vertices in G is equal to the number of edges joining the corresponding vertices in H, then the graphs are said to be *isomorphic* which is denoted by $G \cong H$. Less formally, two graphs are isomorphic if one or the other can be redrawn such that both graphs look identical.

A graph is called an *r-partite* graph if its vertex set V can be partitioned into r pairwise disjoint sets of vertices, i.e., $V_1 \cup V_2 \cup \ldots \cup V_r = V$ and $V_i \cap V_j = \emptyset$, where $1 \leq i < j \leq r$, such that every edge $uv \in E(G)$ has its end vertices in different

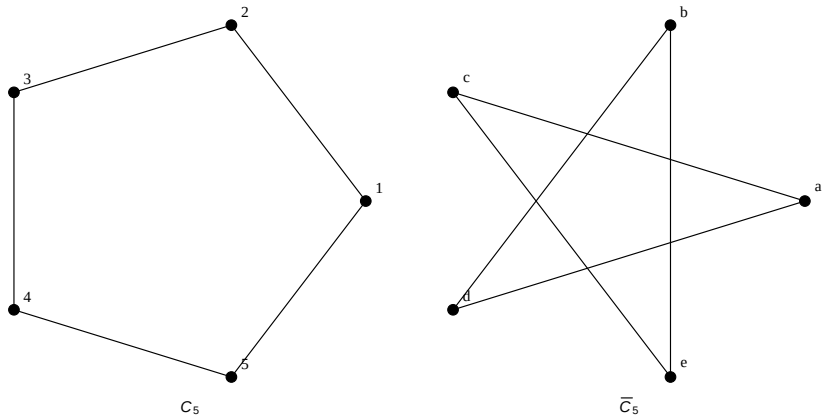

Figure 2.4. Complement and isomorphic graphs. The graph C_5 and its complement $\overline{C}_5$. Since there is a mapping that preserves adjacencies: $\{1, 2, 3, 1, 5\} \rightarrow \{a, c, e, b, d\}$, both graphs are also isomorphic. Adapted from Diestel (2018, p. 4).

partitions, i.e., $u \in V_i$ and $v \in V_j$, where $i \neq j$. Thus, vertices that are in the same vertex partition cannot be adjacent. For $r = 2$ the graph is called *bipartite*. A complete bipartite graph has every possible edge between the two sets of vertices present and is denoted by $K_{i,j}$ where $i = |V_1|$ and $j = |V_2|$. If one of the vertex partitions in a complete bipartite graph consists of a single vertex only, e.g., $K_{1,5}$, then the graph is called a *star graph*. For star graphs it suffices to specify only the number of vertices other than its centre, i.e., $K_{1,6} = S_6$. Figure 2.5 shows two bipartite graphs, one of which is a star graph.

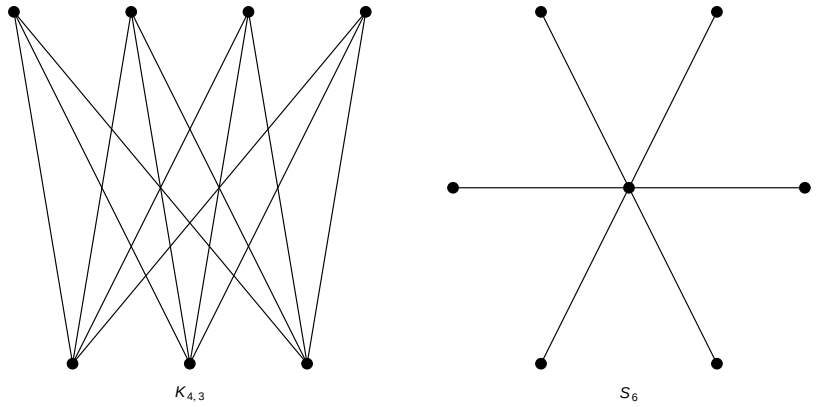

Figure 2.5. Bipartite graphs. The figure shows a complete bipartite graph $K_{4,3}$ on the left, and a star graph S_6 on the right.

2.1.5 Neighbourhood

Adjacent vertices of a vertex are called its *neighbours* and the set of all neighbours of a vertex is called (open) *neighbourhood*. The *open* neighbourhood of a vertex v in a graph G is denoted by $N_G(v) = \{u \,|\, uv \in E(G)\}$. The set of neighbours together with a vertex itself is called *closed* neighbourhood and is denoted by $N_G[v] = N_G(v) \cup v$. For example, the open neighbourhood of vertex 2 in Figure 2.1a is $N_G(2) = \{1, 3, 5\}$, whereas its closed neighbourhood is $N_G[2] = \{2, 1, 3, 5\}$.

2.1.6 Degree and Centrality

The number of neighbours of a vertex v equals the number of edges it is incident with and is referred to as its *degree*. The degree of a vertex is denoted by $\deg_G(v) = |N_G(v)|$. The *minimum degree* of a graph G is $\delta(G) = \min\{\deg_G(v) \,|\, v \in G\}$. Similarly, *the maximum degree* of a graph G is $\Delta(G) = \max\{\deg_G(v) \,|\, v \in G\}$. For the minimum and maximum degree of a graph it holds that $0 \leq \delta(G) \leq \Delta(G) \leq (n-1)$. If a vertex has degree of $(n-1)$ then it is connected to all other vertices in the graph. If instead a vertex has zero degree then it is not connected at all, and thus called *isolated*. A graph G where every vertex has the same degree r, i.e., $\deg_G(v) = r \,\forall\, v \in V(G)$, is called *$r$-regular*. Clearly, if G is r-regular, then $\delta(G) = \Delta(G) = r$. For example, Figure 2.4 shows the cycle C_5, cycles are 2-regular. Figure 2.3 shows complete graphs, K_n, on up to $n = 7$ vertices, complete graphs are $(n-1)$-regular.

In directed graphs the degree of a vertex can be further distinguished, since its neighbourhood can be divided into other vertices that can reach the vertex and other vertices that are reachable by the vertex. Let $N_G^{\text{in}}(v) = \{u \,|\, uv \in E(G)\}$ denote the set of vertices in G that can reach v and $N_G^{\text{out}}(v) = \{u \,|\, vu \in E(G)\}$ denote the set of vertices that can be reached by v, then $\deg_G^{\text{in}}(v) = |N_G^{\text{in}}(v)|$ and $\deg_G^{\text{out}}(v) = |N_G^{\text{out}}(v)|$ denote its *in-degree* and *out-degree*, respectively.

A useful property of the adjacency matrix of a directed graph G is that summing the i-th row yields the out-degree of vertex i and summing the i-th column yields its in-degree, i.e., $\sum_{j \in V(G)} a_{ij} = \deg_G^{\text{out}}(i)$ and $\sum_{j \in V(G)} a_{ji} = \deg_G^{\text{in}}(i)$. Since the adjacency matrix of an undirected graph is symmetric, its row and column sums are equal, hence, the out- and in-degree of a vertex are equal, i.e., $\deg_G^{\text{out}}(i) = \deg_G^{\text{in}}(i) = \deg_G(i)$. Sometimes, for reasons of clarity, we use the symbol k_i' to denote the degree of vertex i when it is clear from the context which network is meant.

The simplest definition of *centrality* states that the most central vertices are the most active ones in the sense that they have the most connections to other vertices in the network, cf. (Wasserman & Faust, 1994, p. 178). Based on this definition, a centrality measure equally simple has been introduced for both undirected and directed networks by Nieminen (1973, 1974). In an undirected network, the *degree centrality* of a vertex is simply its degree. The measure is an index of the potential *communication activity*

of a vertex. Vertices for which their degree centrality is high are expected to use their connections to communicate actively and therefore take central positions in the network. Vertices with low degree centrality are expected to take less central positions as far as complete decentralized positions when vertices have no connections and therefore are unable to communicate at all.

As with vertex degree, degree centrality can be further distinguished in a directed network. Then, the out-degree of a vertex is an index for its activity, as before, and its in-degree can be seen as a simple measure of its *popularity* (or sometimes prestige).[3]

Moreover, dividing degree centrality by its maximum value, which is $(n-1)$, yields a normalized degree centrality measure that is comparable across networks of different orders n, cf. Freeman (1978). Degree centrality then corresponds to the proportion of vertices that a vertex is adjacent to.

In this thesis, we focus on degree centrality, as this is the view of centrality that is adopted when analysing the assortativity in its original form. However, by linking different views of centrality to the distinct structural attributes of a vertex, alternative definitions become available. For example, for a particular vertex, its *control of communication* is linked to the proportion of the shortest paths between any two vertices of the network that pass through that particular vertex, and is referred to *betweenness centrality*, cf. Freeman (1978). Central vertices according to this definition maintain the communication activity of the network, but are also capable of withholding or distorting information. The independence or *efficiency of communication* of a vertex is linked to the inverse average distance between itself and all other vertices, where the obtained measure, which is referred to as *closeness centrality*, determines how quickly information produced by that vertex reach the rest of the network, cf. Sabidussi (1966) and Magnani and Marzolla (2014). Finally, there is an approach to centrality, where a vertex is considered to be central only if it is pointed to by many other central vertices. The corresponding measure to this view of centrality is referred to *eigenvector centrality*, cf. Bonacich (1987).

2.2 Basic Random Graph Models

In this section we discuss the *Erdős-Rényi random graph* (ER) and the Barabási–Albert (BA) model, which will be analysed in an extended version in Chapter 4. Both models are very popular and commonly used as benchmark models.

[3]Eventually, it is worth mentioning that one has to be cautious when interpreting popularity or prestige as its meaning strongly depends on the application, more precisely, on the definition of edges and whether they describe positive or negative effects. The interpretation would have to be reversed in case of negative effects.

2.2.1 Erdős-Rényi Random Graph Model

The *Erdős-Rényi random graph* (ER) model is a term that usually refers to two closely related models. One is the $G_{n,M}$ model, introduced by Erdös and Rényi (1959, 1960), who laid the foundation for random graph theory as a mathematical field, cf. Dorogovtsev (2010), and the other one is the $G_{n,p}$ model, introduced by Gilbert (1959). In this context, $G_{n,M}$ denotes an ensemble of networks, G, with fixed order n and fixed size M, of which members are all equally likely to realize. However, $G_{n,p}$ denotes an ensemble of networks, G, with fixed order n and a given probability, p, that any two vertices in the network are connected by an edge.

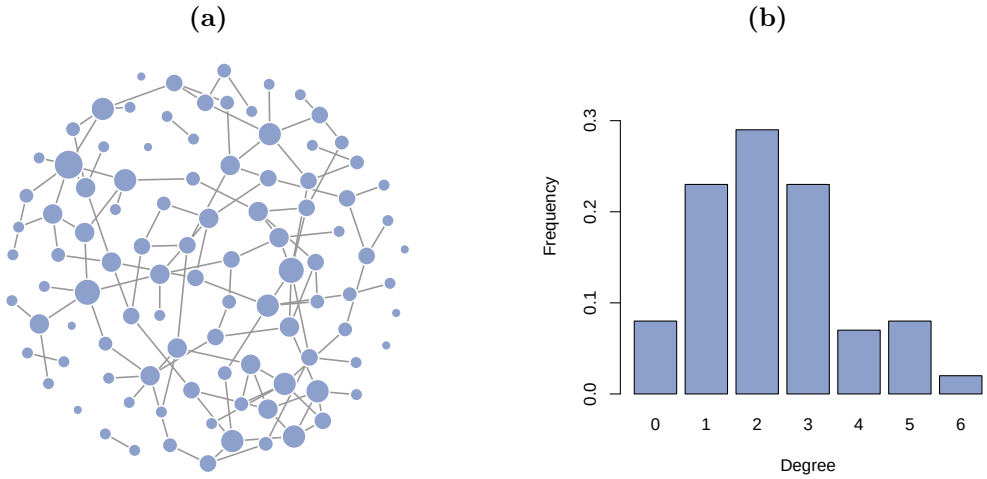

Figure 2.6. Realization of sampling the ER model. The figures visualize (a) the network structure of the resulting ER sample, with order $n = 100$ and connection probability $p = 0.025$, and (b) a bar diagram of the degree distribution.

Figure 2.6 shows a realization of sampling the ER model. For each entry of the (100×100) dimensional adjacency matrix, the flip of a p-biased coin with $p = 0.025$ determines if an edge is present between the corresponding vertices or not. The bar diagram on the right shows the *degree distribution* of the sample graph, i.e., the probability distribution that a randomly chosen vertex has degree k. In general, the degree distribution of the ER model is the binomial distribution:

$$P(k) = \binom{N-1}{k} p^k (1-p)^{N-1-k},$$

which in the case of large N is sometimes approximated by the Poisson distribution, $P(k) = z^k \, \mathrm{e}^{-z}/k!$, where z is the mean degree, cf. Newman, Strogatz, and Watts (2001).

2.2.2 Barabási–Albert Model

The Barabási–Albert (BA) model by Barabási and Albert (1999) is another famous network model, which we like to consider in this Thesis. The BA model has been proposed in order to address two implied assumptions of the ER model that are violated in many real-world networks, which are: (1) Networks have a *fixed number of vertices*; (2) Vertices are assumed to connect randomly to others with a *constant probability*. Barabási and Albert (1999) overcome this by incorporating both a *growth-* and *preferential attachment mechanism* into their model.

Network growth is considered by initializing a random BA network to a number of m_0 arbitrarily connected vertices, such that each vertex is incident with at least one edge, and then, let it grow over a time horizon T. At each time step $t = 1, \ldots, T$ a vertex is added to the network by forming m ($m \leq m_0$) edges between the newly added vertex and some already existing vertex. The process of link formation is governed by a preferential attachment mechanism, i.e., the probability, p_i, that the newly created vertex connects to an existing vertex i depends on the degree k' of vertex i in such a way that:

$$p_i = \frac{k'_i}{\sum_{i=1}^{m_0+t-1} k'_i}. \tag{2.1}$$

Apparently, a new vertex has a higher probability to connect to an existing high degree vertex than to connect to an existing low degree vertex, which, eventually, will lead to the formation of hubs.

After T time steps, a network generated by the BA model consists of $m_0 + T$ vertices and $m_0 + mT$ edges. Moreover, it is *scale free*, i.e., its degree distribution, particularly for large k', is a power law function of the form $P(k') \sim (k')^{-\gamma}$ where the power law exponent $\gamma = 3$, cf. Barabási and Albert (1999), Barabási, Albert, and Jeong (1999) and Bollobás, Riordan, Spencer, and Tusnády (2001).

Fig. 2.7 illustrates the scale free property for a small network generated by sampling the BA model for the parameters $m_0 = 5$, $m = 2$ and $T = 500$. The figure on the right shows the degree distribution on the log-log scale, where the solid black line indicates the observed degrees, and the dashed red line indicates a power law fit. The slope of the dashed line corresponds to the power law exponent γ. Since the dashed line represents a good fit for the solid line, the BA sample appears to have a scale-free degree distribution, as expected.

The above described model is the *simplest* form of the BA model, thus, we therefore refer to it as the simple BA model or simple preferential attachment model. A plethora of extensions to the simple preferential attachment scheme have been suggested over time, in order to alter the characteristic topological features that it induces. For example, Garcia-Domingo, Juher, and Saldaña (2008), Deijfen and Lindholm (2009) and

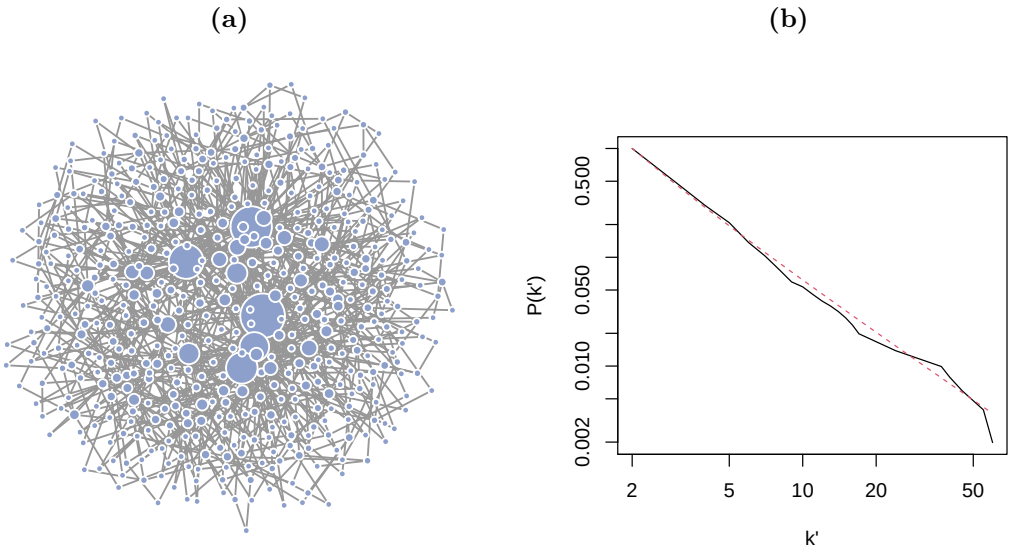

Figure 2.7. Realization of sampling the BA model. The figures visualize (a) the network structure of the resulting BA sample, with parameters $m_0 = 5$, $m = 2$ and $T = 500$, and (b) the degree distribution of the network on the log-log scale. Lines indicate observed degrees (solid black) and a corresponding power law fit (dashed red).

Brot, Honig, Muchnik, Goldenberg, and Louzoun (2013) also consider the *deletion* of edges or vertices. The *ageing* of vertices is considered by Dorogovtsev and Mendes (2000) and Hajra and Sen (2005). With ageing vertices, the probability of a newly added vertex connecting to an existing vertex i is positively weighted by its degree k'_i but, at the same time, negatively weighted by its age x_i, i.e., the preferential attachment scheme is altered such that the probability p_i is proportional to the ratio k'_i/x_i, indicating that older vertices are less likely to be chosen by new ones to connect to. More generally, Bianconi and Barabási (2001) and Borgs, Chayes, Daskalakis, and Roch (2007) introduce an additional *fitness* value η_i for existing vertices and add new ones with probability proportional to $\eta_i k'_i$.[4] Many more extensions have been suggested, of which a non-exhaustive overview is given by Coolen, Annibale, and Roberts (2017).

Weighted extensions of the basic models presented in this section are considered in Chapter 4 as benchmark models for our local assortativity measures. First, however, we want to define the concept of assortativity and review the state of the literature on this topic. Moreover, we propose a new coefficient for the measurement of assortativity in the subsequent chapter.

[4]The concept of fitness of a vertex is closely related to ageing, e.g., by letting $\eta_i = 1/x_i$ the same preferential attachment scheme as with ageing is obtained.

3 Assortative Mixing in Weighted Directed Networks

As previously noted, assortativity is the tendency of a vertex to bond with another based on their similarity, with similarity being usually measured via vertex degree. The most popular assortativity measure is the assortativity coefficient, which is defined as the Pearson correlation coefficient between the excess degrees of both ends of an edge. In this chapter we propose a more general coefficient of assortativity that nests previous assortativity measures as special cases, and that can be applied to unweighted and undirected as well as weighted and directed networks. Moreover, we show that the use of this general coefficient enables us to determine the underlying assortativity structure in weighted networks more precisely. Furthermore, we propose a procedure to assess the statistical significance of assortativity using jackknife, bootstrap and rewiring techniques. An abridged version of this chapter has already been published in *Physica A: Statistical Mechanics and its Applications*, cf. U. Pigorsch and M. Sabek (2022).

The remainder of the chapter is structured as follows: Section 3.1 provides a review of the related literature and motivates the use of excess strength for the computation of assortativity. In Section 3.2 we introduce our generalized assortativity coefficient, elaborate on the importance of considering excess strength rather than total strength, and propose procedures for the interpretation and statistical assessment of assortativity in weighted networks. Section 3.3 illustrates the application and interpretation of assortativity in weighted real-world networks. In Section 3.4 we discuss our empirical results and give suggestions for future research.

3.1 Background and Related Literature

The assortativity coefficient r^{N} has been proposed by Newman (2002) and is defined as the Pearson correlation coefficient between the excess degrees (sometimes: remaining degrees) of both ends of an edge. Excess or remaining degrees are defined to be one less than the ends' degrees, i.e., they are the degrees of the ends prior to the formation of the particular edge which is currently considered. The coefficient is obtained by computing

$$r^{\mathrm{N}} = \frac{M^{-1}\sum_i j_i k_i - \left[M^{-1}\sum_i \frac{1}{2}(j_i + k_i)\right]^2}{M^{-1}\sum_i \frac{1}{2}(j_i^2 + k_i^2) - \left[M^{-1}\sum_i \frac{1}{2}(j_i + k_i)\right]^2}, \tag{3.1}$$

where j_i and k_i are the excess degrees of the ends j and k of edge i, where $i = 1, \ldots, M$, and M is the number of edges in the network. Since r^{N} is a correlation coefficient it

lies in the range $-1 \leq r^{\mathrm{N}} \leq 1$, and has the advantage that assortativity coefficients can be compared across different networks. The coefficient in Equation (3.1) has been proposed for *undirected unweighted* networks.

Newman (2003) has also proposed an extension towards *directed unweighted* networks. He defines assortativity in directed networks as the correlation coefficient between the excess out-degree of the vertex that the i-th edge leads out of and the excess in-degree of the vertex that the i-th edge leads into. In addition to this, Piraveenan et al. (2012) find it sensible to also consider both the correlation between (excess) out-degrees of both ends of an edge and the correlation between (excess) in-degrees of both ends of an edge. Therefore, they propose alternative definitions for assortativity in directed networks, namely out-assortativity and in-assortativity, which are the tendencies of vertices to bond with others of similar out-degree and in-degree as themselves, respectively. This results in four different variants of the assortativity coefficient in directed networks.

For our empirical analysis, we refer to these variants as the *mode of assortativity*. We denote by *out-in* the assortativity coefficient of Newman (2003). The modes *out-out* and *in-in* refer to the out- and in-assortativity according to Piraveenan et al. (2012), respectively. Finally, by *in-out* we denote the correlation coefficient between the in-degree of the vertex that the i-th edge leads out of and the out-degree of the vertex that the i-th edge leads into, see also Piraveenan et al. (2012).

The corresponding assortativity coefficient for *directed* networks is given by:

$$r_d^{\mathrm{N}} = \frac{\sum_i j_i' k_i' - M^{-1}(\sum_i j_i')(\sum_i k_i')}{\sqrt{\left[\sum_i (j_i')^2 - M^{-1}(\sum_i j_i')^2\right]\left[\sum_i (k_i')^2 - M^{-1}(\sum_i k_i')^2\right]}}, \tag{3.2}$$

where this time j_i' and k_i' are the (excess) in- or out-degrees of ends j and k of the i-th edge, and $i = 1, \ldots, M$.

The coefficient in Equation (3.2) has been introduced for *directed unweighted* networks. However, it is capable of handling *undirected unweighted* networks as well, if the network is slightly modified, i.e., by replacing each undirected edge by two directed ones that point in opposite directions, see Newman (2003). Indeed, the formulation in Equation (3.1) is a simplification of the more general formulation in Equation (3.2) that makes use of the property of symmetry of the adjacency matrix of an undirected network.

According to Noldus and van Mieghem (2015), assortativity in weighted networks has been insufficiently studied, so far. One exception is the coefficient of Leung and Chau (2007), which, for example, has been used by Chang, Su, Zhou, and He (2007),

where the following extension of the assortativity coefficient towards *undirected weighted* networks is suggested

$$r^{\mathrm{LC}} = \frac{H^{-1}\sum_i \omega_i(j_i k_i) - [H^{-1}\sum_i \frac{1}{2}\omega_i(j_i + k_i)]^2}{H^{-1}\sum_i \frac{1}{2}\omega_i(j_i^2 + k_i^2) - [H^{-1}\sum_i \frac{1}{2}\omega_i(j_i + k_i)]^2}, \tag{3.3}$$

where, as in Equation (3.1), j_i and k_i are the excess degrees of the ends j and k of edge i, ω_i denotes the weight of the i-th edge and $H = \sum_i \omega_i$ is the sum of edge weights where the sum is over all edges. Obviously, if all edge weights equal one, i.e., the network is unweighted, the coefficient in Equation (3.3) reduces to the original assortativity coefficient in Equation (3.1).

The underlying mechanism of this assortativity coefficient, can easily be illustrated. For the ease of exposition and without loss of generality suppose integer-valued weights (as real-valued weights can be linearly mapped to integers with arbitrary precision, see Rubinov, 2016).[5] Then incorporating edge weights is equivalent to replacing each ω-weighted edge by ω edges with weight one. Thus, high-weighted edges amplify the impact of their connections and therefore contribute more to the overall assortativity.

Although this is a reasonable approach, we instead propose a generalization of assortativity to weighted networks that is based on the correlation between the *excess strengths* of both ends of an edge. Considering excess strength is quite intuitive here, as vertex degree generalizes to vertex strength in weighted networks, see Barrat, Barthélemy, Pastor-Satorras, and Vespignani (2004). He defines the strength of a vertex u as $s_u = \sum_{v \in V} w_{uv}$, where V is the vertex set and w_{uv} is the weight of the edge between u and v.

In fact, note that the emergence of assortativity in a weighted network consists of two mechanisms. The first one is the just mentioned *amplification effect*, which occurs if a connection is considered according to the respective edge weight when computing the correlation between the vertex values. The second one is the *connection effect*, which occurs if, instead of unweighted vertex values (e.g., excess degrees), weighted vertex values are considered (e.g., excess strengths). More precisely, consider two arbitrary adjacent vertices and suppose they have the same degrees but different strengths, as depicted in Figure 3.1. The connection between them, weighted or not, is assortative if degrees are used as vertex values, but is disassortative if strengths are used. The connection effect might also occur vice versa, for example, if two adjacent vertices have different degrees but similar strengths. Noteworthy, the connection effect is ignored in the definition of the assortativity coefficient of Equation (3.3). In the following section we propose a generalized assortativity coefficient that incorporates both of these effects.

[5] For example, $w_{\mathrm{int}} = \mathrm{round}(w_{\mathrm{real}} \cdot 10^{\mathrm{precision}})$ is a mapping that linearly maps real-valued weights to integers with arbitrary precision.

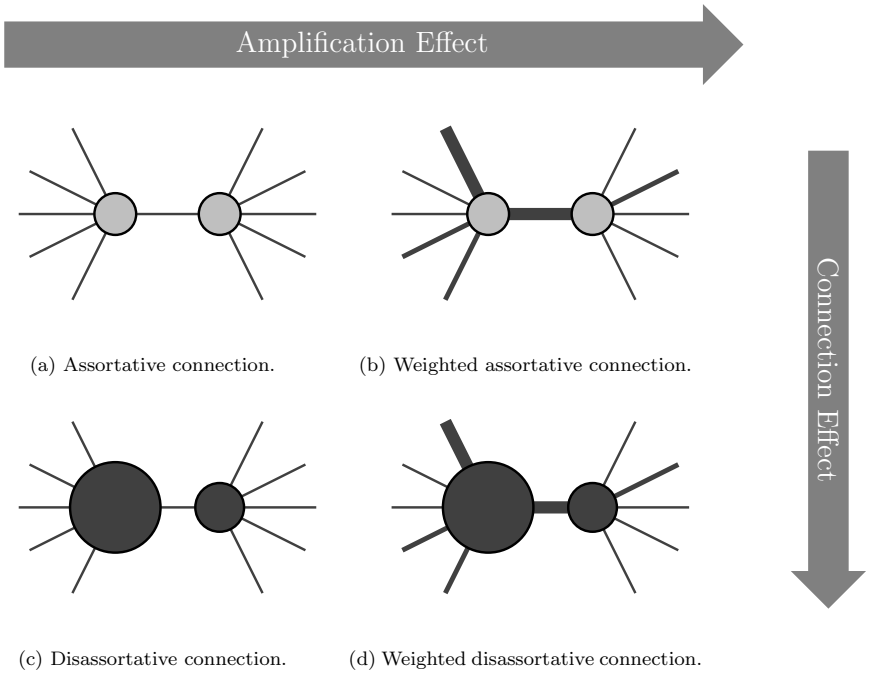

(a) Assortative connection. (b) Weighted assortative connection.

(c) Disassortative connection. (d) Weighted disassortative connection.

Figure 3.1. Illustration of the *connection effect* and the *amplification effect*. All figures show the same exemplary connection between two arbitrary vertices with similar degrees but different strengths. The size of a vertex is proportional to its excess degree in (a) and (b), whereas it is proportional to its excess strength in (c) and (d). Edges have the same widths in (a) and (c), whereas their widths are proportional to their weights in (b) and (d). Arrows then indicate the direction in which the respective mechanisms operate, i.e., when determining the assortativity, the amplification effect occurs if additionally the weight of a given connection is considered, whereas the connection effect occurs if strengths are considered instead of degrees.

3.2 A Generalized Assortativity Coefficient

To account for both effects, we include vertex strength in addition to vertex degree into our assortativity coefficient, which is defined in Section 3.2.1. In Section 3.2.2, we elaborate on the importance of considering excess strength rather than total strength, a distinction that is rarely made explicitly in the context of vertex degree in the existing literature. Moreover, our proposed generalized assortativity coefficient nests four different assortativity coefficients. We suggest computing and interpreting all of them, as their comparison provides new insights on the assortativity structure of weighted networks. This is detailed in Section 3.2.3. We further supplement the analysis by proposing a procedure for assessing both the statistical significance of the four assortativity coefficients and whether the observed assortativity structure has social, organizational origins or has been randomly generated, see Section 3.2.4.

3.2.1 Definition of the Generalized Assortativity Coefficient

In the following, we introduce our generalized weighted assortativity coefficient, that takes the amplification effect as well as the connection effect into account. To this end, let $s'_u = \sum_{v \in V} w_{uv}^{\alpha}$, $\alpha \in \{0, 1\}$, be a modified version of vertex strength. Clearly, if $\alpha = 1$ then $s'_u = s_u$, whereas for $\alpha = 0$ it reduces to ordinary vertex degree. Our generalized weighted assortativity coefficient is then defined as

$$r^{\omega}_{(\alpha,\beta)} = \frac{\sum_i \omega_i^{\beta} l_i m_i - \Omega^{-1}(\sum_i \omega_i^{\beta} l_i)(\sum_i \omega_i^{\beta} m_i)}{\sqrt{\left[\sum_i (\omega_i^{\beta} l_i^2) - \Omega^{-1}(\sum_i \omega_i^{\beta} l_i)^2\right]\left[\sum_i (\omega_i^{\beta} m_i^2) - \Omega^{-1}(\sum_i \omega_i^{\beta} m_i)^2\right]}}, \tag{3.4}$$

where l_i and m_i are the excess (in- or out-) strengths of the ends l and m of edge i. For example, $l_i = s'_l - \omega_i^{\alpha}$ is the excess strength of end l of edge i. Furthermore, $\Omega = \sum_i \omega_i^{\beta}$ with $\beta \in \{0, 1\}$. Obviously, if $\beta = 1$ then $\Omega = H$, whereas for $\beta = 0$ it reduces to the total number of edges in the network, i.e., $\Omega = M$. The generalization is achieved by introducing α and β, which account for the two different mechanisms, i e. the connection effect and the edge amplification effect, respectively. As such the previous definitions of assortativity are nested as special cases, in particular $r^{\omega}_{(\alpha=0,\beta=1)} = r^{\mathrm{LC}}$ and $r^{\omega}_{(\alpha=0,\beta=0)} = r^{\mathrm{N}}$.

Note that r^{LC} is based on the formulation of r^{N} introduced Newman (2002), whereas our coefficient $r^{\omega}_{(\alpha,\beta)}$ is based on the formulation r^{N}_{d} of Newman (2003) and Farine (2014). Thus, it is capable of handling *directed* (*weighted*) networks as well as *undirected* (*weighted*) networks by replacing, as before, each undirected edge by two directed ones that point in opposite directions.

Our assortativity coefficients $r^{\omega}_{(\alpha,\beta)}$ is also inline with the definition of the weighted correlation coefficient, see Da Costa (2011), which is defined as:

$$r_w = \frac{\sum_i w_i X_i Y_i - \sum_i w_i X_i \sum_i w_i Y_i}{\sqrt{\left(\sum_i w_i X_i^2 - (\sum_i w_i X_i)^2\right)\left(\sum_i w_i Y_i^2 - (\sum_i w_i Y_i)^2\right)}}. \tag{3.5}$$

The sums are over observations i; X_i and Y_i are the pair of values of variables X and Y that correspond to the i-th observation; w_i is the weight attributed to this observation, and the sum of edge weights equals unity, i.e., $\sum_i w_i = 1$. Furthermore, if all weights w_i are equal they cancel out and Equation (3.5) reduces to the usual formula for the Pearson correlation coefficient, i.e., the unweighted correlation coefficient. By defining variables $X_i = l_i$ and $Y_i = m_i$ and weights $w_i = \omega_i^{\beta}$, it becomes immediately clear that Equation (3.4) and Equation (3.5) are equivalent.[6]

[6] The additional requirement that $\sum_i \omega_i^{\beta} = \Omega = 1$ can be met without loss of generality by a suitable remapping of the observed edge weights.

To summarize, assortativity in weighted networks is not unambiguously defined. In fact, there are four different ways edge weights can be treated, resulting in four different versions of the assortativity coefficient. First, if present edge weights are neglected, assortativity can be measured as the correlation between the excess degrees of both ends of an edge, $r^{\omega}_{(0,0)}$, which is the classical definition of assortativity introduced by Newman (2002), henceforth referred to as the benchmark assortativity coefficient, also cf. Figure 3.1 (a). Leung and Chau (2007) suggest to measure assortativity by the weighted correlation between the excess degrees of both ends of an edge, $r^{\omega}_{(0,1)}$, cf. Figure 3.1 (b). This partly accounts for edge weights keeping vertex values still unweighted. The remaining two versions of the assortativity coefficient have not been considered in the literature so far, and are both based on excess vertex strength, i.e., $\alpha = 1$, rather than excess vertex degree. In particular, we can either partly incorporate edge weights, this time, by computing the unweighted correlation of weighted vertex values, i.e., excess strength, resulting in the assortativity coefficient $r^{\omega}_{(1,0)}$, or fully incorporate edge weight, i.e., $\alpha = 1$ and $\beta = 1$, by computing the weighted correlation between the excess strengths of both ends of an edge, cf. Figure 3.1 (c) and (d). We denote the latter by $r^{\omega}_{(1,1)}$ and refer to it as the generalized assortativity coefficient.

When analysing the assortativity structure of a real weighted network, we suggest to focus on both, the generalized assortativity coefficient and the benchmark coefficient, i.e., to fully consider edge weights or to neglect them entirely. For example, if the interest is exclusively on the binary network edges, it might be reasonable to neglect edge weights, and to focus on the benchmark assortativity coefficient. However, in many cases edge weights provide additional information, which in turn can be fully explored using the generalized assortativity coefficient. In contrast, focusing exclusively on assortativity coefficients that only partially consider edge weights, falls short, as each includes just one of the two effects of edge weights. Nevertheless, as we will detail in Section 3.2.3, using them as supplementary measures allows drawing more distinct conclusions about the assortativity structure and as such they are also of interest.

3.2.2 Excess (Out- or In-) Strengths in Directed Weighted Networks

The existing literature on the measurement of assortativity rarely explicitly addresses whether total degrees or excess degrees are used; rather, it is often times just referred to "degree". However, Newman (2002) defines the assortativity coefficient for undirected and unweighted networks to be the correlation coefficient between the excess degrees rather than the total degrees of both ends of an edge. The reason for this is that a vertex's tendency to bond with another one is based on the degree it has prior to forming the particular edge, i.e., its own excess degree as well as the other vertex's excess degree, cf. Noldus and van Mieghem (2015). Consequently, using *excess* strengths in case of weighted networks is the obvious choice.

We can only assume that the above-mentioned imprecision is due to the fact that for *unweighted* networks it makes no difference whether correlation is computed based on excess degrees or on total degrees, as both result in the same value of the assortativity coefficient. This holds as the excess degrees of the ends of an edge and the total degrees of the ends of an edge differ by a constant (i.e., by one) and the correlation between two random variables does not change if a constant is added or subtracted to either or both variables. As opposed to this, in a *weighted* network it indeed makes a difference whether excess or total strength is used. The reason is that the excess strengths of the ends of an edge differ from total strengths of the ends of an edge by the weight of the particular edge and this difference is not constant. Therefore, the resulting assortativity coefficient based on excess strengths will be drastically different from the one based on total strengths.

In the following we give a brief example that illustrates the consequences of using total strengths rather than excess strengths for assessing a network's assortativity structure. To this end we consider the weighted and directed network, considered in Yuan, Yan, and Zhang (2021), which is depicted in Figure 3.2. The directed edges are marked by their weights. For example, the first edge of the network connects vertices A and B with an edge of weight 10 pointing from A to B, i.e., $\omega_1 = w_{AB} = 10$. The seventh edge of the network points from C to A with an edge weight of 1, i.e., $\omega_7 = w_{CA} = 1$.

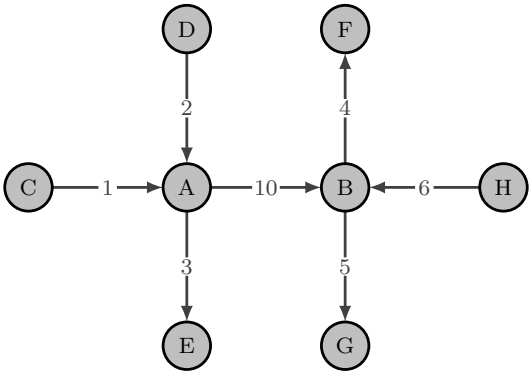

Figure 3.2. Sample weighted directed network. Adapted from Yuan et al. (2021).

The corresponding edge list of the network is depicted in Table 3.1. The edge list is expanded by the excess out- and in-strengths as well as the total out- and in-strengths. The excess out-strength of the source end l of edge i is defined as its total out-strength less the edge weight, i.e., $\tilde{s}^{out}_{(l,i)} = s^{out}_l - \omega_i$. Similarly, the excess in-strength of the target end m of edge i is defined as its total in-strength less the edge weight, i.e., $\tilde{s}^{in}_{(m,i)} = s^{in}_m - \omega_i$. The excess in-degree of the source end l of edge i as well as the excess out-strength of the target end m of edge i are not separately listed in Table 3.1, since $\tilde{s}^{in}_{(l,i)} = s^{in}_l$ and $\tilde{s}^{out}_{(m,i)} = s^{out}_m$, respectively, as reasoned in Section 3.2.1. The total strengths are obtained as usual.

i	l_i	m_i	ω_i	$\tilde{s}^{out}_{(l,i)}$	$\tilde{s}^{in}_{(m,i)}$	s^{out}_l	s^{in}_l	s^{in}_m	s^{out}_m
1	A	B	10	3	6	13	3	16	9
2	H	B	6	0	10	6	3	16	0
3	B	G	5	4	0	9	16	5	0
4	B	F	4	5	0	9	16	4	0
5	A	E	3	10	0	13	0	3	13
6	D	A	2	0	1	2	0	3	13
7	C	A	1	0	2	1	0	3	9

Table 3.1. Edge list of sample network in Figure 3.2. The edge list has been expanded by excess and total out- and in-strengths.

For example, the excess out-strength of vertex A with respect to the first edge is given by $\tilde{s}^{out}_{(A,1)} = 13 - 10 = 3$ and, at the same time, the excess out-strength of vertex A with respect to the fifth edge is given by $\tilde{s}^{out}_{(A,5)} = 13 - 3 = 10$. Also, the excess in-strength of vertex A with respect to the seventh edge is given by $\tilde{s}^{in}_{(A,7)} = 3 - 1 = 2$ and, at the same time, the excess in-strength of vertex A with respect to the sixth edge is $\tilde{s}^{in}_{(A,6)} = 3 - 2 = 1$. This clearly shows that the excess (out- or in-) strengths of the ends of an edge depend on the weight of the edge that is currently considered. As opposed to this, the total strengths of the ends remain the same for all edges.

We will now illustrate the emerging consequences of using total strengths rather than excess strengths when computing the weighted assortativity coefficient. To this end, let $\tilde{\rho} = r^{\omega}_{(\alpha=1,\beta=1)}$ be the generalized assortativity coefficient as defined in Equation (3.4) which is based on excess strengths and ρ be the assortativity coefficient based on total strengths as in Yuan et al. (2021). For the given network, the generalized assortativity coefficients for the different modes of assortativity are $\tilde{\rho}_{out\text{-}in} = -0.65, \tilde{\rho}_{out\text{-}out} = -0.76, \tilde{\rho}_{in\text{-}in} = -0.70$ and $\tilde{\rho}_{in\text{-}out} = -0.82$. On the contrary, the coefficients based on total strengths are $\rho_{out\text{-}in} = 0.29, \rho_{out\text{-}out} = -0.29, \rho_{in\text{-}in} = -0.56$ and $\rho_{in\text{-}out} = -0.82$.

Yuan et al. (2021), therefore, conclude that the example network simultaneously shows assortative and disassortative mixing, whereas, as a matter of fact, the network shows no assortative tendencies at all. The network is purely disassortative. Except for the *in-out* mode of assortativity, the resulting coefficients based on total strengths are throughout greater compared to those of the generalized coefficient. As mentioned before, for the *in-out* mode of assortativity the excess in- and out-strengths equal the total in- and out-strengths of the ends of an edge, respectively, and thus, $\tilde{\rho}$ and ρ coincidentally exhibit the same value. Other than that, using total strengths rather than excess strengths for computing the assortativity coefficient for a weighted network will lead to an overestimation towards the assortative direction, since high weighted edges necessarily connect vertices with high total strengths. Hence, a connection between two vertices that might be disassortative will appear more assortative as the vertex values are artificially inflated by the weight of the edge that connects the two vertices when

total strengths are used. Thus, it is crucial to use excess strengths in order to properly determine the underlying assortativity structure of a network.

In order to show this, consider the relative difference d between two variables $x \geq 0$ and $y \geq 0$ defined as $d = \frac{|x-y|}{(x+y)}$, for which we set $d = 0$ if $x = y = 0$. Computing d with respect to the vertex values of a network yields an indicator of the magnitude of assortativity of a particular connection. To be precise, if d is small, within its bounds $[0, 1]$, then the considered vertices are similar with respect to their vertex values. Vice versa, if d is large, then the considered vertices are different with respect to their vertex values, which basically equals the definition of assortative mixing.

Focusing on the *out-in* mode of assortativity, for the edges of the network in Figure 3.2 we obtain the following relative differences with respect to excess (out- and in-) strengths $d_{(\tilde{s}^{out},\tilde{s}^{in})} = \{0.33, 1, 1, 1, 1, 1, 1\}$. It can be seen that edges 2 to 7 are correctly identified as disassortative. They all tie a connected vertex to a vertex that is not connected at all, which is the most disassortative connection one can think of. The edge connecting vertices A and B is identified as rather assortative, since its value of $d_{(\tilde{s}^{out},\tilde{s}^{in}),1} = 0.33$ is rather small. By comparing this to the relative differences with respect to total (out- and in-) strengths $d_{(s^{out},s^{in})} = \{0.1, 0.63, 0.38, 0.29, 0.5, 0.2, 0.45\}$, which is possible because both $d_{(\tilde{s}^{out},\tilde{s}^{in})}$ and $d_{(s^{out},s^{in})}$ are dimensionless and of the same scale, it can be seen that every single edge is considered more assortative than it actually is, since $d_{(s^{out},s^{in}),i} < d_{(\tilde{s}^{out},\tilde{s}^{in}),i}$ for all edges i. This explains why the results $\tilde{\rho}_{out\text{-}in}$ and $\rho_{out\text{-}in}$ differ so drastically.

Based on this reasoning, we further recommend the following proper utilization of either excess or total strengths (or degrees) when computing the assortativity coefficient for different modes of assortativity for *directed* networks. Excess strengths are used for both out- and in-strengths when the mode of assortativity is *out-in*. Excess out- and total out-strengths are used when the mode is *out-out*, and total in- and excess in-strengths are used when the mode is *in-in*. For the mode *in-out* the correlation between both total in- and out-strengths should be used.

To see this, suppose, for example, of interest is the out-assortativity of a directed *weighted* network. Consider a particular edge leading out of vertex u and into vertex v, then, the out-strength of vertex u is affected by the edge weight whereas the out-strength of vertex v is not. More precisely, consider the out-strengths of both vertices that the particular edge connects prior to forming it. The excess out-strength for vertex u is its out-strength less the edge weight, whereas the excess out-strength for vertex v equals its total out-strength, in this case. For the other modes the reasoning is similar. Technically, the same holds true for directed *unweighted* networks, however, the results are the same no matter if one computes the correlation between excess or total (in- or out-) degrees (or any combination), as before.

We have recently noticed that, in independent and concurrent research, Yuan et al. (2021) have proposed a measure for assortativity in weighted networks similar to ours. Their measure, however, is based on the total strengths between the ends of an edge, which leads to misleading results as outlined above. Moreover, their paper focuses on the assortativity of theoretical network models. However, our key contribution is the introduction of a procedure that allows for both a more precise assessment and interpretation of the assortativity of weighted real-world networks and its analysis with respect to the statistical significance of the network's assortativity.

3.2.3 Procedure for Assessing and Interpreting Assortativity

In order to assess and interpret a network's assortativity, we suggest the following procedure: Firstly, compute $r^{\omega}_{(\alpha,\beta)}$ for all four parameter combinations (α, β), where $\alpha, \beta \in \{0, 1\}$, i.e., we compute the benchmark assortativity coefficient $r^{\omega}_{(0,0)}$, the generalized assortativity coefficient $r^{\omega}_{(1,1)}$ as well as both supplementary measures $r^{\omega}_{(1,0)}$ and $r^{\omega}_{(0,1)}$.

The values of the benchmark assortativity coefficient as well as the generalized assortativity coefficient range between -1 and 1. They give an indication of the underlying assortativity structure of the network with respect to the corresponding vertex values, which are degrees in case of $r^{\omega}_{(0,0)}$ and strengths in case of $r^{\omega}_{(1,1)}$. Similar to the interpretation of the original assortativity coefficient, for both coefficients, positive values indicate an overall assortative structure of the network, and negative values indicate an overall disassortative structure of the network, for zero values of the coefficients the network is considered to be non-assortative.

Secondly, compare the benchmark and the generalized assortativity coefficient. The values of $r^{\omega}_{(0,0)}$ and $r^{\omega}_{(1,1)}$ might be similar in magnitude for some networks, for others they might differ. Thus, a comparison of both values provides information on the impact of edge weights on the underlying assortativity structure of the network. For example, if $r^{\omega}_{(0,0)} > r^{\omega}_{(1,1)}$, then the consideration of edge weights leads to a decrease in assortativity or an increase in disassortativity of the network. In contrast, if $r^{\omega}_{(0,0)} < r^{\omega}_{(1,1)}$, the corresponding weighted network is more assortative than the network where edge weights are neglected.

An even more precise distinction regarding the effects that make up the network's assortativity structure is possible if, in a third step, the supplementary measures $r^{\omega}_{(1,0)}$ and $r^{\omega}_{(0,1)}$ are included into the comparison. For example, since the connection effect is captured by the parameter α, a comparison of $r^{\omega}_{(0,0)}$ with $r^{\omega}_{(1,0)}$, and $r^{\omega}_{(0,1)}$ with $r^{\omega}_{(1,1)}$, respectively, provides information on how the assortativity of the network varies with respect to using weighted vertex values instead of unweighted ones (i.e., strengths rather than degrees). Particularly, if $r^{\omega}_{(0,0)} < r^{\omega}_{(1,0)}$, then incorporating vertex strength leads to an increase in assortativity, suggesting that *unweighted* connections are more assortative

or less disassortative with respect to strengths as compared to degrees. Whereas, if $r^{\omega}_{(0,0)} > r^{\omega}_{(1,0)}$, then incorporating vertex strength leads to a decrease in assortativity, suggesting that *unweighted* connections are less assortative or more disassortative with respect to strengths as compared to degrees. Similarly, the connection effect can be interpreted for edge weighted connections, i.e., if $r^{\omega}_{(0,1)} < r^{\omega}_{(1,1)}$, then incorporating vertex strength leads to an increase in assortativity. This suggests that *weighted* connections are more assortative or less disassortative with respect to strengths as compared to degrees. As opposed to this, if $r^{\omega}_{(0,1)} > r^{\omega}_{(1,1)}$, then incorporating vertex strength leads to a decrease in assortativity, suggesting that *weighted* connections are less assortative or more disassortative with respect to strengths as compared to degrees.

By the same logic, since the amplification effect is captured by the parameter β, comparisons of $r^{\omega}_{(0,0)}$ with $r^{\omega}_{(0,1)}$, and $r^{\omega}_{(1,0)}$ with $r^{\omega}_{(1,1)}$, respectively, reveal how assortativity changes if edge weights are considered in terms of using weighted connections instead of unweighted ones in the computation of the assortativity coefficient for fixed vertex values (strengths or degrees). To be more precise, if $r^{\omega}_{(0,0)} < r^{\omega}_{(0,1)}$, then the increase in assortativity suggests that high weighted connections tend to be more assortative or less disassortative *by degree* than low weighted ones. Vice versa, if $r^{\omega}_{(0,0)} > r^{\omega}_{(0,1)}$, there is a decrease in assortativity, suggesting that high weighted connections are less assortative or more disassortative *by degree* than low weighted ones. Similarly, if $r^{\omega}_{(1,0)} > r^{\omega}_{(1,1)}$, then the increase in assortativity suggests that high weighted connections tend to be more assortative or less disassortative *by strength* than low weighted ones. Again, if, vice versa, $r^{\omega}_{(1,0)} < r^{\omega}_{(1,1)}$, then the decrease in assortativity suggests that high weighted connections tend to be less assortative or more disassortative *by strength* than low weighted ones.

If the assortativity of a network increases due to one of the two effects, we call the respective effect assortative, if, however, the assortativity of a network decreases, we call the respective effect disassortative. As can be seen from the above, both effects are twofold as they might operate differently with respect to the way in which edge weights are considered. For example, for the same network, the assortativity might vary differently for *unweighted* and *weighted connections* if edge weights are considered via weighted vertex values as with the connection effect. The same holds true for the amplification effect where the assortativity with respect to both *unweighted vertex values* and *weighted vertex values* might vary differently if edge weights are considered in terms of weighted connections.

We call the effects *consistent* if, considered individually, they operate in the same way, and *inconsistent* the other way round. For example, a connection effect which reduces the assortativity of the network for both unweighted and weighted connections if edge weights are considered with respect to weighted vertex values is considered *consistent*, in this particular case consistently disassortative. Contrary to this, an amplification effect that increases assortativity by degree on the one hand but decreases assortativity by

Summary 3.2.1 Procedure for assessing and interpreting assortativity.

(a) Compute $r^{\omega}_{(\alpha,\beta)}$ for all four parameter combinations (α, β).

(b) An indication of the overall assortativity is given by the values of $r^{\omega}_{(0,0)}$ and $r^{\omega}_{(1,1)}$:

- if values $> 0 \Rightarrow$ assortative
- if values $< 0 \Rightarrow$ disassortative
- if values $= 0 \Rightarrow$ non-assortative

(c) Obtain the edge weight effect on assortativity by comparing the generalized with the benchmark assortativity coefficient:

- if $r^{\omega}_{(0,0)} > r^{\omega}_{(1,1)} \Rightarrow$ weighted network is less assortative
- if $r^{\omega}_{(0,0)} < r^{\omega}_{(1,1)} \Rightarrow$ weighted network is more assortative

(d) Interpret assortativity effects by comparing the generalized with the benchmark assortativity coefficient:

- *Connection effect*
  - if $r^{\omega}_{(0,0)}(>) < r^{\omega}_{(1,0)} \Rightarrow$ most *unweighted* connections tend to be (less) more assortative by strength as by degree
  - if $r^{\omega}_{(0,1)}(>) < r^{\omega}_{(1,1)} \Rightarrow$ most *weighted* connections tend to be (less) more assortative by strength as by degree
- *Edge amplification effect*
  - if $r^{\omega}_{(0,0)}(>) < r^{\omega}_{(0,1)} \Rightarrow$ high weighted connections tend to be (less) more assortative *by degree*
  - if $r^{\omega}_{(1,0)}(>) < r^{\omega}_{(1,1)} \Rightarrow$ high weighted connections tend to be (less) more assortative *by strength*
- Both effects
  - if one or both effects operate in the same (different) direction with respect to the way in which edge weights are considered $\Rightarrow$ respective effect is consistent (inconsistent)
  - if $r^{\omega}_{(1,1)} < \min(r^{\omega}_{(1,0)}, r^{\omega}_{(0,1)}) \vee r^{\omega}_{(1,1)} > \max(r^{\omega}_{(1,0)}, r^{\omega}_{(0,1)}) \Rightarrow$ consensual
  - if $r^{\omega}_{(1,1)} \in \left[\min(r^{\omega}_{(1,0)}, r^{\omega}_{(0,1)}), \max(r^{\omega}_{(1,0)}, r^{\omega}_{(0,1)})\right] \Rightarrow$ opposing

strength on the other is considered *inconsistent*. In this case, there exists an assortative amplification effect with respect to unweighted vertex values but, at the same time, a disassortative amplification effect with respect to weighted vertex values.

Finally, we can determine whether the effects are *consensual* or *opposing*. The effects are consensual if the assortativity coefficient for which one of the effects has already been taken into account increases or decreases even further if the other effect is additionally taken into account. This is the case if $r^{\omega}_{(1,1)} < \min(r^{\omega}_{(1,0)}, r^{\omega}_{(0,1)})$ or $r^{\omega}_{(1,1)} > \max(r^{\omega}_{(1,0)}, r^{\omega}_{(0,1)})$. If, however, $r^{\omega}_{(1,1)} \in \left[\min(r^{\omega}_{(1,0)}, r^{\omega}_{(0,1)}), \max(r^{\omega}_{(1,0)}, r^{\omega}_{(0,1)})\right]$, then, this indicates that the effects are opposing because there is an effect that results in a more disassortative or assortative coefficient, respectively, if the other one is not considered, i.e., the impact of the first effect is reduced by the second.

The outlined procedure is summarized in summary box 3.2.1, and we will illustrate its application to empirical networks in Section 3.3.

3.2.4 Assessing the Significance of Assortativity

As mentioned above, there are four different ways of measuring assortativity in weighted networks. If we interpret each of them to be an estimator of the respective unknown population parameter, then computing the values for the coefficients based on a real network yields the corresponding point estimates. However, the associated estimation uncertainty is unknown, such that inference on the individual assortativity coefficients is infeasible, unless standard errors are computed, which is a challenging task in network analysis, as there is usually just one realization of a real network and no sample of realizations available. Therefore, resampling methods such as the jackknife or bootstrap method are employed, which generate artificial samples of networks based on which an estimate of the standard error can be derived, cf. Quenouille (1956), Tukey (1958) and Efron (1979). This allows to conduct significance tests for the respective assortativity coefficient.

When assessing a specific network characteristic, it is often times of interest whether the observed characteristic is due to some underlying social or organizational process or due to structural constraints (e.g., finite size), see Maslov and Sneppen (2004), Serrano, Boguñá, and Pastor-Satorras (2006) and Yang, Pan, and Zhou (2017). In this thesis, we will therefore compare the observed assortativity coefficients to the values one would have obtained if edges had formed randomly, i.e., the assortativity of a null model, which we obtain based on a link rewiring technique.

In the following, we present the resampling methods as well as the link rewiring technique adopted in this thesis. Thereafter, we summarize our procedure for the statistical assessment of the assortativity coefficients.

3.2.4.1 Resampling Methods for Networks

In order to resample the networks in our empirical analysis, we follow Newman (2003) in order to obtain jackknife estimates of the standard error of the generalized assortativity coefficient, which we denote by $\hat{\sigma}_{r^{\omega}_{(\alpha,\beta)},J}$. The idea behind the jackknife method is as follows: For a dataset that consists of n sample variables, n artificial subsamples are created by successively removing the i-th sample variable, $i = 1, \ldots, n$. For networks, there are different approaches of adopting the jackknife method. One can either consider the n vertices of a network as sample variables and create subsamples by removing the vertices in turn, thus, a single subsample is the induced subgraph of the $(n-1)$ remaining vertices, cf. Snijders and Borgatti (1999), or one considers the jackknife with respect to the m edges, i.e., by removing the edges in turn as suggested by Newman (2003).

We use the latter for our analysis, as it already has been suggested for the original assortativity coefficient, and since then, has also been used for other network quantities such as *reciprocity*, see e.g., Garlaschelli and Loffredo (2004) and Squartini, Picciolo, Ruzzenenti, and Garlaschelli (2013). The jackknife estimate of standard error of the generalized assortativity coefficient, $\hat{\sigma}_{r^{\omega}_{(\alpha,\beta)},J}$, is defined as

$$\hat{\sigma}_{r^{\omega}_{(\alpha,\beta)},J} = \sqrt{\sum_{i=1}^{m} \left(r^{\omega}_{(\alpha,\beta),(-i)} - r^{\omega}_{(\alpha,\beta)}\right)^2}, \tag{3.6}$$

where $r^{\omega}_{(\alpha,\beta),(-i)}$ is the value of coefficient for the network where the i-th edge is removed. Note that in large networks with many edges this approach can be computationally intensive. In such cases, where computation times are prohibitively long, it might be sensible to consider the jackknife with respect to the vertices instead, since the count of vertices is usually much lower than the count of edges.

Alternatively, we also consider the bootstrap method by following the non-parametric approach of Snijders and Borgatti (1999), which is referred to as the *vertex bootstrap*.[7,8] The idea of the bootstrap is, again for a dataset that consists of n sample variables, to consider the data as a population itself. A subsample is then generated by sampling n variables with replacement from the observed data. Thus, a subsample might contain multiple copies of some variables, and at the same time, no copies of some other variables. For the vertex bootstrap, we sample with replacement from the vertices of

[7] In a later publication this procedure is more formally defined as the *empirical graphon bootstrap*, see Green and Shalizi (2022).

[8] An alternative parametric bootstrapping approach with respect to the edges of a network has been suggested by Rosvall and Bergstrom (2010). Given the observed weighted edges $\omega_1, \ldots, \omega_m$, a sample of size m is drawn by resampling every edge weight from a Poisson distribution with mean equal to the observed edge weights, i.e., $\omega_i^* \sim \text{Pois}(\omega_i), \quad i = 1, \ldots, m$, for a single bootstrap replicate. However, according to the authors, this approach is not suitable in the case of an unweighted network or when the assumption of a Poisson distribution is not appropriate. We therefore do not consider it further in this thesis.

an observed network.[9] More precisely, consider the weighted $n \times n$ adjacency matrix $\boldsymbol{W} = [w_{ij}]$ of the observed network, where n is the number of vertices and the elements w_{ij} represent the weights of the edges connecting some vertices i and j. If, however, i and j are not connected then $w_{ij} = 0$.[10] A sample with replacement is drawn from the sequence of vertices $i = 1, \ldots, n$, and denoted by $i(1), \ldots, i(n)$. A single bootstrap network is created by letting $\boldsymbol{W}^* = [w^*_{hk}]$, where its elements are obtained from the observed weighted adjacency matrix

$$w^*_{hk} = w_{i(h)i(k)}, \quad i(h) \neq i(k). \tag{3.7}$$

In the case of $i(h) = i(k)$, i.e., $i(h)$ and $i(k)$ correspond to the same vertex in the observed network, the weight w^*_{hk} is sampled randomly from the set of all observed edges, since self-edges or loops are usually not considered in real networks. After this, the generalized assortativity coefficient of the bootstrapped network $\hat{\theta}^* = r^{\omega}_{(\alpha,\beta)}(\boldsymbol{W}^*)$ is computed. Repeating the above procedure B independent times yields an ensemble of B bootstrap replications of the estimate of assortativity, $\hat{\theta}^*_1, \ldots, \hat{\theta}^*_B$. The bootstrap estimate of standard error of the generalized assortativity coefficient, denoted by $\hat{\sigma}_{r^{\omega}_{(\alpha,\beta)},B}$, can be obtained according to:

$$\hat{\sigma}_{r^{\omega}_{(\alpha,\beta)},B} = \hat{\sigma}_{\hat{\theta},B} = \sqrt{\frac{1}{B-1}\sum_{b=1}^{B}\left(\hat{\theta}^*_b - \bar{\hat{\theta}}^*\right)^2}, \tag{3.8}$$

where $\bar{\hat{\theta}}^*$ is the mean of the B bootstrap replications. The computational cost of bootstrapping depends on the number of generated subsamples B. Indeed, the number of bootstrap samples B has to be large enough to adequately approximate the distribution of the generalized assortativity coefficient. However, if B is less than the number of vertices n as well as the number of edges m in a network, then the bootstrap requires less computation than both the jackknife with respect to vertices and the jackknife with respect to edges, cf. Cameron and Trivedi (2012).

For the sake of completeness, we report in our empirical analysis both, jackknife and bootstrap standard error estimates for the generalized assortativity coefficient, together

[9] Since the assortativity coefficient is basically a correlation coefficient, an obvious thought that comes into one's mind is to use the standard non-parametric bootstrapping approach for the correlation coefficient, cf. Efron (1979). That corresponds to drawing a sample with replacement from the pairs $(x_i, y_i), i = 1, \ldots, n$. In the context of networks this corresponds to drawing a sample with replacement from the edges of the network. Thus, multiple edges between vertices may emerge. Such edges can be merged into a single edge with a combined edge weight, in weighted networks. However, it is not clear how to proceed with multiple edges in case of an unweighted network. We therefore do not consider it further in this thesis.

[10] We focus on directed weighted networks. Nevertheless, the approach is capable of handling any kind of (un)directed and (un)weighted network.

with 95 percent *normal approximation* confidence intervals, cf. Davison and Hinkley (2013); Efron (1987), which are defined as:[11]

$$CI_{r^{\omega}_{(\alpha,\beta)},0.95,*} = [r^{\omega}_{(\alpha,\beta)} - d, r^{\omega}_{(\alpha,\beta)} + d], \quad d = z_{0.975} \cdot \hat{\sigma}_{r^{\omega}_{(\alpha,\beta)},*}, \tag{3.9}$$

where $\hat{\sigma}_{r^{\omega}_{(\alpha,\beta)},*}$ are either jackknife or bootstrap estimates of the standard error, as defined in Equations (3.6) and (3.8), respectively, and $z_{0.975}$ is the 97.5 percent quantile of the standard normal distribution.

We find that in almost all considered cases the results based on the bootstrap are in line with those based on the jackknife. In rare cases, where the results are ambiguous, we rely on the method that produced its results based on the larger set of subsamples. Thus, we prefer the bootstrap over the jackknife in small networks ($B > m$) and vice versa in large networks ($B < m$).

3.2.4.2 Generation of a Null Model by Link Rewiring

Newman (2003) gives an attempt at an explanation for the phenomenon of assortative mixing (by degree). A distinction is made between the degree correlations that originate from social or organizational processes (e.g., attraction or affiliation) and others that are artefacts resulting from structural constraints that are imposed on the type of network (e.g., structural disassortativity as discussed by Maslov & Sneppen, 2004).

To assess whether a network's assortativity is due to some underlying social or organizational process or due to structural constraints, we adopt the general approach of Maslov and Sneppen (2004) to detect and analyse topological patterns in networks, to the context of assortativity. Maslov and Sneppen (2004) suggest that a statistically significant deviation of a topological property of a network from the one of an appropriate null model presumably reflects that the property has real social or organizational origins.

Consequently, if there is no significant deviation, the pattern appears to be random with respect to the type of network. This means one will commit a mistake by attaching too much importance to it as it appears to be a result from structural constraints, such as finite size. In this context, Yang et al. (2017) show that for (undirected) finite-size unweighted scale-free networks the lower bound of the assortativity coefficient does not approach -1 in the limit of large network sizes, but instead, depends on the power law exponent γ of the degree distribution $p(k) \sim k^{-\gamma}$ of the network. Furthermore, Ser-

[11] For our purpose, we verify its validity by analysing the histogram and Q-Q plots of the distribution of the bootstrap replications, see Figures A.1 to A.6 in the appendix. Alternatively, statistical tests, such as the *Jarque-Bera* or *Anderson-Darling* test, can be employed to check the normality assumption, though, in our case the bootstrap diagnostic plots were conclusive. If the normal distribution assumption is not appropriate, more advanced bootstrap confidence intervals can be used, cf. Efron (1981, 1982, 1987), DiCiccio and Efron (1996), and the excellent overview given in Davison and Hinkley (2013).

rano et al. (2006) show that due to structural constraints purely uncorrelated weighted networks cannot exist. Hence, an absolute consideration of observed assortativity coefficients as well as their comparison across networks, which are heterogeneous with respect to basic features, will yield misleading results. The coefficients would either have to be interpreted within their respective bounds or —as we do— compared to the values of a null model.

A null model is a random network that is matched for basic properties other than the one of interest, such as order, size and degree distribution, see Fornito, Zalesky, and Bullmore (2016). As our focus is on weighted networks we expand these basic properties by the network's strength distribution and weight distribution. The null distribution is sampled by employing a switching based graph generating approach where Markov chains are used to generate an ensemble of randomized networks, see Milo, Kashtan, Itzkovitz, Newman, and Alon (2003); Ying and Wu (2009).

In order to create a single random network we apply the two-step algorithm suggested by Rubinov and Sporns (2011).[12] Initially, the binary edges of the observed network are rewired such that the degree distribution is preserved. To this end we use the well-known algorithm by Maslov and Sneppen (2002), which carries out a series of k Monte Carlo switching steps, where a single step consists of sampling two edges and rewiring them, such that the origin of the first edge is connected to the target of the second edge, and the origin of the second edge is connected to the target of the first edge, provided that by the rewiring no multiple edges or loops are created, i.e., rewiring edges $(a,b),(c,d) \in E$ and $(a,d),(c,b) \notin E$, where $a \neq d \wedge c \neq b$, such that $(a,d),(c,b) \in E$ and $(a,b),(c,d) \notin E$.

Afterwards, the edge weights of the original network are assigned to the edges of the randomized network in such a way that the observed strengths are closely approximated. This is done by randomly selecting an element a_{uv} from the randomized network, observing its expected weight rank i and assigning it to the i-th highest previously unassigned observed edge weight w_{uv}. The weight of an edge connecting vertices u and v, with strengths s_u and s_v, respectively, which we would expect if edges formed randomly is defined as $e_{uv} = \frac{s_u s_v}{\nu}$, where $\nu = \sum_{uv} w_{uv}$ is the sum of all edge weights. The expected (unassigned) weight magnitude of an element a_{uv} is $\tilde{e}_{uv} \propto \left(s_u - \sum_h \tilde{w}_{uh}\right)\left(s_v - \sum_h \tilde{w}_{hv}\right)$, where $\tilde{w}_{uv}$ are the already assigned weights of the randomized network. Clearly, $\tilde{e}_{uv}$ is a version of e_{uv} that corrects for weights that were already assigned, hence, if no weights have been previously assigned, i.e., if all assigned weights equal zero, i.e., $\tilde{w}_{uv} = 0$, then $\tilde{e}_{uv} = e_{uv}$. Arranging a_{uv} by $\tilde{e}_{uv}$ yields the expected weight rank i. After assigning the weight w_{uv} to the edge a_{uv} the pair is removed from further consideration. The remaining elements are then re-arranged by $\tilde{e}_{uv}$ and the procedure repeats by randomly selecting another element a_{uv} until all elements have been assigned an observed edge

[12] Alternatively, the algorithm proposed by Serrano et al. (2006) can be used in order to generate a suitable null model.

weight. According to Rubinov and Sporns (2011) re-arranging the elements in every step is necessary in order to allow for convergence to the original strengths. This might be computationally expensive in large networks with many edges. For those networks however, according to the authors, a less frequent re-arranging will not impair the accuracy.

A random network generated by the algorithm outlined above preserves the degree sequence of the original network and, thus, the (in- and out-) degree distribution, exactly. It also preserves the weight distribution but not the weight sequence. Therefore, the observed strengths of the original network will only be closely approximated. However, a review of the relevant literature shows that, so far, there is no null model of weighted networks that preserves observed strengths exactly. We therefore follow Rubinov and Sporns (2011) and check whether the correlation between the pre- and post-randomization strength sequences is high. Moreover, the *Kolmogorov-Smirnov* two-sample test indicates that the pre- and post-randomization strength sequences follow the same distribution.[13] We therefore conclude that the considered null model is appropriate for our purpose.

3.2.4.3 Statistical Assessment of Assortativity

In the following we make use of the standard errors obtained from the jackknife and bootstrap method, in order to test for the significance of the generalized assortativity coefficient. Moreover, we construct confidence intervals implied by the null model, in order to determine, whether the observed assortativity is due to organizational or social effects, or due to structural constraints.

In particular, to test, whether the assortativity coefficient is significantly different from zero, we check whether the 95 percent jackknife or bootstrap confidence interval of the generalized assortativity coefficient, covers the value zero. If zero is not included, we conclude that the generalized assortativity coefficient is significantly different from zero at the 5 percent significance level. Furthermore, a comparison of the mean of the assortativity of the null model with the observed value of assortativity allows to assess the origins of the assortativity. More precisely, if the 95 percent confidence interval of the mean assortativity of the null model does not encompass the observed assortativity coefficient, we conclude that the assortativity is due to some social or organizational processes. Vice versa, if the computed interval covers the observed assortativity coefficient, this indicates that the assortativity structure of the observed network is due to structural constraints, and thus random with respect to basic features of the network. The procedure is summarized in summary box 3.2.2.

[13] Results are available from the authors upon request.

Summary 3.2.2 Procedure for assessing significance of assortativity.

(a) Estimate $\hat{\sigma}_{r^{\omega}_{(\alpha,\beta)},*}$ for all four parameter combinations (α, β) using a suitable method (e.g., jackknife or bootstrap method, as defined in Equations (3.6) and (3.8), respectively)

(b) Compute confidence intervals, $\mathrm{CI}_{r^{\omega}_{(\alpha,\beta)},S,*}$, for a predefined confidence level S, e.g., $S = 95\%$ (e.g., jackknife or bootstrap normal approximation confidence intervals as in Equation (3.9)), and interpret according to:

- if $0 \notin \mathrm{CI}_{r^{\omega}_{(\alpha,\beta)},S,*} \Rightarrow$ statistically *significant* assortative mixing
- if $0 \in \mathrm{CI}_{r^{\omega}_{(\alpha,\beta)},S,*} \Rightarrow$ assortative mixing statistically *insignificant*

(c) Determine the distribution of the assortativity of a respective null model by a suitable method (e.g., link rewiring as described) and estimate its mean, $r^{\omega}_{(\alpha,\beta),\mathrm{rnd}}$

(d) Compute confidence intervals, $\mathrm{CI}_{r^{\omega}_{(\alpha,\beta),\mathrm{rnd}},S}$, of the mean assortativity of the null model, for a predefined confidence level S, e.g., $S = 95\%$, and interpret according to:

- if $r^{\omega}_{(\alpha,\beta)} \notin \mathrm{CI}_{r^{\omega}_{(\alpha,\beta),\mathrm{rnd}},S} \Rightarrow$ network's assortativity structure appears to have social or organizational origins
- if $r^{\omega}_{(\alpha,\beta)} \in \mathrm{CI}_{r^{\omega}_{(\alpha,\beta),\mathrm{rnd}},S} \Rightarrow$ network's assortativity structure appears to be random with respect to basic features of the network (e.g., size, order)

3.3 Application: Assortativity of Real-World Weighted Directed Networks

In the following we apply our generalized assortativity coefficient to several (un)directed weighted real-world networks and illustrate its usefulness in assessing and interpreting the assortativity structure of these networks by incorporating weighted edges. To this end, we follow the procedures outlined in summary boxes 3.2.1 and 3.2.2. For our analysis, we focus on real-world networks, for which both a content-related interpretation is easily accessible, and the data sets are generally available, such that our results can be easily reproduced.[14] The analysed networks are taken from the website of the *Koblenz Network Collection* project (KONECT), cf. Kunegis (2013), and have also

[14] Of course, our procedure is also applicable to synthetically generated networks, e.g., ones with scale-free degree (or strength) distributions, generated by one of the various network models. However, we do not consider synthetic networks in this chapter, as in such networks edge weights typically do not have a substantial interpretation.

already been considered in previous literature. Table 3.2 presents for each network the assortativity coefficients $r^{\omega}_{(\alpha,\beta)}$ for the different parameter combinations (α, β) along with the corresponding jackknife and bootstrap estimates of the standard error, $\hat{\sigma}_{r^{\omega}_{(\alpha,\beta)},J}$ and $\hat{\sigma}_{r^{\omega}_{(\alpha,\beta)},B}$, respectively, as well as the 95 percent confidence intervals, $\mathrm{CI}_{r^{\omega}_{(\alpha,\beta)},0.95,J}$ and $\mathrm{CI}_{r^{\omega}_{(\alpha,\beta)},0.95,B}$. Bootstrap results are based on $B = 1499$ bootstrap replications. [15] We estimate the mean $r^{\omega}_{\mathrm{rnd}}$ and standard deviation $\hat{\sigma}_{r^{\omega}_{\mathrm{rnd}}}$ of the assortativity of the respective null models based on an ensemble of 1000 randomizations of the observed network, where the number of switching steps per randomization is set to $k = 20m$, as recommended by Fornito et al. (2016); Ying and Wu (2009).[16] The lower and upper bounds of the 95 percent confidence intervals $\mathrm{CI}_{r^{\omega}_{\mathrm{rnd}},0.95}$ are obtained by computing the respective quantiles of the distribution of the randomized assortativity. Subsequently, a detailed analysis of the assortativity structure of each of the networks is given.

3.3.1 NetScience Scientific Collaboration Network

The NetScience network is an undirected collaboration network of scientists working on network theory which has been constructed by Newman (2001). A node in the network represents a scientist and an edge between two scientists indicates that both co-authored one or more publications. In total 2742 co-authorships of 1589 scientists have been included. The intensity of the relation between two scientists is incorporated by positive edge weights, which are defined as $w_{ij} = (n_k - 1)^{-1} \sum_k \delta^k_i \delta^k_j$, where $\delta^k_i = 1$ if scientist i was co-author of paper k, and n_k is the total number of co-authors of a paper k. As such, edge weights take into account that co-authors of large collaborations might know each other less than co-authors of smaller collaborations. Consequently, the interpretations of both vertex degree and vertex strength have to be considered carefully. In particular, vertex degree corresponds to the number of different co-authors scientist i has collaborated with, whereas vertex strength corresponds to the number of papers scientist i has co-authored with others, cf. Newman (2001).

According to our empirical results, the NetScience network is an overall assortative network indicating that scientists have a tendency to collaborate with others that are similar based on the number of co-authors (degree) or based on the number of papers they have been co-authors of (strength), since both the benchmark assortativity coefficient, $r^{\omega}_{(0,0)} = 0.4616$, and the generalized assortativity coefficient, $r^{\omega}_{(1,1)} = 0.1928$, have positive values.

However, since $r^{\omega}_{(0,0)} > r^{\omega}_{(1,1)}$, the network is less assortative if edge weights are considered. On the one hand, this is partly due to a consistently disassortative connection

[15] Based on Davidson and MacKinnon (2000) where a minimum of $B = 399$ bootstrap replications for tests at the 0.05 level and a minimum of $B = 1499$ bootstrap replications for tests at the 0.01 level is suggested, we choose $B = 1499$, although we test at the 0.05 level.

[16] Alternatively, $k = 100m$ can be chosen, cf. Milo et al. (2003), but this is computationally more demanding.

Measure	$\alpha = 0$		$\alpha = 1$	
	$\beta = 0$	$\beta = 1$	$\beta = 0$	$\beta = 1$
		NetScience		
r^{ω}	0.4616	0.3405	0.1016	0.1928
r^{ω}_{rnd}	-0.0436	-0.0051	-0.0691	-0.0988
$\hat{\sigma}_{r^{\omega},J}$	0.0715	0.0618	0.0282	0.0527
$\hat{\sigma}_{r^{\omega},B}$	0.0944	0.1054	0.0978	0.1223
$\hat{\sigma}_{r^{\omega}_{\text{rnd}}}$	0.0173	0.0339	0.0138	0.0305
$\text{CI}_{r^{\omega},0.95,J}$	$[0.3215, 0.6017]$	$[0.2194, 0.4616]$	$[0.0463, 0.1569]$	$[0.0895, 0.2961]$
$\text{CI}_{r^{\omega},0.95,B}$	$[0.2766, 0.6466]$	$[0.1339, 0.5471]$	$[-0.0901, 0.2933]$	$[-0.0469, 0.4325]$
$\text{CI}_{r^{\omega}_{\text{rnd}},0.95}$	$[-0.0709, -0.0143]$	$[-0.0586, 0.0498]$	$[-0.0910, -0.0462]$	$[-0.1452, -0.0459]$
		Windsurfers		
r^{ω}	-0.1470	-0.0170	-0.1710	-0.0769
r^{ω}_{rnd}	-0.2182	-0.1187	-0.1880	-0.2266
$\hat{\sigma}_{r^{\omega},J}$	0.0654	0.1285	0.0481	0.1077
$\hat{\sigma}_{r^{\omega},B}$	0.0465	0.0833	0.0343	0.0901
$\hat{\sigma}_{r^{\omega}_{\text{rnd}}}$	0.0324	0.0740	0.0251	0.0760
$\text{CI}_{r^{\omega},0.95,J}$	$[-0.2752, -0.0188]$	$[-0.2689, 0.2349]$	$[-0.2653, -0.0767]$	$[-0.2880, 0.1342]$
$\text{CI}_{r^{\omega},0.95,B}$	$[-0.2381, -0.0559]$	$[-0.1803, 0.1463]$	$[-0.2382, -0.1038]$	$[-0.2535, 0.0997]$
$\text{CI}_{r^{\omega}_{\text{rnd}},0.95}$	$[-0.2711, -0.1654]$	$[-0.2434, -0.0016]$	$[-0.2299, -0.1492]$	$[-0.3530, -0.0965]$
		Macaques		
out-in				
r^{ω}	-0.3709	-0.3801	-0.2479	-0.2578
r^{ω}_{rnd}	-0.1475	-0.0394	-0.1525	-0.0526
$\hat{\sigma}_{r^{\omega},J}$	0.0377	0.0483	0.0381	0.0476
$\hat{\sigma}_{r^{\omega},B}$	0.0555	0.0638	0.0533	0.0668
$\hat{\sigma}_{r^{\omega}_{\text{rnd}}}$	0.0174	0.0240	0.0173	0.0242
$\text{CI}_{r^{\omega},0.95,J}$	$[-0.4448, -0.2970]$	$[-0.4748, -0.2854]$	$[-0.3226, -0.1732]$	$[-0.3511, -0.1645]$
$\text{CI}_{r^{\omega},0.95,B}$	$[-0.4797, -0.2621]$	$[-0.5051, -0.2551]$	$[-0.3524, -0.1434]$	$[-0.3887, -0.1269]$
$\text{CI}_{r^{\omega}_{\text{rnd}},0.95}$	$[-0.1765, -0.1201]$	$[-0.0790, -0.0010]$	$[-0.1809, -0.1238]$	$[-0.0922, -0.0128]$
out-out				
r^{ω}	0.4162	0.4294	0.3145	0.3251
r^{ω}_{rnd}	0.1022	0.0375	0.0877	0.0269
$\hat{\sigma}_{r^{\omega},J}$	0.0400	0.0491	0.0424	0.0513
$\hat{\sigma}_{r^{\omega},B}$	0.0551	0.0641	0.0507	0.0559
$\hat{\sigma}_{r^{\omega}_{\text{rnd}}}$	0.0200	0.0259	0.0195	0.0246
$\text{CI}_{r^{\omega},0.95,J}$	$[0.3378, 0.4946]$	$[0.3332, 0.5256]$	$[0.2314, 0.3976]$	$[0.2246, 0.4256]$
$\text{CI}_{r^{\omega},0.95,B}$	$[0.3082, 0.5242]$	$[0.3038, 0.5550]$	$[0.2151, 0.4139]$	$[0.2155, 0.4347]$
$\text{CI}_{r^{\omega}_{\text{rnd}},0.95}$	$[0.0698, 0.1354]$	$[-0.0055, 0.0810]$	$[0.0564, 0.1197]$	$[-0.0127, 0.0678]$
in-in				
r^{ω}	0.4030	0.4586	0.2277	0.2828
r^{ω}_{rnd}	0.1032	0.0260	0.0771	0.0132
$\hat{\sigma}_{r^{\omega},J}$	0.0386	0.0440	0.0468	0.0520
$\hat{\sigma}_{r^{\omega},B}$	0.0566	0.0677	0.0471	0.0570
$\hat{\sigma}_{r^{\omega}_{\text{rnd}}}$	0.0194	0.0246	0.0198	0.0263
$\text{CI}_{r^{\omega},0.95,J}$	$[0.3273, 0.4787]$	$[0.3724, 0.5448]$	$[0.1360, 0.3194]$	$[0.1809, 0.3847]$
$\text{CI}_{r^{\omega},0.95,B}$	$[0.2921, 0.5139]$	$[0.3259, 0.5913]$	$[0.1354, 0.3200]$	$[0.1711, 0.3945]$
$\text{CI}_{r^{\omega}_{\text{rnd}},0.95}$	$[0.0723, 0.1360]$	$[-0.0144, 0.0679]$	$[0.0445, 0.1100]$	$[-0.0301, 0.0559]$
in-out				
r^{ω}	-0.4884	-0.5214	-0.3933	-0.4195
r^{ω}_{rnd}	-0.0745	-0.0320	-0.0586	-0.0287
$\hat{\sigma}_{r^{\omega},J}$	0.0234	0.0300	0.0283	0.0391
$\hat{\sigma}_{r^{\omega},B}$	0.0505	0.0586	0.0440	0.0545
$\hat{\sigma}_{r^{\omega}_{\text{rnd}}}$	0.0211	0.0281	0.0214	0.0283
$\text{CI}_{r^{\omega},0.95,J}$	$[-0.5343, -0.4425]$	$[-0.5802, -0.4626]$	$[-0.4488, -0.3378]$	$[-0.4961, -0.3429]$
$\text{CI}_{r^{\omega},0.95,B}$	$[-0.5874, -0.3894]$	$[-0.6363, -0.4065]$	$[-0.4795, -0.3071]$	$[-0.5263, -0.3127]$
$\text{CI}_{r^{\omega}_{\text{rnd}},0.95}$	$[-0.1084, -0.0405]$	$[-0.0793, 0.0145]$	$[-0.0919, -0.0243]$	$[-0.0748, 0.0179]$

Table 3.2. Generalized assortativity analysis. Reported are: Generalized assortativity coefficient r^{ω}, randomized assortativity, r^{ω}_{rnd}, jackknife, bootstrap and randomized assortativity standard errors, $\hat{\sigma}_{r^{\omega},J}$, $\hat{\sigma}_{r^{\omega},B}$ and $\hat{\sigma}_{r^{\omega}_{\text{rnd}}}$ as well as 95 percent jackknife, bootstrap and randomized assortativity confidence intervals, $\text{CI}_{r^{\omega},0.95,J}$, $\text{CI}_{r^{\omega},0.95,B}$ and $\text{CI}_{r^{\omega}_{\text{rnd}},0.95}$, respectively, for all four parameter combinations (α, β). A description of the networks is given in the text.

effect, as $r^{\omega}_{(0,0)} = 0.4616 > r^{\omega}_{(1,0)} = 0.1015$ as well as $r^{\omega}_{(0,1)} = 0.3407 > r^{\omega}_{(1,1)} = 0.1928$, which indicates that most interconnected scientists tend to be more similar based on the number of co-authors they have collaborated with and less similar regarding the number of co-authored papers.

On the other hand, there is a disassortative amplification effect when degrees are used as vertex values, since $r^{\omega}_{(0,0)} = 0.4616 > r^{\omega}_{(0,1)} = 0.3407$, suggesting that the stronger co-author relationships persist between scientists that are less similar based on the number of co-authors they have collaborated with. However, since $r^{\omega}_{(1,0)} = 0.1015 < r^{\omega}_{(1,1)} = 0.1928$, the amplification effect is inconsistent and, thus, there is an assortative amplification effect when strengths are used as vertex values, which means that the stronger co-author relationships tend to persist between scientists that are more similar based on the number of papers they have published with others.

Apparently, both effects are opposing as $r^{\omega}_{(1,1)} = 0.1928 \in [\min(r^{\omega}_{(1,0)}, r^{\omega}_{(0,1)}) = 0.1015, \max(r^{\omega}_{(1,0)}, r^{\omega}_{(0,1)}) = 0.3405]$. Consequently, scientists tend to collaborate with others that are either different based on the number of co-authors they have collaborated with or that are similar based on the number of papers they have published.

In order to assess the significance of the above results, we compute 95 percent jackknife and bootstrap confidence intervals for the coefficients and find that the NetScience network is significantly assortative. Moreover, as the 95 percent confidence intervals of the randomized assortativity do not cover the respective observed assortativity, i.e., $r^{\omega}_{(0,0)} = 0.4616 \notin \mathrm{CI}_{r^{\omega}_{(0,0),\mathrm{rnd}},0.95} = [-0.0709, -0.0143]$ and $r^{\omega}_{(1,1)} = 0.1928 \notin \mathrm{CI}_{r^{\omega}_{(1,1),\mathrm{rnd}},0.95} = [-0.1452, -0.0459]$, we can conclude at the 5 percent significance level, that the observed strong assortative structure is due to some social or sociological process. The network would have been disassortative if edges had formed randomly.[17]

3.3.2 Windsurfers Social Network

The Windsurfers network is an undirected network which is formed by data that was collected while studying the social behaviour of 43 windsurfers on a beach in southern California during the fall of 1986, see Freeman, Freeman, and Michaelson (1988). A node in the network represents a windsurfer and an edge between two windsurfers indicates interpersonal contact. Information on the frequency of this interpersonal contact is incorporated by positive edge weights where a high edge weight indicates a more frequent contact and vice versa. An edge weight of 1 indicates a one-time contact. Thus, the degree of a vertex corresponds to the number of acquaintanceships, whereas

[17] For the measures $r^{\omega}_{(1,0)}$ and $r^{\omega}_{(1,1)}$ the jackknife and the bootstrap intervals seem inconclusive. The respective coefficients differ indeed significantly from the null assortativity, though the bootstrap intervals of the observed assortativity encompass zero. However, in these cases we rely on the jackknife intervals as, for the NetScience network, they are based on the larger set of subsamples, as $B = 1499 < m = 2742$.

vertex strength corresponds to the frequency of encounters. The network consists of 336 weighted edges.

The Windsurfers network is overall disassortative, suggesting that there is a tendency that windsurfers connect to other windsurfers that are more interconnected than themselves. However, the weighted network is less disassortative, as can be seen by comparing the benchmark assortativity coefficient with the generalized assortativity coefficient, $r^{\omega}_{(0,0)} = -0.1470 < r^{\omega}_{(1,1)} = -0.0769$. Analysing both effects, the network indeed shows a consistently disassortative connection effect, which indicates that most interconnected windsurfers differ by the number of acquaintanceships, but differ even more by the frequency of encounters, since $r^{\omega}_{(0,0)} = -0.1470 > r^{\omega}_{(1,0)} = -0.1710$ and $r^{\omega}_{(0,1)} = -0.0170 > r^{\omega}_{(1,1)} = -0.0769$ and, thus, most connections persist between two windsurfers where one is more interconnected than the other. However, there is a consistently assortative edge amplification effect, since $r^{\omega}_{(0,0)} = -0.1470 < r^{\omega}_{(0,1)} = -0.0170$ and $r^{\omega}_{(1,0)} = -0.1710 < r^{\omega}_{(1,1)} = -0.0769$, indicating that, although the network is overall disassortative, the high weighted connections tend to be rather assortative, i.e., windsurfers tend to stay in touch with others more frequently, mostly, if they are as interconnected as themselves, for example, with other windsurfers that either have an equal number of acquaintances or have equally frequent encounters. Since $r^{\omega}_{(1,1)} = -0.0769 \in [\min(r^{\omega}_{(1,0)}, r^{\omega}_{(0,1)}) = -0.1710, \max(r^{\omega}_{(1,0)}, r^{\omega}_{(0,1)}) = -0.0170]$, we have opposing effects for the Windsurfers network. Additionally, because both effects are consistent and because the magnitude of disassortativity is reduced by incorporating both effects, we can reason that the edge amplification effect might be the stronger one.

Considering the significance of the assortativity, the findings are somewhat inconclusive. On the one hand, the respective 95 percent confidence intervals of the randomized assortativity, $\mathrm{CI}_{r^{\omega}_{(\alpha,\beta),\mathrm{rnd}},0.95}$, do not cover the values of $r^{\omega}_{(0,0)}$ and $r^{\omega}_{(1,1)}$, on the other hand, they cover the values of $r^{\omega}_{(0,1)}$ and $r^{\omega}_{(1,0)}$ indicating that the windsurfers network is indeed significantly more disassortative than we would expect if edges had formed randomly, but our previous conclusions regarding the connection effect as well as the amplification effect have to be questioned, as the auxiliary measures $r^{\omega}_{(0,1)}$ and $r^{\omega}_{(1,0)}$ appear to be insignificant with respect to the null model. Additionally, both the jackknife and the bootstrap 95 percent confidence intervals of the observed assortativity r^{ω} overlap the respective null assortativity coefficient $r^{\omega}_{\mathrm{rnd}}$, for all parameter combinations (α, β) indicating that the disassortative structure of the Windsurfers network might also be, at least partially, structural and dependent on the type of the network.

3.3.3 Macaques Dominance Relationship Network

The Macaques network is a directed network which is formed by data that was collected while studying the dominance relationships of 62 female Japanese monkeys (Macaca

fuscata) during the nonmating season from April to early October 1976, see Takahata (1991).

A node in the network represents a specific monkey and directed edges between the nodes represent dominance relationships. Thus, an edge connecting two monkeys points from the dominating monkey to the one which has been dominated during an encounter where food was involved, and edge weights indicate how often such encounters happened. Since the network is directed we can differentiate between in- and out-degrees as well as in- and out-strengths. Thus, four different modes of assortativity are possible, which are denoted by *out-in, out-out, in-in* and *in-out*, where *out-in*, for example, corresponds to the correlation between the excess out- and in-degrees (or strengths) of two interconnected monkeys. The out-degree of a monkey corresponds to the number of different other monkeys it has dominated during an encounter, whereas its in-degree corresponds to the number of different other monkeys it has been dominated by. The out-strength, on the other hand, corresponds to the number of times when a monkey has dominated others, and the in-strength corresponds to the number of times it has been dominated by others. In total, the network consists of 1187 weighted edges. The edge weight sum of 2435 corresponds to the total number of observed encounters.

The network is overall *out-in* as well as *in-out* disassortative, since all the measures $r^{\omega}_{(0,0),\text{out-in}} = -0.3709$, $r^{\omega}_{(1,1),\text{out-in}} = -0.2578$, $r^{\omega}_{(0,0),\text{in-out}} = -0.4884$ as well as $r^{\omega}_{(1,1),\text{in-out}} = -0.4195$ are negative. This implies that monkeys who dominate many others, or dominate others more frequently, preferably dominate other monkeys who are dominated by only a few, or are dominated less frequently. Vice versa, monkeys who dominate few others, or dominate others less frequently, tend to dominate other monkeys who are dominated by many others, or are dominated more frequently. Comparing the respective benchmark with the generalized assortativity coefficient reveals that a full consideration of edge weights reduces the overall disassortativity of the network for both modes of assortativity, although not as much for the *in-out* mode, as the difference between $r^{\omega}_{(0,0),\text{in-out}}$ and $r^{\omega}_{(1,1),\text{in-out}}$ compared to the difference between $r^{\omega}_{(0,0),\text{out-in}}$ and $r^{\omega}_{(1,1),\text{out-in}}$ shows.

At the same time, the network exhibits assortative tendencies with respect to the *out-out* and *in-in* modes, since $r^{\omega}_{(0,0),\text{out-out}} = 0.4162$, $r^{\omega}_{(1,1),\text{out-out}} = 0.3251$, $r^{\omega}_{(0,0),\text{in-in}} = 0.4030$ as well as $r^{\omega}_{(1,1),\text{in-in}} = 0.2828$ are all positive. This indicates that dominating monkeys tend to dominate other dominating monkeys. Also, inferior monkeys usually dominate other inferior monkeys. The network is less *out-out* as well as *in-in* assortative if edge weights are considered, since $r^{\omega}_{(0,0),\text{out-out}} > r^{\omega}_{(1,1),\text{out-out}}$ and $r^{\omega}_{(0,0),\text{in-in}} > r^{\omega}_{(1,1),\text{in-in}}$. The decrease in disassortativity for the *out-in* and *in-out* modes as well as the decrease in assortativity for the *out-out* and *in-in* modes can be explained by analysing the respective connection and amplification effects.

There is a consistently assortative connection effect for the *out-in* and *in-out* modes, since $r^{\omega}_{(0,0),\text{out-in}} = -0.3709 < r^{\omega}_{(1,0),\text{out-in}} = -0.2479$ and $r^{\omega}_{(0,1),\text{out-in}} = -0.3801 < r^{\omega}_{(1,1),\text{out-in}} = -0.2578$ as well as $r^{\omega}_{(0,0),\text{in-out}} = -0.4884 < r^{\omega}_{(1,0),\text{in-out}} = -0.3933$ and $r^{\omega}_{(0,1),\text{in-out}} = -0.5214 < r^{\omega}_{(1,1),\text{in-out}} = -0.4195$, but a consistently disassortative connection effect for the *out-out* and *in-in* modes, as $r^{\omega}_{(0,0),\text{out-out}} = 0.4162 > r^{\omega}_{(1,0),\text{out-out}} = 0.3145$ and $r^{\omega}_{(0,1),\text{out-out}} = 0.4294 > r^{\omega}_{(1,1),\text{out-out}} = 0.3251$ as well as $r^{\omega}_{(0,0),\text{in-in}} = 0.4030 > r^{\omega}_{(1,0),\text{in-in}} = 0.2277$ and $r^{\omega}_{(0,1),\text{in-in}} = 0.4586 > r^{\omega}_{(1,1),\text{in-in}} = 0.2828$. This means that, for the *out-in* and *in-out* modes, *most* interconnected monkeys differ less based on the number of times they have dominated or have been dominated by others, and vice versa, respectively, compared to the number of different monkeys they dominated or have been dominated by. On the contrary, for the *out-out* and *in-in* modes, *most* interconnected monkeys differ more based on both the number of times they have dominated others and the number of times they have been dominated by others compared to the number of different monkeys they dominated or have been dominated by, respectively.

Furthermore, there is a consistently disassortative amplification effect for the *out-in* and the *in-out* modes, because $r^{\omega}_{(0,0),\text{out-in}} = -0.3709 > r^{\omega}_{(0,1),\text{out-in}} = -0.3801$ and $r^{\omega}_{(1,0),\text{out-in}} = -0.2479 > r^{\omega}_{(1,1),\text{out-in}} = -0.2578$ as well as $r^{\omega}_{(0,0),\text{in-out}} = -0.4884 > r^{\omega}_{(0,1),\text{in-out}} = -0.5214$ and $r^{\omega}_{(1,0),\text{in-out}} = -0.3933 > r^{\omega}_{(1,1),\text{in-out}} = -0.4195$, but a consistently assortative amplification effect for the *out-out* and *in-in* modes, since $r^{\omega}_{(0,0),\text{out-out}} = 0.4162 < r^{\omega}_{(0,1),\text{out-out}} = 0.4294$ and $r^{\omega}_{(1,0),\text{out-out}} = 0.3145 < r^{\omega}_{(1,1),\text{out-out}} = 0.3251$ as well as $r^{\omega}_{(0,0),\text{in-in}} = 0.4030 < r^{\omega}_{(0,1),\text{in-in}} = 0.4586$ and $r^{\omega}_{(1,0),\text{in-in}} = 0.2277 < r^{\omega}_{(1,1),\text{in-in}} = 0.2828$. Indicating that dominant monkeys *less frequently* dominate inferior monkeys, and vice versa. Also, monkeys dominate others that are similarly dominant or inferior, respectively, *more frequently*.

The connection effect and the amplification effect are opposing for all four modes, as can be seen by the fact that if one is assortative the other is disassortative and vice versa, as well as by the fact that $r^{\omega}_{(1,1)} \in [\min(r^{\omega}_{(1,0)}, r^{\omega}_{(0,1)}), \max(r^{\omega}_{(1,0)}, r^{\omega}_{(0,1)})]$ for all four modes. Additionally, since all effects are consistent, and since the weighted network is less disassortative for the *out-in* and *in-out* modes, but less assortative for the *out-out* and *in-in* modes, the connection effect can be regarded as the stronger effect for all four modes. Finally, since all coefficients are significantly different from zero, and the 95 percent confidence intervals of the randomized assortativity do not cover any observed coefficient, we can conclude that the observed assortativity structure of the Macaques network has real social or sociological or organizational origins rather than being random with respect to basic network characteristics such as order, size, distribution of degrees, strengths, or weights.

3.4 Discussion and Future Work

Based on the preceding analysis of the assortativity of the weighted example real-world networks, precise statements of their network topology are now possible. For example, consider the Macaques network —without having actually plotted the network graphically in advance, but having verified our observations afterwards— we conclude that the network has a multi-tiered, almost tree-like hierarchical structure, that branches out into star-like configurations, where cycles are possible for the lower tiers, and where the higher weighted edges tend to form either between vertices where the out-degree or -strength of the one is different from the in-degree or -strength of the other, and vice versa, or between vertices of similar in-degree or -strength as well as vertices of similar out-degree or -strength.

Based on this reasoning, we chose to visualize the network with the layout algorithm by Reingold and Tilford (1981) in Figure 3.3b. This is quite unusual, since the layout is specially designed for trees, but the network under consideration is not a tree because it contains cycles. However, the tree layout captures the structure of the network quite well. For example, the top tier node represents the alpha-female of the group, and also the dominance relationships between the other low-ranking monkeys are clearly visible. To make a comparison, in Figure 3.3a we also visualize the network with the layout algorithm by Kamada and Kawai (1989), which is one of the most popular graph layout algorithms. Apparently, this visualization gives almost no indication of the topological

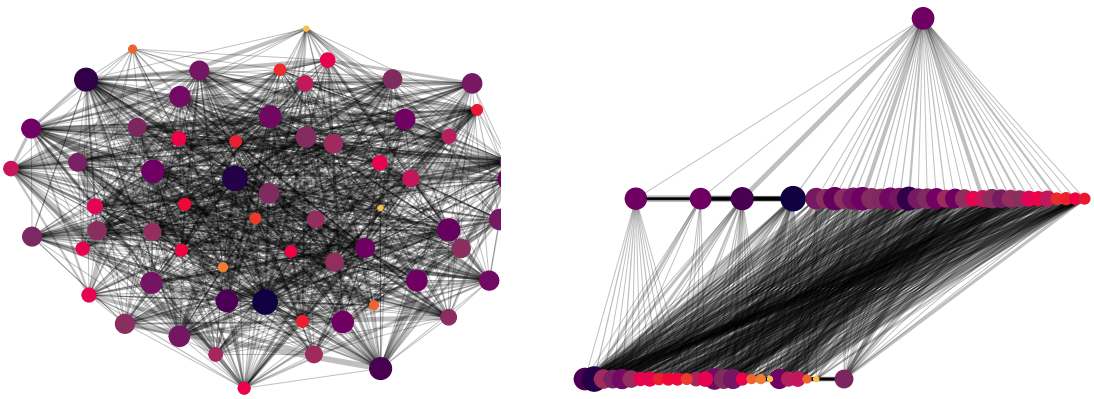

(a) Kamada and Kawai graph layout. **(b)** Reingold and Tilford graph layout.

Figure 3.3. Visualization of the graph structure of the *Macaques* network using different layout algorithms. Both figures show the same network, using (a) the layout algorithm by Kamada and Kawai (1989) and (b) the layout algorithm for trees by Reingold and Tilford (1981). The vertex out-strengths are colour-coded, where darker colours indicate higher strengths, and lighter colours indicate lower strengths. The size of the coloured hull of a vertex is proportional to its out-degree. Moreover, thicker edges indicate higher edge weights.

Admittedly, these observations also could have been obtained by studying the weighted adjacency matrix of the network, moreover, they are quite unsurprising even, given that dominance relationships between animals have been exhaustively studied for several species in the past. However, the fact that our proposed procedure of assessing the assortativity of a weighted network reveals the structural features of each example network precisely is exactly what we aim for.

Moreover, the use of the generalized assortativity coefficient together with the procedure of identifying its significance can help, if the interest is in understanding the mechanics of the underlying network formation process. For example, for the Windsurfers network we find that its assortativity appears to be structure-dependent, such that the corresponding network model can be simplified, as degree (or strength) correlations can be omitted. As opposed to this, for the NetScience network degree (or strength) correlations would have to be explicitly considered when modelling the network.

We think that in the case of networks which are larger by several orders of magnitude than the ones we considered for illustrative purposes in this chapter, and for which the topology or the formation process is not-well known, our generalized assortativity coefficient will provide useful insights.

Moreover, the concept of generalizing assortativity to weighted networks, shown in this work, easily extends to more complex definitions of assortativity, for example, the ones by Meghanathan (2016) or Arcagni, Grassi, Stefani, and Torriero (2017, 2021), as they are, at their core, still based on the Pearson correlation. Meghanathan (2016) considers assortativity based on centrality measures other than degree (or strength), such as *betweenness*, *eigenvector*, and *closeness* centrality. Arcagni et al. (2017, 2021) define *higher order assortativity*, which is the tendency of similar vertices to bond via indirected connections, such as paths, shortest paths or random walks.

In this chapter we have shown that assortativity, the tendency of vertices to bond with others based on similarities (usually excess vertex degree), in weighted networks is more complex than in unweighted networks. Previously published research focuses on seeking a single measure that describes the underlying assortativity structure. We pointed out, however, that focusing on a single measure might lead to information loss, and, therefore, proposed a generalized assortativity coefficient that nests previous measures and that utilizes available information at the best.

To this end, we proposed to use as vertex values excess vertex strength, which has never been considered in the assortativity literature so far and which is the generalization of excess vertex degree in weighted networks. We broke down assortativity in weighted networks into its components and identified two mechanisms that essentially affect the assortativity structure of a network, which we refer to as the connection effect as well as the amplification effect. Furthermore, we provided procedures that allow for a detailed

interpretation and assessment of assortativity in weighted networks as well as for the assessments of its statistical significance. For the latter we introduced appropriate resampling and link rewiring techniques.

We demonstrated the application and usefulness of our generalized assortativity coefficient for assessing and interpreting the assortativity of three commonly used weighted real-world networks, both directed and undirected. Albeit being often times considered in the literature, the analysed networks are admittedly not very complex. However, our procedure can straightforwardly be applied to analyse the assortativity structure of also more realistic networks, as we will detail in Chapter 5 when we analyse the network of cryptocurrencies.

But first, based on our developments in this chapter, we will extend the concept of generalized assortativity to local assortativity in the subsequent Chapter 4. This allows us to identify those vertices and edges that contribute the most to the global assortativity of a network.

4 Local Assortativity in Weighted and Directed Complex Networks

So far we have focused on global assortativity. We proposed a new assortativity coefficient and showed its usefulness. We now turn our focus on local assortativity, which is the contribution of individual vertices or edges to the global assortativity structure. Since assortativity is a measure of the stability of a network, this is particularly important as it can help to understand which vertices or edges are particularly stability-threatening and which are stability-protective. This can help with developing efficient strategies for both breaking up a network (e.g., with vaccination in disease spreading social networks) and protecting particularly vulnerable networks (e.g., financial networks or technological networks, such as the Internet), cf. Newman (2002). As compared with global assortativity, local assortativity can be considered as a *third-order* graph metric as it provides further differentiation in graphs that have the same degree distribution (*first-order* metric) as well as the same assortativity structure (*second-order* metric), cf. Noldus and van Mieghem (2015). For example, both the ER and BA model are known to generate (global) non-assortative networks, see Newman (2002), however, only the ER model generates graphs that also show local non-assortative tendencies, whereas vertices that join the network at an earlier point in time tend to be local disassortative, in the BA model. In this chapter we propose a more general coefficient of local assortativity, which nests previous local assortativity measures as special cases and is flexible in the sense that it can be either vertex based or edge based. Moreover, our local assortativity measure will be applicable to unweighted and undirected as well as weighted and directed networks.

The remainder of the chapter is structured as follows: Section 4.1 provides a review of the related literature on local assortativity in unweighted networks. Moreover, we are able to demonstrate the equivalence of two allegedly different previous definitions of local assortativity, namely the one by Piraveenan et al. (2008) and the one by Zhang et al. (2012). To the best of our knowledge, we are the first to recognize the equivalence of both definitions. The unified approach will then serve as point of reference for our generalized local assortativity coefficient, which we introduce in Section 4.2. In Section 4.3 we illustrate the application and usefulness of our local assortativity measure based on simulated networks, and analyse local assortativity of two real-world networks. Thereby, we also demonstrate how to compute local assortativity profiles, which are very

helpful for characterizing the local assortativity pattern of a network. In Section 4.4 we discuss our empirical results and give suggestions for future research.

4.1 Background and Related Literature

As with global assortativity, there exist multiple definitions of local assortativity in undirected as well as directed yet unweighted networks. In the following, we will briefly review those aspects from the previous literature that are most relevant to our subsequent analysis. The concept of local assortativity has been first introduced by Piraveenan et al. (2008, 2010) for undirected networks, and later extended towards directed networks, cf. Piraveenan et al. (2012). The authors define local assortativity as the *scaled difference between the average excess degree of the neighbours of a vertex and the global average excess degree*. Their local assortativity coefficient is a *vertex based* measure.

An allegedly different approach has been proposed by Zhang et al. (2012), who refer to their measure as the *universal assortativity coefficient* (UAC). The UAC is denoted by ρ^{UAC}, and is defined as the sum of so-called *edge assortativeness values*, ρ_e, of a targeted edge set, E_{target}. Thereby, these assortativeness values, ρ_e, can serve well as an *edge based* local assortativity measure. By consolidating the edge assortativeness values of the set of edges that emanate from a vertex, so-called *vertex assortativeness values* are obtained, which can be considered as a *vertex based* local assortativity measure.

In the following we present a comprehensive description of the derivation of the measure of Zhang et al. (2012). However, we will reconsider the one proposed by Piraveenan et al. (2008, 2010, 2012) by demonstrating the equivalence of the local assortativeness values of Zhang et al. (2012) and the vertex based assortativity measure of Piraveenan et al. (2008), at the end of this section.

To this end, let $p(k') = p_{k'}$ denote the degree distribution, i.e., the probability of a randomly chosen vertex having degree k'; $q(k) = q_k$ denotes the remaining (or excess) degree distribution, i.e., the probability that a vertex reached by following a randomly chosen edge has excess degree k. Since the excess degree k is the total degree k' of a vertex less one, i.e., $k = k' - 1$, it is distributed proportional to $(k+1)p_{k+1}$. Thus, the distribution q_k is given by:

$$q_k = \frac{(k+1)p_{k+1}}{\sum_{k'} k' p_{k'}},$$

where $\sum_{k'} k' p_{k'}$ is the expected degree of a vertex.

Let e_{jk} denote the joint distribution of excess degrees of either end of an edge, i.e., the probability that a randomly chosen edge connects two vertices with excess degrees j and k, see Callaway, Hopcroft, Kleinberg, Newman, and Strogatz (2001) and Newman (2002).

Then, given the above, the edge assortativeness values, ρ_e, are derived from the definition of assortativity, r, of Newman (2002) by rearranging the right-hand side of the equation by applying the *König–Huygens formula*[18] reversely for the covariance in the numerator:

$$r = \frac{1}{\sigma_{q_k}^2} \sum_{jk} jk(e_{jk} - q_j q_k) \tag{4.1}$$

$$= \frac{\sum_{jk} jke_{jk} - \sum_j jq_j \sum_k kq_k}{\sigma_{q_k}^2} \tag{4.2}$$

$$= \frac{E[JK] - U_{q_k}^2}{\sigma_{q_k}^2}$$

$$= \frac{E[JK] - U_{q_k}^2 - U_{q_k}^2 + U_{q_k}^2}{\sigma_{q_k}^2} \tag{4.3}$$

$$= \frac{E[JK] - E[J]U_{q_k} - E[K]U_{q_k} + E[U_{q_k}^2]}{\sigma_{q_k}^2}$$

$$= \frac{E[JK - JU_{q_k} - KU_{q_k} + U_{q_k}^2]}{\sigma_{q_k}^2}$$

$$= \frac{E[(J - U_{q_k})(K - U_{q_k})]}{\sigma_{q_k}^2}, \tag{4.4}$$

where J and K are the excess degrees of the ends of an edge and U_{q_k} denotes the mean of the distribution q_k, which is the mean excess degree of an end of an edge and $\sigma_{q_k}^2$ is the variance of the distribution q_k. For Equation (4.2), since both ends of an edge have the same expected excess degree it holds that $\sum_j jq_j = E[J] = \sum_k kq_k = E[K] = U_{q_k}$, and thus, $\sum_j jq_j \sum_k kq_k = U_{q_k}^2$. For Equation (4.3), a constructive zero is added.

By estimating the theoretical quantities in Equation (4.4) by their sample counterparts (by averaging over the edges of the network), the assortativity coefficient of a real *undirected* network can be obtained by computing[19]:

$$r = \frac{\frac{1}{M}\sum_{e=1}^{M}(j_e - \bar{U}_{q_k})(k_e - \bar{U}_{q_k})}{\hat{\sigma}_{q_k}^2}, \tag{4.5}$$

where j_e and k_e are the excess degrees of the ends of edge e; $\bar{U}_{q_k} = \frac{1}{M}\sum_{e=1}^{M}\frac{1}{2}(j_e + k_e)$ and $\hat{\sigma}_{q_k} = \sqrt{\frac{1}{M}\sum_{e=1}^{M}\frac{1}{2}(j_e^2 + k_e^2) - \bar{U}_{q_k}^2}$ are the sample mean and standard deviation of the excess degree of an end of an edge, and M is the number of edges in the network.[20]

[18] With the König–Huygens formula, the variance of a random variable X can be expressed in terms of its raw moments $E(X)$ and $E(X^2)$, i.e., $\mathrm{Var}(X) = E[(X - E(X))^2] = E(X^2) - E(X)^2$.

[19] Whether to apply *Bessel's correction*, i.e., using $\frac{1}{M-1}$ instead of $\frac{1}{M}$ as a correction factor is just a minor technicality as it cancels out anyway when computing the Pearson correlation coefficient.

[20] In an undirected network, each edge e has two ends j_e and k_e, and thus, there are $2M$ ends in total. Therefore, the mean excess degree of an end of an edge is obtained by averaging the mean of the excess degrees of the ends of an edge over all edges of the network. This extends to computing the standard deviation of the excess degree of an end of an edge.

From this representation it becomes apparent that the (direct) contribution of an individual edge, e, to the assortativity coefficient, r, is determined by ρ_e, which is the scaled product of the differences between the excess degrees of both ends of an edge and the mean excess degree of an end of an edge:

$$\rho_e = \frac{(j_e - \bar{U}_{q_k})(k_e - \bar{U}_{q_k})}{M\hat{\sigma}^2_{q_k}}. \tag{4.6}$$

An important result is the fact that the assortativeness values in Equation (4.6) can be interpreted as an *edge based* local assortativity measure. In particular, an edge is considered assortative if its contribution to the global assortativity coefficient is positive, i.e., $\rho_e > 0$, and disassortative, in case its contribution is negative, i.e., $\rho_e < 0$.

Defining local assortativity on an edge basis is advantageous, since this allows for determining the assortativity of sets of edges by summing the values ρ_e for a particular target edge set, E_{target}, which is used by Zhang et al. (2012) to define their UAC as:

$$\rho^{\text{UAC}} = \sum_{e \in E_{\text{target}}} \rho_e. \tag{4.7}$$

Setting the target edge set E_{target} in Equation (4.7) to the entire edge set E consisting of the M edges of the network yields the assortativity coefficient r by Newman (2002), i.e., $\sum_{e=1}^{M} \rho_e = r$.

Moreover, Zhang et al. (2012) argue that the assortativeness values ρ_e can be used to easily derive a *vertex based* local assortativity measure ρ_v for some vertex v simply by setting the target edge set E_{target} to the edges emanating from that vertex v. More precisely, for undirected networks this gives:

$$\rho_v = \sum_{u=1}^{n} \rho_{e_{vu}}, \tag{4.8}$$

where $\rho_{e_{vu}}$ is the assortativeness value of the edge e that has end vertices v and u. A vertex is considered as assortative if $\rho_v > 0$, and as disassortative if $\rho_v < 0$.

Note that the computation of ρ_v in Equation (4.8) is similar to the computation of the vertex degree k'_v of vertex v in an undirected network, however, instead of summing the elements of the network's adjacency matrix $\boldsymbol{A} = [a_{vu}]$, the sum is over the local edge assortativeness values of connected vertices. Hence, the summation of ρ_v for all vertices yields:[21]

$$\sum_{v=1}^{n} \rho_v = \sum_{uv} \rho_{e_{uv}} = 2r. \tag{4.9}$$

[21] As compared with the sum of all vertex degrees in an undirected network, which is $\sum_{v=1}^{n} k'_v = \sum_{uv} a_{uv} = 2M$.

In order to show that the values, ρ_v, as defined in Equation (4.9), are equivalent to those defined by Piraveenan et al. (2008), consider again Equation (4.8). By replacing the right-hand side of the equation by its definition in Equation (4.6) we obtain:

$$\begin{aligned}
\rho_v = \sum_{u=1}^{n} \rho_{e_{vu}} &= \sum_{u=1}^{n} \frac{(j_v - \bar{U}_{q_k})(k_u - \bar{U}_{q_k})}{M\hat{\sigma}^2_{q_k}} \\
&= \sum_{u=1}^{n} \frac{(j_v k_u - \bar{U}^2_{q_k})}{M\hat{\sigma}^2_{q_k}} && (4.10) \\
&= \frac{\sum_{u=1}^{n} j_v k_u - \sum_{u=1}^{n} \bar{U}^2_{q_k}}{M\hat{\sigma}^2_{q_k}} \\
&= \frac{j_v \sum_{u=1}^{n} k_u - \sum_{u=1}^{n} \bar{U}^2_{q_k}}{M\hat{\sigma}^2_{q_k}} \\
&= \frac{j_v k'_v \bar{k}_u - k'_v \bar{U}^2_{q_k}}{M\hat{\sigma}^2_{q_k}} && (4.11) \\
&= \frac{k'_v (j_v \bar{k}_u - \bar{U}^2_{q_k})}{M\hat{\sigma}^2_{q_k}}, && (4.12)
\end{aligned}$$

where Equation (4.10) is an equivalent transformation, cf. Newman (2002, eq. (4)). Equation (4.11) results because the number of neighbours of a vertex corresponds to its degree, and thus, $\frac{1}{k'_v} \sum_{u=1}^{n} k_u = \bar{k}_u \Leftrightarrow \sum_{u=1}^{n} k_u = k'_v \bar{k}_u$, where $\bar{k}_u$ is the mean excess degree of the neighbours of vertex u. Finally, Equation (4.12) shows that the vertex based local assortativity measure ρ_v is precisely the definition of local assortativity by Piraveenan et al. (2008).

This demonstrates that both definitions of local assortativity, the one by Zhang et al. (2012) and the one by Piraveenan et al. (2008) are equivalent. Note that Piraveenan et al. (2008) scale their local measure, such that summing over the local vertex assortativeness values yields the assortativity coefficient r. This, however, is a matter of choice, and is achieved by multiplying the denominator in Equation (4.12) by 2, because $\sum_{v=1}^{n} \rho_v = 2r \Leftrightarrow r = \sum_{v=1}^{n} \frac{\rho_v}{2}$.

Piraveenan et al. (2010) give a slightly different definition of local assortativity. More precisely, using our notation, then, modifying the numerator of Equation (4.12) to be $j_v k'_v(\bar{k}_u - \bar{U}_{qk})$ yields the local vertex assortativeness values by Piraveenan et al. (2010). However, in order to derive this definition Piraveenan et al. (2010) had to make a questionable assumption on how to split the contribution to the global assortativity among vertices, whereas our definition, and thus, the definition by Piraveenan et al. (2008), copes without additional assumptions. Moreover, the resulting local vertex assortativeness by Piraveenan et al. (2010) additionally would have to be scaled, as their summation does not equal the global assortativity coefficient any more. This is because the definition in Equation (4.12) obeys this rule, and unless $\bar{U}_{qk} = 0 \vee j_v \neq 0$ or $\bar{U}_{qk} = j_v \neq 0$ both definitions are different, in general. Therefore, we

consider the modified local assortativity coefficient by Piraveenan et al. (2010) as the inferior measure. It seems that their first intuition was right, i.e., the local assortativity coefficient as proposed by Piraveenan et al. (2008), as we arrive at the same result differently.

With the help of both assortativeness values, ρ_e and ρ_v, the following measures can be derived in order to further differentiate the local connectivity tendencies of a network: The relative frequency of assortative edges is denoted by $P(\rho_e > 0)$; similarly, The relative frequency of assortative vertices is denoted by $P(\rho_v > 0)$. Zhang et al. (2012) also derive two measures they refer to as the *average assortative (or disassortative) strength* of an edge. However, this might lead to confusion, as the term strength refers to something different in the context of weighted networks, as we will detail in a bit. Instead, for the two measures, we will refer to them as what they actually are. More precisely, the *mean absolute magnitude of assortative edges*, which we denote by $\overline{(\rho_e)_+}$, and similarly, the *mean absolute magnitude of disassortative edges*, which we denote by $\overline{(\rho_e)_-}$.

Finally, we consider the *edge based* definition of local assortativity by Zhang et al. (2012) as the more flexible approach, especially as it also allows us to obtain precisely the vertex based assortativeness values by Piraveenan et al. (2008). We therefore adopt this formulation for the derivation of our generalized local assortativity measure, in the subsequent section.

4.2 Generalized Local Assortativity

Recall that in weighted complex networks, vertex degree generalizes to vertex strength, see Barrat et al. (2004). He defines the strength of a vertex u to be the total weight of its connections, i.e., $s'_u = \sum_{v \in V} w_{uv}$ where V is the vertex set and w_{uv} is the weight of the edge that connects vertices u and v. Thus, it is sensible to also generalize the definition of the assortativity coefficient, r, in Equation (4.1) by incorporating excess vertex strengths rather than excess vertex degrees in weighted networks. This allows for deriving a weighted local assortativity measure similarly to the global one. Initially, Zhang et al. (2012) derive their measure for undirected networks only. They indeed point out that an extension towards directed networks is straightforward, but do not provide any details. In the following, we will first derive a weighted local assortativity measure for undirected networks and, thereafter, give a detailed description of the necessary steps for extending the newly obtained definition to directed networks.

4.2.1 Undirected Weighted Networks

In order to derive weighted local assortativity for undirected weighted networks, we define the following quantities: let $p_{s'}$ denote the strength distribution, i.e., the prob-

ability that a randomly chosen vertex has strength s'; q_s denotes the excess strength distribution, i.e., the probability that a vertex reached by following a randomly chosen edge of weight ω has excess strength s. Note that the excess strength s of a vertex depends on the weight ω of the edge we arrived along. It is the total strength of the vertex less the edge weight ω, i.e., $s = s' - \omega$, and hence is distributed proportional to $(s+\omega)p_{s+\omega}$. Analogously to the previous derivation for q_k, the distribution is given by:

$$q_s = \frac{(s+\omega)p_{s+\omega}}{\sum_{s'} s' p_{s'}},$$

where $\sum_{s'} s' p_{s'}$ is the expected strength of a vertex. We denote by e_{st} the joint distribution of excess strengths of either end of an edge, i.e., the probability that a randomly chosen edge connects two vertices with excess strengths s and t. Having generalized these quantities, a similar representation of assortativity as in Equation (4.1), but with weighted vertex values, is given by:

$$r^{\omega} = \frac{1}{\sigma_{q_s}^2} \sum_{st} st(e_{st} - q_s q_t), \tag{4.13}$$

which, by a similar rearranging of the right-hand side as before, is equivalent to:

$$r^{\omega} = \frac{E[(S - U_{q_s})(T - U_{q_s})]}{\sigma_{q_s}^2}, \tag{4.14}$$

where, this time, S and T are the excess strengths of the ends of an edge and U_{q_s} denotes the mean of the distribution q_s, which is the mean excess strength of an end of an edge and $\sigma_{q_s}^2$ is the variance of the distribution q_s.

In order to quantify the amount of assortative mixing Newman (2002) follows Callaway et al. (2001) by employing the (unweighted) connected degree-degree correlation function. This is suitable for *unweighted* networks. However, in *weighted* networks information on the weights of the observational pairs s_e and t_e are incorporated via edge weights ω_e of the connecting edge e. The extension of the definition of assortativity to incorporate connection weights when computing the correlation coefficient between the weighted vertex values is straightforward, as weighted statistical functions for arithmetic means, covariances, and variances are readily available, see Price (1972).

Thus, we can estimate the theoretical quantities in Equation (4.14) by their *weighted* sample counterparts (again by averaging over the edges of the network), and obtain the following weighted assortativity coefficient:

$$r^{\omega} = \frac{\frac{1}{H}\sum_{e=1}^{M} \omega_e (s_e - \bar{U}_{q_s}^{\omega})(t_e - \bar{U}_{q_s}^{\omega})}{(\hat{\sigma}_{q_s}^{\omega})^2}, \tag{4.15}$$

where s_e and t_e are the excess strengths of the ends of edge e, the sum of edge weights is denoted by $H = \sum_{e=1}^{M} \omega_e$; $\bar{U}^{\omega}_{q_s} = H^{-1} \sum_{e=1}^{M} \frac{1}{2}\omega_e(s_e + t_e)$ is the weighted sample mean and $\hat{\sigma}^{\omega}_{q_s} = \sqrt{H^{-1} \sum_{e=1}^{M} \frac{1}{2}\omega_e(s_e^2 + t_e^2) - (\bar{U}^{\omega}_{q_s})^2}$ the weighted sample standard deviation of the excess strength of an end of an edge.

The coefficient, r^{ω}, in Equation (4.15) corresponds to the weighted correlation coefficient between the weighted vertex values (excess strengths) of the ends of an edge, as introduced in Chapter 3. It is the weighted counterpart of the assortativity coefficient, r, by Newman (2002) as in Equation (4.5), which is the unweighted correlation coefficient between the unweighted vertex values (excess degrees) of the ends of an edge.

Furthermore, we denote by ρ^{ω}_e the extension of the assortativeness values as in Equation (4.6) towards weighted networks. The weighted assortativeness values ρ^{ω}_e are defined as:

$$\rho^{\omega}_e = \frac{\omega_e(s_e - \bar{U}^{\omega}_{q_s})(t_e - \bar{U}^{\omega}_{q_s})}{H(\hat{\sigma}^{\omega}_{q_s})^2}. \tag{4.16}$$

Edges are considered disassortative if the values are negative, i.e., if $\rho^{\omega}_e < 0$, and assortative of the values are positive, i.e., $\rho^{\omega}_e > 0$.

Similar to the generalized assortativity coefficient in Chapter 3 (see Equation (3.4)), we introduce tuning parameters $\alpha, \beta \in \{0, 1\}$, that function as switches and allow for controlling the degree of generalization of the local assortativity coefficient. More precisely, the parameter α switches between the use of excess degrees or strengths as vertex values, and β switches between the computation of unweighted or weighted correlation between the vertex values of the ends of an edge. Moreover, these tuning parameters allow for nesting previous (local) assortativity measures as special cases, as we will detail in the following. To this end, let $s^*_u = \sum_{v \in V} w^{\alpha}_{uv}$ be a modified version of vertex strength s'_u. Clearly, if $\alpha = 1$, then s^* equals the vertex strength, i.e., $s^* = s'$, whereas, if $\alpha = 0$, then s^* reduces to ordinary vertex degree, i.e., $s^* = k'$. Furthermore, let $\Omega = \sum_{e=1}^{M} \omega^{\beta}_e$. Obviously, if $\beta = 1$, then $\Omega = H$, i.e., Ω corresponds to the sum of edge weights, whereas, if $\beta = 0$, then $\Omega = M$, i.e., Ω equals the number of edges in the network. Based on these parameters, (α, β), we define the corresponding weighted assortative values as:

$$\rho^{\omega}_e(\alpha, \beta) = \frac{\omega^{\beta}_e[l_e - \bar{U}^{\omega}_{q_s}(\alpha, \beta)][m_e - \bar{U}^{\omega}_{q_s}(\alpha, \beta)]}{\Omega[\hat{\sigma}^{\omega}_{q_s}(\alpha, \beta)]^2}, \tag{4.17}$$

where l_e and m_e are the vertex values of the ends of edge e. For example, $l_e = s^*_l - \omega^{\alpha}_e$; the (weighted) sample mean and standard deviation expressed as functions of the parameters (α, β) are $\bar{U}^{\omega}_{q_s}(\alpha, \beta) = \Omega^{-1} \sum_{e=1}^{M} \frac{1}{2}\omega^{\beta}_e(l_e + m_e)$ and $\hat{\sigma}^{\omega}_{q_s}(\alpha, \beta) = \sqrt{\Omega^{-1} \sum_{e=1}^{M} \frac{1}{2}\omega^{\beta}_e(l_e^2 + m_e^2) - [\bar{U}^{\omega}_{q_s}(\alpha, \beta)]^2}$. The expression in Equation (4.17) is the most general version of the (weighted) assortativeness values (for undirected networks) as

it nests all previous (local) assortativity measures as follows: for the combination $\alpha = 0$ and $\beta = 0$, the values $\rho_e^\omega(\alpha, \beta)$ reduce to the original assortativeness values as proposed by Zhang et al. (2012) (see Equation (4.6)), i.e., $\rho_e^\omega(0,0) = \rho_e$, such that, $\sum_{e=1}^{M} \rho_e^\omega(0,0) = r$. Whereas, for the combination $\alpha = 1$ and $\beta = 1$, the values equal the weighted assortativeness values (see Equation (4.16)), i.e., $\rho_e^\omega(1,1) = \rho_e^\omega$, and thus, $\sum_{e=1}^{M} \rho_e^\omega(1,1) = r^\omega$. Generally, summing the values $\rho_e^\omega(\alpha, \beta)$ for all edges M in the network yields the *generalized assortativity coefficient*, $r^\omega(\alpha, \beta)$, i.e., $\sum_{e=1}^{M} \rho_e^\omega(\alpha, \beta) = r^\omega(\alpha, \beta)$. We therefore refer to the values $\rho_e^\omega(\alpha, \beta)$ as the *generalized edge assortativeness values*. The summation of the generalized edge assortativeness values over the edges emanating from a vertex v yields the *generalized vertex assortativeness values*, $\rho_v^\omega(\alpha, \beta) = \sum_{u=1}^{n} \rho_{e_{vu}}^\omega(\alpha, \beta)$.

Additionally, by using the same naming convention as used by Zhang et al. (2012), we refer to the assortativity coefficient that results by summing the generalized edge assortativeness values for an arbitrary target edge set E_{target} as the *generalized universal assortativity coefficient* (GUAC), and define it as:

$$\sum_{e \in E_{\text{target}}} \rho_e^\omega(\alpha, \beta) = \rho^{\text{GUAC}} \tag{4.18}$$

The GUAC is a versatile coefficient that, e.g., can be used to determine the contribution of either a set of vertices or edges to the global assortativity. It is up to the researcher to choose which vertices and edges are interesting to consider. Possible interesting vertices can include the top n most assortative or most disassortative vertices (or edges). However, it can also be interesting to examine the vertices that can be combined into a community (or the edges connecting them) with regard to their aggregated assortativity. Another interesting example, which is considered in the following, is the determination of the assortativity of isomorphic components in a network.

Figure 4.1 shows the advantage of the GUAC of being capable of identifying the differences of weighted local connectivity patterns of isomorphic components. The example undirected network on $n = 70$ vertices with $M = 71$ edges is based on the one depicted in Zhang et al. (2012), but is complemented by randomly assigned edge weights, except for edges that are incident with vertices of components A or B, which have the same weight of one. The network is overall disassortative with respect to degrees, as $r^\omega(0,0) = -0.800$, and also (even slightly more) overall disassortative with respect to strengths, as $r^\omega(1,1) = -0.828$. However, the components A and B show different local connectivity patterns in the sense of how they connect to the rest of the network. In order to quantify this behaviour the GUAC of the components is computed by summing the local edge assortativeness values that connect each component to the rest of the network, respectively. Although they are isomorphic components, A tends to connect degree disassortatively to the rest of the network, $\rho_A^{\text{GUAC}}(0,0) = -0.034$,

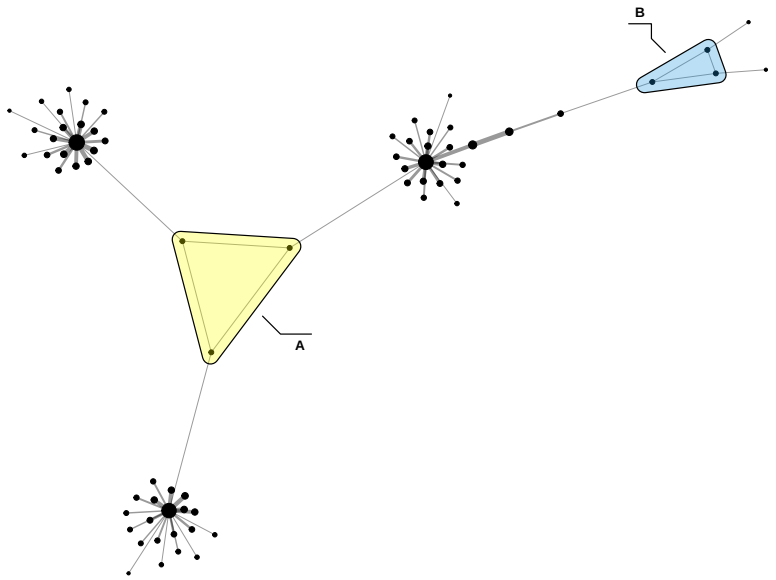

Figure 4.1. Differences of local connectivity patterns of isomorphic components (A and B). The example weighted undirected graph on $n = 70$ vertices with $M = 71$ edges is based on the one depicted in Zhang et al. (2012), but is complemented by randomly assigned edge weights (except for the edges that are incident with vertices of components A or B, which have the same weight of one). Higher edge weights are indicated by thicker edges. The depicted size of vertices is proportional to the vertex' total vertex strength.

whereas B forms degree assortative connections, $\rho_B^{\mathrm{GUAC}}(0,0) = 0.025$. This can be verified, again, by considering Figure 4.1, where the component A, of which the vertices have a relatively low degree, is surrounded by high-degree vertices, whereas component B is connected to also low degree vertices. If, however, edge weights are considered, then, the components A and B are almost non-assortative, as $\rho_A^{\mathrm{GUAC}}(1,1) = -0.009$ and $\rho_B^{\mathrm{GUAC}}(1,1) = 0.007$. The signs of $\rho_A^{\mathrm{GUAC}}(1,1)$ and $\rho_B^{\mathrm{GUAC}}(1,1)$ still differ, because of the way each component connects to the rest of the network, i.e., A is surrounded by vertices with high strengths, whereas B connects to low strength vertices. However, the contribution to the overall disassortativity of the network is equally small for both components A and B. This is because of the comparatively low weights of the edges that connect the components to the rest of the network (all equal one).

As a result, the components A and B show different local connectivity patterns with respect to their degrees, but show similar local connectivity patterns with respect to their strengths. Thus, the GUAC allows to further distinguish between local connectivity patterns of components and their contribution to the global assortativity of the network, if edge weights are additionally considered.

Moreover, with the help of both generalized edge and vertex assortativeness values, generalizations of the unweighted measures can be derived, that allow for further differentiation of the local connectivity tendencies of a weighted network, such as the

proportion of assortative edges, $P(\rho_e^\omega(\alpha,\beta) > 0)$, the proportion of assortative vertices, $P(\rho_v^\omega(\alpha,\beta) > 0)$, the mean absolute magnitude of assortative edges $\overline{(\rho_e^\omega(\alpha,\beta))_+}$ and the mean absolute magnitude of disassortative edges, $\overline{(\rho_e^\omega(\alpha,\beta))_-}$.

Finally, with the help of the generalized edge assortativeness values it is possible to determine local assortativity measures, which have not been considered in the literature, so far. For example, $\rho_e^\omega(1,1)$ is a local assortativity measure that corresponds to the global generalized assortativity coefficient, which we proposed in Chapter 3. Moreover, $\rho_e^\omega(0,1)$ is a local assortativity measure corresponding to the (global) assortativity coefficient suggested by Leung and Chau (2007)

So far we have considered undirected networks. Now we will extend the proposed local assortativity measures for directed networks.

4.2.2 Directed Weighted Networks

In the following, we extend the definition of generalized local assortativity for directed weighted networks, similar to Newman (2003) and Piraveenan et al. (2012) for unweighted networks. We therefore define the following quantities: $p_{s'}^{\text{out}}$ denotes the *out-strength* distribution, i.e., the probability that a randomly chosen vertex has out-strength s'. The *in-strength* distribution, i.e., the probability that a randomly chosen vertex has in-strength s' is denoted by $p_{s'}^{\text{in}}$.

In order to define the *excess out-* or *in-strength* distributions we have to distinguish between the cases in which an edge *leads out of* a vertex and those in which an edge *leads into* a vertex, respectively. We indicate the latter by a superscript asterisk symbol.

To this end, for the *excess out-strength*, let q_s^{out} denote the excess out-strength distribution of the end that a directed edge *leads out of*, i.e., the probability that a vertex reached by *backtracing* a randomly chosen directed edge of weight ω has excess out-strength s. However, $q_s^{*\text{out}}$ denotes the excess out-strength distribution of the end that a directed edge *leads into*, i.e., the probability that a vertex reached by *following* a randomly chosen directed edge of weight ω has excess out-strength s. In case of q_s^{out} the excess out-strength s of an end depends on the edge weight ω, thus, it is the total out-strength less the edge weight, i.e., $s = s' - \omega$, hence, q_s^{out} is distributed according to $(s+\omega)p_{(s+\omega)}^{\text{out}}$, and, as before, normalization results in:

$$q_s^{\text{out}} = \frac{(s+\omega)p_{(s+\omega)}^{\text{out}}}{\sum_{s'} s' p_{s'}^{\text{out}}}.$$

As opposed to this, in case of $q_s^{*\text{out}}$ the excess out-strength s of an end does not depend on the edge weight ω, and thus, the excess out-strength is equal to the total out-strength in this case, i.e., $s = s'$, hence, $q_s^{*\text{out}}$ is distributed according to $p_{s'}^{\text{out}}$.

Similarly, for the *in-strength*, we denote by $q_s^{*\text{in}}$ the excess in-strength distribution of an end that a directed edge *leads into*, i.e., the probability that a vertex reached by

following a randomly chosen directed edge of weight ω has excess in-strength s. The excess in-strength distribution of an end that a directed edge *leads out of* is denoted by q_s^{in}, i.e., the probability that a vertex reached by *backtracing* a randomly chosen directed edge of weight ω has excess in-strength s. This time vice versa, in case of $q_s^{*\text{in}}$ the in-strength of an end depends on the edge weight ω, thus, it is the total in-strength less the edge weight, i.e., $s = s' - \omega$, hence, $q_s^{*\text{in}}$ is distributed according to $(s+\omega)p_{(s+\omega)}^{\text{in}}$, where normalization yields:

$$q_s^{*\text{in}} = \frac{(s+\omega)p_{(s+\omega)}^{\text{in}}}{\sum_{s'} s' p_{s'}^{\text{in}}}.$$

Contrary, if we consider q_s^{in} the excess in-strength of an end does not depend on the edge weight ω, thus, the excess in-strength is equal to the total in-strength in this case, i.e., $s = s'$, such that q_s^{in} is distributed according to $p_{s'}^{\text{in}}$.

Furthermore, we define $e_{st}^{\text{out–in}}$ to be the joint distribution of excess out- and in-strengths, i.e., the probability that a randomly chosen directed edge *leads out of* a vertex with excess out-strength s and *into* a vertex with excess in-strength t. The joint distributions for the other *modes of assortativity*, which are *out–out*, *in–in* and *in–out*, are defined accordingly. For reasons of clarity, we only show the derivation for the *out–in* mode. The derivation for the other modes is analogous.

Using the above, we define a directed weighted assortativity coefficient as:

$$r_{\text{out–in}}^{\omega} = \frac{1}{\sigma_{q^{\text{out}}}\sigma_{q^{*\text{in}}}} \sum_{st} st(e_{st}^{\text{out–in}} - q_s^{\text{out}} q_t^{*\text{in}}). \tag{4.19}$$

Apparently the representation in Equation (4.19) is a directed version of the coefficient in Equation (4.13), and thus, corresponds to the (vertex value) weighted version of the directed assortativity coefficient by Newman (2003), i.e., it is the correlation between the excess out-strength of the outgoing end and the excess in-strength of the incoming end of an edge.

Once more, we rearrange the right-hand side of Equation (4.19), estimate the theoretical quantities by their weighted sample counterparts, and introduce (α, β) and the mode of assortativity as parameters. We then define the *directed* weighted assortativeness values as:

$$\rho_e^{\omega}(\alpha, \beta, \text{out–in}) = \frac{\omega_e^{\beta}[l_e^{\text{out}} - \bar{U}_{q_s^{\text{out}}}^{\omega}(\alpha,\beta)][m_e^{\text{in}} - \bar{U}_{q_s^{*\text{in}}}^{\omega}(\alpha,\beta)]}{\Omega \cdot \hat{\sigma}_{q_s^{\text{out}}}^{\omega}(\alpha,\beta) \cdot \hat{\sigma}_{q_s^{*\text{in}}}^{\omega}(\alpha,\beta)}, \tag{4.20}$$

where l_e^{out} and m_e^{in} are similarly defined, as before, with the addition that the direction of edge e is incorporated, i.e., if $\alpha = 1$, the quantities denote the excess out-strength of the end l that edge e leads out of and the excess in-strength of the end m that edge e leads into. If, however, the parameter $\alpha = 0$, the vertex values re-

duce to the excess out- and in-degree, respectively; $\bar{U}^{\omega}_{q_s^{\text{out}}}(\alpha,\beta) = \Omega^{-1}\sum_{e=1}^{M}\omega_e^{\beta} l_e^{\text{out}}$ and $\bar{U}^{\omega}_{q_s^{*\text{in}}}(\alpha,\beta) = \Omega^{-1}\sum_{e=1}^{M}\omega_e^{\beta} m_e^{\text{in}}$ are the (weighted) sample mean out- and in-strengths of the outgoing and incoming ends, respectively; and the respective (weighted) sample standard deviations are given by $\hat{\sigma}^{\omega}_{q_s^{\text{out}}}(\alpha,\beta) = \sqrt{\Omega^{-1}\sum_{e=1}^{M}\omega_e^{\beta}(l_e^{\text{out}})^2 - [\bar{U}^{\omega}_{q_s^{\text{out}}}(\alpha,\beta)]^2}$ and $\hat{\sigma}^{\omega}_{q_s^{*\text{in}}}(\alpha,\beta) = \sqrt{\Omega^{-1}\sum_{e=1}^{M}\omega_e^{\beta}(m_e^{\text{in}})^2 - [\bar{U}^{\omega}_{q_s^{*\text{in}}}(\alpha,\beta)]^2}$.[22]

If $\beta = 1$ weighted sample mean and standard deviation of the vertex value of an end of an edge are used. However, if $\beta = 0$, the unweighted mean and standard deviation are used. Just like Equation (4.17) for undirected networks, the expression in Equation (4.20) is the most general version of the (weighted) assortativeness values for a directed network.[23] For example, consider the parameter combination $(\alpha = 0, \beta = 0)$, the *summation of the generalized weighted and directed assortativeness values*, $\rho_e^{\omega}(\alpha,\beta,\text{mode})$, for the *out–in* mode of assortativity corresponds to the directed assortativity coefficient, r_d, by Newman (2003), whereas for the *out–out* and *in–in* modes it corresponds to the so-called *out-assortativity*, r_{out}, and *in-assortativity*, r_{in}, respectively, see Piraveenan et al. (2012).

Mode	$\alpha = 0$		$\alpha = 1$	
	$\beta = 0$	$\beta = 1$	$\beta = 0$	$\beta = 1$
undirected	r^{N}, [1]	r^{LC}, [2]	–	r^{ω}
out–in	r_d, [3]	–	–	$r^{\omega}_{\text{out–in}}$
out–out	r_{out}, [4]	–	–	$r^{\omega}_{\text{out–out}}$
in–in	r_{in}, [4]	–	–	$r^{\omega}_{\text{in–in}}$
in–out	–	–	–	$r^{\omega}_{\text{in–out}}$

[1] Newman (2002)
[2] Leung and Chau (2007)
[3] Newman (2003)
[4] Piraveenan et al. (2012)

Table 4.1. Overview of previous assortativity measures that are obtainable by summing $\rho_e^{\omega}(\alpha,\beta,\text{mode})$, as in Equation (4.20) for the various parameter combinations (α,β) for the different modes of assortativity. We indicate assortativity measures, which have been previously used in the literature by their references (no claim to completeness). Measures that have not been focused by the literature, so far, are indicated by '–'. Note that the generalized assortativity coefficient $r^{\omega}_{\text{mode}}(\alpha,\beta)$ technically nests all measures, however, its focus is on the parameter combination $(\alpha = 1, \beta = 1)$, and thus, we decide to forgo placing a reference in each cell of the table for reasons of clarity.

[22] Unlike in undirected networks, in a directed network each edge has one outgoing and one incoming end. Therefore, the mean excess out-degree or out-strength of an end of an edge is obtained by averaging the excess out-degrees or -strengths of the outgoing ends over all edges in the network. The mean excess in-degree or -strength of an end of an edge is obtained, accordingly. This also applies to the computation of the standard deviation of the excess out- or in-degree or -strength of an end of an edge.

[23] Technically, Equation (4.20) is capable of handling undirected networks as well, however, a slight modification to the network is necessary, i.e., replacing each undirected edge by two directed ones that point in opposite directions, alternatively Equation (4.17) can be used, cf. Newman (2003).

Table 4.1 gives an overview of previous assortativity measures that are obtainable by summing the generalized weighted and directed assortativeness values for the various parameter combinations for the five different modes of assortativity (we consider *undirected* as a fifth mode here). For example, $\sum_{e=1}^{M} \rho_e^{\omega}(0, 0, \textit{undirected}) = r^{\mathrm{N}}$, which is the assortativity coefficient by Newman (2002).

Moreover, in directed networks, the vertex assortativeness values can be further differentiated. The sum can either be computed using the edge assortativeness values of the outgoing edges or the incoming edges. This results in two representations of vertex assortativeness values, which we refer to as the *generalized vertex out-assortativeness values* and *generalized vertex in-assortativeness values*, respectively. The generalized vertex out-assortativeness and in-assortativeness values of a vertex v are denoted by $\rho_v^{\omega}(\alpha, \beta, \textit{out})$ and $\rho_v^{\omega}(\alpha, \beta, \textit{in})$, respectively, and they are defined as:

$$\rho_v^{\omega}(\alpha, \beta, \textit{out}) = \sum_{u=1}^{n} \rho_{e_{vu}}^{\omega}(\alpha, \beta, \mathrm{mode}), \qquad \rho_v^{\omega}(\alpha, \beta, \textit{in}) = \sum_{u=1}^{n} \rho_{e_{uv}}^{\omega}(\alpha, \beta, \mathrm{mode}).$$

We suggest that the directed vertex assortativeness values are chosen in accordance with the considered mode of assortativity. For example, both generalized vertex out- and in-assortativeness values can be determined for the *out–in* mode of assortativity. For the generalized vertex out-assortativeness, the contribution to the global assortativity is assigned to the vertex from which the edge originates. In the case of generalized vertex in-assortativeness values, the contribution to global assortativity is assigned to the vertex pointed to by an edge. It depends on the research setting, in particular which vertex is responsible for a connection, whether the former or the latter should be preferred. Finally, the generalized vertex out- and in-assortativeness values obey the following summation rule:

$$\sum_{v=1}^{n} \rho_v^{\omega}(\alpha, \beta, \textit{out}) = \sum_{v=1}^{n} \rho_v^{\omega}(\alpha, \beta, \textit{in}) = \sum_{uv} \rho_{e_{uv}}^{\omega}(\alpha, \beta, \mathrm{mode}) = r^{\omega}(\alpha, \beta, \mathrm{mode}). \quad (4.21)$$

In summary, by generalizing the concept of local assortativity towards directed and weighted networks, we obtain the generalized edge and vertex assortativeness values, ρ_e^{ω} and ρ_v^{ω} (see Equations (4.20) and (4.21), respectively), yielding measures for the contribution to global assortativity of individual edges and vertices, respectively. Moreover, the generalized universal assortativity coefficient, ρ^{GUAC} (see Equation (4.18)), measures the assortativity of network components by aggregating the assortativeness values of edges of an arbitrary edge subset. For all measures, the parameters are $(\alpha, \beta, \mathrm{mode})$, where the parameter α indicates if vertex degrees or strengths shall be used and β indicates whether to compute the unweighted or weighted correlation, for the respective mode of assortativity. We proceed with a demonstration on how to use the newly

obtained measures for an in-depth analysis of local assortativity of a network in the subsequent section.

4.3 Empirical Analysis of Local Assortativity Patterns

In the following, we demonstrate the usefulness of our generalized local assortativity measures by presenting an in-depth analysis of the generalized local assortativity of theoretical network models as well as of real world networks. Section 4.3.1 considers weighted generalizations of the *Erdős-Rényi random graph* (ER) and Barabási-Albert (BA) models. In Section 4.3.2 we consider two real world networks, one undirected the other one directed.

4.3.1 Selected Network Models

The models considered below are weighted extensions of models that are known to be (global) non-assortative. We therefore expect that the weighted extensions will have a similar assortativity structure, especially since the extended models contain their respective counterparts as unweighted projections (for which we measure the assortativity with the parameter combination $(\alpha = 0, \beta = 0)$). A main purpose of the analysis is to verify that our generalized local assortativeness measures are able to identify a known (global) non-assortative network, and also to uncover differences in the local structures. The differences in the local assortativity structures can then help to further differentiate the topology of networks with similar global assortativity.

4.3.1.1 The Weighted Random Graph Model

The *weighted random graph* (WRG) model by Garlaschelli (2009) is an extension of the *Erdős-Rényi random graph* (ER) model towards weighted networks. It seizes on the $G_{n,p}$ ensemble (see Chapter 2), but incorporates edge weights ω. The derivation is analogous to the ER model, see Park and Newman (2003), Maslov and Sneppen (2004), Garlaschelli and Loffredo (2008, 2009) and Garlaschelli (2009) for a thorough derivation of the model. In essence, the WRG model is completely specified by the probability that any two vertices i and j are connected by an edge of weight ω, which is given by:

$$P(W_{ij} = \omega) = P(\omega) = p^{\omega}(1 - p). \tag{4.22}$$

The probability that there is no edge between two vertices is denoted by $P(0)$, and thus, $1 - P(0) = p$ is the probability of two vertices being connected by an edge of any (non-zero) weight. The choice of the symbol p is, according to Garlaschelli (2009), justified by the fact that the projection of the WRG model onto an unweighted graph yields

the ER random graph with connection probability p.[24] Consider Equation (4.22) and let $\tilde{q} = (1 - p)$, with this, note that the random weights W_{ij} are distributed according to a *geometric distribution* with success probability $\tilde{q}$, i.e., $W_{ij} \sim \text{Geo}(\tilde{q})$. Usually, the parameter of the geometric distribution is denoted by p. In this paper, however, p is defined in terms of the complement, hence, we introduce the substitution $\tilde{q} = (1 - p)$ for reasons of traceability. In this case, the geometric distribution is the probability distribution of the number of consecutive fails ω that can be observed, in a series of independent *Bernoulli* trials with success probability $\tilde{q}$, before the first success occurs, cf. Krishnamoorthy (2020). In order to draw samples from the geometric distribution, the parameter $\tilde{q}$ can be determined by equating the network's average edge weight $\bar{\omega}$ to the mean of the distribution $\text{Geo}(\tilde{q})$, i.e., $\bar{\omega} = \frac{1-\tilde{q}}{\tilde{q}} \Leftrightarrow \tilde{q} = \frac{1}{\bar{\omega}+1}$, which, by resubstitution, leads to the identity $p = \frac{\bar{\omega}}{\bar{\omega}+1} \Leftrightarrow \bar{\omega} = \frac{p}{1-p}$.

With the above, we can generate *directed* samples from the WRG model, with a given order n and mean edge weight $\bar{\omega}$, simply by forming a weighted $n \times n$ adjacency matrix $\mathbf{W} = [w_{ij}]$ from the realizations, w_{ij}, of $n(n-1)$ randomly drawn edge weights, $W_{ij} \sim \text{Geo}(\tilde{q})$, such that the diagonal elements of $\mathbf{W}$ are zero.[25] For *undirected* samples only the upper triangle of $\mathbf{W}$ has to be populated with randomly drawn weights, due to symmetry of the adjacency matrix (the lower triangle is populated, such that $w_{ij} = w_{ji}$, afterwards).[26]

Figure 4.2 shows networks of order $n = 100$, which result of sampling the WRG model for different target mean edge weights $\bar{\omega}$, and thus, different target connection probabilities p. For the ER model, the condition for the emergence of a *giant component* is $p > \frac{1}{n-1}$, i.e., a giant component emerges if the mean degree of the network exceeds unity ($\bar{k}' > 1$), in other words, each vertex is on average connected to at least one other vertex, cf. Erdös and Rényi (1960), Bollobás (2008) and Barabási (2016). For the WRG model, this translates to the following condition for the emergence of a giant component: $\bar{\omega} > \frac{1}{n-2}$. Interestingly, by comparing Figures 4.2a to 4.2c, the transition from a *subcritical regime*, where there is no giant component, to a *supercritical regime*, where there is a giant component together with small clusters, to a *connected regime*, where there is single giant component and no small clusters, can be observed.

[24] Note that, for the purpose of fitting the model to a real network, the maximum likelihood estimates p^* of the connection probability p are different for the WRG and the ER model, see Garlaschelli and Loffredo (2008), more precisely:

$$p^*_{\text{WRG}} = \frac{2H}{n(n-1) + 2H} \quad \text{, whereas} \quad p^*_{\text{ER}} = \frac{2M}{n(n-1)}.$$

[25] See Devroye (1986) and Krishnamoorthy (2020) for algorithms for sampling random numbers from a geometric distribution.

[26] Alternatively, pseudocode of the algorithm that generates undirected samples from the WRG model, as presented in Garlaschelli (2009), which can be easily generalized for directed networks, can be found in Coolen et al. (2017)

Measure	$\bar{\omega} = 0.02$			
	$\alpha = 0$		$\alpha = 1$	
	$\beta = 0$	$\beta = 1$	$\beta = 0$	$\beta = 1$
undirected				
r^ω	-0.002	-0.002	-0.002	-0.002
$P(\rho_e^\omega > 0)$	0.500	0.500	0.502	0.501
$\overline{(\rho_e^\omega)_+}$	6.48e-05	6.48e-05	6.43e-05	6.44e-05
$\overline{(\rho_e^\omega)_-}$	6.53e-05	6.53e-05	6.52e-05	6.53e-05
$P(\rho_v^\omega > 0)$	0.499	0.499	0.499	0.499
out–in				
r^ω	-0.001	-0.001	-0.001	-0.001
$P(\rho_e^\omega > 0)$	0.500	0.500	0.501	0.501
$\overline{(\rho_e^\omega)_+}$	3.26e-05	3.26e-05	3.23e-05	3.23e-05
$\overline{(\rho_e^\omega)_-}$	3.27e-05	3.27e-05	3.25e-05	3.25e-05
$P(\rho_v^\omega(\text{out}) > 0)$	0.499	0.499	0.500	0.500
$P(\rho_v^\omega(\text{in}) > 0)$	0.500	0.500	0.500	0.501
out–out				
r^ω	-4.25e-04	-2.63e-04	-4.09e-04	-2.46e-04
$P(\rho_e^\omega > 0)$	0.500	0.500	0.501	0.501
$\overline{(\rho_e^\omega)_+}$	3.26e-05	3.26e-05	3.23e-05	3.23e-05
$\overline{(\rho_e^\omega)_-}$	3.27e-05	3.27e-05	3.25e-05	3.25e-05
$P(\rho_v^\omega(\text{out}) > 0)$	0.499	0.500	0.498	0.499
$P(\rho_v^\omega(\text{in}) > 0)$	0.500	0.501	0.500	0.500
in–in				
r^ω	-0.001	-0.001	-0.001	-0.001
$P(\rho_e^\omega > 0)$	0.500	0.500	0.501	0.501
$\overline{(\rho_e^\omega)_+}$	3.25e-05	3.25e-05	3.22e-05	3.22e-05
$\overline{(\rho_e^\omega)_-}$	3.27e-05	3.27e-05	3.25e-05	3.25e-05
$P(\rho_v^\omega(\text{out}) > 0)$	0.499	0.498	0.499	0.499
$P(\rho_v^\omega(\text{in}) > 0)$	0.497	0.499	0.499	0.500
in–out				
r^ω	-4.49e-04	-0.001	-4.05e-04	-4.77e-04
$P(\rho_e^\omega > 0)$	0.501	0.501	0.503	0.503
$\overline{(\rho_e^\omega)_+}$	3.26e-05	3.26e-05	3.22e-05	3.22e-05
$\overline{(\rho_e^\omega)_-}$	3.27e-05	3.27e-05	3.26e-05	3.26e-05
$P(\rho_v^\omega(\text{out}) > 0)$	0.499	0.499	0.499	0.499
$P(\rho_v^\omega(\text{in}) > 0)$	0.499	0.499	0.499	0.499

Table 4.2. Generalized local assortativity analysis of the WRG model. Reported are the generalized assortativity coefficient r^ω, fraction of local assortative edges $P(\rho_e^\omega > 0)$, average absolute magnitude of assortative edges $\overline{(\rho_e^\omega)_+}$, average absolute magnitude of disassortative edges $\overline{(\rho_e^\omega)_-}$, fraction of local assortative vertices $P(\rho_v^\omega > 0)$ (undirected), and fraction of local out- and in-assortative vertices $P(\rho_v^\omega(\text{out}) > 0)$ and $P(\rho_v^\omega(\text{in}) > 0)$ (directed), respectively, for the WRG model, for a target mean edge weight $\bar{\omega} = 0.02$, for all four parameter combinations (α, β). An ensemble of 100 weighted random graphs (WRG) of order $n = 1000$ is drawn for each mode of assortativity. The results are averaged over the samples of the respective ensembles.

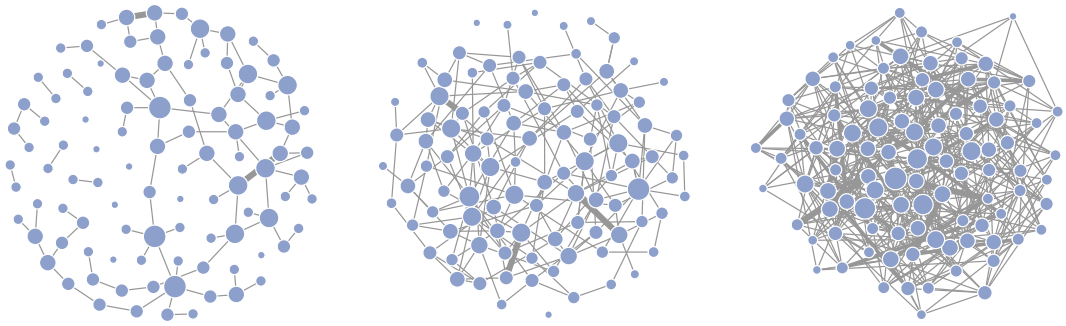

(a) Subcritical regime. **(b)** Supercritical regime. **(c)** Connected regime.

Figure 4.2. Realizations of sampling the WRG model from different regimes. The graphs are on $n = 100$ vertices. The probability of two vertices being connected by an edge of any (non-zero) weight is, for (a) $p = 0.0099$ resulting in a mean edge weight $\bar{\omega} = 0.01$, for (b) $p = 0.0196$ and $\bar{\omega} = 0.02$, and for (c) $p = 0.0476$ and $\bar{\omega} = 0.05$. The size of a vertex is proportional to its (total) strength. Moreover, thicker edges indicate higher edge weights.

Since most real-world networks are supercritical, cf. Barabási (2016), we base our local assortativity analysis of the WRG model on that regime. For each mode of assortativity, i.e., *undirected*, *out–in*, *out–out*, *in–in* and *in–out*, we sample an ensemble of 100 networks. We set the average edge weight of a sample to $\bar{\omega} = 0.02$. This way we ensure that the resulting samples are in the supercritical regime. The range of p for which the supercritical regime results is $\frac{1}{N} < p < \frac{\ln N}{N}$, cf (Barabási, 2016, p. 86). An average edge weight of $\bar{\omega} = 0.02$ corresponds to a connection probability $p = 0.0196$, which lies in between $\frac{1}{100} = 0.01 < 0.0196 < 0.0461 = \frac{\ln 100}{100}$. Any other value from this range would be appropriate, too.

Table 4.2 shows the averaged results of the local assortativity analysis (over the samples of the respective ensembles) for the four different parameter combinations $(\alpha, \beta) \in \{0, 1\}$. Note that, for the parameter combination $(\alpha = 0, \beta = 0)$, the WRG model is projected onto an unweighted graph, i.e., analysing the generalized assortativity of the WRG model is the same as analysing the assortativity of the ER model, for this combination. The following detailed description refers to all modes and parameter combinations, as the results are quite similar. For example, the generalized assortativity coefficient $r^{\omega}(\alpha, \beta)$ equals almost zero, indicating that the WRG model generates networks that do not show any degree or strength correlations, as expected.[27] Moreover, there is an equal proportion of assortative and disassortative edges, as $P(\rho_e > 0) \approx 0.5$. Also, assortative and disassortative edges tend to be equally strong as the average absolute magnitude of assortative and disassortative edges is fairly balanced. Finally, there is an equal proportion of assortative and disassortative vertices, as $P(\rho_v > 0) \approx 0.5$.

[27] The fact that the coefficient is not exactly zero might be explained by structural constraints, i.e., the finite size of the network sample, cf. Serrano et al. (2006) and Yang et al. (2017).

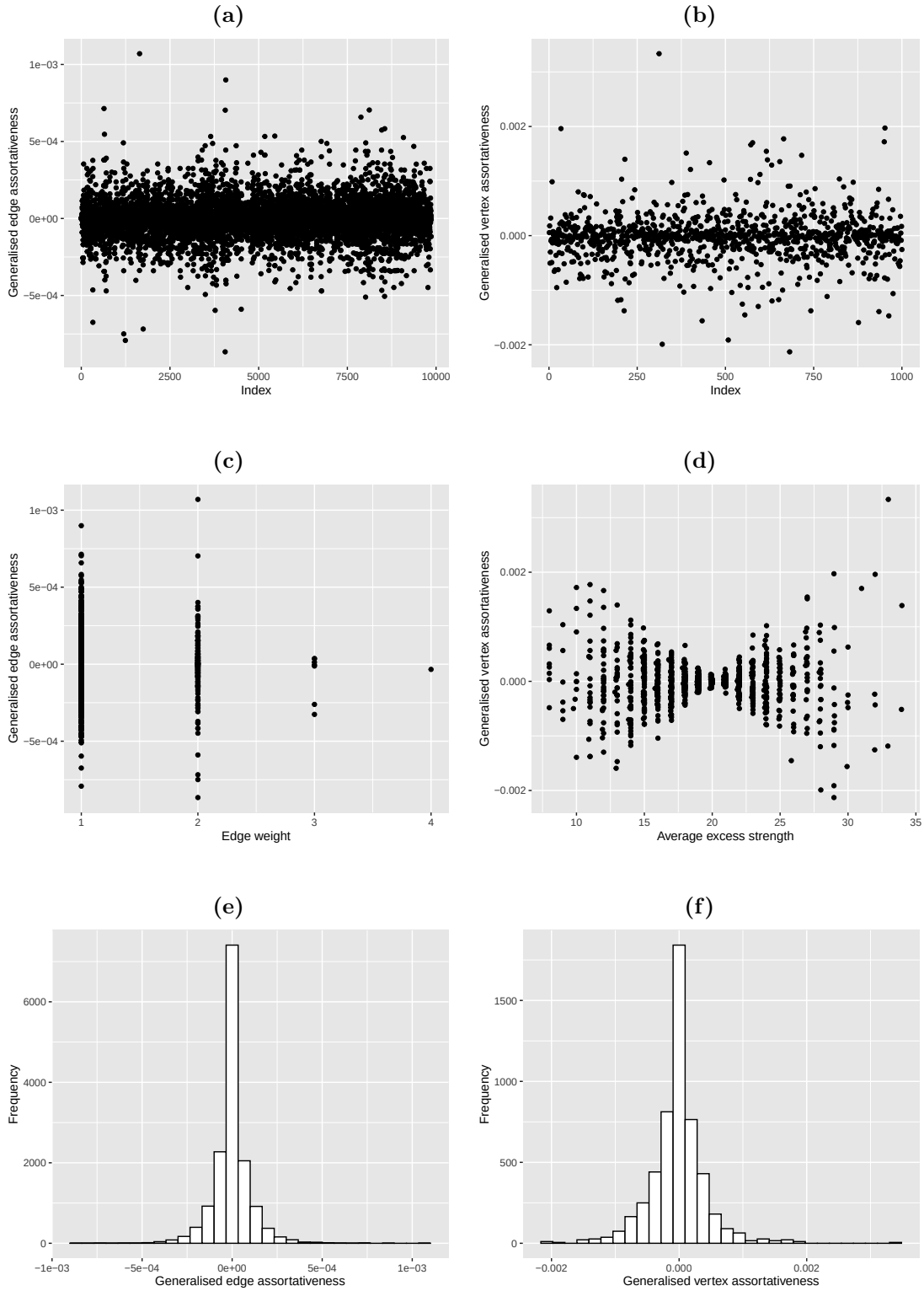

Figure 4.3. Generalized local assortativity plots of the WRG model. The plots are for a single undirected sample of the WRG model of order $n = 1000$ with an average edge weight $\bar{\omega} = 0.02$, for the parameter combination $(\alpha = 1, \beta = 1)$.

Figures 4.3a to 4.3f provide a graphical analysis of the local assortativity pattern of the undirected WRG model, for the parameter combination $(\alpha = 1, \beta = 1)$.[28] More precisely, Figure 4.3a shows a scatter plot of the relation between the edge assortativeness values and the position of an edge in the edge list or adjacency matrix. If the elements of the edge list or adjacency matrix of the network are ordered from a content perspective, this depiction will provide a facility of analysing the edge assortativeness with respect to this ordering. In the case of the theoretical WRG, however, there is no particular ordering of vertices or edges. Therefore, Figures 4.3a and 4.3b emphasize once more that no degree or strength correlations are present in this model, as positive as well as negative edge and vertex assortativeness values are evenly distributed among edges and vertices, respectively. This observation is also supported by the histograms in Figures 4.3e and 4.3f. However, Figure 4.3d shows an interesting pattern. Although vertices tend to be local non-assortative on average, the figure shows that there is more variation in the vertex assortativeness values for vertices with an average excess strength either below or above a particular value.[29] The value for which the variation of generalized vertex values is lowest (≈ 20) happens to be the global average excess strength of the ends of an edge. This, however, is due to the way how (vertex based) local assortativity is defined, as the definition pivots on the global average excess strength, $\bar{U}_{q_s}$, cf. Equation (4.12).

A main purpose of the preceding analysis is verifying that our generalized local assortativeness measures are able to identify a known non-assortative network. It is, thus, pleasant to see that the results coincide with our expectations, as the WRG model shows neither global nor local assortative or disassortative tendencies, just as its unweighted counterpart the ER model with unweighted assortativity.

We continue with another theoretical model that, similar to the WRG, is known (global) non-assortative, but is structurally different with respect to local assortativity. We show that these different structures can be uncovered by our local assortativity measures.

4.3.1.2 Weighted Preferential Attachment Models

Yook, Jeong, Barabási, and Tu (2001) consider weighted scale free networks. Their model, which they refer to as the *weighted scale free model* (WSF), expands the simple BA model by a weight assignment scheme, i.e., edges are created according to the simple preferential attachment scheme in Equation (2.1), to which weights are assigned afterwards. In order to derive the weight assignment scheme, the following assumptions

[28] We forgo showing figures for both the other parameter combinations and modes of assortativity because of their similar visual appeal.

[29] The average excess strength of a vertex corresponds to the total strength less the mean of the weights of the edges emanating from that particular vertex. Figure B.1 illustrates how the average excess degree and strength of a vertex are obtained.

are made: (1) the weight of a newly created edge between a new vertex j and an existing one i is proportional to the degree k'_i; (2) it is assumed that vertices have reasonably uniform total *resources* for linking to others. Thus, for each new vertex entering the network, its total strength is fixed,[30] and normalized, such that the sum of weights of m newly created edges equals unity, i.e., $\sum_{\{i'\}} w_{ji'} = 1$, where $\{i'\}$ is the set of vertices to which a new vertex j is connected to. As a result of combining the two assumptions, weights are assigned to newly created edges between vertices j and i according to the following scheme:

$$w_{ji} = \frac{k'_i}{\sum_{\{i'\}} k'_{\{i'\}}}. \tag{4.23}$$

Furthermore, Yook et al. (2001) propose two variants of the model, by altering either the preferential attachment scheme or the weight assignment scheme. The former is referred to as *weight driven connectivity*, whereas the latter is referred to as *weight driven weight*. With weight driven connectivity, the preferential attachment scheme in Equation (2.1) is altered, such that the probability of choosing an existing vertex i is proportional to its strength s'_i, instead of its degree k'_i. Similarly, in the weight driven weight case, degrees k' are replaced by strengths s' in the weight assignment scheme in Equation (4.23). Moreover, Zheng, Trimper, Zheng, and Hui (2003) contribute to this by adding a *stochastic weight assignment* scheme to the WSF model. At first, random fitness values η are assigned to the vertices, where, for simplicity, $\eta_i \sim U_{[0,1]}$ for each vertex i.[31] With probability p, edge weights are then assigned to newly created edges according to Equation (4.23), and, with probability $(1 - p)$ edge weights are assigned according to the scheme:

$$w_{ji} = \frac{\eta_i}{\sum_{\{i'\}} \eta_{\{i'\}}}. \tag{4.24}$$

For $p = 1$ the *connectivity driven weight* scheme suggested by Yook et al. (2001) is recovered, whereas, for $p = 1$ weights are driven entirely by vertex fitness. For values in the range $0 < p < 1$, weights are stochastically assigned, mimicking the real-world behaviour of newcomers entering a network, and choosing to connect to others either based on their popularity or based on other non-popularity related attributes captured by the fitness value. As with the simple BA model, there exist a growing number of extensions to the weighted BA model. Among the above-mentioned extensions for the simple BA model, of which some might also be applicable to the weighted BA model, there exist extensions specifically developed for the weighted model. For example, Barthélemy, Barrat, Pastor-Satorras, and Vespignani (2005) argue that the presence of a new edge

[30] Vertices increase their strength by attracting new connections over the course of time, though.

[31] However, the fitness values are not restricted to be uniformly distributed, but rather can be distributed according to any distribution $P(\eta)$, cf. Zheng et al. (2003).

can introduce variations of existing weights across a network, such that a local rearrangement of weights might be sensible.

The simple BA model immediately becomes more complex when *directed* networks are considered. Bollobás, Borgs, Chayes, and Riordan (2003) have suggested a directed version of the *unweighted* simple BA model by introducing a set of additional parameters $\alpha, \beta, \gamma, \delta_{\text{out}}, \delta_{\text{in}}$, which are non-negative real numbers, where $\alpha + \beta + \gamma = 1$, together with a set of rules on how to proceed in each time step t. A network is generated by the following rules:

(A) with probability α, a new vertex j is added to the network and connected to an existing vertex i by forming an edge that points from j to i, where the probability of choosing i is proportional to $(k'_{\text{in}}(i) + \delta_{\text{in}})$.

(B) with probability β, two existing vertices j and i are connected by forming an edge that points from j to i, where j and i are chosen independently, with probabilities proportional to $(k'_{\text{out}}(j) + \delta_{\text{out}})$ and $(k'_{\text{in}}(i) + \delta_{\text{in}})$, respectively.

(C) with probability γ, a new vertex j is added to the network and connected to an existing vertex i by forming an edge that points from i to j, where the probability of choosing i is proportional to $(k'_{\text{out}}(i) + \delta_{\text{out}})$.

Apparently, parameters α, β, γ can be interpreted as probabilities of a biased three-sided coin, and δ_{in} and δ_{out} are tuning parameters that allow for vertices with zero in- or out-degree, k'_{in} or k'_{out}, respectively, to still be considered as an end to connect to.

To the best of our knowledge, so far, there is no established model for producing random *directed and weighted* scale free networks. Indeed, an attempt at a definition of such a model has been made by Yuan et al. (2021), in order to generalize the model by Bollobás et al. (2003). However, the generalization is not complete in that sense that the case (B) is not contained in the model by Yuan et al. (2021), moreover, their choice of assigning edge weights in the process of link formation seems a bit arbitrary to us, as they randomly sample integer values ranging from 1 to 10.[32] We conclude that this model needs further investigation, and therefore, only consider the undirected WSF model in this Thesis. We postpone the analysis of directed weighted scale-free models to future research.

For our assortativity analysis, we consider the WSF model with stochastic weights assignment scheme, for which we set $m_0 = 5$, $T = 10000$, $m = 2$ and $p = 0.5$, as a representative of a weighted network with a scale free degree (and strength) distribution. Table 4.3 shows the results of the local assortativity analysis for the WSF model, as averages over the individual samples of the ensemble. Interestingly, the results of our analysis show that the model generates predominantly disassortative networks, as

[32] We aim at analysing the influence of edge weights on the local (edge) assortativity, and thus, it does not seem sensible to us to set edge weights arbitrarily and then to interpret them.

the generalized assortativity coefficient, r^ω, is negative for all parameter combinations (α, β). This is the result of the fact that, on the one hand, the proportion of disassortative edges is slightly higher, i.e., $P(\rho_e^\omega > 0) > 0.5$, and, on the other hand, the average absolute magnitude of disassortative edges is higher than that of assortative edges, i.e., $\overline{(\rho_e^\omega)_-} > \overline{(\rho_e^\omega)_+}$. Furthermore, most of the nodes are disassortative, since $P(\rho_v^\omega > 0) > 0.5$.

Measure	$\alpha = 0$		$\alpha = 1$	
	$\beta = 0$	$\beta = 1$	$\beta = 0$	$\beta = 1$
r^ω	-0.042	-0.079	-0.039	-0.074
$P(\rho_e^\omega > 0)$	0.671	0.718	0.706	0.748
$\overline{(\rho_e^\omega)_+}$	6.48e-06	5.57e-06	5.53e-06	4.87e-06
$\overline{(\rho_e^\omega)_-}$	1.95e-05	2.81e-05	1.98e-05	2.91e-05
$P(\rho_v^\omega > 0)$	0.692	0.702	0.714	0.725

Table 4.3. Generalized assortativity analysis of the WSF model. Generalized assortativity coefficient r^ω, fraction of local assortative edges $P(\rho_e^\omega > 0)$, average absolute magnitude of assortative edges $\overline{(\rho_e^\omega)_+}$, average absolute magnitude of disassortative edges $\overline{(\rho_e^\omega)_-}$, fraction of local assortative vertices $P(\rho_v^\omega > 0)$ for the WSF model, for all four parameter combinations (α, β). An ensemble of 100 samples of the WSF model with $m_0 = 5$, $T = 10000$, $m = 2$ and $p = 0.5$ is drawn. The results are averaged over the samples of the ensemble.

The BA model, of which the WSF model is an extension of, can be shown to be non-assortative in the limit of large n, cf. Newman (2002). However, due to structural constraints such as the finite size of the network samples, the model does not produce purely non-assortative networks, cf. Maslov and Sneppen (2004), Serrano et al. (2006) and Yang et al. (2017). Apparently, the WSF model shares this property.

Unlike the WRG model, Figure 4.4 shows patterns in the local assortativity structures for the WSF model. Note that in preferential attachment models, if vertices and edges are numbered consecutively when entering the network or when forming, then the respective indices correspond to the times at which a vertex was created or at which an edge was formed. For example, in Figures 4.4a and 4.4b it can be seen that nodes that join the network earlier tend to be disassortative, and edges that form early tend to be assortative, cf. Noldus and van Mieghem (2015), who note a similar pattern in the BA model.

On the other hand, plotting the edge assortativeness values against the corresponding edge weight, cf. Figure 4.4c shows that highly weighted edges tend to be disassortative. Similarly, for the vertex assortativeness values, when plotted against the average excess strength of a node, cf. Figure 4.4d shows that the vertices with higher excess strength tend to be disassortative. However, the analysis of the histograms in Figures 4.4e and 4.4f indicates that the majority of edges and vertices are non-assortative.

Moreover, most of the assortative edges can be traced back to connections between the disassortative hubs, which in turn are the product of the initialization of the model,

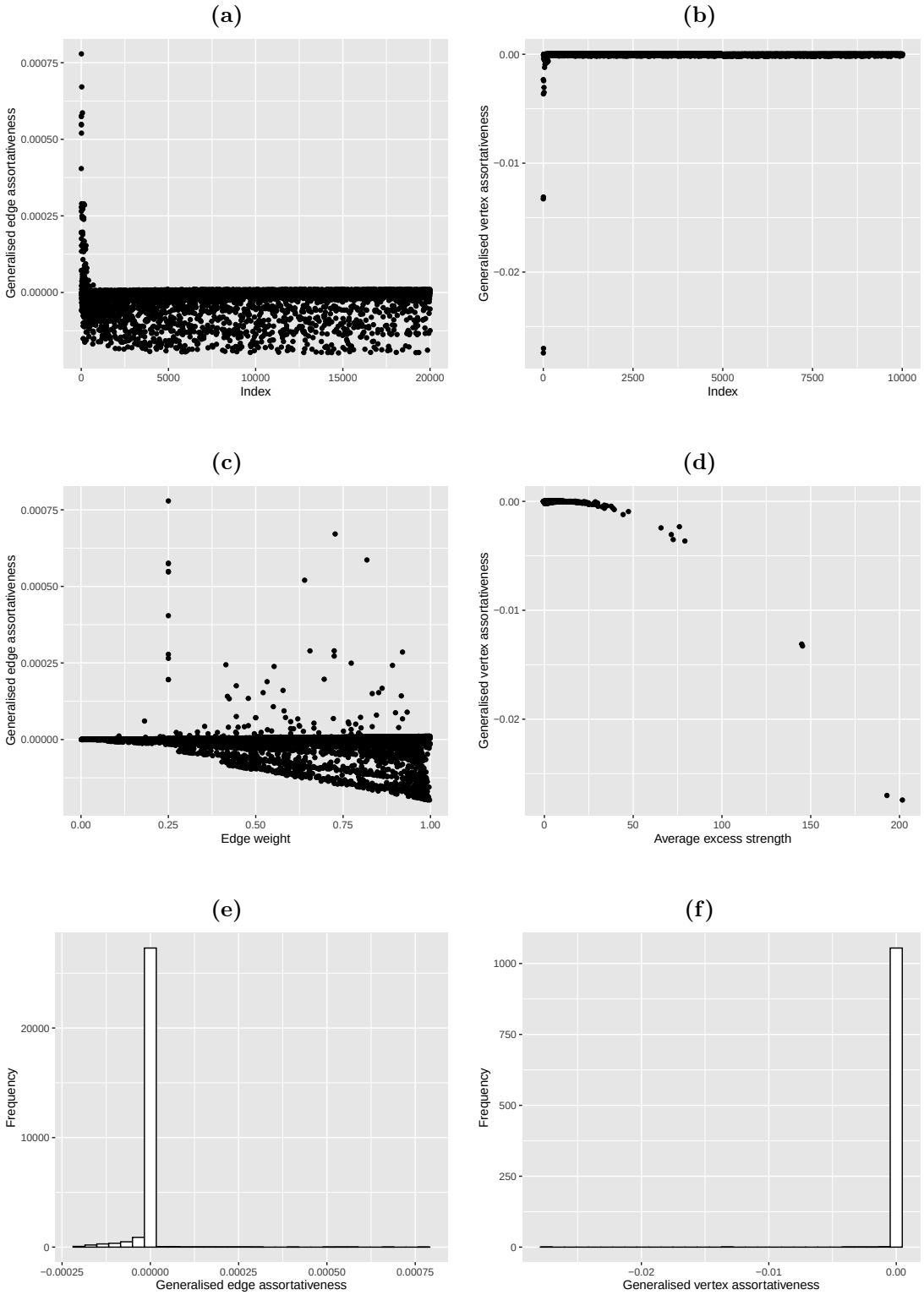

Figure 4.4. Generalized local assortativity plots of the WSF model. The plots are for a single sample of the WSF model with $m_0 = 5$, $T = 10000$, $m = 2$ and $p = 0.5$, for the parameter combination $(\alpha = 1, \beta = 1)$.

i.e., vertices that belong to the initial set of vertices, m_0. Apparently, it takes some time for these initialization effects to average out, and $T = 10000$ does not seem to be long enough for the model to adopt an overall non-assortative structure. Xu, Zhang, Sun, and Small (2009) and others consider cases in which the assortativity structure of (scale free) networks is significantly influenced by super rich nodes. They argue that it may be sensible to exclude these super rich nodes from consideration when calculating certain network measures, e.g, assortativity. Considering the above, this might also be useful if the WSF model is to be used.

Interestingly, both the WRG and the WSF model show very different local assortativity patterns, even though they are weighted extensions of models that are considered to generate global non-assortative networks. This implies that networks may exhibit a similar global assortativity, but the underlying local structures can differ substantially. Accordingly, it seems sensible to also consider the local assortativity structures of a network in order to describe its topology as precisely as possible. In the following, we turn our focus to analysing the local assortativity patterns of two real-world networks.

4.3.2 Real World Networks

To exemplarily demonstrate the analysis of generalized local assortativity, we consider two weighted real-world networks, one undirected, the other directed. We reconsider therefore the *NetScience* network of Chapter 3 as an example for an undirected network as well as the neural network of the nematode worm *Caenorhabditis elegans* (C. Elegans) as an example for a directed network. Both networks are commonly used examples in the literature. In addition, the datasets are publicly available, which ensures that the results below can be easily reproduced.

4.3.2.1 NetScience Scientific Collaboration Network

Recall from the previous chapter, that the NetScience network is an undirected collaboration network of scientists working on network theory, where vertices represent scientists and edges indicate if both co-authored one or more publications, cf. Newman (2001). The intensity of the relation between two scientists is incorporated by positive edge weights. In particular, degrees in the network correspond to the number of different co-authors of a scientist, whereas strengths correspond to the number of papers a scientist has co-authored with others, cf. Newman (2001).

Figure 4.5 shows a visualization of the graph structure of the *NetScience* network. It can be clearly seen that the network consists of a larger connected component and many smaller components, which are often basic configurations such as dyads, triangles, edge-triangles or bow ties. According to our empirical results, presented in Chapter 3, the *NetScience* network is an overall assortative network indicating that scientists have a tendency to collaborate with others that are similar based on the number of co-authors

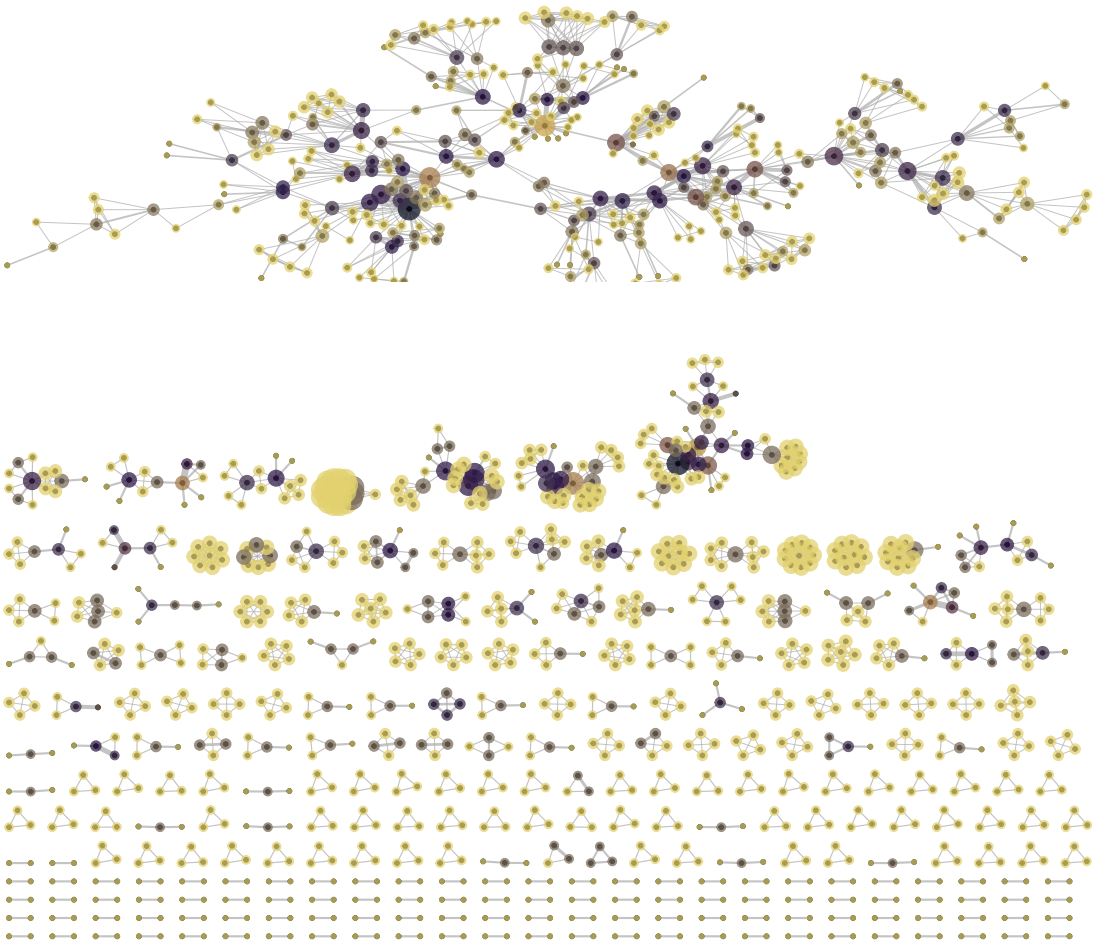

Figure 4.5. Visualization of the graph structure of the *NetScience* network. The figure shows both the largest connected component of the network, which consists of $n_1 = 379$ vertices out of the $n = 1589$ vertices of the complete network, and the remaining small components of which the network also is composed of (128 isolated vertices have been omitted in the figure). The (total) vertex strengths are indicated by colour-coded hulls, where lighter colours indicate lower strengths, and darker colours indicate higher strengths. The size of the coloured hull of a vertex is proportional to its (total) degree. Moreover, thicker edges indicate higher edge weights.

(degree) or based on the number of papers they have been co-authors of (strength), since both the benchmark assortativity coefficient, $r^{\omega}_{(0,0)} = 0.4616$, and the generalized assortativity coefficient, $r^{\omega}_{(1,1)} = 0.1928$, have positive values.

Table 4.4 presents the results of the local assortativity analysis of this network. Well over 70 percent of the edges are assortative, since $P(\rho^{\omega}_e > 0) > 0.7$, for all parameter combinations (α, β). The proportion of assortative vertices is of a similar order of magnitude, with the proportion of $P(\rho^{\omega}_v > 0) = 68.9$ percent for the combination $(1, 0)$ standing out as rather low.

Recall from Chapter 3, that there is a consistently disassortative *connection effect* for the network. However, there is an inconsistent *amplification effect*, since it is disassortative if degrees are used as vertex values but assortative if strengths are used. Interestingly, this can be confirmed and even specified if we compare the average absolute magnitude of assortative and disassortative edges. We then notice that the ratio changes if we use weighted rather than unweighted vertex values, i.e., excess strengths instead of degrees. For example, the average absolute magnitude of assortative edges is higher than that for disassortative edges when considering the combinations $(0, 0)$ and $(0, 1)$. On the other hand, if we look at the parameter combinations $(1, 0)$ and $(1, 1)$, we find that the average absolute magnitude of disassortative edges is greater than that of the assortative edges. This appears to be an indication of the connection effect.

In contrast, if we compare the average absolute magnitudes of assortative and disassortative edges for a given value of the parameter α, the amplification effect becomes apparent. For example, for $\alpha = 0$, the difference in the average absolute magnitudes between assortative and disassortative edges is reduced if $\beta = 1$ instead of $\beta = 0$, since the magnitude of assortative edges is reduced in this case. For $\alpha = 1$, on the other hand, the difference in the average absolute magnitudes is reduced if $\beta = 1$ instead of $\beta = 0$, because the magnitude of assortative edges increases more than for disassortative edges.

Figures 4.6a and 4.6b, depict the vertex assortativeness values plotted against the average excess degree (or strength) of a vertex. Moreover, the edge assortativeness values are plotted against the corresponding weight of an edge, which is shown in Figure 4.6c. By considering Figures 4.6a and 4.6b, for the combinations $(0, 1)$ and $(1, 1)$, it becomes apparent that the higher the average excess degree or strength of a vertex, the more assortative it is. For combinations $(0, 0)$ and $(1, 0)$, vertices tend to be non-assortative up to a medium average excess degree or strength, then assortative, and then non-assortative again. In terms of content, there seems to be a certain degree or strength where authors prefer to form connections with other equally well-connected authors. Below or above, research collaborations seem to be of a more disassortative nature, both in terms of degrees and in terms of strength. However, recurring collaborations tend to exist between well-connected authors, recognizable by the slope of the curves when the weighted correlation is calculated, i.e., for parameters $(0, 1)$ and $(1, 1)$.

From Figure 4.6c, we see that edges tend to be more assortative the greater the edge weight, with this effect being stronger in the case of degrees than in the case of strengths. Again, the inconsistent amplification effect can be observed since the curve for the combination $(0, 1)$ is above that of $(0, 0)$, but that for $(1, 1)$ is below that for $(1, 0)$.

Also interesting to examine in general is the question of which vertices or edges are particularly assortative or disassortative. For the network under consideration a particular assortative vertex corresponds to an author collaborating usually with others

Measure	$\alpha = 0$		$\alpha = 1$	
	$\beta = 0$	$\beta = 1$	$\beta = 0$	$\beta = 1$
		NetScience		
r^ω	0.462	0.340	0.102	0.193
$P(\rho_e^\omega > 0)$	0.772	0.772	0.713	0.749
$\overline{(\rho_e^\omega)_+}$	2.76e-04	2.18e-04	1.16e-04	1.55e-04
$\overline{(\rho_e^\omega)_-}$	1.96e-04	1.93e-04	1.59e-04	1.83e-04
$P(\rho_v^\omega > 0)$	0.755	0.737	0.689	0.738
		C. Elegans		
out–in				
r^ω	-0.233	-0.355	-0.181	-0.292
$P(\rho_e^\omega > 0)$	0.511	0.494	0.610	0.633
$\overline{(\rho_e^\omega)_+}$	1.19e-04	1.18e-04	6.18e-05	8.21e-05
$\overline{(\rho_e^\omega)_-}$	3.27e-04	4.14e-04	2.94e-04	4.80e-04
$P(\rho_v^\omega > 0)$	0.306	0.350	0.455	0.495
out–out				
r^ω	0.099	0.269	0.065	0.148
$P(\rho_e^\omega > 0)$	0.562	0.564	0.591	0.593
$\overline{(\rho_e^\omega)_+}$	2.74e-04	3.50e-04	1.99e-04	2.24e-04
$\overline{(\rho_e^\omega)_-}$	2.55e-04	1.89e-04	2.20e-04	1.71e-04
$P(\rho_v^\omega > 0)$	0.643	0.640	0.646	0.640
in-in				
r^ω	-0.092	-0.132	-0.068	-0.098
$P(\rho_e^\omega > 0)$	0.572	0.677	0.694	0.734
$\overline{(\rho_e^\omega)_+}$	1.14e-04	1.12e-04	6.14e-05	9.66e-05
$\overline{(\rho_e^\omega)_-}$	2.44e-04	4.08e-04	2.34e-04	4.23e-04
$P(\rho_v^\omega > 0)$	0.549	0.616	0.582	0.636
in–out				
r^ω	-0.026	0.138	0.061	0.125
$P(\rho_e^\omega > 0)$	0.531	0.530	0.645	0.658
$\overline{(\rho_e^\omega)_+}$	2.28e-04	3.19e-04	1.66e-04	1.92e-04
$\overline{(\rho_e^\omega)_-}$	2.82e-04	2.35e-04	2.27e-04	2.13e-04
$P(\rho_v^\omega > 0)$	0.532	0.549	0.660	0.653

Table 4.4. Generalized local assortativity analysis of real-world networks. Reported are the generalized assortativity coefficient r^ω, fraction of local assortative edges $P(\rho_e^\omega > 0)$, average absolute magnitude of assortative edges $\overline{(\rho_e^\omega)_+}$, average absolute magnitude of disassortative edges $\overline{(\rho_e^\omega)_-}$, fraction of local assortative vertices $P(\rho_v^\omega > 0)$, for all four parameter combinations (α, β), for two real-world weighted networks, one undirected, the other one directed. The networks are: a co-authorship network of scientists working on network theory (Newman, 2001), in which authors are connected if they have co-authored one or more papers; the neural network of the nematode worm C. Elegans (Watts & Strogatz, 1998; White et al., 1986), in which edges indicate that two neurons are connected by either a synapse or a gap junction.

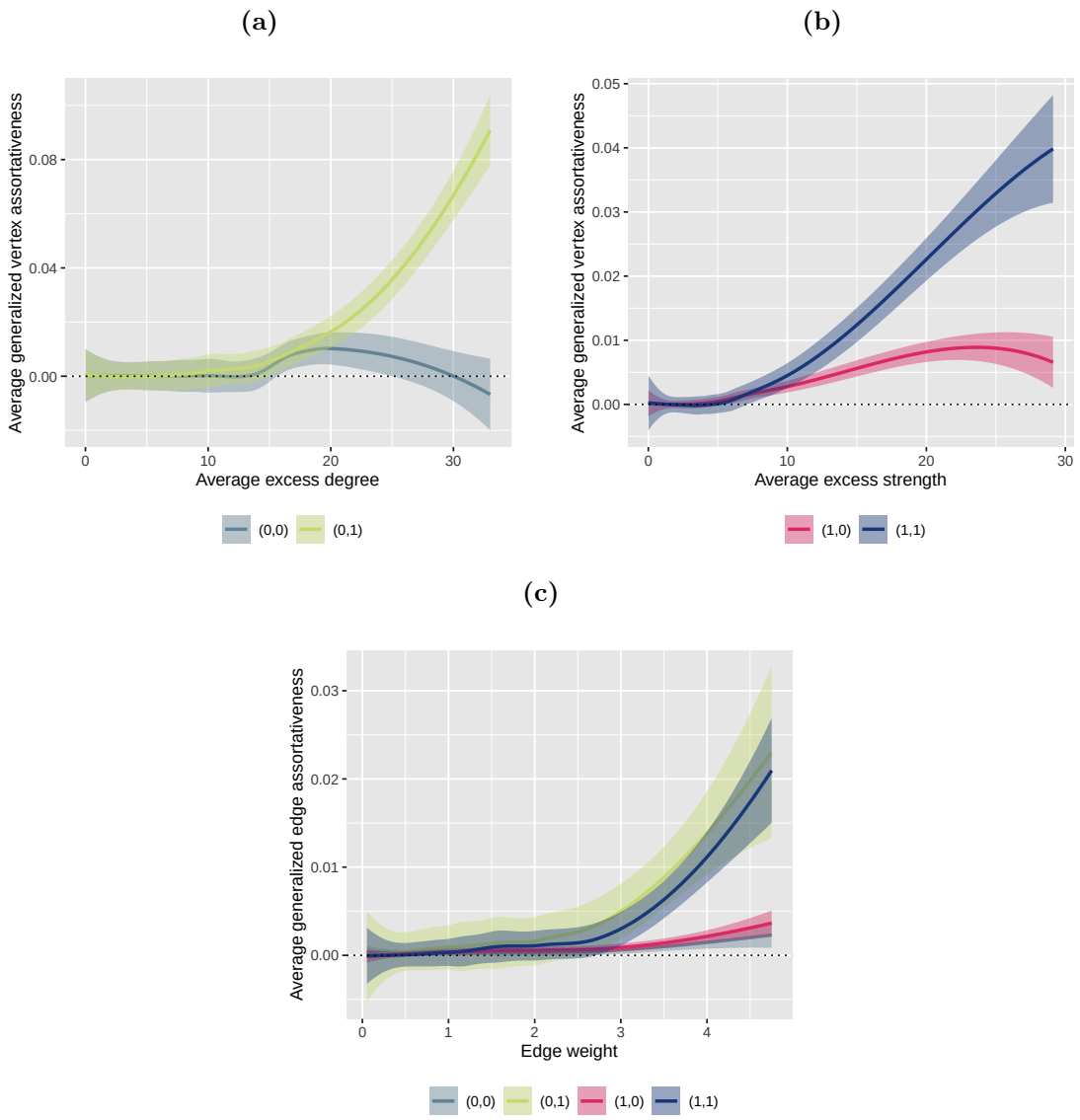

Figure 4.6. Generalized vertex and edge assortativeness profiles of the *NetScience* network. Generalized vertex degree assortativeness (a) and strength assortativeness (b) and edge assortativeness (c) profiles of the *NetScience* network for all four parameter combinations (α, β). The profiles are obtained by smoothing the data with loess regression (the shaded area indicates 95 percent confidence bands).

that have a similar number of co-authors (degree assortative) or a similar number of co-authored publications (strength assortative). Disassortative vertices, on the other hand, correspond to authors that usually collaborate with others who are unlike them, i.e., authors with many co-authors (degree disassortative) or co-authored publications (strength disassortative) tend to collaborate with others that have few co-authors or few co-authored publications, respectively, and vice versa. Assortative edges connect authors with a similar number of co-authors (degree assortative) or co-authored pub-

lications (strength assortative), whereas disassortative edges connect authors that are dissimilar. However, since we will not go into this further below, the interested reader will find tables listing the top assortative and disassortative vertices and edges in the appendix of this work, cf. Tables B.1 and B.2.

4.3.2.2 Caenorhabditis Elegans Neural Network

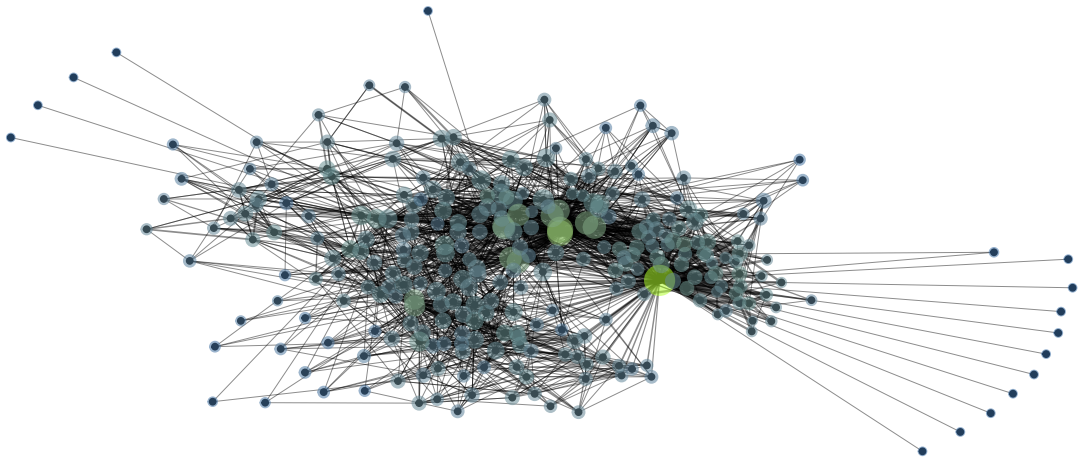

Figure 4.7. Visualization of the graph structure of the *C. Elegans* network. The (total) vertex strengths are indicated by colour-coded hulls, where lighter colours indicate higher strengths, and darker colours indicate lower strengths. The size of the coloured hull of a vertex is proportional to its (total) degree. Moreover, thicker edges indicate higher edge weights.

The neural network of the nematode worm *Caenorhabditis elegans* (C. Elegans) is an example of a completely mapped neural network, cf. Watts and Strogatz (1998) and White et al. (1986). A node in the directed and weighted network represents a neuron and an edge between two neurons indicates that they are connected by either a synapse or a gap junction. However, we could not find any information on how edge weights are defined in this network, so we must assume that they somehow reflect the cost or capacity of communication between the neurons (e.g., distance, speed, volume, or bandwidth) as it is the usual way to define edge weights in brain networks of that type, cf. Faskowitz, Betzel, and Sporns (2022).

Figure 4.7 shows a visualization of the graph structure of the *C. Elegans* network. We have not analysed the *C. Elegans* network in detail in Chapter 3, and thus, will briefly describe the generalized assortativity structure of the network. Overall, the network is disassortative for the modes *out–in* and *in–in* for all combinations (α, β). Moreover, the network is assortative for the modes *out–out* and *in–out* for all combinations (α, β), except for the mode *in–out* for the combination $(0, 0)$, for which the network is also disassortative. Table 4.4 shows the results of the local assortativity analysis of the *C.*

Elegans network. However, instead of giving a repetitive local assortativity analysis, which would be largely identical to the procedure just described for the *NetScience* network but for four modes instead of just one, we proceed directly with describing the local vertex and edge assortativeness profiles.

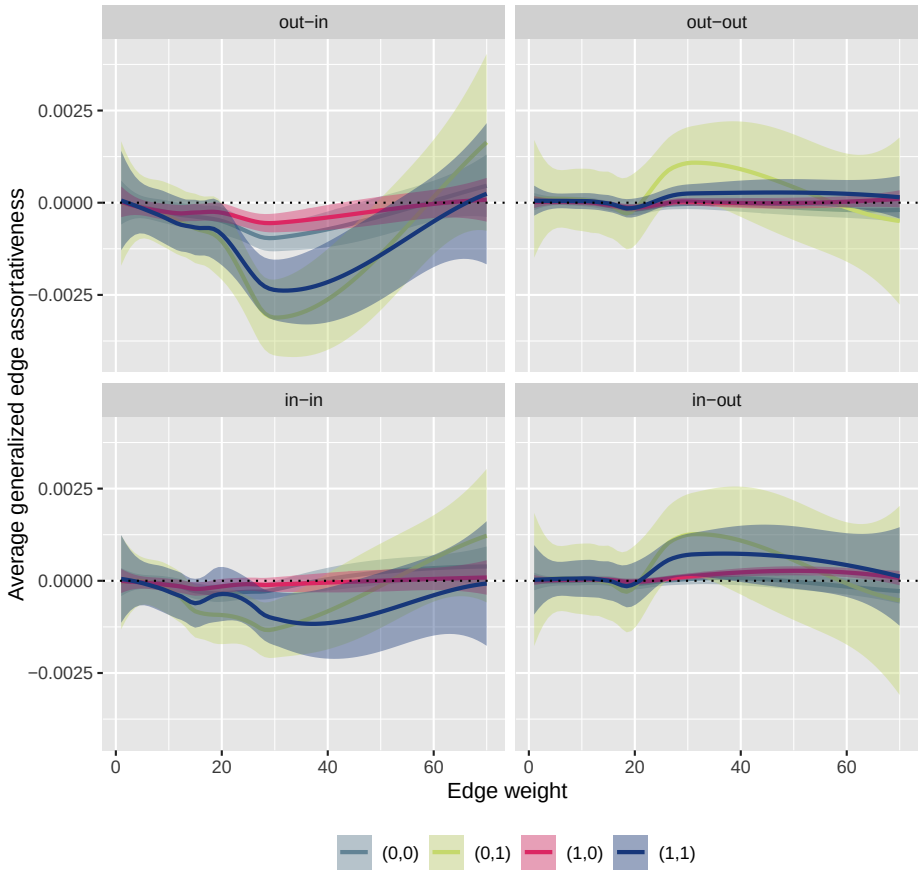

Figure 4.8. Generalized edge assortativeness profiles of the *C. Elegans* network. Generalized edge assortativeness profiles of the *C. Elegans* neural network for all four parameter combinations (α, β) for all four modes of assortativity. The profiles are obtained by smoothing the data with loess regression (the shaded area indicates 90 percent confidence bands).

Figure 4.8 shows the average edge assortativeness values plotted against the corresponding edge weight. In Figures 4.9 and 4.10 the average vertex assortativeness values are plotted against the corresponding average excess out-degree or -strength of a vertex. For reasons of clarity, we consider the averages of the edge and vertex assortativeness values for this network. Since we are considering four modes of assortativity at the same time, it would not otherwise be possible to clearly identify patterns.

Considering the edge assortativeness values first, we see that the modes *out–in* and *in–in* as well as *out–out* and *in–out* turn out be structurally quite similar. For the

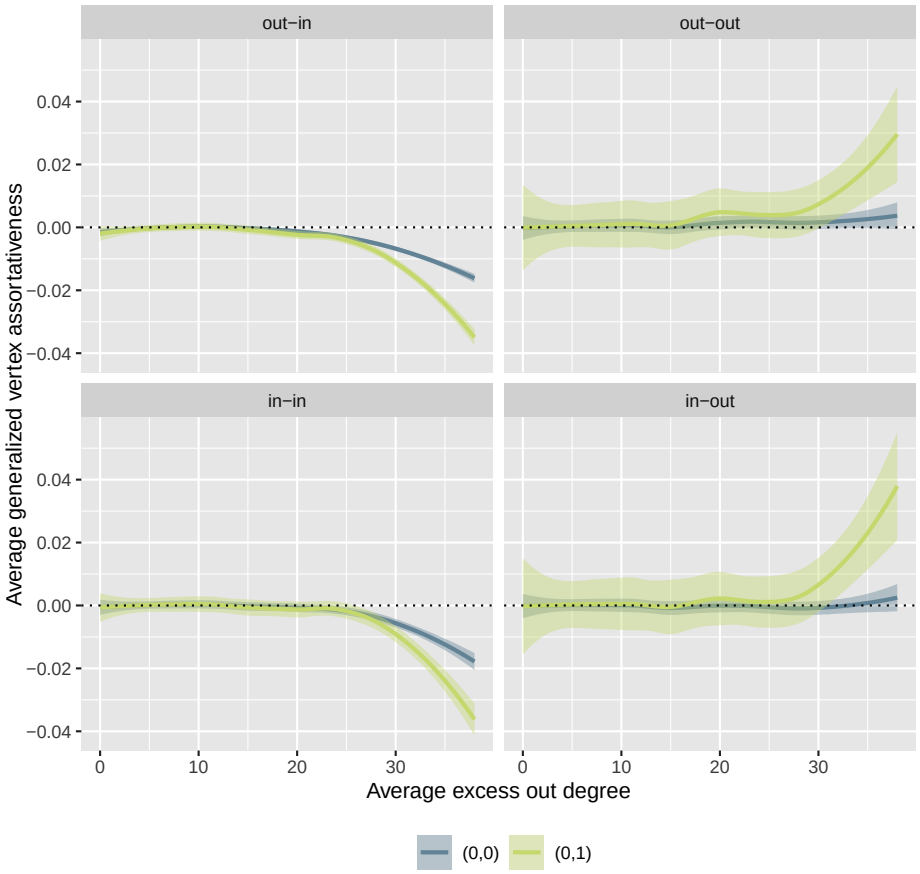

Figure 4.9. Generalized vertex degree assortativeness profiles of the *C. Elegans* network. Generalized vertex degree assortativeness profiles of the *C. Elegans* neural network for the two parameter combinations (α, β), for which degrees are used as vertex values, for all four modes of assortativity. The profiles are obtained by smoothing the data with loess regression (the shaded area indicates 95 percent confidence bands).

out–in mode, edges with low edge weights tend to be non-assortative, for the area of medium edge weights disassortative, and beyond that again non-assortative. For medium edge weights, the *out–in* edge assortativeness values decrease more clearly for the combinations $(0, 1)$ and $(1, 1)$ than for the combinations $(0, 0)$ and $(1, 0)$. This is again an indication of the amplification effect, this time consistent since the curve for $(0, 1)$ is below that of $(0, 0)$ just as the curve for $(1, 1)$ is below that of $(1, 0)$. The above is structurally similar for the *in–in* mode, but not as pronounced. For the *out–out* mode, the edge assortativeness values tend to be non-assortative for all combinations (α, β), except for $(0, 1)$ in the middle edge weight range, for which the edges tend to be assortative. In addition, for the structurally similar *in–out* mode, the curve bends slightly in the area of middle edge weights also for the parameter combination $(1, 1)$.

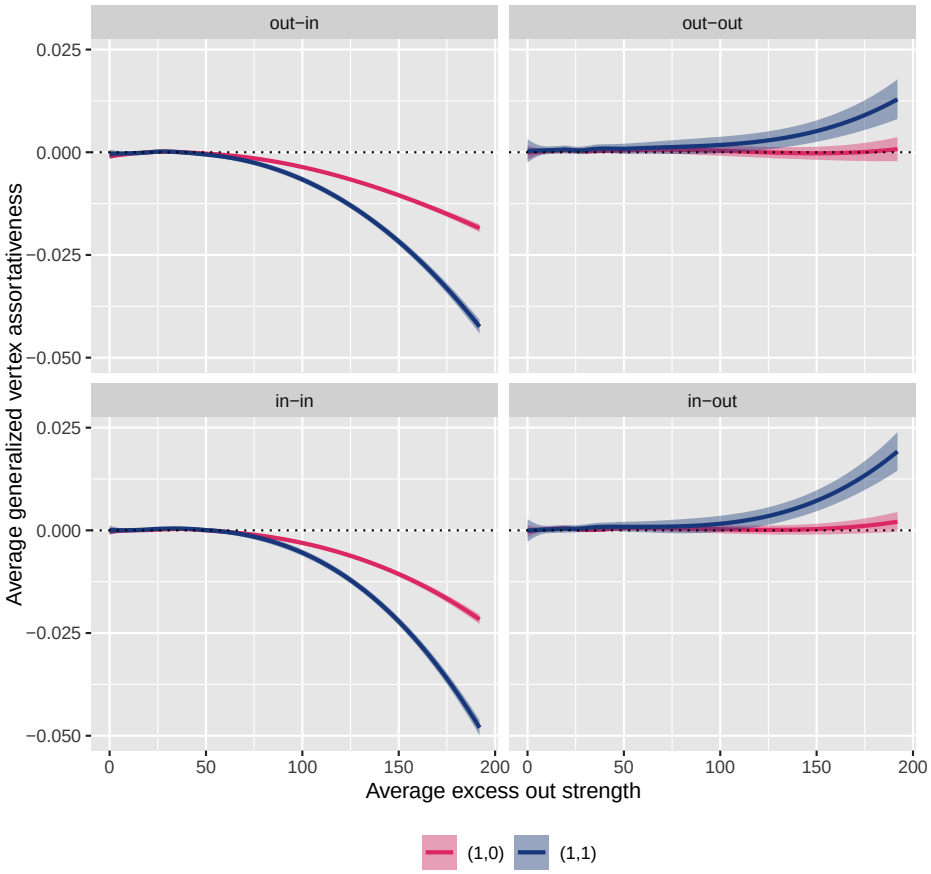

Figure 4.10. Generalized vertex strength assortativeness profiles of the *C. Elegans* network. Generalized vertex strength assortativeness profiles of the *C. Elegans* neural network for the two parameter combinations (α, β), for which strengths are used as vertex values, for all four modes of assortativity. The profiles are obtained by smoothing the data with loess regression (the shaded area indicates 95 percent confidence bands).

By considering Figures 4.9 and 4.10, we see that with increasing average excess out-degree or -strength, vertices tend to become more disassortative for the *out–in* and *in–in* modes of assortativity. Conversely, for the modes *out–out* and *in–out*, vertices tend to be more assortative with increasing average excess out-degree or -strength. However, for all modes, the pattern is more pronounced when the weighted correlation is considered, i.e., $\beta = 1$ instead of $\beta = 0$.

The local assortativity analysis revealed how the global assortativity structure of a network is composed. The *C. Elegans* network is *out–in* disassortative because edges with a mid-range edge weight are disassortative, while low-weighted edges and high-weighted edges tend to be non-assortative (see Figure 4.8). The netscience network, on the other hand, is assortative, since edges tend to be more assortative the higher the

edge weight. The effect is more or less pronounced for both networks, depending on whether degrees or strengths are used as vertex values. Being able to recognize these fine differences has only become possible through the generalized local assortativity consideration. Thus, the analysis of the local assortativity can therefore help to further break down the assortativity structure for a network. For a comparison across networks, this also allows to further differentiate the topology of networks that exhibit a similar global assortativity, as we have shown for the theoretical models. In summary, the generalized local assortativity consideration provides valuable information when examining the assortativity of a network.

4.4 Discussion and Future Work

In this chapter, we have extended local assortativity for weighted networks. By having unified two approaches used in the literature, we were able to derive distinct measures that allow us to determine the assortativeness of individual edges and vertices as well as of entire components of a weighted network. We demonstrated the usefulness of these measures by applying them to various theoretical and real-world networks. Along the way, we also explained how to compute local assortativity profiles, which are informative about the pattern of local assortativity either with respect to edge weight or vertex strength. Such profiles have been analysed by Piraveenan et al. (2008) for their unweighted vertex-based local assortativity measure. Since our generalized local assortativity can be either vertex-based or edge-based, we have extended the assortativity profiles accordingly in order to be able to gain as much information from them as possible, when considering weighted networks.

Thedchanamoorthy et al. (2014) suggest an alternative definition of local assortativity that, contrary to the definition by Piraveenan et al. (2008, 2010), does not pivot on the global mean excess degree (or strength) of the ends of an edge, $\bar{U}_{q_k}$. They claim, that the definition of Piraveenan et al. (2008, 2010) is counter-intuitive, in that sense, that an edge, which connects two vertices with different degrees, but both higher than $\bar{U}_{q_k}$, is considered assortative, whereas an edge that connects two vertices with similar degrees, where one has a degree higher than $\bar{U}_{q_k}$, and the other one has a degree lower than $\bar{U}_{q_k}$, is considered disassortative. We have shown, however, that this definition inherently rests upon the definition of assortativity by Newman (2002), and departing from it does not seem quite sensible, as it is widely accepted. Moreover, Thedchanamoorthy et al. (2014) state that their approach is computationally less expensive, which is also not quite right, as the generalized edge assortativeness values, $\rho_e^{\omega}(\alpha, \beta, mode)$, are immediately available when computing the assortativity coefficient of a network, and thus, our definition of local assortativity does not bear any additional computational costs. We, therefore, did not consider the approach by Thedchanamoorthy et al. (2014) in this thesis.

We noticed that by analysing the local assortativity structure of a network via the generalized edge assortativeness values, $\rho_e^{\omega}(\alpha, \beta, mode)$, only the direct contribution of an edge e to the global assortativity coefficient is captured. More precisely, because of the way the generalized assortativeness values are defined, i.e., as a product of the scaled differences of the excess degrees (or strengths) of both ends of an edge and their respective means, edges are considered in isolation. However, if a vertex u is incident with more than one edge, then, the presence of edge e increases the excess degree (or strength) of that vertex when considering any edge other than e, which can be seen as an indirect contribution to the global assortativity. This potential indirect contribution is neglected in the definition of the generalized assortativeness values, but is also neglected in the previous local assortativity definitions by Piraveenan et al. (2008, 2010, 2012) and Thedchanamoorthy et al. (2014). In order to decide if this is a drawback, a more in-depth analysis is necessary. We plan on revisiting this topic in future research where we will compare the generalized assortativeness values to an alternative local edge assortativity measure that also captures indirect contributions to the global assortativity. For example, an unsophisticated alternative local edge assortativity measure is the following:

$$\rho_e^J = \tilde{r} \frac{\Delta\tilde{r}(e)}{\sum_{i=1}^{M} \Delta\tilde{r}(i)}, \tag{4.25}$$

where $\tilde{r}$ is any global assortativity coefficient of choice, e.g., the generalized assortativity coefficient, then $\tilde{r} = r^{\omega}_{(\alpha,\beta)}$; $\Delta\tilde{r}(e) = \tilde{r} - \tilde{r}_{(-e)}$ is the difference between the global assortativity $\tilde{r}$ of a network and the jackknife statistic $\tilde{r}_{(-e)}$, i.e., the global assortativity of the same network but with the e-th edge removed. Apparently, the measure in Equation (4.25) is based on the jackknife method, and thus, we denote it by ρ_e^J and refer to it as the jackknife local (edge) assortativeness values. The measure ρ_e^J captures the direct as well as the above-mentioned indirect contribution of an edge e to the global assortativity of a network. However, as compared to the generalized local assortativeness values as in Equation (4.20), the computational cost is considerably larger for the jackknife local edge assortativeness values. In fact, it increases by a factor of $(M + 1)$. Nevertheless, for small- and medium-sized networks, the jackknife local edge assortativeness values can serve as a benchmark for determining the accuracy of the generalized local assortativeness values, though. So far, we conjecture that the indirect influence on the assortativity of an edge becomes negligible the bigger the network is, which leads us to believe that the use of the generalized local assortativeness values for measuring the local edge assortativity is appropriate in most cases, especially when analysing very large real world networks, for which computing the local assortativity based on the jackknife statistics would result in a prohibitively large computational cost.

Moreover, as for global assortativity, it also applies to local assortativity that the concept of generalizing local assortativity to weighted networks, shown in this work, easily extends to the more complex definitions of assortativity of Meghanathan (2016) or Arcagni et al. (2017, 2021). Recall, that they are, at their core, still based on the Pearson correlation.

Finally, in future research we will address the assessment of significance of local assortativity profiles. Since local assortativity is a *third-order* graph metric one would have to employ a feature preserving graph rewiring algorithm in order to decide whether the observed local assortativity profile significantly deviates from one of a suitable null model (either generative or by link-rewiring). However, such a rewiring algorithm would have to preserve also the global assortativity of the network, and thus, the link-rewiring algorithm by Rubinov and Sporns (2011), which we utilized in order to assess the significance of the global generalized assortativity coefficient, is not applicable here as it only preserves the degree and strength distribution of the observed network. However, a review of the relevant literature shows that, so far, there exists no null model of weighted networks that preserves the observed generalized assortativity.

In future research we will also focus on epidemic spreading. Wu, Xu, and Wang (2005) study the properties of weighted scale free networks, in particular, the epidemic spreading process via a *susceptible-infected* (SI) model. It would be interesting to also analyse the epidemic spreading in scale free networks that also show assortative or disassortative mixing. We might consider the *mutual attraction* model, introduced by Wang, Hu, Wang, and Yan (2006) for generating assortative and disassortative networks, for which we will analyse the generalized (local) assortativity. We are curious if a network's resilience against exogenous shocks can indeed be increased by the removal of edges with certain local assortativeness values, i.e., the epidemic spreading process can be slowed down. Based on such findings, policy advice can be given, which can also be interesting for financial networks such as the cryptocurrency network.

And we will therefore now move our attention towards the analysis of the assortativity structure of the cryptocurrency network. To this end we will apply not only our global measure of assortativity but also the generalized local assortativity measures derived in this chapter, in order to analyse its resilience.

5 The Robustness of the Network Structure of the Cryptocurrency Market

The market of cryptocurrencies is a $932B market that comprises approximately $10,000$ active cryptocurrency projects.[33] Thus, cryptocurrencies appear to be more than a fad, and one can no longer deny the market's increasing importance for the global economy. In this context, great interest is taken in assessing the stability of the market, i.e., its systemic risk, as cryptocurrencies are well known for their high volatility. Another question that arises is whether and how cryptocurrencies are related to each other. Combining the above, the question arises if there is a network formed by cryptocurrencies and, if so, whether it is robust.

This chapter is dedicated to the analysis of the robustness of the network topology of cryptocurrencies by means of analysing its generalized assortativity structure. To this end, we employ the Diebold and Yilmaz (2014) (DY) *connectedness* index methodology in order to construct the cryptocurrency network's adjacency matrix from cryptocurrency price data. The remainder of this chapter is therefore structured as follows: Section 5.1 provides a review of the related literature on financial networks. In Section 5.2 we give a detailed description of the DY methodology and the estimation of high-dimensional financial networks based on vector autoregression with regularization. Building on this foundation, the network of cryptocurrencies is analysed thoroughly in Section 5.3. We analyse the relationship between financial connectedness, as a measure of systemic risk, and generalized assortativity of a network, as an indicator of network stability. By analysing the evolvement of the generalized assortativity coefficient of the volatility connectedness network, we are able to empirically show that both measures are inversely related, which opens up new possibilities of monitoring systemic risk, especially since there are indications that connectedness might not be suitable for an absolute comparison across different markets, which we will also discuss. In Section 5.4 we discuss our empirical findings and give suggestions for future research.

5.1 Background and Related Literature

The recent financial crises have led to a greater awareness of systemic risk and financial contagion, and as a result, network analysis has also found its way into financial market analysis and has become increasingly important. Even textbooks on network analysis,

[33] Information sourced from `coinmarketcap.com`, current as of June 30, 2022.

such as, e.g., Caldarelli (2007), devote an entire chapter to this subject. The author presents an overview of different types of financial networks. There are simple networks in which the connections between the objects are directly observable. For example, as with the *board of directors*, where a network is formed either by joining directors sitting on the same board or by joining boards that share a common director, cf. Caldarelli (2007, p. 234). Other examples of networks with somehow directly observable relations are, e.g., networks formed by global import and export trade relationships among countries such as the *world trade web*, cf. Serrano and Boguñá (2003) and Garlaschelli and Loffredo (2004). Or, networks representing interbank markets, where edges correspond to interbank lending, cf. Soramäki, Bech, Arnold, Glass, and Beyeler (2007), Bech and Atalay (2010), Craig and von Peter (2014), in 't Veld and van Lelyveld (2014) and Fricke and Lux (2015).

Interbank markets are special in that the bilateral trade relationships can be observed directly, but the data usually is non-disclosed and often times only available to researchers in central banks. In such cases, the application of more sophisticated methods is needed in order to estimate the network structure from publicly available data. For example, Torri, Giacometti, and Paterlini (2018) estimate the dependence structure of a sample of European banks in terms of their partial correlations from credit default swap time series data.

Another frequently used method to infer the network structure in cases where direct relationships cannot be observed is by analysing cross-correlation patterns. There exists a strand of literature that analyses the stock network topology by means of minimum spanning tree (MST), c.f. Mantegna (1999), Brida and Risso (2010), Bonanno, Caldarelli, Lillo, and Mantegna (2003), Onnela, Chakraborti, Kaski, Kertész, and Kanto (2003) and Vandewalle, Brisbois, and Tordoir (2001), where a network is created by linking two companies based on their stock return correlation. Mantegna (1999) and Onnela et al. (2003) show that the resulting network structure exhibits groups corresponding to industry sectors. Moreover, using the MST methodology, Bonanno et al. (2003) find that popular models of portfolio dynamics fail to capture topological properties of real financial markets. Furthermore, the MST of such a stock network is scale-free, see Onnela et al. (2003) and Vandewalle et al. (2001), such that insights gained from studying (theoretical) scale-free networks can be applied stock networks as well. The MST methodology has also been used by Zięba, Kokoszczyński, and Śledziewska (2019) in order to analyse the cryptocurrency market.

Diebold and Yilmaz (2009, 2012, 2014, 2015a, 2015b) propose a framework for defining, measuring and monitoring *connectedness*. To this end they propose several measures at different levels of granularity, from disaggregated *pairwise connectedness* through aggregated *system-wide connectedness*. The authors refer to connectedness as describing how strongly or weakly a financial system is connected overall. The term is also as-

sociated with various types of financial risks (e.g., market risk, portfolio concentration risk, credit risk, business cycle risk or systemic risk), cf. Diebold and Yilmaz (2015a). But it is most commonly associated with *systemic risk* and some authors use the terms connectedness and systemic risk interchangeably, see, e.g., Baruník and Křehlík (2018).

Systemic risk is *"[the risk of] ... breakdowns in an entire system, as opposed to breakdowns in individual parts and components"* (George G. Kaufman & Kenneth E. Scott, 2003, p. 371), which aligns with our interpretation of systemic risk in this thesis. There exists a variety of approaches in order to quantify systemic risk, for example, the *marginal expected shortfall* (MES) proposed by V. V. Acharya, Pedersen, Philippon, and Richardson (2017), which tracks the sensitivity of a financial firm's returns to market-wide extreme or systemic events; the *SRISK* (SRISK) of V. Acharya, Engle, and Richardson (2012) and Brownlees and Engle (2017), which, depending on a systemic event, measures the capital shortfall that financial firm is expected to experience; the aggregated SRISK can be therefore viewed as the amount of capital that the government would have to provide to sustain the financial system; and the *conditional value-at-risk* (Δ CoVaR) of Adrian and Brunnermeier (2016), which is defined as the change in *value-at-risk* (VaR) of the financial system conditional on shifting from the median return of a firm to its return when in distress. These metrics are the most important market-data based measures in the systemic risk literature, see Benoit, Colliard, Hurlin, and Pérignon (2017) for a thorough review of this topic. According to Diebold and Yilmaz (2014), their connectedness measures and the above systemic risk measures are indeed different, but measure similar things and can therefore be related to each other. More precisely, MES measures exposures of firms to systemic shocks from the system, whereas Δ CoVaR measures contributions of firms to systemic events, which corresponds exactly to what is measured by pairwise connectedness. Moreover, system-wide connectedness provides a measure of systemic risk comparable to the aggregated SRISK. In the following, we therefore consider connectedness as a proxy for systemic risk and use this index to monitor crises in the cryptocurrency market.

Since Diebold and Yilmaz (2014) established the connection between their connectedness index methodology and network theory, this approach has also been used very frequently to estimate the underlying network structure of various markets. For example, Uluceviz and Yilmaz (2020) recently applied it to analyse the real-financial connectedness in the Swiss economy by means of analysing the connectedness between a real economic activity proxy (KOF barometer) and several financial variables (e.g., the Switzerland stock market index). Bostanci and Yilmaz (2020) estimate and analyse the global network structure of sovereign credit risk, a network constructed from daily log returns of sovereign credit default swaps (SCDS) spreads.

Recent studies, who apply the DY connectedness methodology to the cryptocurrency market, are, e.g., Koutmos (2018) and Kamisli, Kamisli, and Temizel (2019). Koutmos

(2018) studied the connectedness among 18 cryptocurrencies from August 2015 to July 2018 (1,076 daily observations). The author finds that Bitcoin (BTC) is the dominant contributor of return and volatility connectedness. Moreover, the degree of connectedness increases with media attention regarding cryptocurrencies. Also, connectedness among cryptocurrencies has risen over the years.

Kamisli et al. (2019) study the return and volatility connectedness between Bitcoin (BTC) and stock markets (stock indices) from different (global) regions from analysing weekly data on Bitcoin (BTC) and regional stock index returns from August 2011 to February 2019. There appears to be limited pairwise directional return and volatility connectedness between Bitcoin and regional stock markets, where the strength of connectedness varies locally. For example, Bitcoin tends to receive more connectedness from Asian regions, whereas it tends to emit more connectedness to stock markets of America.

However, there are quite a number of studies examining the cryptocurrency market using alternative methods as well, for an extensive survey we refer to Kyriazis (2019). For example, Bouri, Gabauer, Gupta, and Tiwari (2021) analyse the time-varying volatility connectedness of 15 cryptocurrencies from August 2015 to March 2020 (1679 daily observations) based on the framework introduced by Gabauer (2020), which is an alternative to the DY framework based on the DCC-GARCH model originally proposed by Engle (2002).

What we do find, however, is that there is a lot of untapped potential. Many of the studies analyse the connectedness between cryptocurrencies or between cryptocurrencies and other variables (stock indexes, gold, exchange traded funds or other currencies such as USD, EUR, or GBP) and sometimes find more or less connectedness. More rarely, however, do we see network theoretical methods being applied to the underlying network, as suggested by Diebold and Yilmaz (2014).

To the best of our knowledge, by analysing the assortativity structure of the cryptocurrency network, we are the first to consider assortativity for a connectedness network. This is surprising, as assortativity is often associated with network robustness, where robustness is defined as the ability of a system to maintain its core functionality, even if individual components fail, cf. Barabási (2016). However, if connectedness measures systemic risk, which is the risk of a system losing its core functionality due to the failure of individual components, there must be a link between the two concepts that is worth investigating. Moreover, our study stands out from others, as we analyse a more exhaustive set of data, both in terms of the time span and in terms of the number of considered cryptocurrencies. Other studies either look at a similar length of time as we do, but only analyse a handful of cryptocurrencies, or consider a similar number of cryptocurrencies as we do, but for a much shorter period of time.

The problem that arises when considering a large amount of cryptocurrencies is that the model complexity increases very quickly, in the sense that the number of parameters to be estimated becomes very large. In cases where the available data is not sufficient to compensate for the loss of degrees of freedom, this leads to overfitting or even to the fact that the model can no longer be estimated. Regularization methods are then needed to be applied to restrict the number of parameters used for estimation, cf. Torri et al. (2018) and Sánchez García and Cruz Rambaud (2022). In the context of connectedness, Demirer, Diebold, Liu, and Yilmaz (2018) are the first to propose a regularization approach for the DY framework in order to estimate also high-dimensional networks.

5.2 Financial Networks Based on Variance Decompositions

Ever since vector autoregression (VAR) has been introduced by Sims (1980) it has become a popular method for modelling the time-varying relationship between multiple variables. Its fields of application are thereby manifold and range from the joint analysis of multivariate time series over forecasting to structural inference and policy analysis, cf. Stock and Watson (2001). An advantage of VAR models is that current and lagged values from multiple time series are used for the estimation, thereby capturing comovements of variables that would have gone undetected in the case of uni- or bivariate models, cf. Stock and Watson (2001).

In the following we will give a detailed description of the DY connectedness index framework. Therefore, the VAR(p) model is introduced in Section 5.2.1. Section 5.2.2 introduces generalized impulse response functions and variance decompositions, on which the DY connectedness measures are based on. An overview of the connectedness measures, and an explanation of how they relate to networks is given in Sections 5.2.3 and 5.2.4, respectively. Finally, since the estimated VAR(p) model is indispensable for the subsequent assessment of connectedness, we explore regularization techniques that ensure that the model can be estimated even in high dimensions in Section 5.2.5.

5.2.1 The VAR(p) Model

The foundation of the DY framework is the N-variable covariance stationary process, which is modelled by the VAR(p) model as:[34]

$$\boldsymbol{x}_t = \sum_{i=1}^{p} \boldsymbol{\Phi}_i \boldsymbol{x}_{t-i} + \boldsymbol{\varepsilon}_t, \tag{5.1}$$

[34]Note that we consider the mean-adjusted process here. Also, we use the same notation as in Pesaran and Shin (1998), for reasons of clarity and comprehensibility. However, the presentation of the fundamentals of the VAR(p) model is also based on Hamilton (1994), Lütkepohl (2007) and Tsay (2014).

where $\boldsymbol{x}_t = (x_{1,t}, \ldots, x_{N,t})'$ is a $(N \times 1)$ vector of *random variables* at points in time $t = 1, \ldots, T$, and $\boldsymbol{\Phi}_i$ are *fixed* $(N \times N)$ coefficient matrices at lags $i = 1, \ldots, p$. Eventually, the error term $\boldsymbol{\varepsilon}_t = (\varepsilon_{1,t}, \ldots, \varepsilon_{N,t})'$ is an N-dimensional *white noise* or *innovation process*, i.e., $E(\boldsymbol{\varepsilon}_t) = 0$, $E(\boldsymbol{\varepsilon}_t \boldsymbol{\varepsilon}_t') = \boldsymbol{\Sigma} = [\sigma_{ij}]$, $i, j = 1, \ldots, N$, for all t, and $E(\boldsymbol{\varepsilon}_t \boldsymbol{\varepsilon}_s') = 0$, for $s \neq t$. Moreover, the covariance matrix of the errors, $\boldsymbol{\Sigma}$, is assumed to be non-singular. Because $\boldsymbol{x}_t$ is assumed to be covariance stationary, Equation (5.1) can also be formulated based on its infinite vector moving average representation:

$$\boldsymbol{x}_t = \sum_{i=0}^{\infty} \boldsymbol{A}_i \boldsymbol{\varepsilon}_{t-i}, \tag{5.2}$$

where $\boldsymbol{A}_i$ are $(N \times N)$ matrices of moving average coefficients, which can be obtained using the coefficient matrices $\boldsymbol{\Phi}_i$, once the model has been estimated, by the recursive relations:

$$\boldsymbol{A}_i = \boldsymbol{\Phi}_1 \boldsymbol{A}_{i-1} + \boldsymbol{\Phi}_2 \boldsymbol{A}_{i-2} + \ldots + \boldsymbol{\Phi}_p \boldsymbol{A}_{i-p}, \tag{5.3}$$

where $\boldsymbol{A}_0 = \boldsymbol{I}_N$ and $\boldsymbol{A}_i = 0$ for $i < 0$. Sometimes Equation (5.3) is represented in a more convenient form, by using the lag operator L of $L^p \boldsymbol{x}_t = \boldsymbol{x}_{t-p}$. With the $(N \times N)$ matrix lag polynomial $\boldsymbol{\Phi}(L) = [\boldsymbol{I}_N - \boldsymbol{\Phi}_1 L - \ldots - \boldsymbol{\Phi}_p L^p]$ the model in Equation (5.1) can be rewritten as $\boldsymbol{\Phi}(L)\boldsymbol{x}_t = \boldsymbol{\varepsilon}_t$, and Equation (5.2) as $\boldsymbol{x}_t = \boldsymbol{A}(L)\boldsymbol{\varepsilon}_t$, where $\boldsymbol{\Phi}(L) = [\boldsymbol{A}(L)]^{-1}$, which demonstrates the recursive relations from Equation (5.3) in terms of the matrix lag polynomials. The matrix polynomial $\boldsymbol{A}(L)$ contains an infinite number of lags, and thus, has to be approximated by the moving average coefficients, $\boldsymbol{A}_h$, calculated at different horizons $h = 1, \ldots, H$.

5.2.2 Generalized Impulse Response Functions and Variance Decompositions

The DY connectedness measures are based on variance decompositions, which are transformations of the elements $\boldsymbol{A}_h$, cf. Baruník and Křehlík (2018). In order to produce these variance decompositions, the DY approach utilizes the generalized VAR framework by Koop, Pesaran, and Potter (1996) and Pesaran and Shin (1998) (KPPS), which has the advantage of being invariant to variable ordering.[35]

KPPS define the generalized impulse response function, $\boldsymbol{GI}_x$. To this end, let $\boldsymbol{\Omega}_{t-1}$ be the non-decreasing set of available information up to $t-1$, and δ_j denotes a shock

[35] In order to circumvent the problem of the dependence on the variable ordering, DY switched from using the identification scheme based on the Cholesky factorization suggested by Sims (1980), which orthogonalizes the system, to the KPPS framework, cf. Diebold and Yilmaz (2009, 2012). If the interest is in the topology of the resulting network, KPPS should be preferred, especially if there exist no profound economic theory on the true ordering of the variables of interest, since, with KPPS, the network is completely determined by the data, cf. Wiesen, Beaumont, Norrbin, and Srivastava (2018).

to the j-th element of $\boldsymbol{\varepsilon}_t$, then, the generalized impulse function of $\boldsymbol{x}_t$ at horizon h is defined as:

$$\boldsymbol{GI}_x(h, \delta_j, \boldsymbol{\Omega}_{t-1}) = E(\boldsymbol{x}_{t+h}|\varepsilon_{jt} = \delta_j, \boldsymbol{\Omega}_{t-1}) - E(\boldsymbol{x}_{t+h}|\boldsymbol{\Omega}_{t-1}). \tag{5.4}$$

By using Equation (5.2) in Equation (5.4), the above equation reduces to:

$$\boldsymbol{GI}_x(h, \delta_j, \boldsymbol{\Omega}_{t-1}) = \boldsymbol{A}_h E(\boldsymbol{\varepsilon}_t|\varepsilon_{jt} = \delta_j).$$

Additionally assume that $\boldsymbol{\varepsilon}_t$ has a multivariate normal distribution,[36] then:

$$E(\boldsymbol{\varepsilon}_t|\varepsilon_{jt} = \delta_j) = (\sigma_{1j}, \sigma_{2j}, \ldots, \sigma_{Nj})'\sigma_{jj}^{-1}\delta_j = \boldsymbol{\Sigma}\boldsymbol{e}_j\sigma_{jj}^{-1}\delta_j, \tag{5.5}$$

where $\boldsymbol{e}_j$ is a selection vector whose j-th element is 1, and all other elements are 0. The *unscaled* generalized impulse response function of the effect of a shock to the j-th equation at time t on $\boldsymbol{x}_{t+h}$ is then given by:

$$\boldsymbol{GI}_x(h, \delta_j, \boldsymbol{\Omega}_{t-1}) = \frac{\boldsymbol{A}_h\boldsymbol{\Sigma}\boldsymbol{e}_j\delta_j}{\sigma_{jj}} = \frac{\boldsymbol{A}_h\boldsymbol{\Sigma}\boldsymbol{e}_j}{\sqrt{\sigma_{jj}}} \cdot \frac{\delta_j}{\sqrt{\sigma_{jj}}}. \tag{5.6}$$

Defining $\delta_i = \sqrt{\sigma_{jj}}$, in Equation (5.6), the *scaled* generalized impulse response function, $\Psi_j^{\mathrm{g}}(h)$, is obtained as:

$$\Psi_j^{\mathrm{g}}(h) = \sigma_{jj}^{-\frac{1}{2}}\boldsymbol{A}_h\boldsymbol{\Sigma}\boldsymbol{e}_j. \tag{5.7}$$

With Equation (5.7), the (i, j)-th element of the H-step-ahead generalized forecast error variance decomposition (GFEVD) matrix, $\boldsymbol{\theta}^{\mathrm{g}}(H)$, is then defined as:

$$\boldsymbol{\theta}_{ij}^{\mathrm{g}}(H) = \frac{\sigma_{jj}^{-1}\sum_{h=0}^{H}(\boldsymbol{e}_i'\boldsymbol{A}_h\boldsymbol{\Sigma}\boldsymbol{e}_j)^2}{\sum_{h=0}^{H}\boldsymbol{e}_i'\boldsymbol{A}_h\boldsymbol{\Sigma}\boldsymbol{A}_h'\boldsymbol{e}_i}, \tag{5.8}$$

where the numerator accumulates the squared impulse responses of the effect of a unit shock (i.e., one standard deviation) to the j-th innovation at time t on the future value of $x_{i,t+h}$ over the horizon $h = 1, \ldots, H$, and the denominator accumulates the impulses of variable i to all influences over the same horizon, i.e., it corresponds to the mean squared error of the H-step-ahead forecast of variable i.

Thus, $\boldsymbol{\theta}_{ij}^{\mathrm{g}}(H)$, measures the contribution of the j-th variable to the H-step-ahead forecast error variance of the i-th variable. In order to preserve the interpretation of the contribution to the forecast error variances as percentages, the rows of the GFEVD

[36] Note that, by using the KPPS framework, an additional normality assumption for the historically observed error distribution is required. However, in this thesis, we consider log volatilities, which are well-approximated as Gaussian, see Diebold and Yilmaz (2015a), and thus, the KPPS framework appears to be appropriate.

matrix have to be normalized, as they might not sum to unity, i.e., due to the non-zero covariance between the non-orthogonalised shocks, in general $\sum_{j=1}^{N} \boldsymbol{\theta}_{ij}^{\mathrm{g}}(H) \neq 1$, cf. Pesaran and Shin (1998). The rows of the GFEVD matrix are normalized according to:

$$\tilde{\boldsymbol{\theta}}_{ij}^{\mathrm{g}}(H) = \frac{\boldsymbol{\theta}_{ij}^{\mathrm{g}}(H)}{\sum_{j=1}^{N} \boldsymbol{\theta}_{ij}^{\mathrm{g}}(H)}.$$

Hence, by construction, the sums of the rows of the normalized GFEVD matrix equal unity, i.e., $\sum_{j=1}^{N} \tilde{\boldsymbol{\theta}}_{ij}^{\mathrm{g}}(H) = 1$, and thus, the sum of all elements of $\tilde{\boldsymbol{\theta}}^{\mathrm{g}}(H)$ is equal to N.

5.2.3 Measures of Financial Connectedness

In the context of the DY framework, the elements of $\tilde{\boldsymbol{\theta}}_{ij}^{\mathrm{g}}(H)$ yield a measure of *pairwise directional* connectedness between the variables i and j at horizon H, and thus, the notation is converted to $C_{i\leftarrow j}^{H}$, for reasons of clarity and comprehensibility, i.e., $C_{i\leftarrow j}^{H} \equiv \tilde{\boldsymbol{\theta}}_{ij}^{\mathrm{g}}(H)$, cf. Demirer et al. (2018) and Diebold and Yilmaz (2014).

Along with the pairwise directional connectedness measure, $C_{i\leftarrow j}^{H}$, the DY framework introduces two measures of *total directional* connectedness, where one is the total connectedness from all other variables j to variable i, which is defined as the i-th off-diagonal row sum of the GFEVD matrix:

$$C_{i\leftarrow \bullet}^{H} \equiv \sum_{j=1, i\neq j}^{N} \tilde{\boldsymbol{\theta}}_{ij}^{\mathrm{g}}(H).$$

The total *from-others-connectedness*, $C_{i\leftarrow \bullet}^{H}$, measures the share of variable i's forecast error variance that is due to the forecast error of all the other variables j. By looking at this the other way round, the total *to-others-connectedness*, $C_{\bullet\leftarrow i}^{H}$, of variable i is the amount of forecast error variance of all other variables j that is induced by variable i, which is defined as the i-th off-diagonal column sum of the GFEVD matrix:[37]

$$C_{\bullet\leftarrow i}^{H} \equiv \sum_{j=1, i\neq j}^{N} \tilde{\boldsymbol{\theta}}_{ji}^{\mathrm{g}}(H).$$

[37] Note that Demirer et al. (2018) define from-others- and to-others-connectedness differently. The authors additionally scale both measures by a factor N^{-1}. Thus, from-others-connectedness becomes $C_{i\leftarrow \bullet}^{H}/N$ and to-others-connectedness becomes $C_{\bullet\leftarrow i}^{H}/N$. By scaling, the interpretation of the measures changes slightly, as they have to be interpreted relative to the forecast error variance of the entire system. Moreover, by scaling, the total system-wide connectedness is obtained as the sum (instead of the mean) of either one of the measures (from-others or to-others).

Additionally, the measure, C^H, referred to as total *system-wide* connectedness is available, which is defined as the scaled sum of the off-diagonal elements of the GFEVD matrix:

$$C^H \equiv \frac{\sum_{i,j=1,i\neq j}^{N} \tilde{\boldsymbol{\theta}}_{ij}^{\mathrm{g}}(H)}{\sum_{i,j=1}^{N} \tilde{\boldsymbol{\theta}}_{ij}^{\mathrm{g}}(H)} = \frac{\sum_{i,j=1,i\neq j}^{N} \tilde{\boldsymbol{\theta}}_{ij}^{\mathrm{g}}(H)}{N} = 1 - \frac{\mathrm{Tr}\left(\tilde{\boldsymbol{\theta}}^{\mathrm{g}}(H)\right)}{N}.$$

The total system-wide connectedness measures the share of the total forecast error variance of the system that is not self-induced by the variables, thus, it equals the mean of the total directional connectedness values of the variables of the system (either *from-others* or *to-others*).[38]

Note that the above measures are defined only in relation to a *"reference universe"*, i.e., a specific set of variables $\boldsymbol{x}_t$, which implies that they will generally not be robust to the choice of variables, cf. Diebold and Yilmaz (2015a, p. 19). This means that adding or removing variables from consideration can change the resulting connectedness value. However, this is an indication that the measures might not be suitable for an absolute comparison (of percentages) across markets or that the results of such a comparison at least have to be viewed with caution.

5.2.4 Connectedness Networks

In order to relate the DY connectedness indices to networks, recall that a network can be represented as a graph $G = (V, E)$ of order n and size m. The finite set $V = \{v_1, v_2, \ldots, v_n\}$ is the vertex set, and $E = \{e_1, e_2, \ldots, e_m\}$ is a set of 2-subsets of V referred to as the edge set. The graph or network G is a directed network, if each edge has a direction associated to it. This means that the ordering of its end vertices becomes significant, which is the case if edges v_1v_2 and v_2v_1 refer to distinct edges in the network. Moreover, the network is a weighted network, denoted by the pair (G, f) if the function $f : E(G) \to \mathbb{R}$ is a weight function that assigns a weight to each edge of the network. Furthermore, G can be represented by its weighted $(n \times n)$ adjacency matrix $\boldsymbol{W}$, where the elements $w_{ij} = f(w_{ij})$ if vertices i and j are connected, and $w_{ij} = 0$ otherwise. The network is called simple network if there are no loops, i.e., the diagonal elements of the (weighted) adjacency matrix of G are zero.

Diebold and Yilmaz (2014) note that (disregarding its diagonal elements) the GFEVD matrix can be interpreted as a weighted adjacency matrix that forms a *connectedness network*, where the pairwise directional connectedness values C_{ij}^H correspond to the weights of edges between variables (or vertices) i and j.[39] However, what is a bit

[38] Note that the measures would have to be multiplied by 100, in order to obtain percentages.

[39] Note, that Diebold and Yilmaz (2014) utilize a similar notation as Newman (2018) where the weighted edge $C_{ij}^H \equiv w_{ij}$ leads out of vertex j and into vertex i. However, the reverse is also commonly used, i.e., to define an edge that leads out of vertex i and into vertex j as w_{ij}. Eventually, this is a matter of taste, as the adjacency matrix can be transposed such that it complies with the definition,

misleading is the fact that they associate their measures with degrees when they are actually strengths since the network is weighted. More precisely, the from-others- and to-others-connectedness values can be related to the in- and out-strengths of a vertex, respectively, and the system-wide connectedness corresponds to either the mean in- or out-strength. Recognizing this is beneficial, since this implies that, by utilizing the methods of network theory, additional tools for analysing connectedness become available.

5.2.5 Regularization for High-Dimensional VAR Estimation

The complexity of a VAR(p) model can grow rapidly fast, as the number of parameters that have to be estimated depends on both the dimension of $\boldsymbol{x}_t$ and the lag order p. If both the number of considered variables N and the number of considered lags p are high then a correspondingly large number of parameters must be estimated. The problem with a model with too many parameters is that it is prone to overfit the data. In order to ensure that the model in Equation (5.1) can be estimated even in high dimensions, *regularization* techniques are available for recovering some degrees of freedom. Regularization refers to the technique of imposing a constraint on the magnitude of the parameters of a model, in order to control for its complexity, cf. Lever, Krzywinski, and Altman (2016). A popular regularization method, which we will utilize in this thesis, is the *elastic net* proposed by Zou and Hastie (2005). The elastic net is a compromise between the *ridge regression* (RR), which has been first introduced by Hoerl and Kennard (1970a, 1970b) and the *least absolute shrinkage and selection operator* (LASSO) by Tibshirani (1996).

RR coefficients minimize a penalized residual sum of squares (RSS) by imposing a limit on the squared ℓ_2 norm of the coefficients, which is the sum of squares of parameters, in cases where there is a vector of coefficients. In a VAR model the coefficients are collected in matrices, and thus, RR limits the squared ℓ_2 matrix norm, which is the squared singular value of the coefficient matrix.[40] RR has the advantage that it provides a unique parameter solution, in cases where different models yield the same minimal RSS due to multiply correlated variables, a problem we might also encounter when estimating high-dimensional VAR(p) models. However, regardless of how large the value of the penalty parameter λ is chosen, RR only shrinks coefficients towards zero, but is unable to set them to zero.

but one has to be careful, when using software, to prevent confusion (e.g., with out- or in-degrees of vertices). For example, the *igraph* package (Gabor Csardi & Tamas Nepusz, 2006) for the *R* language (R Core Team, 2021) implements the latter definition, using this package, we have to transpose the GFEVD matrix before forming the network.

[40] For a matrix A, it holds that: $\|A\|_2 = \sqrt{\lambda_{\max}(A'A)} = \sigma_{\max}(A)$ (*spectral norm*), where $\lambda_{\max}(A'A)$ denotes the largest eigenvalue of the matrix $A'A$, and $\sigma_{\max}(A)$ denotes its square root, i.e., the largest singular value of A, cf. Gentle (2017). Moreover, $\|A'A\|_2 = \|AA'\|_2 = \|A\|_2^2 = \sigma_{\max}(A)^2$, by singular value decomposition, cf. Meyer (2008).

LASSO on the other hand performs well in variable selection, i.e., setting the coefficients of variables to zero. It does so by imposing a limit on the ℓ_1 norm of the coefficients, which is the sum of the absolute values of the parameters, in cases where there is a vector of coefficients. In the context of a VAR model, this corresponds to limiting the ℓ_1 matrix norm, which is the maximum column sum of the coefficient matrix.[41]

By combining the above, the elastic net penalty is given by:

$$\min_{\mathbf{\Phi}} \sum_{t=1}^{T} \|\boldsymbol{x}_t - \sum_{l=1}^{p} \mathbf{\Phi}_l \boldsymbol{x}_{t-l}\|_2^2 + \lambda(\alpha\|\mathbf{\Phi}\|_1 + (1-\alpha)\|\mathbf{\Phi}\|_2^2) \tag{5.9}$$

where the first term of the sum is the RSS and the second term corresponds to the penalty, where $\|\cdot\|_1$ and $\|\cdot\|_2$ denote the ℓ_1 and ℓ_2 matrix norms, $\mathbf{\Phi} = [\mathbf{\Phi}_1, \ldots, \mathbf{\Phi}_p]$ denotes the coefficient matrix, $\lambda \geq 0$ is a penalty or complexity parameter that controls the amount of shrinkage, and the parameter α balances the LASSO and RR penalties. While the λ parameter is usually obtained by a *cross-validation* procedure (CV), the α parameter can be chosen either on qualitative grounds or alternatively by CV, cf. Hastie, Tibshirani, and Friedman (2009), or even adaptively, cf. Zou and Zhang (2009) and Demirer et al. (2018). For our analysis in Section 5.3, we will obtain values for both λ and α by CV.

The elastic net penalty in Equation (5.9) consists of two parts, i.e., the RR regulizer function, $\lambda(1-\alpha)\|\mathbf{\Phi}\|_2^2$, which shrinks coefficients of highly correlated variables towards each other, and the LASSO, $\lambda\alpha\|\mathbf{\Phi}\|_1$, which performs a variable selection. Thus, regularization with elastic net penalty combines the advantages of both RR and LASSO, cf. Lever et al. (2016).

Note, however, that the RR solutions are not equivariant under scaling of the input variables, thus, the inputs are usually standardized (and centred), cf. Hastie et al. (2009), moreover, since we utilize a single penalty parameter, λ, for all model coefficients this problem carries over to the regularization with elastic net penalty. We follow therefore Nicholson, Matteson, and Bien (2017) and Nicholson, Wilms, Bien, and Matteson (2020) for a standardization procedure for regularization in VAR models. This means, prior to estimation, we ensure that all included time series are on the same scale by standardizing each series, such that it has zero mean and unit variance. Furthermore, when considering a rolling estimation window, in order to capture the parameter variation over time, we standardize each series separately in each rolling window, again.

[41] Again, for a matrix A, it holds that: $\|A\|_1 = \max_j \sum_i |a_{ij}|$ (*column-sum norm*), cf. Gentle (2017).

5.3 The Cryptocurrency Network

We apply the DY methodology to the cryptocurrency market and analyse its volatility connectedness as well as the resulting volatility connectedness network. When analysing financial connectedness, volatility connectedness is of particular interest for its aptitude for real-time monitoring systemic risk. This is because volatilities tend to move together primarily in financial crises, whereas returns tend to move together in both calm and turbulent times, cf. Diebold and Yilmaz (2015a). Apart from Figure 5.6 in Section 5.3.4, where we show the dynamic total system-wide return connectedness for illustrating the afore-mentioned behaviour of asset returns, we will focus on analysing volatility connectedness, as our interest is in analysing the systemic risk and correspondingly the stability of the cryptocurrency market and the corresponding cryptocurrency network. Henceforth, we mean volatility connectedness, when referring to connectedness, unless otherwise stated.

The remainder of this section is structured as follows: in Section 5.3.1 we provide a brief introduction to cryptocurrencies based on the Bitcoin system. The section is therefore primarily of interest for the reader being not familiar with cryptocurrencies and blockchains. A description of the data that we consider in our empirical analysis is given in Section 5.3.2. We present a static and dynamic connectedness analysis in Sections 5.3.3 and 5.3.4, respectively. Section 5.3.5 we analyse the relationship between volatility connectedness, as a measure of systemic risk, and the generalized assortativity coefficient of a network, as an indicator of network stability. In Section 5.3.6 we explore the multiscale backbone of the volatility connectedness network and analyse its community structure.

5.3.1 A Primer on Cryptocurrencies

In the following, we give a simple explanation of a cryptocurrency based on the Bitcoin system in order to convey the basic idea. For the big picture, however, we refer to two extensive, albeit not too technical surveys on this topic, one on Bitcoin in particular, the other one on cryptocurrency systems in general, cf. Ghimire and Selvaraj (2018) and Mukhopadhyay et al. (2016), respectively.

To this end, Figure 5.1 shows a simplified representation of a blockchain. The information carriers of the decentralized system are referred to as *blocks*. A Block has a unique identifier, namely its *hash*. A hash is the result of the application of a cryptographic hash function that takes an input of variable length and generates a fixed length output, hence the name cryptocurrency. Each block consists of the hash of the previous block — this is how blocks are linked together to form a blockchain — together with a list of transactions to be executed and a *proof of work*.

The proof of work makes a block a valid block, and only valid blocks are added to the blockchain. More precisely, the proof of work consists of the task of finding a number referred to as *nonce*,[42] that when hashed together with the other information of a block yields a hash that meets the requirements of a valid block. For a block to be considered valid it is required that its hash begins with a certain number of zeros.[43]

The search for valid blocks in order to propose them to the system is referred to as *mining*. Participants of the system that mine blocks are referred to as *miners*. If a proposed block is accepted, it is added to the blockchain and a reward in form of newly created Bitcoin is granted to the miner that successfully proposed the block (as part of the transactions to be executed of that block). By adding the block to the blockchain the transactions are executed and reported to all participants of the system. Therefore, it is possible for any participant of the system to track the entire transaction history at any time, rendering fraud or double spending uneconomical, as this would be detected immediately.

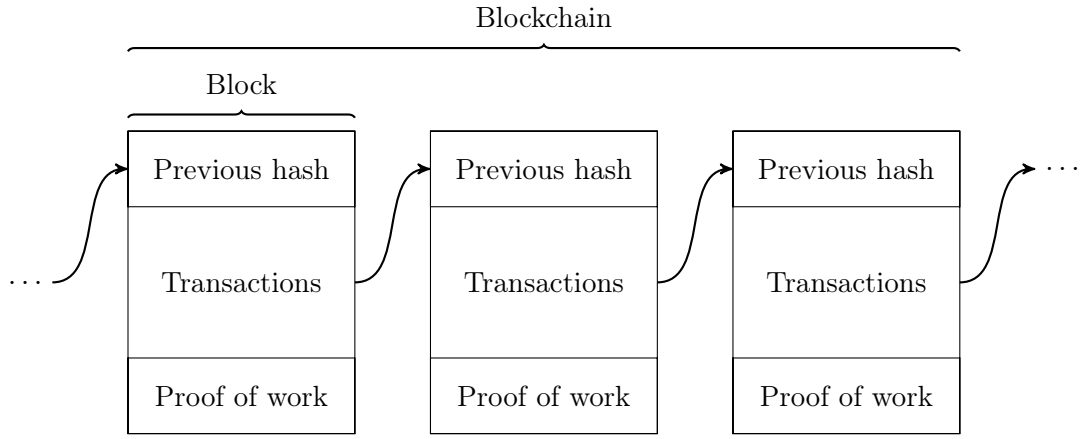

Figure 5.1. Simplified blockchain. Adapted from Ghimire and Selvaraj (2018).

The working principles of other cryptocurrencies are similar to a greater or lesser extend differing, for example, by the way how blocks are validated, where proof of work is just one option, or by the particular hash function that is used for encryption, or by the way how possible transaction fees are considered, or by how fast transactions are executed.

5.3.2 Data

We obtain data from *CoinMarketCap* over the period from July 3, 2017 to June 30, 2022 (1735 daily observations).[44] From the top 500 *active* and *tracked* cryptocurrencies

[42] The term is an acronym and stands for *number only used once*.

[43] It is noteworthy that it is practically impossible to infer from a hash of a valid block what the nonce might have been that has generated this very hash. Computing the hash for a given nonce, on the other hand, can be done fast, so that the proof of work can be easily verified.

[44] `https://coinmarketcap.com/api/`

by market capitalization (as of June, 30 2022), we select those for which consecutive data for at last 5 years are available. The final data sample consists of daily open, high, low, and closing (OHLC) prices of 49 cryptocurrencies.

Table C.1, in the appendix, gives an overview over the selected cryptocurrencies' names and symbols as well as their ranks according to their market capitalization.[45] As of this writing, the selected cryptocurrencies account for a share of approximately 66.2 percent of the market capitalization of the entire market, suggesting that the selection represents the market fairly well. Figure 5.2 shows the percentage share of the accumulated market capitalization as a function of the number of top n cryptocurrencies. Apparently, the cryptocurrency market consists of a few key players who accumulate most of the market capitalization.

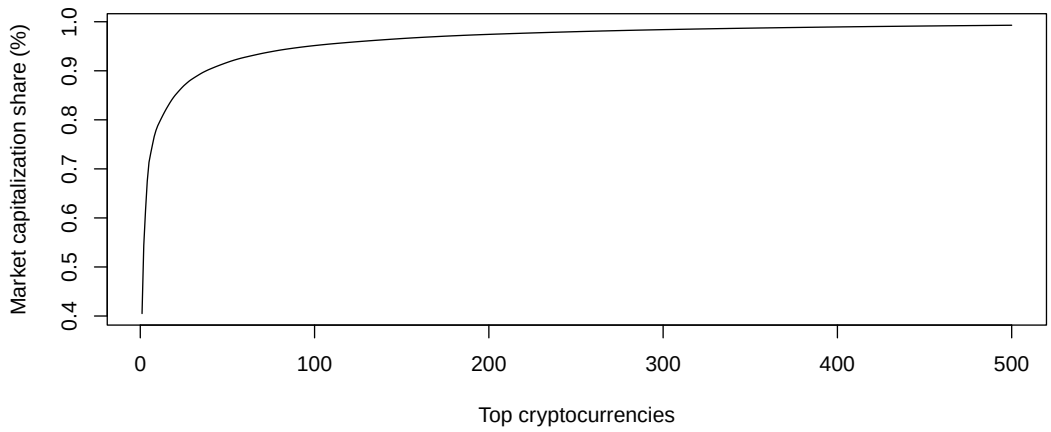

Figure 5.2. Market capitalization share of top cryptocurrencies. For example, the top 100 cryptocurrencies account for approximately 95.1 percent of the market capitalization of the entire market (as of June 30, 2022).

The latent cryptocurrency return volatility has to be estimated. The literature on estimating and modelling volatility is vast, e.g., see Andersen, Bollerslev, Christoffersen, and Diebold (2006) and Andersen, Bollerslev, Christoffersen, and Diebold (2013) for a survey on this topic. In this thesis, since we have daily OHLC price data, we follow Demirer et al. (2018) and utilize the daily range-based volatility estimator, suggested by Garman and Klass (1980), which is defined as:

$$\hat{\sigma}^2_{i,t} = 0.511(u_{i,t} - d_{i,t})^2 - 0.019\Big[c_{i,t}(u_{i,t} + d_{i,t}) - 2u_{i,t}d_{i,t}\Big] - 0.383c^2_{i,t}, \tag{5.10}$$

[45] For each cryptocurrency the market capitalization is determined by multiplying its *circulating supply* with its current price, where circulating supply is the amount of coins that are circulating in the market, and thus, are in public hands, cf. CoinMarketCap (2022). Hence, circulating supply is comparable to the *floating stock* in the stock market, which is the number of shares available for trading of a particular stock.

Table 5.1. Descriptive statistics. Descriptive statistics of annualized volatilities and returns (percentage) in the period from July 3, 2017 to June 30, 2022.

Symbol	Mean	Median	Max.	Min.	Std. dev.	Skewness[1]	Kurtosis[1]
			Annualized volatilities				
BTC	59.315	47.275	460.399	5.851	45.443	0.047	3.002
ETH	75.996	61.615	665.190	7.543	56.466	0.219	3.290
XRP	88.769	63.228	923.949	9.974	86.204	0.431	3.190
Market	115.991	87.057	4204.759	0.222	112.341	-0.996	9.000
			Annualized returns				
BTC	19.446	35.615	6513.372	-18345.153	1478.905	-1.734	25.939
ETH	44.517	89.339	8531.882	-21554.505	1906.077	-1.562	20.527
XRP	-5.133	28.548	16428.659	-19660.993	2285.422	-0.144	17.816
Market	9.902	7.307	58186.267	-35466.463	2580.912	0.215	28.351

[1] For volatility, the values in the table correspond to the skewness and kurtosis of the logarithm of the annualized volatilities.

where $u_{i,t} = H_{i,t} - O_{i,t}$, $d_{i,t} = L_{i,t} - O_{i,t}$ and $c_{i,t} = C_{i,t} - O_{i,t}$ are the normalized high, low and closing prices, and $O_{i,t}, H_{i,t}, L_{i,t}$ and $C_{i,t}$ are the logs of daily OHLC prices of cryptocurrency i at time t.[46] The estimator in Equation (5.10) is an estimator for the daily return variance of a cryptocurrency. In order to obtain an estimator for the annualized daily percentage standard deviation of the returns, i.e., daily return volatility, $\hat{\sigma}_{it}$, we apply the following transformation: $\hat{\sigma}_{it} = 100 \cdot \sqrt{365 \cdot \hat{\sigma}_{it}^2}$. When analysing returns, we consider the *log return* of a cryptocurrency i defined as the difference of log closing prices: $r_t = C_{i,t} - C_{i,t-1}$, cf. Campbell, Lo, and MacKinlay (2012).

In the appendix, for each cryptocurrency, for the sample period from July 3, 2017 to June 30, 2022, Figures C.1 to C.4 show time series plots of the estimated annualized daily volatility and return (percentage). Moreover, Figures C.5 to C.12 present histograms and density estimates of the log annualized daily volatilities and the daily log returns (together with respective normal densities for comparison), respectively, indicating that the log volatilities are well-approximated as Gaussian.[47]

Table 5.1 presents descriptive statistics of the percentage annualized volatilities and percentage annualized log returns averaged over the entire cryptocurrency market, for the sample period. Moreover, descriptive statistics of the top 3 cryptocurrencies, i.e., Bitcoin (BTC), Ethereum (ETH), and Ripple (XRP), are separately shown, for com-

[46] Alternative estimators are available for higher frequency price data. For example, Baruník and Křehlík (2018) use daily *realized volatility* in the context of volatility connectedness, which is the sum of squared (intraday) returns, where they use a sampling period of 5 minutes. However, Alizadeh, Brandt, and Diebold (2002) show that the range-based volatility estimator is almost as efficient as realized volatility, albeit using only four inputs per day.

[47] The log returns on the other hand are not so well-approximated as Gaussian, as was expected, cf. Diebold and Yilmaz (2015a). However, we focus on the volatility connectedness, and take the results for return connectedness with a grain of salt, as they are mainly presented for reasons of completeness anyway.

parison purposes. Evidently, the cryptocurrency market is much more volatile than previously analysed financial markets.

For example, Diebold and Yilmaz (2015a) analyse the connectedness of 10 major global stock markets, by considering daily data on nominal local-currency stock market indexes, over the course of almost 20 years up to the year 2013. The mean of the annualized volatilities averaged over the 10 stock markets is 18.841, cf. Diebold and Yilmaz (2015a, table 4.3, p. 87), whereas the mean of the annualized volatilities averaged over the cryptocurrency market is 115.991. The mean annualized returns on the other hand are much more similar in magnitude. The mean of the annualized returns averaged over the 10 stock markets is 11.410, cf. Diebold and Yilmaz (2015a, table 4.2, p. 86), whereas the mean of the annualized returns averaged over the cryptocurrency market is 9.902.[48]

Additionally, by comparing the skewness and kurtosis values of the annualized volatilities of the top 3 cryptocurrencies with those of the entire market, it becomes apparent that the volatilities of the cryptocurrencies are likely to be on different scales. This can also be confirmed by considering the volatility plots in Figures C.5 to C.8 in the appendix. It seems therefore sensible to utilize a standardization procedure before estimating the VAR model, as mentioned before.

5.3.3 Static Analysis: Full Sample Connectedness

For the full sample analysis of the volatility connectedness, we estimate a VAR($p = 4$) based on the demeaned and standardized logarithms of the annualized return volatilities over the entire sample period from July 3, 2017 to June 30, 2022.[49] For the model, a lag order of $p = 4$ is chosen based on the ACF and PACF functions, respectively.[50] Considering up to four lags is also in accordance with what can be found in the literature, where usually lag orders of $p = 3$ or $p = 4$ are chosen, depending on the frequency of the data, and the number of trading days. For example, cryptocurrencies can be traded 7 days in a week, and thus, the chosen lag order corresponds to exactly half a trading week. The forecast horizon, H, based on which the GFEVD matrix is computed, is set to $H = 12$, which is long enough, for our analysis, to capture the impulse responses entirely. The robustness of the total system-wide volatility connectedness with respect to our parameter choice is supported in Figures C.13 and C.14, in the appendix of this thesis, which show the estimated total system-wide connectedness for a range of alternative lag orders and forecast horizons.

[48] Although the considered time periods differ, the comparison is in so far fair, as there have been calm and turbulent times in both considered time periods.

[49] For each series, we use the Augmented Dickey–Fuller (ADF) test in order to verify its stationarity.

[50] Since it would result in a very large number of figures, we do not present the ACF and PACF functions, but they are available from the authors upon request.

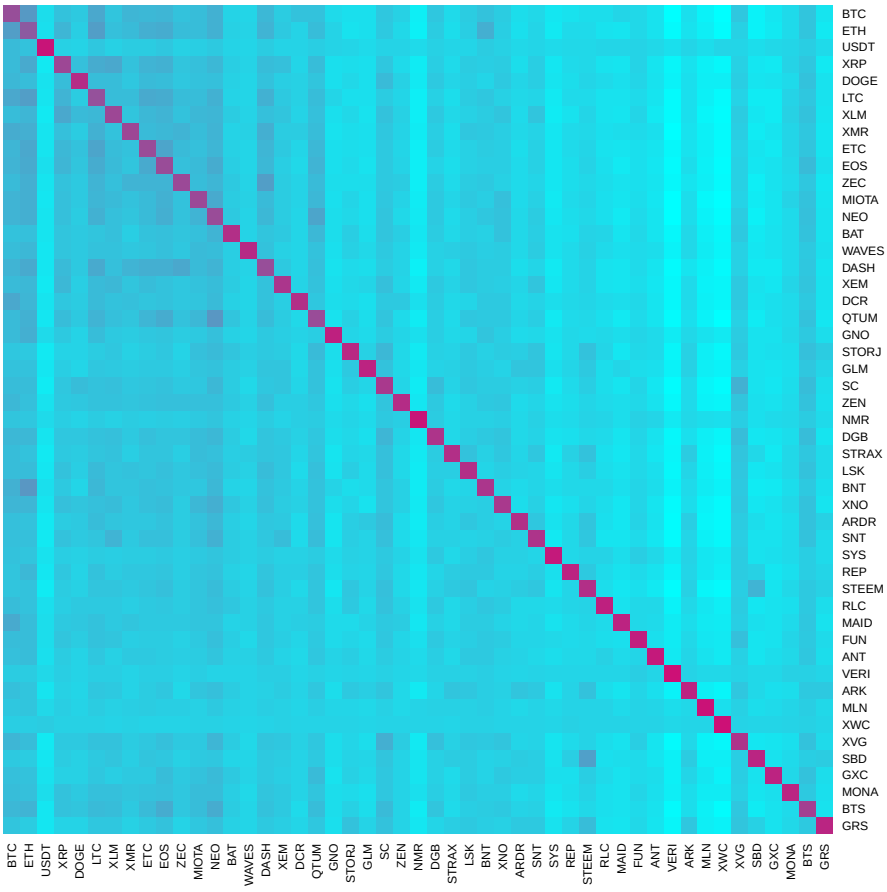

Figure 5.3. Static pairwise directional volatility connectedness. The colours of the tiles of the heatmap correspond to the magnitude of the pairwise directional connectedness between the corresponding cryptocurrencies, light cyan indicates low connectedness, whereas dark deep pink indicates high connectedness.

In the DY methodology the connectedness is usually summarized in a table referred to as *connectedness table* (or sometimes called *spillover table*), cf. Diebold and Yilmaz (2009, 2012, 2014). This is informative if the number of variables, for which the connectedness or spillover effects are investigated, is not too large. However, since our sample consists of 49 cryptocurrencies, such a table would encompass 49^2 pairwise directional connectedness values, which can no longer be presented in a clear way. Instead, we show the pairwise directional volatility connectedness values, $C^H_{i \leftarrow j}$, between two cryptocurrencies i and j in terms of a heatmap, in Figure 5.3.

Each tile of the heatmap corresponds to a pairwise directional connectedness value. The colours of the tiles range from light cyan, for lower connectedness values, to deep pink, for higher connectedness values. The rows and columns of the heatmap correspond to the cryptocurrencies of our sample, which are ordered by their market capitalization rank. Apparently the pairwise directional connectedness is highest for the diagonal

elements, indicating that a large percentage of the forecast error variance of a cryptocurrency is self-induced (sometimes called *own-variable* effects). The colours of the off-diagonal elements on the other hand appear to have a fairly even hue, indicating that the pairwise directional connectedness values tend to be similar in magnitude between one variable and variables other than itself. However, the tiles in the upper left corner of the map appear to be a bit darker than the rest. This might indicate that the pairwise directional connectedness values between cryptocurrencies with a high market capitalization tend to be slightly higher than the others.[51]

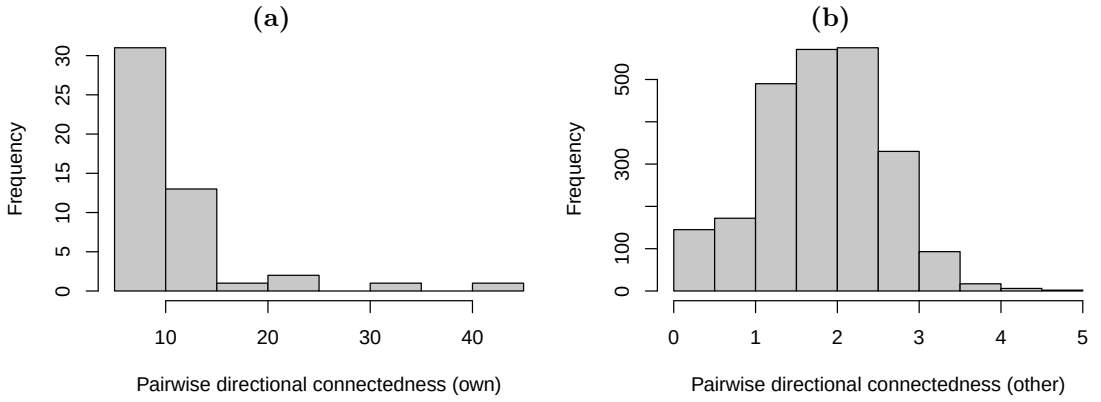

Figure 5.4. Pairwise directional connectedness. Depicted are a histogram of the distribution of the pairwise directional connectedness values, $C^H_{i\leftarrow j}$, separated into directional connectedness from a variable to itself (own), $C^H_{i\leftarrow i}$, and directional connectedness from one variable to a variable other than itself (other), $C^H_{i\leftarrow j}, i \neq j$.

	Min.	1st Qu.	Median	Mean	3rd Qu.	Max.	Std. dev.
Other	0.000	1.297	1.847	1.817	2.360	4.625	0.761
Own	6.336	7.758	8.899	10.979	11.050	44.041	6.803

Table 5.2. Descriptive statistics of pairwise directional connectedness. Reported are the pairwise directional connectedness values, $C^H_{i\leftarrow j}$, separated into directional connectedness from a variable to itself (own), $C^H_{i\leftarrow i}$, and directional connectedness from one variable to a variable other than itself (other), $C^H_{i\leftarrow j}, i \neq j$.

In order to convey a sense of the scale of the pairwise directional connectedness values, Figure 5.4 shows histograms of their distributions separated into own (diagonal) and other (off-diagonal) pairwise directional connectedness, where additional information are provided in the form of descriptive statistics of the pairwise directional connectedness values in Table 5.2. For example, the average of the diagonal pairwise connectedness is approximately 10.9 percent, which is about 5 times as much as the mean of

[51] We verify this later, when we extract the connectedness backbone network, in Section 5.3.6, and find that the more relevant edges are between the large cryptocurrencies.

the off-diagonal pairwise connectedness, which is about 1.8 percent. Most of the off-diagonal pairwise connectedness range between 1 and 3 percent, whereas the minimum of diagonal pairwise connectedness exceeds 6.3 percent. However, the diagonal pairwise connectedness is below 12 percent for 75 percent of the cryptocurrencies. Vice versa, for 75 percent of the cryptocurrencies, at least 88 percent of their forecast error variance are due to shocks to other variables in the system (sometimes called *other-variable* effects).

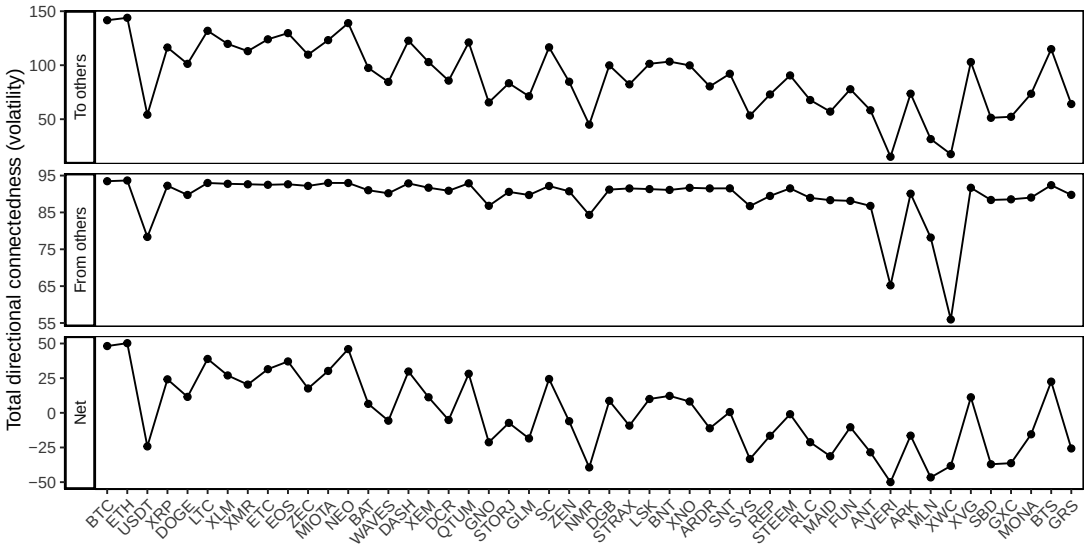

Figure 5.5. Static total directional volatility connectedness. For each cryptocurrency, the figure shows its respective from-others-connectedness, $C^H_{i\leftarrow\bullet}$, to-others-connectedness, $C^H_{\bullet\leftarrow i}$ as well as the net-connectedness, as the difference between from-others- and to-others-connectedness.

Figure 5.5 shows the aggregation of pairwise directional connectedness, $C^H_{i\leftarrow j}$, in the form of the total directional measures to-others-connectedness, $C^H_{\bullet\leftarrow i}$, and from-others-connectedness, $C^H_{i\leftarrow\bullet}$, as well as the net-connectedness, as the difference between from-others- and to-others-connectedness, for each cryptocurrency. In the figure, the cryptocurrencies are, again, ordered according to their market capitalization, such that the market capitalization decreases, from left to right.

A slight decline in the to-others-connectedness for smaller cryptocurrencies is visible. Apparently, larger cryptocurrencies are connected more strongly, and thus, tend to distribute a larger proportion of shocks to the system. The from-others-connectedness on the other hand appears to be fairly even, for all cryptocurrencies, with some exceptions among the smaller ones. However, the measure is quite high overall, indicating that a large proportion of uncertainty is due to shocks received from other cryptocurrencies.

For example, consider Bitcoin (BTC, first from left), 93.47 percent of its forecast error variance is induced by other cryptocurrencies, whereas only 6.53 percent of the uncertainty is self-induced. On the other hand, the to-others-connectedness of Bitcoin

is 141.65 percent (relative to its own forecast error variance), which (by scaling the measure) corresponds to 2.89 percent of the grand total of forecast error variance that is emitted by all variables in the system.[52] We compare our results to Yi, Xu, and Wang (2018) who analyse the volatility connectedness among 8 cryptocurrencies over the period from August 4, 2013 to April 1, 2018 (their observed period and ours overlap by about 9 months). For Bitcoin, they find a from-others-connectedness of 57.72 percent as well as a to-other-connectedness of 58.14 relative to own forecast error variance, which corresponds to 7.27 percent of the systems total forecast error variance. Given that we consider a larger system size (49 cryptocurrencies), it seems plausible that the from-others-connectedness of the cryptocurrency has increased over time ($93.47 > 57.72$), as more cryptocurrencies in the market bring additional uncertainty to the system. If we consider the to-other-connectedness, we find that this has increased relative to the own forecast error variance ($141.65 > 58.14$), but has decreased in relation to the grand total of forecast error variance that is emitted by all variables in the system ($2.89 < 7.27$). This is also sensible, since the contribution of bitcoin in terms of forecast error variance is distributed among more cryptocurrencies.

We observe further that the net-connectedness and to-others connectedness are structurally quite similar, which is due to the (more or less) evenly high from-others-connectedness, for most of the cryptocurrencies. However, the cryptocurrencies can be clearly separated into net *receivers*, for which the net-connectedness is negative, and net *emitters*, for which the net-connectedness is positive. The depiction of the net-connectedness indicates that smaller cryptocurrencies tend to be net receivers of shocks from other, presumably, larger ones. This is because larger cryptocurrencies tend to be net emitters of shocks, with Bitcoin (BTC) and Ethereum (ETH, second from left) being the largest emitters of shocks.

When analysing the aggregated measures, in Figure 5.5, The cryptocurrency Tether (USDT, third from left) stands out a bit. This may be due to the fact that Tether is a cryptocurrency *stablecoin* pegged to the U.S. dollar, and thus, differs inherently from the considered cryptocurrencies.[53]

Finally, averaging either the to-others- or the from-others-connectedness values yields total system-wide connectedness, C^H, which is a proxy of systemic risk (recall, sometimes the terms are used interchangeably). We obtain a total system-wide connectedness of $C^H = 89.02$ percent, for the cryptocurrency market, for the entire period from July 3, 2017, to June 30, 2022. This indicates that 89.02 percent of the volatility forecast error variance in the entire market is due to the connectedness of individual cryptocur-

[52] In this case, the scaling by Demirer et al. (2018) (see Footnote 37) gives a better feel for the scale of the to-others-connectedness measure. However, in the case of the from-others-connectedness measure, we consider it more informative to report the measure relative to the own forecast error variance of the variable.

[53] In our further analysis on the stability of the cryptocurrency network, in Section 5.3.5, it will turn out that Tether plays an important role.

rencies. To put this into perspective, Diebold and Yilmaz (2015a) find that the total system-wide connectedness among 10 major stock markets is approximately 41 percent. It is no secret that the market of cryptocurrencies stands out due to being highly volatile. However, our analysis shows, that apart from being highly volatile, the market is also subject to high systemic risk due to high connectedness. Again, if we compare our results to those of Yi et al. (2018), we note that the increase in systemic risk is a development of recent years, as the total-system-wide connectedness over the period from August 2013 to April 2018 was only 37.79 for the cryptocurrency market (based on a smaller system size).[54]

Diebold and Yilmaz (2015a) already recognized that the full sample connectedness analysis yields a snapshot, which summarizes volatility connectedness dynamics over the considered period. However, in order to capture the evolution of the financial market under consideration during both calm and turbulent times, connectedness would also have to be considered dynamically. Because of this, we proceed with a dynamic analysis of the system-wide volatility connectedness of the cryptocurrency market in the subsequent section.

5.3.4 Dynamic Analysis: Rolling Sample Connectedness

For the dynamic analysis of the system-wide connectedness of the cryptocurrency market, we estimate the VAR($p = 4$) model using 90-day rolling samples, and a forecast horizon $H = 12$ for computing the GFEVD. For a rolling window estimation, setting an appropriate window size, that captures the dynamics well, without smoothing too much on the one hand and also not being too erratic on the other hand, is challenging. Our choice for the window size, $w = 90$, corresponds to a quarterly period, for daily return volatilities (and returns). We additionally compared our parameter choice to alternative rolling window sizes, see Figure C.15, in the appendix, which shows the estimated dynamic total system-wide connectedness for different window sizes. The selected rolling window size provides a good balance between smoothness and sensitivity when capturing the dynamics of connectedness. Increasing the window size leads to a very strong smoothing of the dynamics, such that the waves of connectedness are no longer so clearly visible.

Figure 5.6 presents the dynamic system-wide volatility connectedness, and dynamic system-wide return connectedness, for a comparison. There are several waves of high volatility connectedness clearly visible in the figure, when shocks created a large portion of future uncertainty, and hence strong connectedness, in the system. Volatility connectedness is well above 90 percent for these waves, where the last wave is ongoing since the second quarter of 2022. We will soon discuss the events that might have led

[54] However, using a rolling window estimation of connectedness Yi et al. (2018) find a steadily increasing total system-wide connectedness, which was around 70 percent at the beginning of 2018, which is closer to our results for this period.

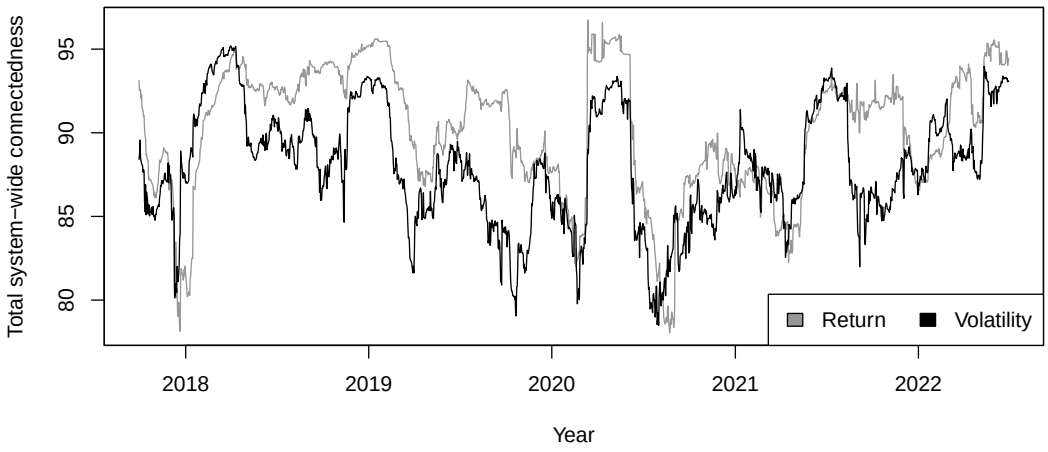

Figure 5.6. Total system-wide return and volatility connectedness. The results are based on a rolling window estimation of a VAR($p = 4$) model using the most recent $w = 90$ observations, and where the GFEVD is based on an H-step-ahead forecast with $H = 12$.

to an increase of volatility connectedness. Obviously, during recovery phases volatility connectedness drops. However, return connectedness stays high also in between volatility connectedness peaks, illustrating that volatilities tend to move together only in financial crises, whereas returns tend to move together in both calm and turbulent times, as mentioned before.

The dynamic total system-wide volatility connectedness of the cryptocurrency market ranges between 78.49 percent and 95.19 percent, with an average of 87.95 percent over the considered period, which is quite high, all things considered. For example, if we consider again the 10 major stock markets, analysed by Diebold and Yilmaz (2015a, fig. 4.3 (b), p. 95), their analysis shows that the volatility connectedness of the stock markets ranges between 24 percent (in 2000) and 65 percent (in 2008). In another study Baruník and Křehlík (2018) analyse the volatility connectedness of 11 major financial U.S. firms, over the course of 16 years (2000–2016), and find that the connectedness among these firms ranges between 55 percent and 85 percent. The cryptocurrency market, therefore, appears to have a very high base level of connectedness, and thus systemic risk, which can increase even further in times of crises. However, the variation of system-wide connectedness of the cryptocurrency market, over time, can be expected because the studied period includes both upswings and downswings, in which shocks transmit across the system with different strengths.

Volatility Connectedness bottoms during calm times over the periods from early 2019 to early 2020 and from mid 2020 to early 2021, creating a less connected system. A

decline in the overall trend of connectedness can be observed over the course of the years before 2020. After 2020, a rising trend of connectedness can be observed. This might be an indication of a business cycle. However, in order to state this assuredly, the considered time span would have to be increased.

Finally, we consider events that might have led to phases of increased connectedness. For example, the first two volatility connectedness peaks in Figure 5.6 occur during the year 2018, which can thereby be attributed to several occurrences over the course of the year. In 2018, the market experienced its biggest crash to date, leading to insiders referring to the year as a *nightmare*, cf. Ouimet (2019). In early 2018, the market had already begun to cool off, after Bitcoin has reached an all-time-high of almost \$20K by December 2017, when rumours of a cryptocurrency exchange ban in South Korea have brought uncertainty to the market, cf. C. Kim and Kim (2018a, 2018b). Additional uncertainty has been brought to the market by the news that Japan's largest cryptocurrency over-the-counter (OTC) market, *Coincheck*, had to suspend trading due to \$530MM worth of the cryptocurrency *NEM* (XEM) being stolen in a cyberattack, the largest ever by then, cf. Mochizuki and Vigna (2018). This has triggered a large sell-off wave resulting in a Bitcoin price as low as $\$6,200$ by February 2018, corresponding to a drop in price by 70 percent within two months. The market did not recover over the course of next months but rather experienced another major price decline at the end of the year, cf. Patterson (2018).

The next volatility connectedness peak appears in the first half of 2020. At that time, the World Health Organization (WHO) declared COVID-19 a pandemic (on March 11, 2020), entailing lockdowns across most countries of the world, cf. Onyeaka, Anumudu, Al-Sharify, Egele-Godswill, and Mbaegbu (2021). Thus, the high connectedness in the cryptocurrency market can be attributed to high uncertainty due to a global, generally precarious economic situation.

In May 2021, first, Elon Musk, Chief Executive Officer (CEO) of Tesla, Inc., a manufacturer for electric vehicles, has stated that the company will no longer accept Bitcoin for car purchases due to the environmental impact of the cryptocurrency, cf. Jin and Singh (2021). At about the same time, China has banned the provision of cryptocurrency related financial services, cf. Shen and Siu (2021), resulting in another connectedness peak.

There has been an ongoing increase in connectedness since early 2022, which can be caused by a variety of reasons, such as repercussions of the (still ongoing) global pandemic (e.g., supply chain troubles), a generally uncertain economic situation due to high inflation and war-related events, or recent plans for cryptocurrency regulation (e.g., the Markets In Crypto Assets (MiCA) framework by the EU, cf. European Commission, 2019). Regulation plans have been reinforced, lately, by the collapse of the algorithmic

stablecoin, *TerraUSD* (UST), and its governance token, *LUNA* (LUNA), in May 2022, which has led to a billion worth loss across the cryptocurrency market, cf. John (2022).

The considerations above suggest that the cryptocurrency market is sensitive to two types of events, those that also affects other (financial) markets (e.g., pandemic, inflation, war-related events), and market specific events (e.g., regulation plans, security gaps), see, e.g., Corbet, Lucey, Urquhart, and Yarovaya (2019) for a comprehensive review on the topic of cryptocurrencies as financial assets. This increases the difficulty of assessing the systemic risk for the cryptocurrency market, and emphasizes the need of a reliable approach for monitoring connectedness, that also gives an indication of the severity of a potential crisis.

5.3.5 Robustness of the Volatility Connectedness Network

The terms robustness and resilience are often used synonymously, however, they are closely related concepts that are nevertheless different, cf. Barabási (2016). Recall that robustness is defined as the ability of a system to maintain its core functionality even if individual components fail. In the context of networks, this means that the core functionality is preserved even if individual vertices or edges are missing. On the other hand, resilience is the ability of the system to adapt the mode of operation to internal or external disturbances, so that the core functionality is preserved. Resilience is therefore a dynamic property that requires a shift in core activities. That means a system might be robust because of its resilience.

In the following we focus on analysing the robustness or resilience of the cryptocurrency connectedness network. Since the assortativity of a network is often considered as a measure of its resilience, we therefore, analyse the assortativity structure of the cryptocurrency connectedness network and its change over the course of time. Recall that assortativity is the tendency of a vertex to bond with another based on their similarity, with similarity being usually measured via vertex degree.

The assortativity structure of a network has a big impact on its percolation behaviour. This is because perturbations or shocks have a higher chance to propagate through the network, if central vertices tend to be connected to each other, i.e., if the network structure is assortative. However, the opposite is true, if the network shows disassortative tendencies, i.e., if central vertices tend not to be connected to each other. This implies that assortative mixing leads to a loss of stability, and that disassortative networks are more robust to the effect of dynamic fluctuations than assortative networks, cf. Brede and Sinha (2005) and Xulvi-Brunet and Sokolov (2004).

These considerations are under the premise that edge weights denote somehow negative effects, which are desirably prevented. For example, in case of the cryptocurrency network, edge weights describe negative effects, as they indicate transmission of risk due to uncertainty. This means that the network is more robust, the more disassortative

it is. There are, however, other forms of financial networks, for which the opposite reasoning applies. Consider, for example, banking networks, where edge weights denote the flow of money (perceived as positive). In such networks, it is crucial to maintain this flow in order to prevent the market from failing. Therefore, banking networks tend to be more robust, the more assortative they are.

The assortativity of a network is obtained by computing the Pearson correlation coefficient between the excess degrees of both ends of an edge. Unfortunately, in the case of the connectedness network, this leads to a problem. Since the network is a complete network by construction, i.e., there exists an edge between any pair of vertices, it is r-regular with $r = (n-1)$, implying that every vertex has the same degree. Thus, the correlation coefficient cannot be computed due to the homogeneous degrees of the vertices. Sometimes, a network is declared to be perfectly assortative, in such a case, arguing that connected vertices are maximally similar with respect to their degrees. Our analysis, however, will show that one might make a mistake by doing so.

By considering vertex strength instead of vertex degree, it becomes possible to determine and analyse assortativity for such r-regular networks, and thus, for the cryptocurrency network as well. The derivations and analyses of Chapters 3 and 4 are therefore of essential use. By using the generalized assortativity coefficient it is possible to compute the assortativity of the network, and furthermore, to assess its statistical significance. Moreover, since the network is also weighted, the maximum of available information is used in order to determine the robustness of the cryptocurrency network.

Recall that the generalized assortativity coefficient has been defined as:

$$r^{\omega}_{(\alpha,\beta)} = \frac{\sum_i \omega_i^{\beta} l_i m_i - \Omega^{-1}(\sum_i \omega_i^{\beta} l_i)(\sum_i \omega_i^{\beta} m_i)}{\sqrt{\left[\sum_i (\omega_i^{\beta} l_i^2) - \Omega^{-1}(\sum_i \omega_i^{\beta} l_i)^2\right]\left[\sum_i (\omega_i^{\beta} m_i^2) - \Omega^{-1}(\sum_i \omega_i^{\beta} m_i)^2\right]}},$$

where l_i and m_i are the excess (in- or out-) strengths of the ends l and m of edge i. For example, $l_i = s'_l - \omega_i^{\alpha}$ is the excess strength of end l of edge i with $\alpha \in \{0,1\}$. Furthermore, $\Omega = \sum_i \omega_i^{\beta}$ with $\beta \in \{0,1\}$. Since degree assortativity cannot be computed for the network, we focus on the parameter combination $(\alpha = 1, \beta = 1)$. For the mode of assortativity, a pre-analysis has shown that the *out–in* and *in–in* modes are structurally very similar as well as the *out–out* and *in–out* modes, see Figure C.18, in the appendix.[55] We focus therefore on the *out–in* mode of the generalized assortativity coefficient, as this is also the suggested mode by Newman (2003).

[55] To the best of our knowledge, we are the first to perform such an analysis. It would be interesting to see if other networks also show this kind of behaviour or if it is unique to the cryptocurrency network. Interestingly, the modes *out–in* and *in–in* as well as *out–out* and *in–out*, respectively, have already shown similar patterns regarding the local assortativity analysis of the *C. Elegans* network in Chapter 4. This might be therefore something worth understanding.

In order to assess the significance of the assortativity of the connectedness network, we use the algorithm by Rubinov and Sporns (2011), as in Chapter 3. This algorithm (approximately) preserves the strength distribution while rewiring the observed network. Since the total system-wide connectedness corresponds to the mean strength of the network (either out or in), it is preserved by the algorithm. This implies that random samples are drawn from the distribution of networks that exhibit the same total system-wide connectedness as the observed network, but for which edges had formed randomly, i.e., random assortativity structure. A comparison of the observed assortativity with the assortativity of the surrogates gives an indication of the significance of the assortativity of the observed network. We draw therefore a sample of 250 random networks for each rolling window estimate of the connectedness network and compare their respective assortativity values. Figure 5.7 shows the evolvement of the assortativity of the connectedness network over time.

The assortativity of the connectedness ranges between -0.36 and 0.08, with an average of -0.07 over the considered period, indicating that there are times when the network is more stable and times when it is less stable. We observe that the peaks and troughs of assortativity and connectedness coincide, respectively, i.e., at times at which the assortativity is low the connectedness is high, and vice versa. Apparently the total system-wide connectedness of the market and the generalized assortativity of the underlying network are inversely related.

By looking at both indicators at the same time, and additionally considering the significance of the generalized assortativity coefficient over time, a more precise assessment is possible as to when the market seems to be in a crisis and when not. The market is in crisis when the underlying network has transformed itself in such a way that it is non-assortative or (in particularly severe crises, such as in 2018) significantly disassortative compared to the corresponding null model, as this structure is as robust as possible against the failure of individual vertices. A crisis appears to subside when the underlying network resumes assortative tendencies over an extended period of time. In addition, the network shows the greatest assortative tendencies during periods of upswing. This is the case, for example, in the phases of the upswing from early 2019 to early 2020 and from mid-2020 to early 2021, and at the time before the last crash in the second quarter of 2022.

Statements of this kind cannot be made by analysing the total system-wide connectedness alone, since this key figure is apparently not suitable for an absolute comparison (of the percentages), as previously suspected.[56] This can be seen, for example, by looking at the periods from the second half of 2018 to early 2019 and from late 2021 to early 2022. The average system-wide connectedness is at a similarly high level for both

[56] If it were the case, that the absolute total system-wide connectedness percentages were suitable for a comparison across markets, we would come to the conclusion that the cryptocurrency market is permanently in a crisis.

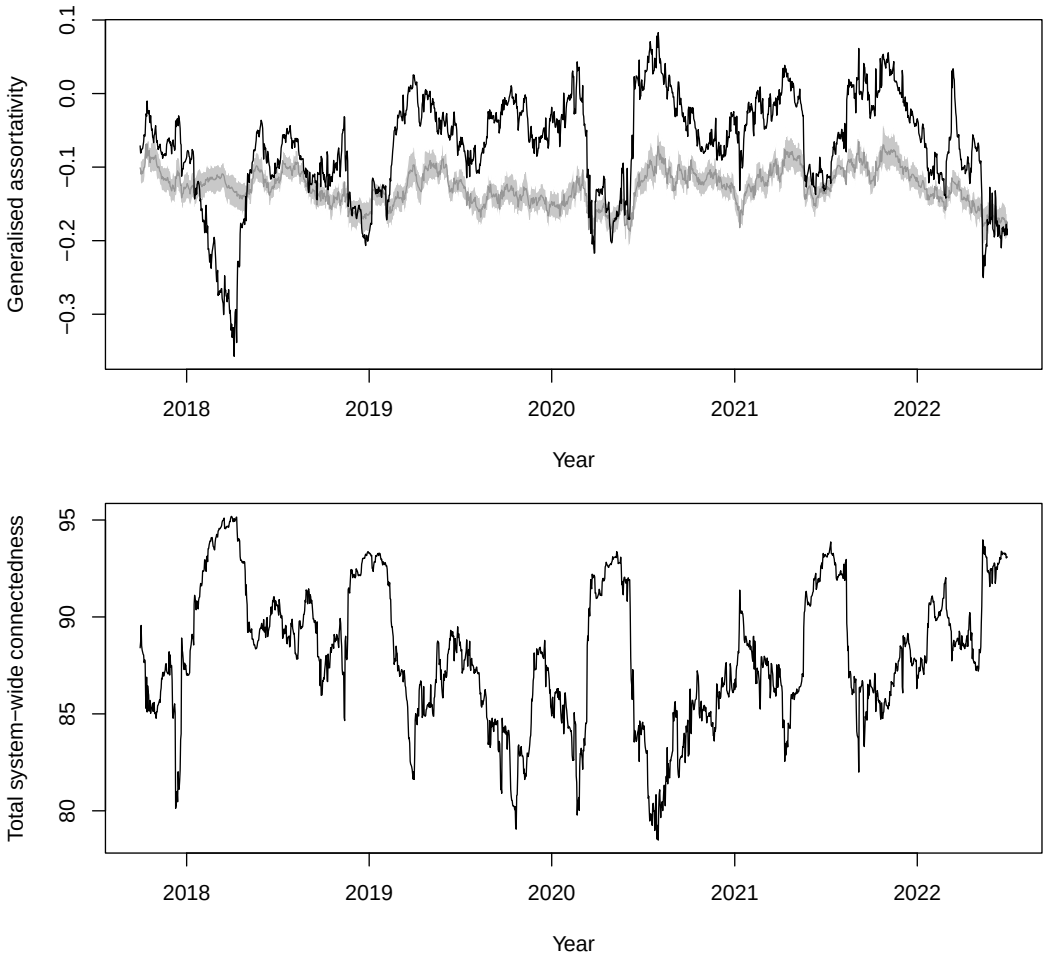

Figure 5.7. Evolvement of generalized *out–in* assortativity of the volatility connectedness network. Depicted are the evolvement of the generalized *out–in* assortativity coefficient ($\alpha = 1, \beta = 1$) for a rolling window estimation of the volatility connectedness network ($w = 90$, $H = 12$, $p = 4$), in the top figure. The dark grey line and grey shaded area indicate the mean of the generalized *out–in* assortativity of a respective null model together with a piecewise 95 percent confidence band, respectively. The bottom figure presents the total system-wide volatility connectedness, for comparison purposes.

periods. However, the market is in crisis in the first period, while the second period is rather calm. Only the additional consideration of the generalized assortativity for both periods enables the correct classification. Another point that shows that the analysis of assortativity provides additional information is the period between the two connectedness peaks at the beginning and end of 2018. Although the connectedness falls slightly during this period, which indicates a less connected system, and thus, a supposedly lower systemic risk, the assortativity shows that the market has not yet overcome the crisis. This is an advantage of the assortativity analysis, since the resulting coefficient can be compared with across networks by comparing it to the null model.

It would be interesting to know which underlying processes lead to the network being formed into an assortative or a disassortative one. Unfortunately, so far there exists no generative model that can be used to construct networks with a given assortativity, which would help explain why assortative mixing arises. All models known to us are based on a random graph with predefined basic features such as order, size, or degree distribution, which is made assortative or disassortative by link rewiring. So to explain how the network manages to form disassortatively in times of crisis and assortatively in upswings, we need to look at the components that make up the network.

In principle, the network is based on the return volatilities, which in turn are based on the returns resulting from the prices of the individual assets, which in turn are the product of supply and demand in the market. The core of the network and in particular its assortativity structure is therefore derived from the aggregated investment decisions of all participants in the market. The way investors act in the market, i.e., whether they sell or hold positions or even buy more, significantly influences the assortativity structure of the underlying network of the market. The assortativity structure of the network may therefore reflect the market sentiment. If the market sentiment is positive, as is the case with upswings, the potential risk of an exogenous shock is collectively assessed as low, which the investors express through their actions. The result is that the network becomes assortative, and the associated loss of stability is apparently tolerated by the market participants. However, if the risk of a shock is collectively perceived as high, as is the case in crises, the instability of the network will then no longer be tolerated, and the adjusted investment decisions lead to the network structure becoming non-assortative or even disassortative, which increases stability. It would be interesting to see if an additional analysis of sentiment indicators and the comparison of their evolvement with those of assortativity can confirm these assumptions. Possible sentiment indicators may be the VIX or the index of Baker and Wurgler (2006), for which Anamika, Chakraborty, and Subramaniam (2021) have shown that they impact the cryptocurrency market. Alternatively, the *VCRIX*, a volatility index specific to cryptocurrencies in the vein of the VIX index of A. Kim, Trimborn, and Härdle (2021) may be considered.

Although we are confident that the inverse relationship between a market's systemic risk and the robustness of its underlying network structure, which we empirically show for the cryptocurrency market, is shared by other financial markets more widely as well. This is something that has to be verified by further research.

However, if our assumption is confirmed, then for example, from a practical application point of view, the results of the joint analysis of connectedness and assortativity can be used to monitor the risk development in real time, not only in the cryptocurrency market but any financial market. It is then possible to identify early when the market is cooling off or is even heading towards a crisis. Moreover, the granularity in which the analysis is carried out can be selected arbitrarily fine, and it only depends on the data

availability whether quarterly, monthly weekly, or daily periods may be considered. We also see no reason why such an analysis should not also be possible on the basis of intraday data.

In the following, however, we want to deepen the assortativity analysis further and focus on the generalized local assortativity. Breaking down the interpretation of global generalized assortativity, as an indicator of the stability of a network, to individual vertices and edges, we come to the conclusion that local assortativity can be an indicator of stabilizing vertices or edges. More precisely, since vertices that have a particularly high (and positive) local vertex assortativeness value contribute the most to the assortative structure of the network, they therefore destabilize the network the most. In contrast, nodes that have a particularly high (and negative) local vertex assortativeness value contribute the most to the disassortative structure of the network, and thus stabilize it the most. The same considerations can be made for edges and their local edge assortativeness values.

The analysis of the local generalized assortativity is based on the full sample volatility connectedness network. For this purpose, Table 5.3 first shows the results of the global generalized assortativity analysis for the consideration of the entire period, again for the parameter combination ($\alpha = 1, \beta = 1, \text{mode} = \textit{out–in}$). Obviously, the network is significantly disassortative, since $r^\omega < r^\omega_{\text{rnd}}$, and $r^\omega \notin [-0.075, -0.050]$, indicating that the market is currently in a (severe) crisis.

r^ω	$\hat{\sigma}_{r^\omega,J}$	r^ω_{rnd}	$\hat{\sigma}_{r^\omega_{\text{rnd}}}$	$\text{CI}_{r^\omega_{\text{rnd}},0.95}$
-0.098	0.032	-0.062	0.006	$[-0.075, -0.050]$

Table 5.3. Generalized assortativity analysis of the static volatility connectedness network. Reported are the values of the generalized assortativity coefficient, r^ω, together with the jackknife estimate of the standard error, $\hat{\sigma}_{r^\omega,J}$, the expected generalized assortativity of the corresponding null model (based on an ensemble size of 250), r^ω_{rnd}, together with its standard error estimate and a 95 percent confidence interval of the generalized assortativity coefficient of the null model, $\text{CI}_{r^\omega_{\text{rnd}},0.95}$, for the parameter combination ($\alpha = 1, \beta = 1, \text{mode} = \textit{out–in}$).

To break down the global generalized assortativity, we calculate the generalized edge assortativeness values, ρ^ω_e, for each edge and the generalized vertex assortativeness values, ρ^ω_v, for each vertex. Recall that the generalized edge assortativeness, ρ^ω_e, are defined as:

$$\rho^\omega_e(\alpha, \beta, \textit{out–in}) = \frac{\omega_e^\beta [l_e^{\text{out}} - \bar{U}^\omega_{q_s^{\text{out}}}(\alpha, \beta)][m_e^{\text{in}} - \bar{U}^\omega_{q_s^{*\text{in}}}(\alpha, \beta)]}{\Omega \cdot \hat{\sigma}^\omega_{q_s^{\text{out}}}(\alpha, \beta) \cdot \hat{\sigma}^\omega_{q_s^{*\text{in}}}(\alpha, \beta)},$$

where the mode of assortativity is *out–in* and is determined by the mode of the global assortativity under consideration, l_e^{out} and m_e^{in} are the excess out-strength of the end l

that edge e leads out of and the excess in-strength of the end m that edge e leads into. The weighted sample mean out- and in-strengths of the outgoing and incoming ends are $\bar{U}^{\omega}_{q_s^{\text{out}}}(\alpha,\beta)$ and $\bar{U}^{\omega}_{q_s^{*\text{in}}}(\alpha,\beta)$, respectively, and the respective weighted sample standard deviations are given by $\hat{\sigma}^{\omega}_{q_s^{\text{out}}}(\alpha,\beta)$ and $\hat{\sigma}^{\omega}_{q_s^{*\text{in}}}(\alpha,\beta)$. Further, recall that the generalized vertex assortativeness values, ρ^{ω}_v, are defined as:[57]

$$\rho^{\omega}_v(\alpha,\beta,\textit{out}) = \sum_{u=1}^{n} \rho^{\omega}_{e_{vu}}(\alpha,\beta,\textit{out-in}).$$

Figure 5.8 visualizes the results of the local assortativity analysis. For example, Figures 5.8a and 5.8c show scatterplots of the generalized edge assortativeness values, and Figure 5.8e shows the corresponding histogram. Since the elements of the adjacency matrix are ordered (i.e., cryptocurrencies are ordered according to their market capitalization), this order carries over to the order in which the edges are considered. Thus, when the edge assortative values are plotted against their index, we can observe that connections between large cryptocurrencies tend to be disassortative and connections between smaller cryptocurrencies tend to be assortative.

When the edge assortativeness values are plotted against the corresponding edge weight, we observe that assortative connections are almost exclusively present in the low edge weight range, whereas disassortative edges tend to have medium to high edge weights, but hardly any low ones. The histogram, shows that the proportion of disassortative edges is slightly higher than the proportion of assortative edges, however, the majority of the edges are non-assortative.

Figures 5.8b and 5.8d show scatterplots and Figure 5.8f shows the corresponding histogram for the generalized vertex assortativeness values. As before, since the elements of the adjacency matrix are ordered, plotting the vertex assortativeness values against their index reveals if there is a relationship between the size of a cryptocurrency and its vertex assortativeness. Apparently, this is not the case as assortative and disassortative vertices tend to be evenly distributed across all indexes. However, the two largest cryptocurrencies are particularly disassortative as compared to the others.

On the other hand, plotting the vertex assortativeness values against the corresponding average excess strength of a vertex, reveals a nonlinear relationship. More specifically, vertices with an average excess strength fairly close to the mean average excess strength, which equals 0.872, tend to be non-assortative. Vertices with an average excess strength above mean tend to be disassortative, while they can be both assortative and disassortative if their average excess strength is below mean. If we look at the his-

[57] Recall that in a directed network it is possible do compute both generalized vertex out-assortativeness values and generalized vertex in-assortativeness values. A preliminary analysis has shown that the results do not differ much, no matter what form of generalized vertex assortativeness value we compute. Thus, we focus on generalized vertex out-assortativeness.

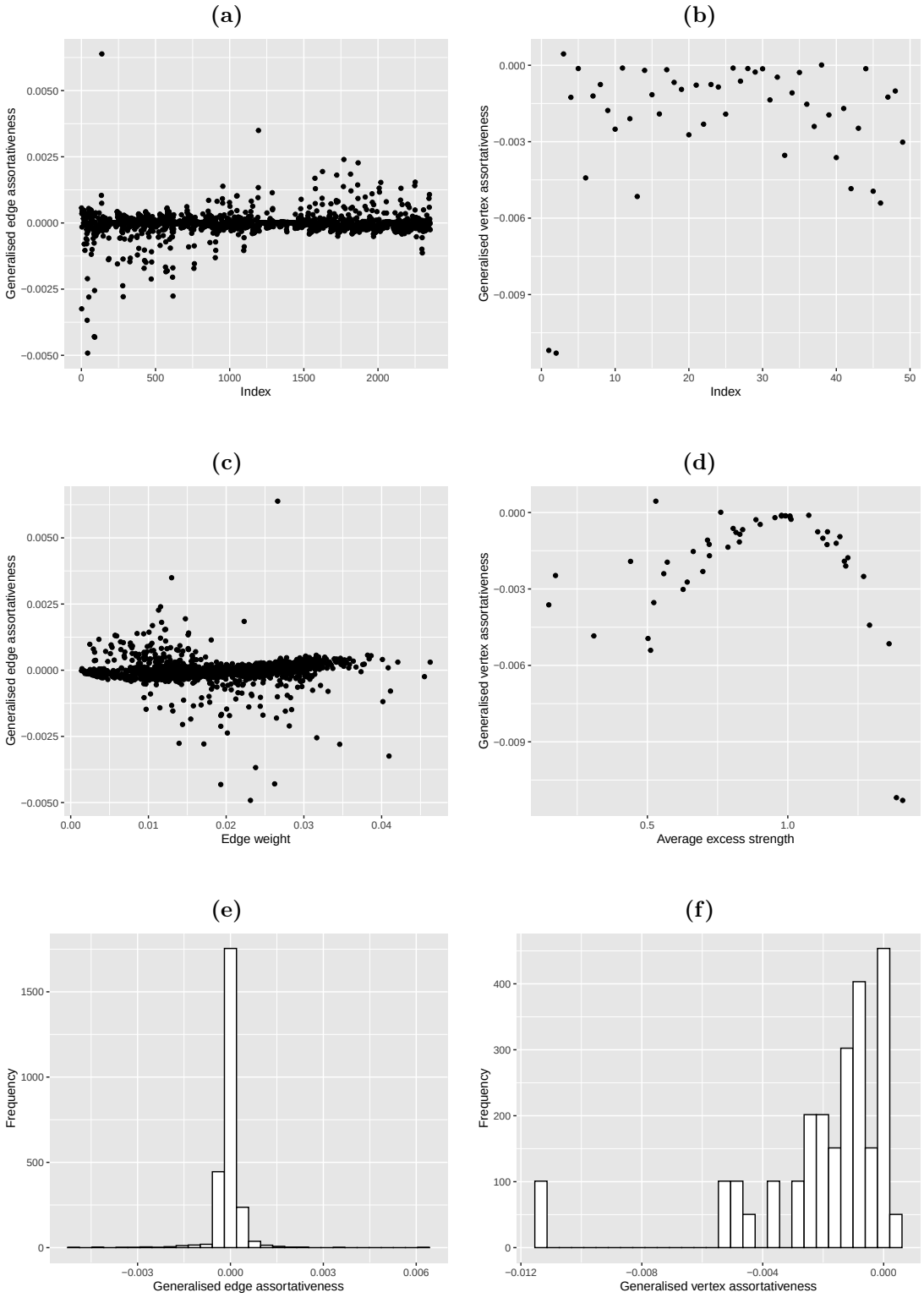

Figure 5.8. Generalized local assortativity of the static volatility connectedness network.

togram, we find that vertices are almost exclusively non-assortative or disassortative. As we shall shortly see, there are only two assortative vertices.

There are various ways of achieving a non-assortative or disassortative structure for a network. For example, if we make the comparison to the WRG or WSF model (see Chapter 4), we find that a network can be non-assortative in that disassortative and assortative vertices or edges balance each other (WRG). Or it takes a non-assortative structure with a slight tendency towards disassortativity in that the predominant part of the network is non-assortative and only a few vertices or edges are very strongly disassortative (WSF). If we consider the edge and vertex assortativeness values in the cryptocurrency network, however, it becomes apparent that the whole network is seeking for robustness, since almost all parts (edges and vertices) tend to be non-assortative or disassortative.

Consider, therefore, Table 5.4 and Table 5.5 where we report the top 5 assortative and disassortative vertices and the top 5 assortative and disassortative edges, with respect to generalized vertex and edge assortativeness, respectively. In the context of stability, we note that Tether (USDT) poses the greatest threat to the stability of the underlying network, while Bitcoin (BTC) and Ethereum (ETC) protect it. The statements refer to the network that is currently in a crisis. It is to be expected that a different picture emerges in upswings. However, to show that a more sophisticated, dynamic analysis of local assortativity is required, which is beyond the scope of this work and which we therefore postpone to future research.

Generalized vertex assortativeness					
Top assortative			Top disassortative		
Rank	Symbol	Assortativeness	Rank	Symbol	Assortativeness
1	USDT	0.0004448	1	ETH	-0.0112978
2	FUN	0.0000101	2	BTC	-0.0111917
3	ZEC	-0.0001088	3	GXC	-0.0054079
4	DGB	-0.0001102	4	NEO	-0.0051509
5	DOGE	-0.0001287	5	SBD	-0.0049446

Table 5.4. Generalized vertex assortativeness ranking of the (static) volatility connectedness network. The table shows the top 5 most assortative as well as the top 5 most disassortative cryptocurrencies with respect to the generalized vertex assortativeness values, ρ_v^ω, for the parameter combination $(\alpha = 1, \beta = 1, \text{mode} = \textit{out–in})$.

Finally, if we translate the results of the generalized local assortativity analysis into recommendations for action with respect to investment decisions during financial crises, the following strategy appears to be fairly reasonable. One might want to consider investing in positions as disassortative as possible, for which the risk of failure due to a direct exogenous shock is low (based on project size or liquidity reserve et cetera). For

Generalized edge assortativeness							
Top assortative				Top disassortative			
Rank	From	To	Assortativeness	Rank	From	To	Assortativeness
1	USDT	XWC	0.0063853	1	BTC	XWC	-0.0049170
2	NMR	XWC	0.0034936	2	ETH	XWC	-0.0043160
3	MAID	XWC	0.0023983	3	ETH	VERI	-0.0042937
4	ANT	XWC	0.0022711	4	BTC	VERI	-0.0036766
5	REP	XWC	0.0019433	5	BTC	USDT	-0.0032437

Table 5.5. Generalized edge assortativeness ranking of the (static) volatility connectedness network. The table shows the top 5 most assortative as well as the top 5 most disassortative connections between cryptocurrencies with respect to the generalized edge assortativeness values, ρ_e^ω, for the parameter combination ($\alpha = 1, \beta = 1, \text{mode} = \textit{out–in}$).

such positions, the risk of failure due to an indirect shock that propagates through the network is lower due to the disassortative tendencies, however, the risk of a direct shock remains, and thus, should be also considered. On the other hand, one might want to consider staying away from or clearing positions that show assortative tendencies, and for which it is unclear if they would stand even indirect shocks (again, based on project size or liquidity reserve et cetera). Such positions have a higher risk of failure due to both direct and indirect shocks.

To illustrate this, we compare the performance of *WhiteCoin* (XWC), a small cryptocurrency with respect to market capitalization, which is the receiving end of the top 5 assortative edges (according to our strategy one to avoid), with those of Bitcoin (BTC), the largest and second most disassortative cryptocurrency (according to our strategy one that should be preferred). WhiteCoin (XWC) experienced an above-average fall in the price of 91.97 percent, since the beginning of 2022. In terms of market capitalization of WhiteCoin, this means that about $565MM vanished. By comparison, the price decline of Bitcoin, is equivalent to (merely) 59.59 percent, over the same time period. The price decline of the more assortative WhiteCoin (as compared with Bitcoin) is more than 50 percent higher than for the more disassortative Bitcoin. However, this is only an indication. Further research has to verify whether the trading strategy is sensible or not. Therefore, one would have to examine the local assortativity dynamically.

Moreover, the analysis of the local edge and vertex assortativeness values can also be particularly helpful with selecting considerable pairwise directional connectedness relationships for an analysis, as analysing of all of them might not possible with justifiable effort. For example, for the considered network, there are a total of 2352 pairwise connectedness relationships. Thus, it seems sensible to select only those pairwise relationships for a more in-depth analysis that are particularly relevant from a risk perspective, e.g, the top assortative and disassortative relationships (see Table 5.5). For the

cryptocurrency network, Figures C.20 and C.21 depicts the evolvement of pairwise directional connectedness over the considered time period, for both the top 5 assortative and disassortative connections between the cryptocurrencies, for example. However, a more in-depth analysis of the pairwise connectedness, in particular the meaningfulness of the results, would require detailed knowledge of the individual cryptocurrency projects. However, that would exceed the scope of this work. We may come back to this in future research.

In addition to the total system-wide and pairwise directional analysis of connectedness, it can sometimes be useful to examine whether cryptocurrencies can be grouped together based on their connectedness, from a robustness perspective. The idea behind it is, that in the event of a shock to a particular cryptocurrency, the surrounding ones that are close tend to be affected sooner or more severely. In network terminology such a phenomenon is referred to as *cascading failures*, i.e., the activity of a vertex depends on the activity of its neighbours, such that the failure of a vertex may induce failures to the vertices it is connected to, cf. Barabási (2016). Cascading failures are common in economic systems and have been the cause of some of the most severe financial crises in the recent past. Consider, for example, the decline in house prices in 2008 in the U.S., which led eventually to a global financial crisis. It is therefore valuable information for both investors and policymakers to know which cryptocurrencies are particularly close in terms of community structure in order to take possible cascading failures into account. To this end we consider briefly the community structure of the cryptocurrency network in the next section.

5.3.6 Backbone Extraction and Community Structure

The backbone of a network refers to a simpler version of the original network that is reduced in size (i.e., some vertices or edges are omitted), such that the core information of the original network is preserved, cf. Dai, Derudder, and Liu (2018). We mentioned above that the cryptocurrency network is a complete network, i.e., each vertex is connected to every other vertex in the network by a weighted edge. In the case of assortativity, we had to extend the assortativity coefficient, in order to be able to compute the measure for the cryptocurrency network. Some methods are in theory applicable to complete networks but fail in practice because of the high edge density. For example, the algorithm that we use for community detection is unable to uncover the communities in the complete network. In order to achieve sparsity of the network, i.e., to determine its backbone, a plethora of techniques is available, of which a comprehensive review is given by Dai et al. (2018).

A simple and straightforward approach is the *global weight thresholding*, cf. Yan, Jeub, Flammini, Radicchi, and Fortunato (2018). When illustrating the resulting net-

work, Diebold and Yilmaz (2014, fig. 7) utilize global weight thresholding,[58] by only depicting edges whose edge weight magnitude is above a certain percentile threshold.[59] Alternatively, the minimum spanning tree can be examined instead of the complete network. In order to find the minimum spanning tree of a network, $(n-1)$ edges are selected such that no cycle is created and the sum of their weights is minimal,[60] see, e.g., Kruskal (1956). Zięba et al. (2019), for example, analyse cryptocurrency networks using their minimum spanning trees.

However, both of these approaches have disadvantages, as they destroy local patterns and neglect the multiscale nature of networks. The minimum spanning tree omits cycles by construction, and thus, produces overly simplified representations of the original network, where clustering hierarchies are destroyed, cf. Serrano, Boguñá, and Vespignani (2009). Moreover, since exactly $(n-1)$ edges are select in finding the minimum spanning tree, its size is fixed. With global weight thresholding, the threshold is usually chosen arbitrarily. In addition, the reduced-size network only contains edges with a relatively high edge weight, since edges whose weight is below the threshold are removed. Hence, global thresholding introduces arbitrariness, structural bias and uniscalarity, cf. Dai et al. (2018).

In order to reduce the density of the network of cryptocurrencies, and extract its backbone, we opt therefore for using a more sophisticated approach, which does not have the above disadvantages. We will use the *disparity filter algorithm* suggested by Serrano et al. (2009).[61] By specifying a null model to define anomalous fluctuations in the edge weights, the disparity filter algorithm preserves those edges of the network that deviate significantly from the local weight assignment scheme under the null hypothesis. The assumed null model considers normalized edge weights, $p_{ij} = w_{ij}/s'_i$, where, as before, $s'_i = \sum_j w_{ij}$ is the strength of vertex i.[62] The normalized edge weights, that correspond to the connections of a particular vertex of degree k', are then considered to be randomly assigned draws from a uniform distribution, $U_{[0,1]}$.

According to Serrano et al. (2009) a somehow conceivable explanation would be to consider the lengths of k subintervals obtained by uniformly sampling $k-1$ breakpoints

[58] However, they do not refer to the term *global weight thresholding* explicitly.

[59] We have also seen others using this approach.

[60] Note, however, that this is the case if edge weights refer to distances. In case of connectedness one would either have to select the edges such that their sum is maximal or use their reciprocals, as a high connectedness indicates a low distance between vertices and vice versa.

[61] Interestingly, the disparity filter algorithm is a special case of the *Pólya filter*, which offers a continuous family of network backbones $\mathcal{P}_a$, as a combinatorial model, based on the Pólya urn, that is driven by a self-reinforcement mechanism governed by a reinforcement parameter a, cf. Marcaccioli and Livan (2019). An example of a Pólya urn is the following: initially, an urn contains B_0 black balls and R_0 red balls; a ball is drawn from the urn, randomly with replacement; when returning the ball, a many new balls of the same colour are added to the urn; this process repeats n times, such that the probability of observing x red balls after n steps follows the Beta-Binomial distribution, cf. Mahmoud (2009). The disparity filter is obtained by setting $a = 1$.

[62] For simplicity, the depiction of the algorithm is for the case of an undirected network, however, it is also suitable for directed networks.

from the interval $[0, 1]$. The lengths of the k intervals then correspond to the expectation of the normalized edge weights, p_{ij}. The probability density function for the normalized edge weights taking on a particular value x is then given by:

$$\rho(x)dx = (k-1)(1-x)^{k-2}dx.$$

With this, for each edge of the original network, the probability of its weight being in accordance with the null model can be determined by:

$$\alpha_{ij} = 1 - (k-1)\int_0^{p_{ij}} (1-x)^{k-2}dx.$$

By prespecifying a significance level $\tilde{\alpha}$, edges that do not comply with the null hypothesis are filtered out, i.e., if $\alpha_{ij} < \tilde{\alpha}$, as they are considered to be the product of network-organizing principles, and thus, form the network backbone. Edges for which $\alpha_{ij} > \tilde{\alpha}$ are removed, as they are considered to be random fluctuations.

Serrano et al. (2009) conclude that values in the range $\tilde{\alpha} = [0.01, 0.5]$ are optimal in the sense that the resulting backbones preserve a large proportion of both the number of vertices and the sum of edge weights, compared to the original network.[63] Moreover, they exhibit the same clustering, and have a stable stationary degree distribution, albeit consisting of a much smaller number of edges.

$\tilde{\alpha}$	$\%H_{\text{orig.}}$	$\%V_{\text{orig.}}$	$\%E_{\text{orig.}}$	$\tilde{\alpha}$	$\%H_{\text{orig.}}$	$\%V_{\text{orig.}}$	$\%E_{\text{orig.}}$
0.50	0.995	1.000	0.982	0.25	0.235	1.000	0.156
0.45	0.980	1.000	0.949	0.20	0.079	0.857	0.046
0.40	0.899	1.000	0.822	0.15	0.018	0.449	0.010
0.35	0.703	1.000	0.580	0.10	0.005	0.143	0.003
0.30	0.479	1.000	0.353	0.05	0.000	0.041	0.000

Table 5.6. Disparity backbone network sizes. The sizes are in relation to the original network, in terms of percentage total edge weight $\%H_{\text{orig.}}$, vertices $\%V_{\text{orig.}}$ and number of edges $\%H_{\text{orig.}}$ for different values of $\tilde{\alpha}$.

For the volatility connectedness network, Table 5.6 gives an overview of resulting backbone network sizes, as compared to the original network, in terms of percentage total edge weight $\%H_{\text{orig.}}$, vertices $\%V_{\text{orig.}}$ and number of edges $\%H_{\text{orig.}}$ and Figure 5.9 shows the corresponding resulting backbone network visuals for different values of the parameter $\tilde{\alpha}$. The vertex labels correspond to the respective market capitalization ranks of the cryptocurrencies, as in Table C.1, in the appendix. For example, the vertex labelled 1 corresponds to Bitcoin (BTC). Apparently, by changing the values

[63] In the case of the volatility connectedness network, the fact that a large proportion of the sum of edge weights is preserved is desirable, as it is proportional to the total system-wide connectedness measure, C^H.

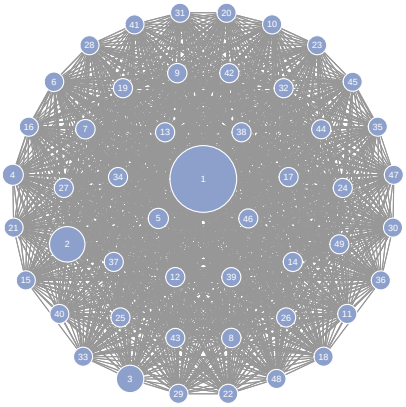

(a) Complete network.

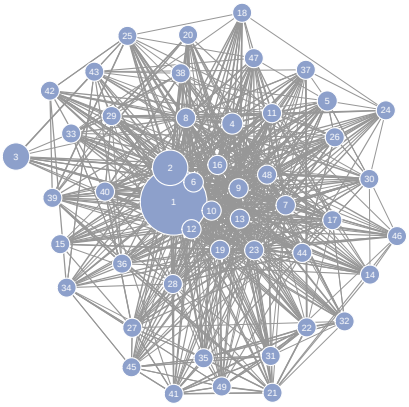

(b) $\tilde{\alpha} = 0.30$

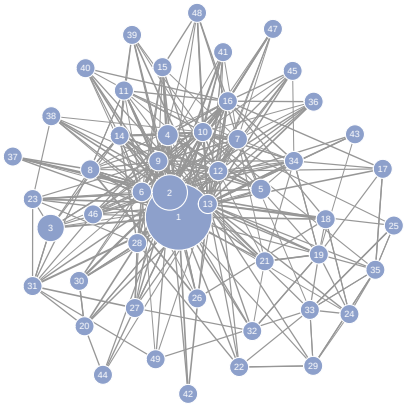

(c) $\tilde{\alpha} = 0.25$

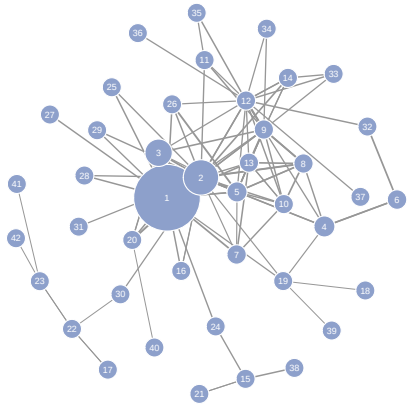

(d) $\tilde{\alpha} = 0.20$

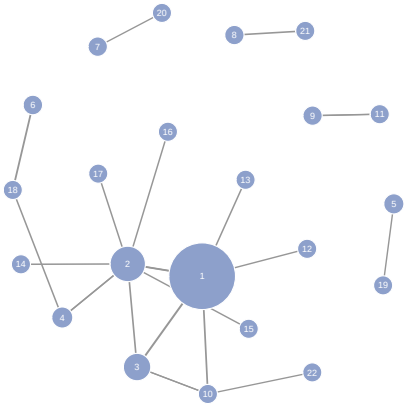

(e) $\tilde{\alpha} = 0.15$

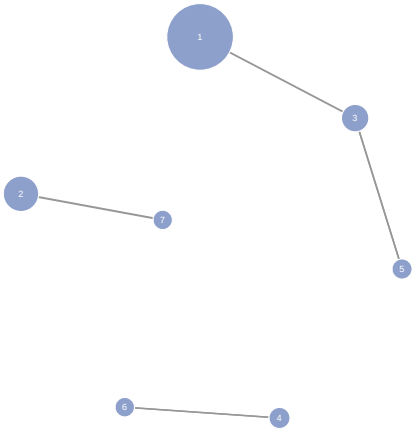

(f) $\tilde{\alpha} = 0.10$

Figure 5.9. Disparity backbone network visualizations.

of $\tilde{\alpha}$, edges are filtered out progressively focusing on more relevant edges.[64] As the figures show, there are more relevant edges between cryptocurrencies with higher market capitalization, as already indicated in Section 5.3.3.

However, with the disparity filter algorithm, not only edges with a high edge weight are considered, but also statistically significant edges with a low edge weight. This means that all important connections are considered on multiple scales at the same time. This would not have been possible with the global weight thresholding approach, since all edges below the scale determined by the threshold are removed. However, all approaches to reducing the complexity of the network have their limitations, including the disparity filter algorithm approach. In particular, the disparity filter algorithm does not work in networks where the edge weights are homogeneously distributed, cf. Serrano et al. (2009). However, this is not a problem in the present case, since the edge weights of the cryptocurrency network are heterogeneously distributed, see Figure 5.4b.

The question arises as to which value of $\tilde{\alpha}$ should be chosen in order to determine the network backbone. Unfortunately, there is no answer that conclusively answers the question. We, therefore, propose to examine a selection of values with regard to their suitability on a case-by-case basis, as we did. In the case of the cryptocurrency network, if we had to commit to a value, we would tend towards 0.2, as this is the value that generates the smallest backbone network with all vertices preserved from the original network. We want the backbone network to be small, limited to only the most relevant edges, but at the same time, we want to keep all vertices of the original network as we want to assign each cryptocurrency to a community. However, there may be cases where it is not necessary to preserve all nodes of the original network, then another value may be more appropriate.

There are a multitude of methods for finding communities in networks, see, e.g., Fortunato and Hric (2016) for an excellent review on community structure detection. For uncovering the communities of the cryptocurrency network we use the very popular *Louvain algorithm*, cf. Blondel, Guillaume, Lambiotte, and Lefebvre (2008).[65] The Louvain algorithm is a greedy algorithm optimizing the network *modularity*. Modularity is a measure that indicates the quality of a network partition in the sense that the within community edge density is high, whereas, at the same time, the in-between community edge density is low, cf. Newman and Girvan (2004), Newman (2004) and Leicht and Newman (2008). Figure 5.10 shows the network backbones for which we determined the communities using the Louvain algorithm, the nodes are coloured according to their

[64] We forgo depicting network visuals for values of $\tilde{\alpha} = \{0.50, 0.45, 0.40, 0.35, 0.05\}$, as the resulting backbone networks either have a similar visual appeal as the complete network or consist of only a single connection between vertices 1 and 2.

[65] The classic Louvain algorithm is designed for undirected networks. Directed networks are usually treated as undirected, as the method is still applicable, then. This is what we have done in this work. However, Dugué and Perez (2015) have proposed a directed version of the algorithm, which we might consider in future research.

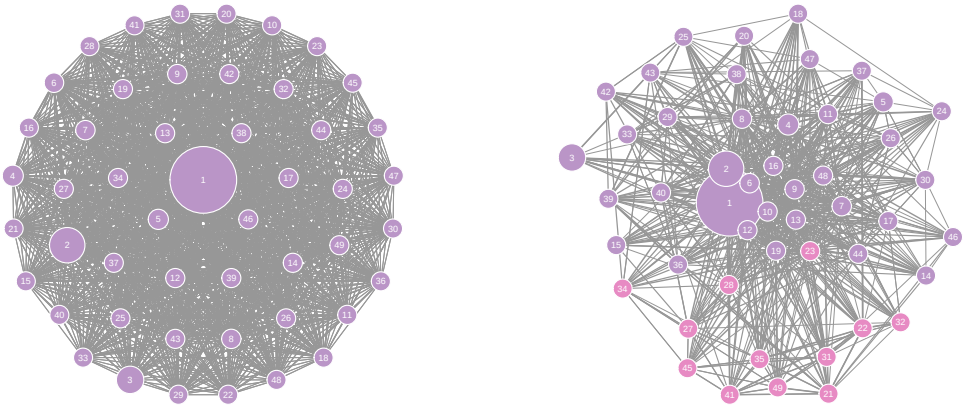

(a) Complete network. **(b)** $\tilde{\alpha} = 0.30$

(c) $\tilde{\alpha} = 0.25$ **(d)** $\tilde{\alpha} = 0.20$

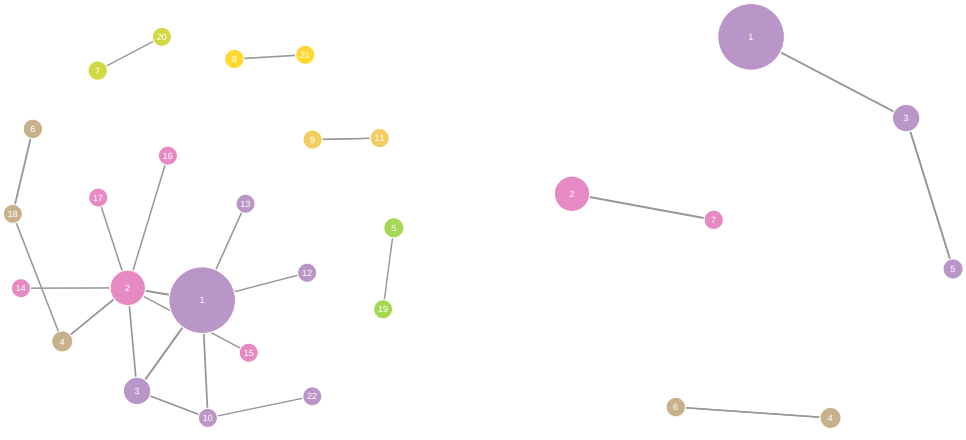

(e) $\tilde{\alpha} = 0.15$ **(f)** $\tilde{\alpha} = 0.10$

Figure 5.10. Disparity backbone network community structure. Application of the Louvain algorithm for community detection.

community affiliation. Apparently, the algorithm is able to uncover the communities the better, the sparser the network is. Depending on the desired level of sparsity, the cryptocurrency network can be divided into between two and seven communities. The information about which cryptocurrencies can be grouped together can now also be used to assess the potential threat that individual cryptocurrencies pose to others. Interestingly, considering the top 3 largest cryptocurrencies, Bitcoin (BTC) and Tether (USDT) are almost always in the same community (the exception is for $\tilde{\alpha} = 0.25$). In contrast, Bitcoin (BTC) and Ethereum (ETH) are in different communities for the sparsest network backbones, where the focus is on the most relevant edges.

5.4 Discussion and Future Work

Our analysis has shown that the total system-wide volatility connectedness, which is a proxy for the systemic risk, can be related to the generalized assortativity coefficient of the corresponding volatility connectedness network, which itself is considered to be a proxy for the stability of the network. Both measures are inversely related, i.e., the one is high when the other is low and vice versa. More precisely, it is in turbulent times of high systemic risk (crisis), when the system-wide connectedness peaks. In those times, the generalized assortativity coefficient of the connectedness network tends to be low, indicating that the network is non-assortative or even disassortative (with respect to a corresponding null model). In phases of upswing, however, the network tends to become assortative. We have shown that analysing both metrics together is beneficial as it allows for a more precise classification of crises and their severity. This was previously not possible with the exclusive consideration of connectedness.

Analysing the generalized local assortativity of the volatility connectedness network has shown that Tether (USDT), being the most assortative vertex in the network, is the greatest threat to the stability of the cryptocurrency network. Whereas the two largest cryptocurrencies Bitcoin (BTC) and Ethereum (ETH) are its strongest protectors, as they contribute most to the disassortative structure of the network. Note, however, that the above reasoning is based on the static local assortativity.

Both global and local generalized assortativity analysis are based on real-time monitoring the market of cryptocurrencies. However, it would be interesting to see if the future evolution of the network, particularly the assortativity, can be predicted. If that were the case, potential crises could be identified at an early stage and recommendations for action could be made. We have not mentioned it explicitly yet, but when we look at the cryptocurrency network dynamically, we obtain a separate adjacency matrix for every point in time. In network science, such networks are referred to as temporal networks for specific methods are available, see, e.g., Holme and Saramäki (2012) and Holme (2017) for a survey on the subject of temporal networks, and Brey, LeBlanc, and Deschamps (2018) for an overview of selected methods for analysing and visual-

izing temporal networks based on the *R* programming language. In this context, two recent publications consider temporal network prediction and interpretation, one using interpretable learning algorithms, such as LASSO regression and random forests, the other one reviewing various approaches, e.g., probabilistic, time series analysis, or deep learning approaches. We will test the above methods for their suitability for predicting the future assortativity structure of the cryptocurrency network, and thus, anticipating times of crisis of the cryptocurrency market, in future research.

Furthermore, it may be interesting to examine the development of the assortativity structure with regard to its timeframe. We are interested in finding out whether there are differences in the short-, medium- and long-term assortativity structure. For the volatility connectedness, in order to account for heterogeneous frequency responses to shocks of variables, Baruník and Křehlík (2018) introduce a framework based on the spectral representation of variance decompositions. This allows for partitioning connectedness in, for example, short-, medium- and long-term financial cycles. Again, we have not yet seen any explicit reference in the literature, but with the approach by Baruník and Křehlík (2018), multiple adjacency matrices at any point in time are obtained, for which the edge weights each have a different meaning. In the case of edge weights referring to short-, medium- and long-term connectedness, there are three adjacency matrices at any point in time. This is a temporal multiplex, which is a special case of a multilayer network, cf. Kivela et al. (2014) for an overview of the topic of multilayer networks. Since there are also separate methods for these kinds of networks, we also see untapped potential for future research here. We want to use these methods to further improve our assortativity analysis of the cryptocurrency network.

Considering the general suitability of the DY framework in combination with KPPS for the derivation of the underlying network structure of the market of interest, Wiesen and Bharadwaj (2021) point out disadvantages: (1) As a consequence of using the *ad hoc* normalized GFEVD matrix, such that rows sum to unity, DY may fail to measure the exact degree of total connectedness, cf. Caloia, Cipollini, and Muzzioli (2019); (2) By summing the directional connectedness values that lead to variable j, in order to obtain the *total to-connectedness*, $C^H_{j\leftarrow\bullet}$, the cross-correlation between the variables (over which the sum is computed) are neglected, and, thus, the use of DY spillover indices may only imprecisely dichotomize forecast error variance into *own-variable* effects and *other-variable* effects, cf. Lastrapes and Wiesen (2021).

Although we conjecture that (2) may not be too drastic, as we utilize a regularization approach in order to estimate the coefficients, and the RR part of the elastic net penalty considers multiple correlated variables. Therefore, as an alternative to the DY framework, we may consider using the *joint spillover index* suggested by Lastrapes and Wiesen (2021), which overcomes the above-mentioned disadvantages, in order to construct the adjacency matrix of the network. It would be interesting to see whether and,

if so, how far the resulting network structure is affected by the use of different spillover indexes.

We find that the data are particularly well suited for analysing risk and robustness, since the market for cryptocurrencies is characterized, among other things, by its high volatility. Moreover, the market had to suffer several shocks in the recent past. These shocks always led to strong fluctuations, as compared to other financial markets, for which a price decline of around 90 percent in 2 months is rather unusual, for example. At the same time, however, this also means that the resulting patterns of the cryptocurrency market are becoming more apparent, which enabled us to recognize the connection between connectedness and assortativity. We find it fascinating that the analysis of the generalized assortativity produces such interesting results and that the patterns are so well pronounced for the cryptocurrency market.

This concludes the analysis. We proceed with a conclusion of this thesis in the last chapter.

6 Conclusion

In this thesis we have shown that assortativity, the tendency of vertices to bond with others based on similarities (usually excess vertex degree), in weighted networks is more complex than in unweighted networks. Previously published research focuses on seeking a single measure that describes the underlying assortativity structure. We pointed out, however, that focusing on a single measure might lead to information loss, and, therefore, proposed a generalized assortativity coefficient that nests previous measures and that utilizes available information at the best.

To this end, we proposed to use as vertex values excess vertex strength, which has never been considered in the assortativity literature so far and which is the generalization of excess vertex degree in weighted networks. We broke down assortativity in weighted networks into its components and identified two mechanisms that essentially affect the assortativity structure of a network, which we refer to as the connection effect as well as the amplification effect. Furthermore, we provided procedures that allow for a detailed interpretation and assessment of assortativity in weighted networks as well as for the assessment of its statistical significance. For the latter we introduced appropriate resampling and link rewiring techniques. We demonstrated the application and usefulness of our generalized assortativity coefficient for assessing and interpreting the assortativity of three commonly used weighted real-world networks, both directed and undirected.

Moreover, we have extended local assortativity for weighted networks. By having unified two approaches used in the literature, we were able to derive distinct measures that allow us to determine the assortativeness of individual edges and vertices as well as of entire components of a weighted network. We demonstrated the usefulness of these measures by applying them to various theoretical and real-world networks. We were able to show that the analysis of generalized local assortativity can help to further break down the assortativity structure for a network. This allows to further differentiate the topology of networks that exhibit a similar global assortativity, as we have shown for the theoretical models. Along the way, we also explained how to compute local assortativity profiles, which are informative about the pattern of local assortativity either with respect to edge weight or vertex strength.

Since (almost) everything can be represented as a network, we were able to analyse the underlying network of the cryptocurrency market, the structure of which we estimated using cryptocurrency price data. By using a regularization approach when estimating the model parameters, we were able to conduct a study that stands out from others.

Since we analyse a more exhaustive set of data, both in terms of the time span and in terms of the number of considered cryptocurrencies. Other studies either look at a similar length of time as we do, but only analyse a handful of cryptocurrencies, or consider a similar number of cryptocurrencies as we do, but for a much shorter period of time. However, by looking at a longer period of time, we were able to better interpret the patterns that emerged.

We have thoroughly studied the network of cryptocurrencies, particularly with regard to the relationship between the network's volatility connectedness, as a measure of systemic risk, and its assortativity structure, as a measure of network resilience. By analysing the evolvement of the generalized assortativity coefficient of the volatility connectedness network, we were able to empirically show that both measures are inversely related. This opens up new possibilities of monitoring systemic risk, since we additionally provide a procedure for determining the significance of generalized assortativity with respect to a null model. For this purpose, we have provided information on how the results of this analysis can be used to develop a corresponding monitoring tool. Without the generalized assortativity measures, this analysis would not have been possible, and this relation would have remained undetected.

Moreover, we demonstrated how the backbone of the cryptocurrency network can be obtained in order to properly determine its community structure. This analysis provides valuable information in terms of assessing and managing risk, as it allows cascading failures in the network to be taken into account.

In addition, we have given references to interesting questions for future research at the appropriate points in this work. What we find most interesting is whether the network structure can be predicted. Based on the results of this work, we conclude that the ability to predict the network structure would be tantamount to the ability to predict crises. For this reason, we will devote more attention to this question.

Finally, we expect that this way of analysing connectedness together with generalized assortativity will be extensively used in analysing financial networks, and we are curious to see whether such an analysis will deliver similar results for other markets. We leave for future research to ascertain whether the inverse relationship between a market's systemic risk and the robustness of its underlying network structure is unique to the cryptocurrency market or is shared by other financial markets more widely.

A Appendix Chapter 3

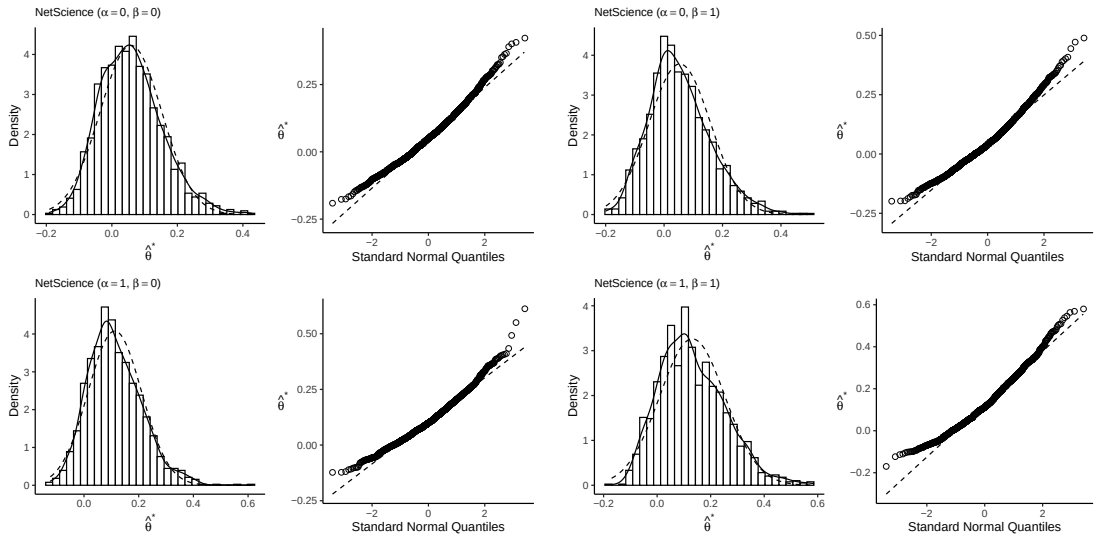

Figure A.1. Histogram and QQ-plot of bootstrap replications *(NetScience).* Histogram and QQ-plot of the distribution of bootstrap replications $\hat{\theta}_b^*, b = 1, \ldots, B = 1499$ for the undirected *NetScience* network for the various parameter constellations $(\alpha, \beta) \in \{0, 1\}$. Lines indicate the kernel density of the bootstrap distribution (solid) and the density of the normal distribution $\mathcal{N}(\bar{\hat{\theta}}_b^*, \hat{\sigma}^2_{\hat{\theta}_b^*})$ (dashed).

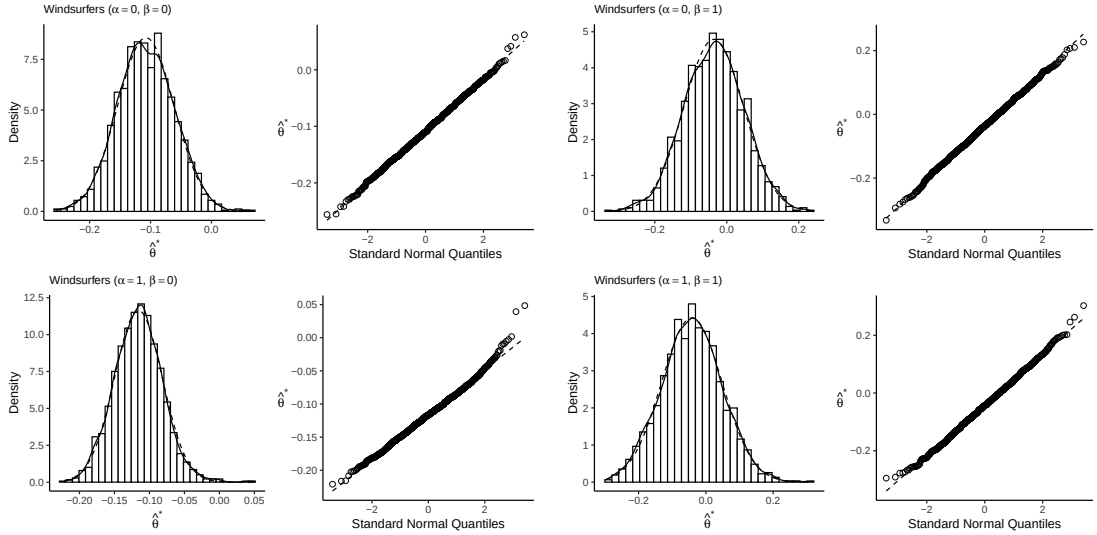

Figure A.2. Histogram and QQ-plot of bootstrap replications *(Windsurfers).* Histogram and QQ-plot of the distribution of bootstrap replications $\hat{\theta}_b^*, b = 1, \ldots, B = 1499$ for the undirected *Windsurfers* network for the various parameter constellations $(\alpha, \beta) \in \{0, 1\}$. Lines indicate the kernel density of the bootstrap distribution (solid) and the density of the normal distribution $\mathcal{N}(\bar{\hat{\theta}}_b^*, \hat{\sigma}^2_{\hat{\theta}_b^*})$ (dashed).

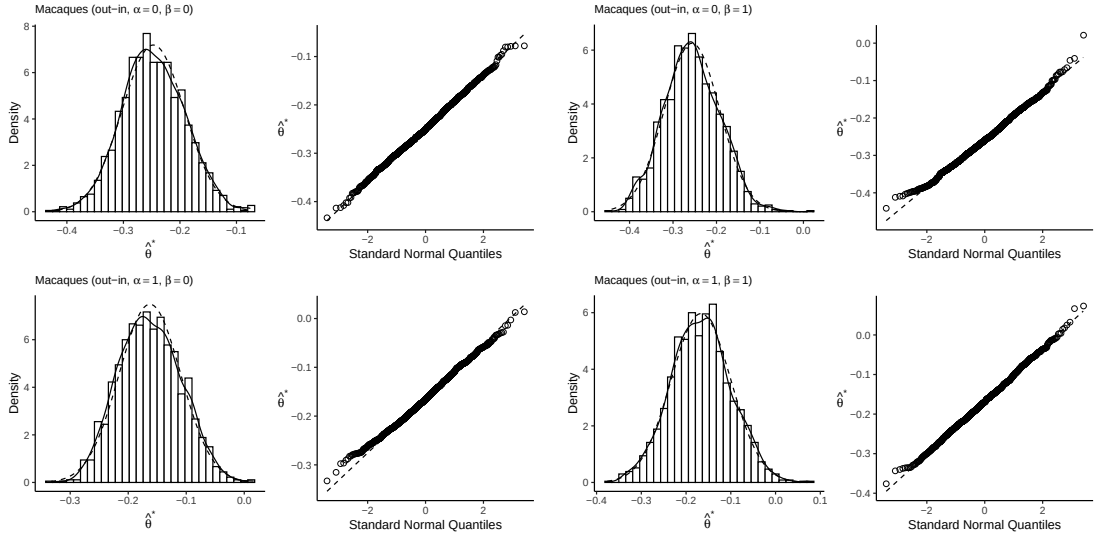

Figure A.3. Histogram and QQ-plot of bootstrap replications *(Macaques, out–in).* Histogram and QQ-plot of the distribution of bootstrap replications $\hat{\theta}_b^*, b = 1, \ldots, B = 1499$ for the *Macaques* network for the various parameter constellations $(\alpha, \beta) \in \{0, 1\}$ for the assortativity mode *out-in*. Lines indicate the kernel density of the bootstrap distribution (solid) and the density of the normal distribution $\mathcal{N}(\bar{\hat{\theta}}_b^*, \hat{\sigma}^2_{\hat{\theta}_b^*})$ (dashed).

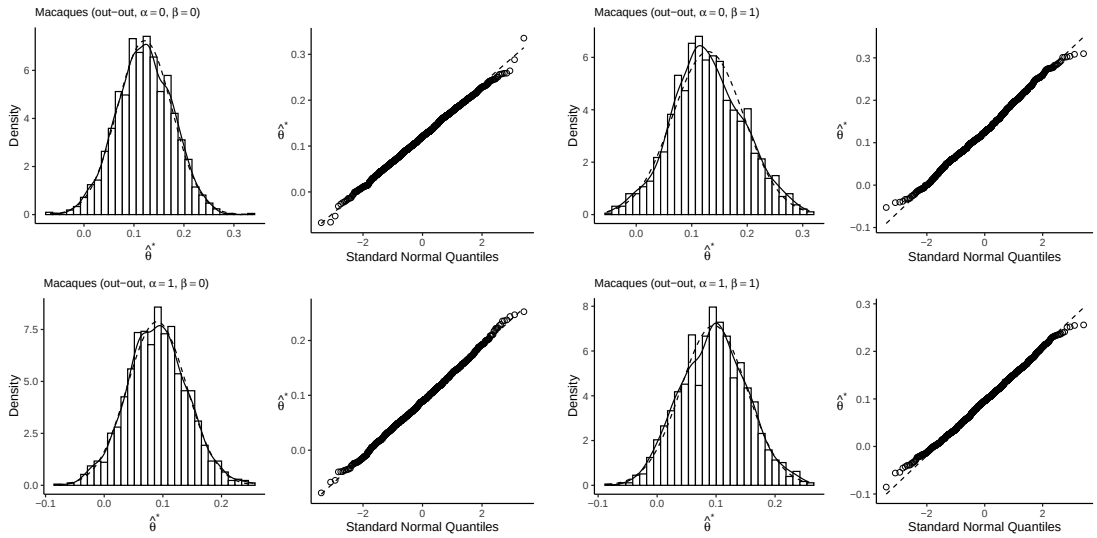

Figure A.4. Histogram and QQ-plot of bootstrap replications *(Macaques, out–out).* Histogram and QQ-plot of the distribution of bootstrap replications $\hat{\theta}_b^*, b = 1, \ldots, B = 1499$ for the *Macaques* network for the various parameter constellations $(\alpha, \beta) \in \{0, 1\}$ for the assortativity mode *out-out*. Lines indicate the kernel density of the bootstrap distribution (solid) and the density of the normal distribution $\mathcal{N}(\bar{\hat{\theta}}_b^*, \hat{\sigma}^2_{\hat{\theta}_b^*})$ (dashed).

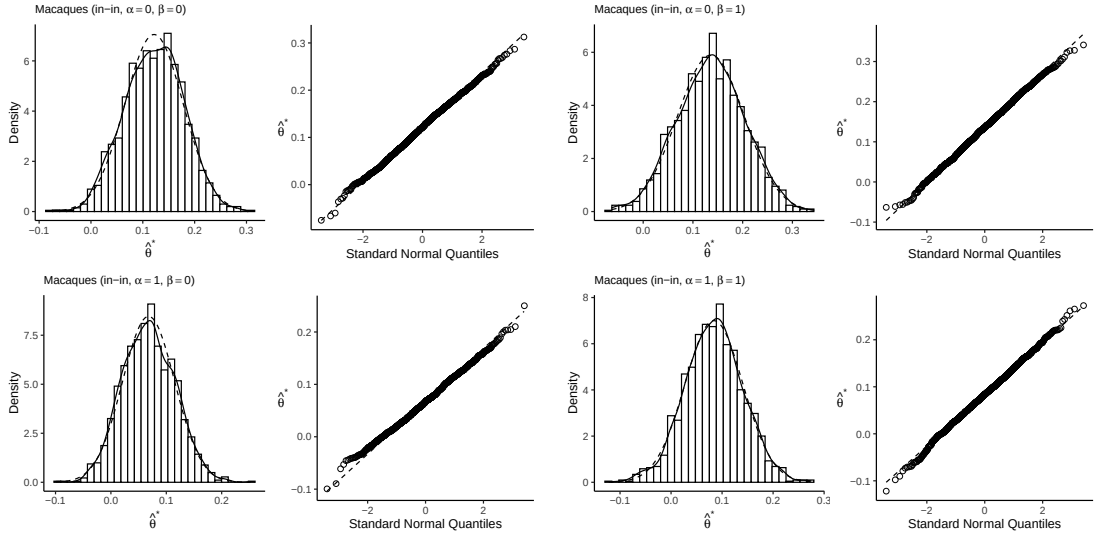

Figure A.5. Histogram and QQ-plot of bootstrap replications *(Macaques, in–in).* Histogram and QQ-plot of the distribution of bootstrap replications $\hat{\theta}_b^*, b = 1, \ldots, B = 1499$ for the *Macaques* network for the various parameter constellations $(\alpha, \beta) \in \{0, 1\}$ for the assortativity mode *in-in*. Lines indicate the kernel density of the bootstrap distribution (solid) and the density of the normal distribution $\mathcal{N}(\bar{\hat{\theta}}_b^*, \hat{\sigma}^2_{\hat{\theta}_b^*})$ (dashed).

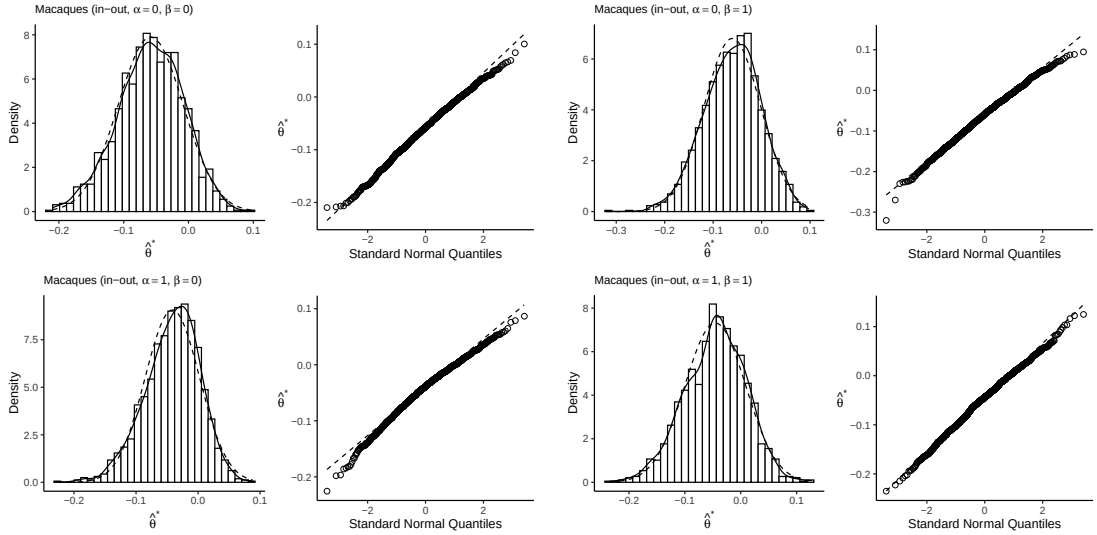

Figure A.6. Histogram and QQ-plot of bootstrap replications *(Macaques, in–out).* Histogram and QQ-plot of the distribution of bootstrap replications $\hat{\theta}_b^*, b = 1, \ldots, B = 1499$ for the *Macaques* network for the various parameter constellations $(\alpha, \beta) \in \{0, 1\}$ for the assortativity mode *in-out*. Lines indicate the kernel density of the bootstrap distribution (solid) and the density of the normal distribution $\mathcal{N}(\bar{\hat{\theta}}_b^*, \hat{\sigma}^2_{\hat{\theta}_b^*})$ (dashed).

B Appendix Chapter 4

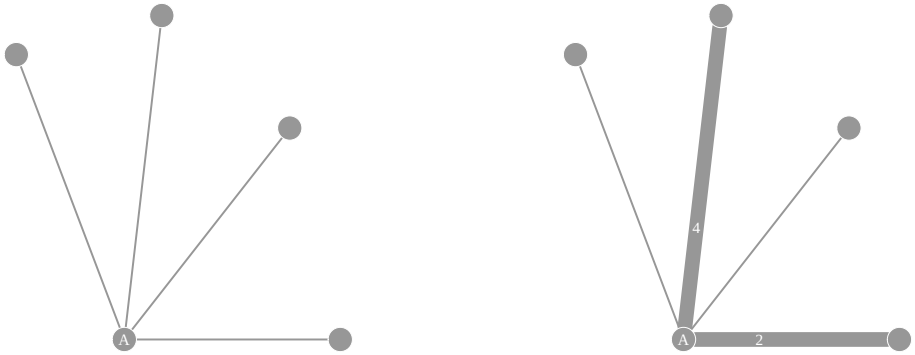

(a) Average excess degree $\bar{k}_A = 3$.

(b) Average excess strength $\bar{s}_A = 6$.

Figure B.1. Average excess degree and strength illustration. Depicted are two graphs, one unweighted (all weights equal 1) (a) and the other one weighted (unlabelled edges have weight 1) (b). The average excess degree of vertex A is computed as the mean of excess degrees that result if edges are, in turn and from left to right, omitted from (a), i.e., $\bar{k}_A = \frac{3+3+3+3}{4} = 3$. Similarly, considering (b), the average excess strength of vertex A is computed as $\bar{s}_A = \frac{7+4+7+6}{4} = 6$.

	$(\alpha = 0, \beta = 0)$			$(\alpha = 1, \beta = 1)$		
Rank	Name	ρ_v^ω	Degree	Name	ρ_v^ω	Strength
1	UETZ, P	0.0159	20	JEONG, H	0.0252	18
2	CAGNEY, G	0.0159	20	BARABASI, A	0.0226	30
3	MANSFIELD, T	0.0159	20	PASTORSATORRAS, R	0.0171	17
4	GIOT, L	0.0150	19	VESPIGNANI, A	0.0119	15
5	JUDSON, R	0.0150	19	OLTVAI, Z	0.0069	10
6	KNIGHT, J	0.0150	19	MORENO, Y	0.0062	15
7	LOCKSHON, D	0.0150	19	VAZQUEZ, A	0.0062	11
8	NARAYAN, V	0.0150	19	VICSEK, T	0.0046	9
9	SRINIVASAN, M	0.0150	19	ALBERT, R	0.0037	8
10	POCHART, P	0.0150	19	SOLE, R	0.0035	15
11	QURESHIEMILI, A	0.0150	19	WATTS, D	0.0029	9
12	LI, Y	0.0150	19	BARTHELEMY, M	0.0021	9
13	GODWIN, B	0.0150	19	HILGETAG, C	0.0021	11
14	CONOVER, D	0.0150	19	DIAZGUILERA, A	0.0020	11
15	KALBFLEISCH, T	0.0150	19	NEWMAN, M	0.0019	23
16	VIJAYADAMODAR, G	0.0150	19	GUIMERA, R	0.0019	10
17	YANG, M	0.0150	19	KAHNG, B	0.0018	11
18	JOHNSTON, M	0.0150	19	STROGATZ, S	0.0016	8
19	FIELDS, S	0.0150	19	YOUNG, M	0.0015	13
20	ROTHBERG, J	0.0150	19	HOLME, P	0.0014	9
⋮						
1442	LEICHT, E	-0.0007	2	ALON, U	-0.0006	8
1443	MACDONALD, P	-0.0008	2	MACDONALD, P	-0.0007	1
1444	BIANCONI, G	-0.0008	4	SMITH, E	-0.0007	2
1445	DOBRIN, R	-0.0008	3	FERRERICANCHO, R	-0.0007	4
1446	BEG, Q	-0.0008	3	VALVERDE, S	-0.0007	5
1447	HU, G	-0.0008	11	PACHECO, A	-0.0007	4
1448	KOVACS, B	-0.0008	4	MASON, S	-0.0007	1
1449	LATORA, V	-0.0008	15	WUCHTY, S	-0.0008	1
1450	GLOT, L	-0.0008	3	HUBERMAN, B	-0.0008	8
1451	SOLE, R	-0.0009	17	BOCCALETTI, S	-0.0009	12
1452	DEZSO, Z	-0.0009	1	BIANCONI, G	-0.0009	3
1453	YOOK, S	-0.0009	4	LATORA, V	-0.0009	11
1454	TU, Y	-0.0009	3	BORNHOLDT, S	-0.0010	8
1455	BOCCALETTI, S	-0.0011	19	YOOK, S	-0.0011	3
1456	WUCHTY, S	-0.0011	2	GASTNER, M	-0.0011	1
1457	DIAZGUILERA, A	-0.0012	15	LUSSEAU, D	-0.0011	1
1458	MASON, S	-0.0013	3	PARK, J	-0.0011	1
1459	YOUNG, M	-0.0016	20	MONTOYA, J	-0.0011	2
1460	BARABASI, A	-0.0022	34	DEZSO, Z	-0.0015	1
1461	NEWMAN, M	-0.0059	27	GIRVAN, M	-0.0020	3

Table B.1. Generalized vertex assortativeness ranking of the *NetScience* network. Reported are the 20 most assortative as well as the 20 most disassortative actors of the network, with respect to generalized vertex assortativeness, $\rho_v^\omega(\alpha, \beta)$, for the two parameter combinations $(\alpha, \beta) = \{(0, 0), (1, 1)\}$.

	$(\alpha = 0, \beta = 0)$							$(\alpha = 1, \beta = 1)$						
Rank	u	v	$\rho^{\omega}_{e_{uv}}$	k'_u	k'_v	$\bar{k}_u$	$\bar{k}_v$	u	v	$\rho^{\omega}_{e_{uv}}$	s'_u	s'_v	$\bar{s}_u$	$\bar{s}_v$
1	BARABASI, A	JEONG, H	0.0058	34	27	33	26	BARABASI, A	JEONG, H	0.0385	30	18	29.1176	17.3333
2	BARABASI, A	OLTVAI, Z	0.0041	34	21	33	20	PASTORSATORRAS, R	VESPIGNANI, A	0.0118	17	15	15.8667	13.9286
3	JEONG, H	OLTVAI, Z	0.0030	27	21	26	20	BARABASI, A	OLTVAI, Z	0.0107	30	10	29.1176	9.5238
4	BARABASI, A	VICSEK, T	0.0026	34	16	33	15	PASTORSATORRAS, R	SOLE, R	0.0084	17	15	15.8667	14.1176
5	NEWMAN, M	SOLE, R	0.0022	27	17	26	16	NEWMAN, M	SOLE, R	0.0078	23	15	22.1481	14.1176
6	JEONG, H	VICSEK, T	0.0019	27	16	26	15	BARABASI, A	VICSEK, T	0.0072	30	9	29.1176	8.4375
7	UETZ, P	CAGNEY, G	0.0018	20	20	19	19	VESPIGNANI, A	MORENO, Y	0.0064	15	15	13.9286	13.9286
8	UETZ, P	MANSFIELD, T	0.0018	20	20	19	19	PASTORSATORRAS, R	MORENO, Y	0.0057	17	15	15.8667	13.9286
9	CAGNEY, G	MANSFIELD, T	0.0018	20	20	19	19	NEWMAN, M	WATTS, D	0.0055	23	9	22.1481	7.7143
10	GIOT, L	UETZ, P	0.0017	19	20	18	19	MORENO, Y	VAZQUEZ, A	0.0050	15	11	13.9286	10.0833
⋮														
2733	BARABASI, A	DOBRIN, R	-0.0011	34	3	33	2	MORENO, Y	PACHECO, A	-0.0013	15	4	13.9286	3.0000
2734	BARABASI, A	BEG, Q	-0.0011	34	3	33	2	SOLE, R	FERRERICANCHO, R	-0.0013	15	4	14.1176	3.0000
2735	BARABASI, A	MASON, S	-0.0011	34	3	33	2	BARABASI, A	BIANCONI, G	-0.0017	30	3	29.1176	2.2500
2736	BARABASI, A	TU, Y	-0.0011	34	3	33	2	BARABASI, A	YOOK, S	-0.0017	30	3	29.1176	2.2500
2737	NEWMAN, M	GASTNER, M	-0.0013	27	1	26	0	NEWMAN, M	GASTNER, M	-0.0021	23	1	22.1481	0.0000
2738	NEWMAN, M	LUSSEAU, D	-0.0013	27	1	26	0	NEWMAN, M	LUSSEAU, D	-0.0021	23	1	22.1481	0.0000
2739	NEWMAN, M	PARK, J	-0.0013	27	1	26	0	NEWMAN, M	PARK, J	-0.0021	23	1	22.1481	0.0000
2740	BARABASI, A	MACDONALD, P	-0.0014	34	2	33	1	SOLE, R	MONTOYA, J	-0.0022	15	2	14.1176	0.0000
2741	BARABASI, A	WUCHTY, S	-0.0014	34	2	33	1	BARABASI, A	DEZSO, Z	-0.0029	30	1	29.1176	0.0000
2742	BARABASI, A	DEZSO, Z	-0.0017	34	1	33	0	NEWMAN, M	GIRVAN, M	-0.0041	23	3	22.1481	1.5000

Table B.2. Generalized edge assortativeness ranking of the *NetScience* network. Reported are the 10 most assortative as well as the 10 most disassortative connections of the network, with respect to generalized edge assortativeness, $\rho^{\omega}_{e_{uv}}(\alpha, \beta)$ together with the mean average excess degree, $\bar{k}$, as well as the degree, $k\prime$, for the combination $(\alpha, \beta) = (0, 0)$, and the mean average excess strength, $\bar{s}$, as well as the strength, $s\prime$, for the combination $(\alpha, \beta) = (1, 1)$, for both ends, u and v, of an edge e.

C Appendix Chapter 5

Rank	Symbol	Name	Rank	Symbol	Name
1	BTC	Bitcoin	26	DGB	DigiByte
2	ETH	Ethereum	27	STRAX	Stratis
3	USDT	Tether	28	LSK	Lisk
4	XRP	XRP	29	BNT	Bancor
5	DOGE	Dogecoin	30	XNO	Nano
6	LTC	Litecoin	31	ARDR	Ardor
7	XLM	Stellar	32	SNT	Status
8	XMR	Monero	33	SYS	Syscoin
9	ETC	Ethereum Classic	34	REP	Augur
10	EOS	EOS	35	STEEM	Steem
11	ZEC	Zcash	36	RLC	iExec RLC
12	MIOTA	IOTA	37	MAID	MaidSafeCoin
13	NEO	Neo	38	FUN	FUNToken
14	BAT	Basic Attention Token	39	ANT	Aragon
15	WAVES	Waves	40	VERI	Veritaseum
16	DASH	Dash	41	ARK	Ark
17	XEM	NEM	42	MLN	Enzyme
18	DCR	Decred	43	XWC	WhiteCoin
19	QTUM	Qtum	44	XVG	Verge
20	GNO	Gnosis	45	SBD	Steem Dollars
21	STORJ	Storj	46	GXC	GXChain
22	GLM	Golem	47	MONA	MonaCoin
23	SC	Siacoin	48	BTS	BitShares
24	ZEN	Horizen	49	GRS	Groestlcoin
25	NMR	Numeraire			

Table C.1. Overview of cryptocurrency selection.

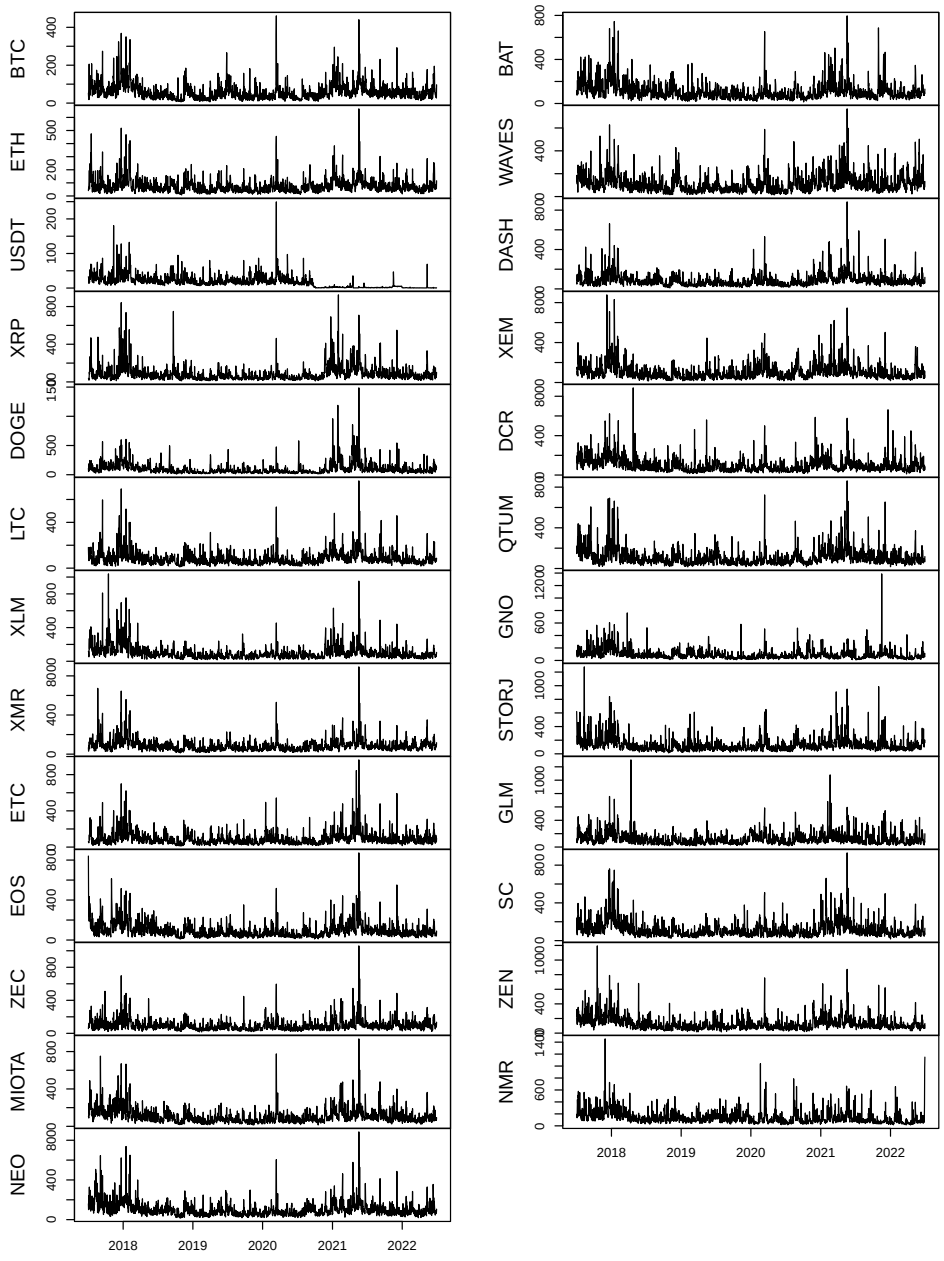

Figure C.1. Annualized daily volatility (percentage) top 1-25.

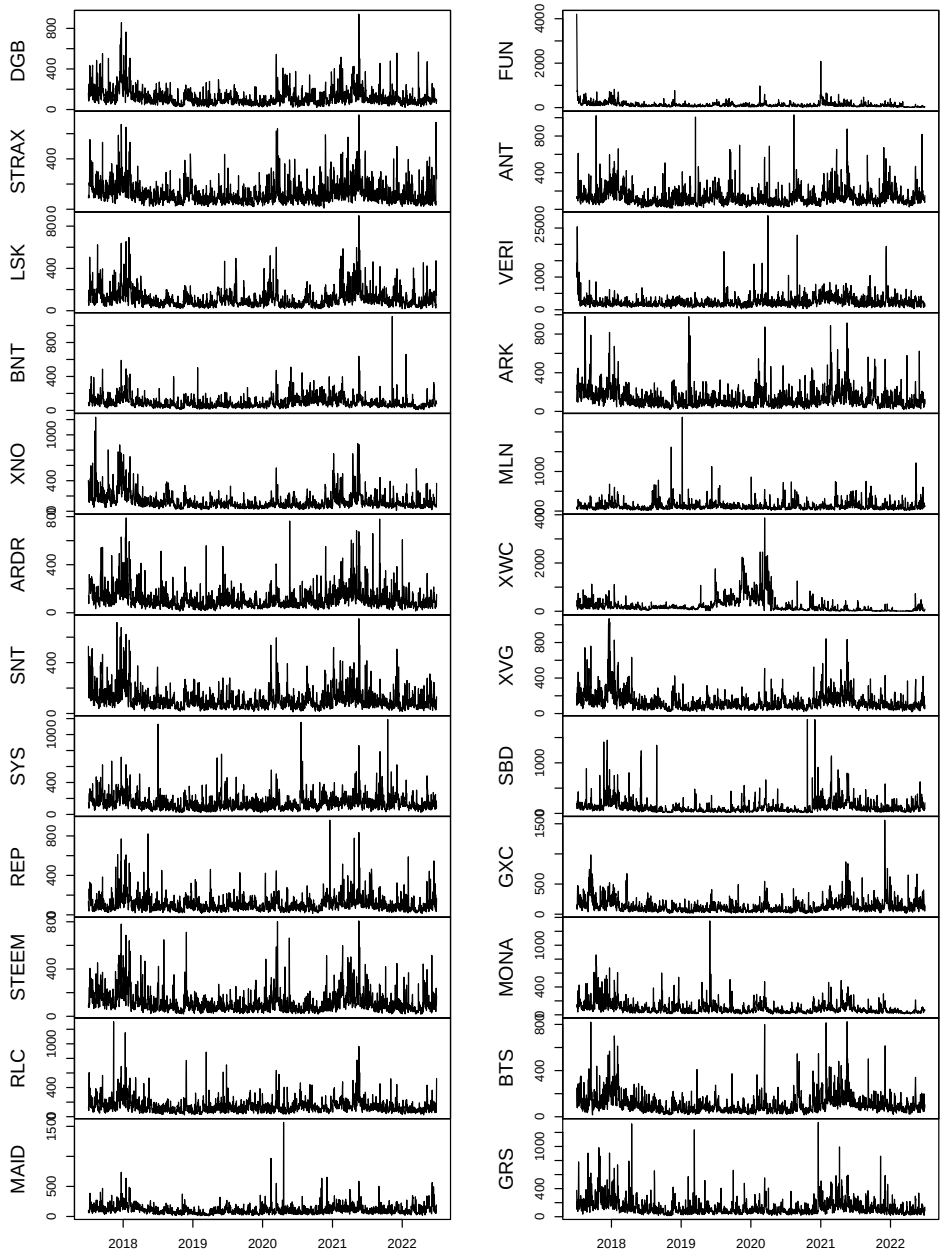

Figure C.2. Annualized daily volatility (percentage) top 26-49.

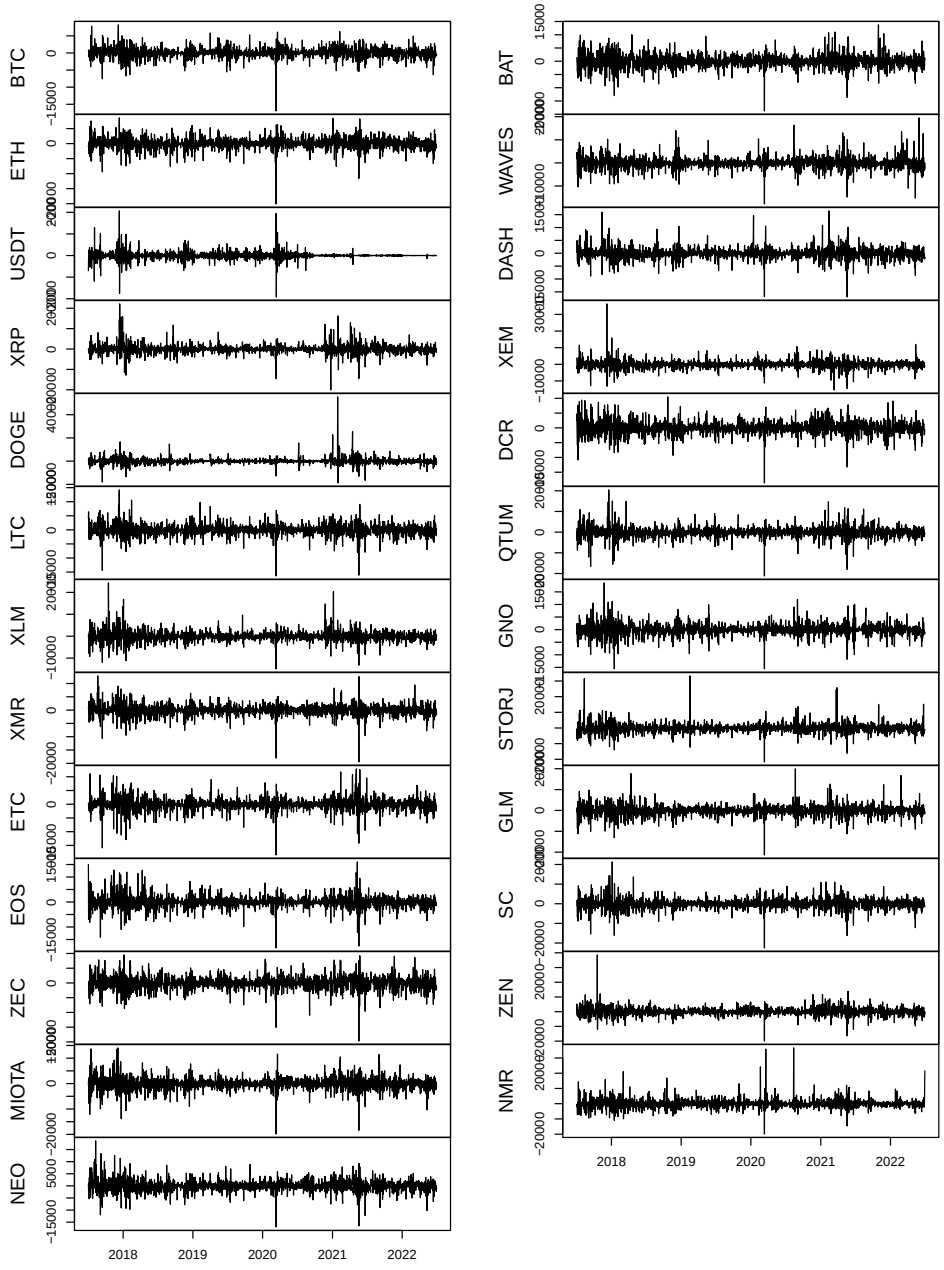

Figure C.3. Annualized daily log returns (percentage) top 1-25.

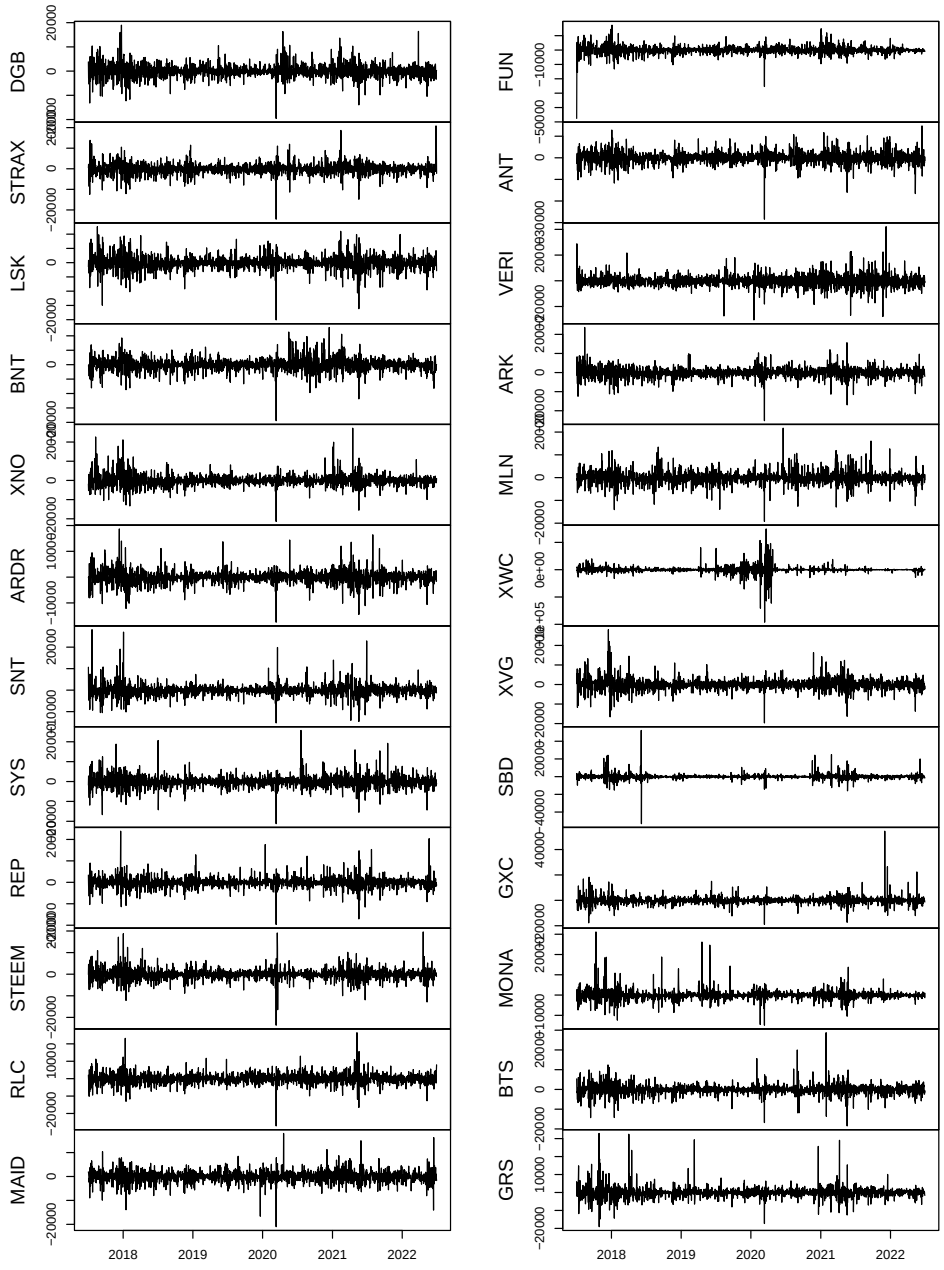

Figure C.4. Annualized daily log returns (percentage) top 26-49.

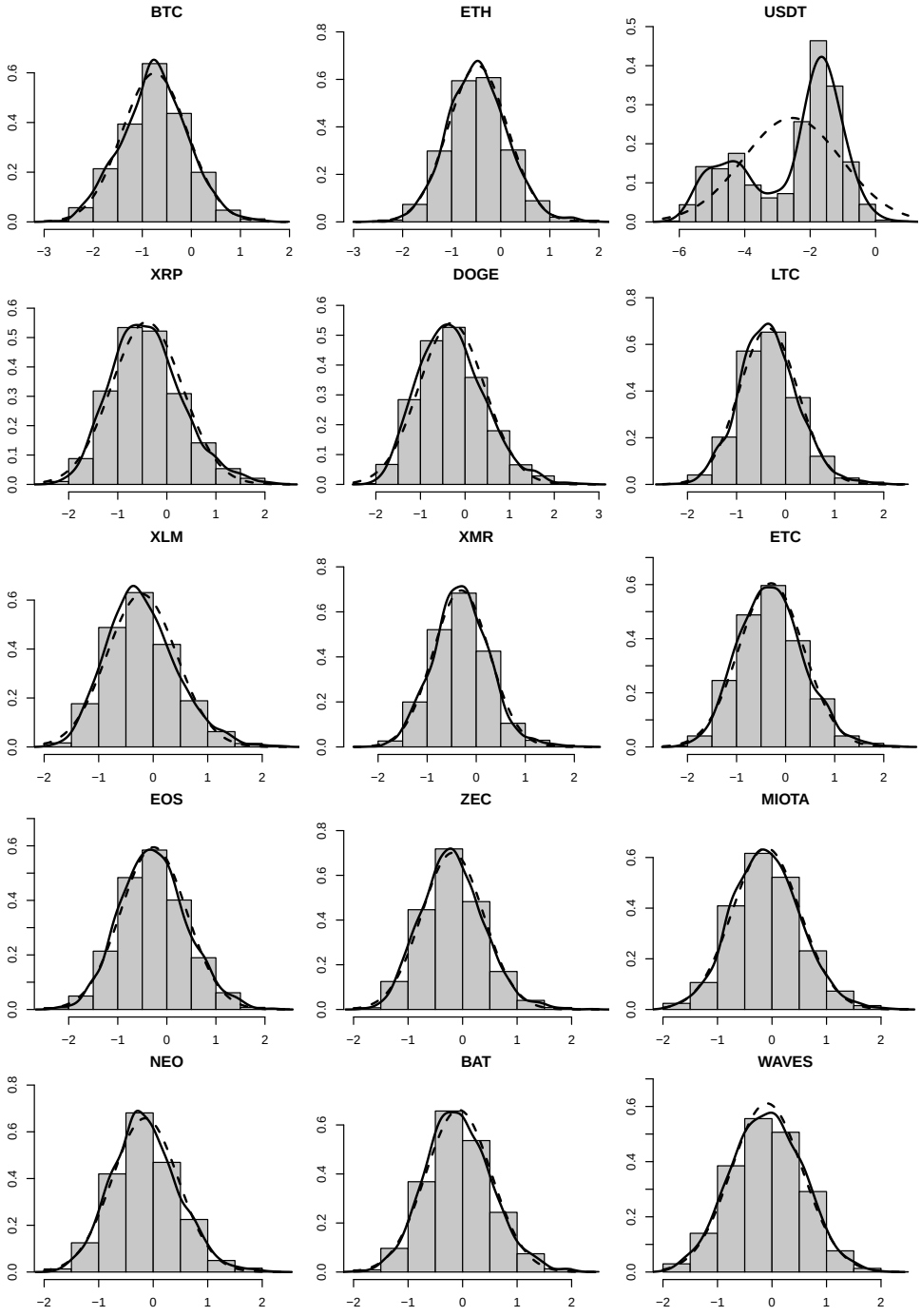

Figure C.5. Histogram of log annualized daily volatilities top 1-15. Lines indicate kernel density estimates (solid black) and the respective normal density (dashed black) for comparison.

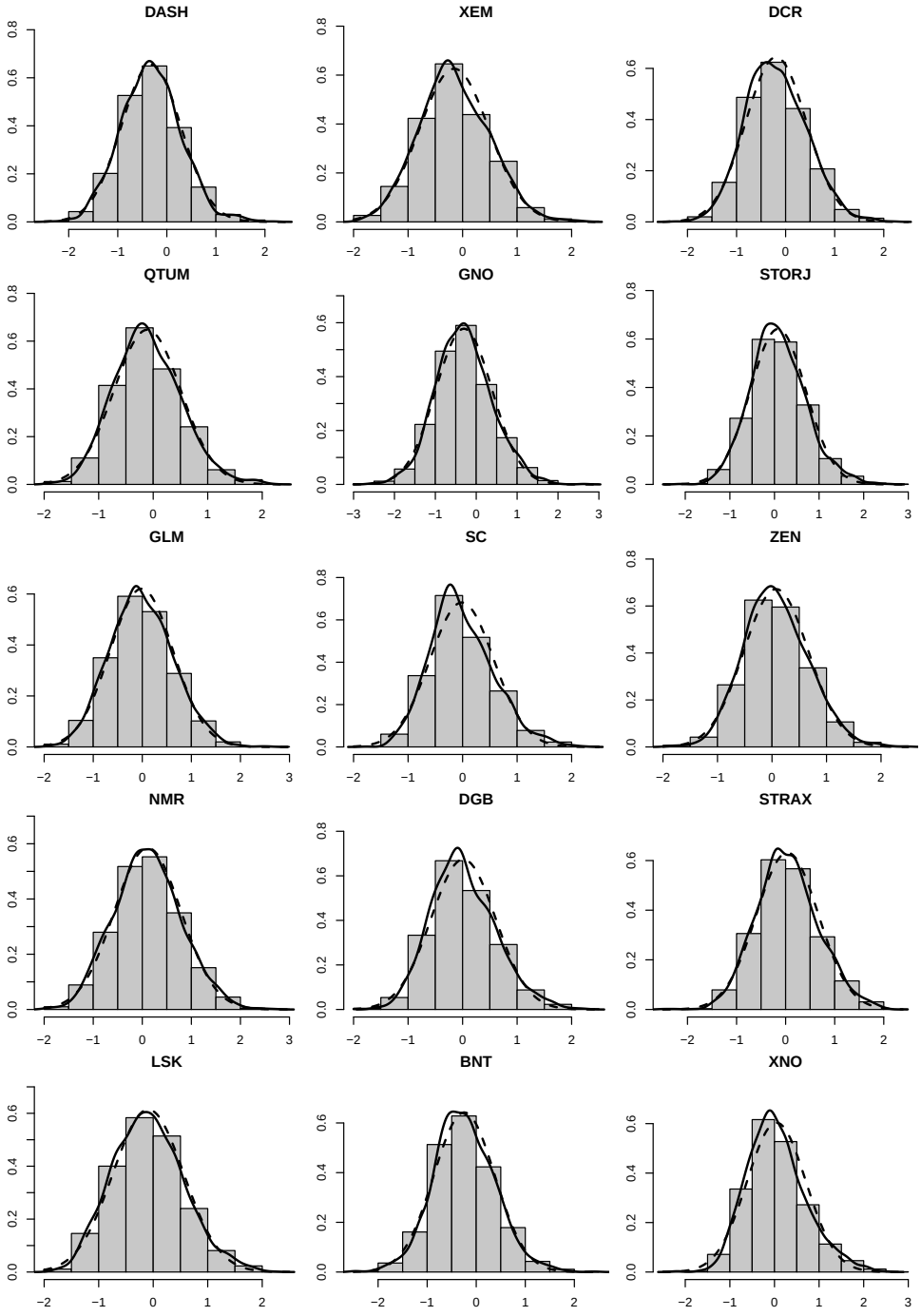

Figure C.6. Histogram of log annualized daily volatilities top 16-30. Lines indicate kernel density estimates (solid black) and the respective normal density (dashed black) for comparison.

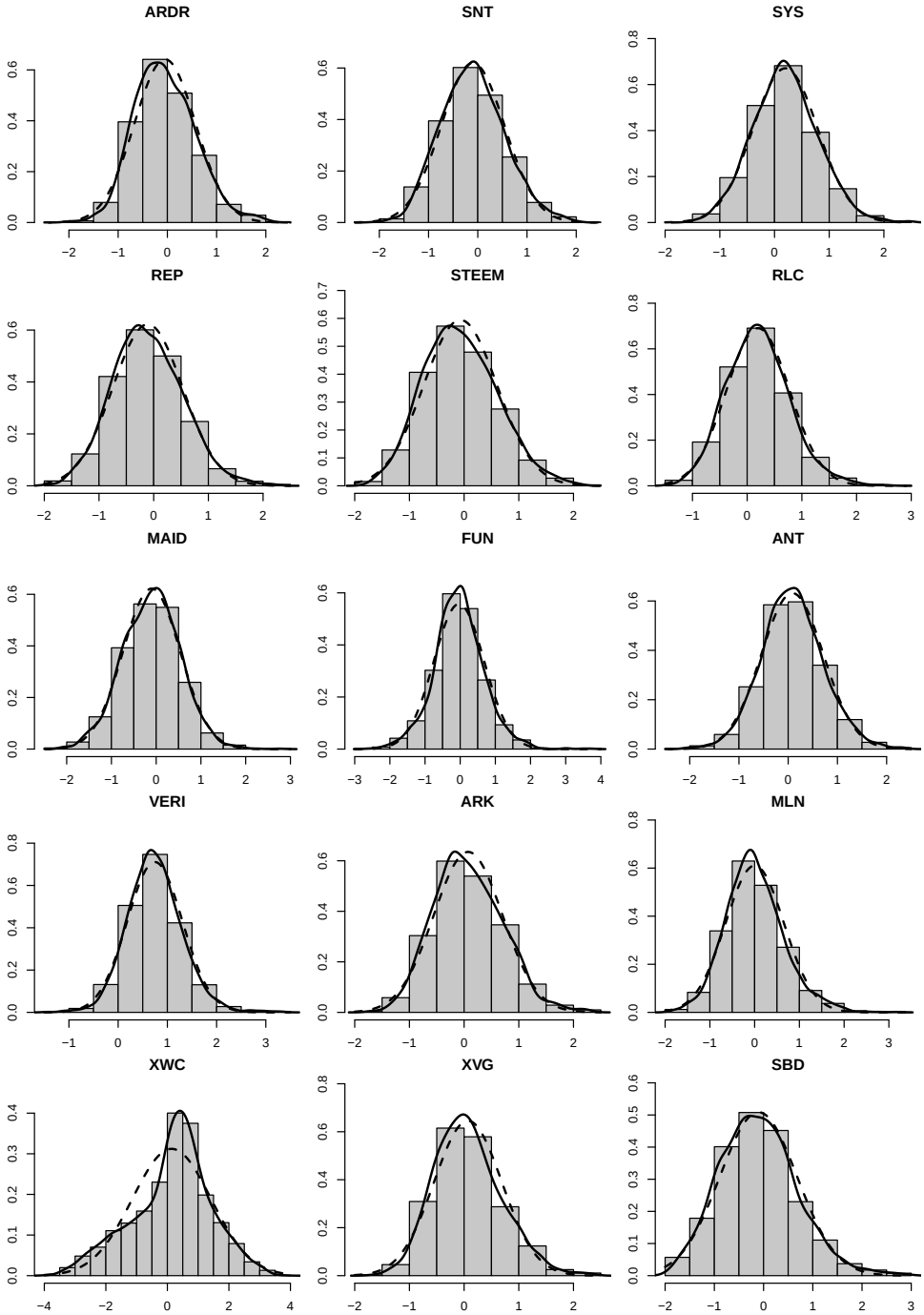

Figure C.7. Histogram of log annualized daily volatilities top 31-43. Lines indicate kernel density estimates (solid black) and the respective normal density (dashed black) for comparison.

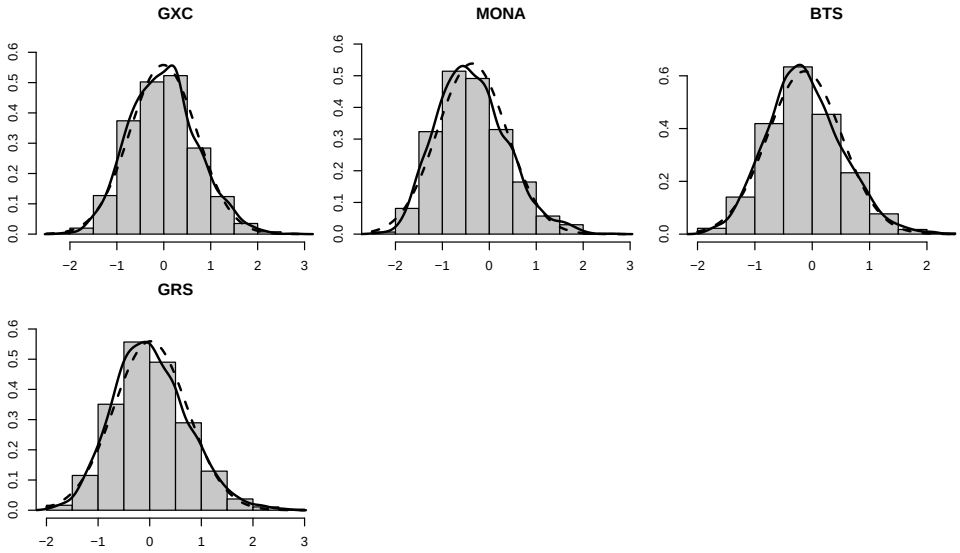

Figure C.8. Histogram of log annualized daily volatilities top 46-49. Lines indicate kernel density estimates (solid black) and the respective normal density (dashed black) for comparison.

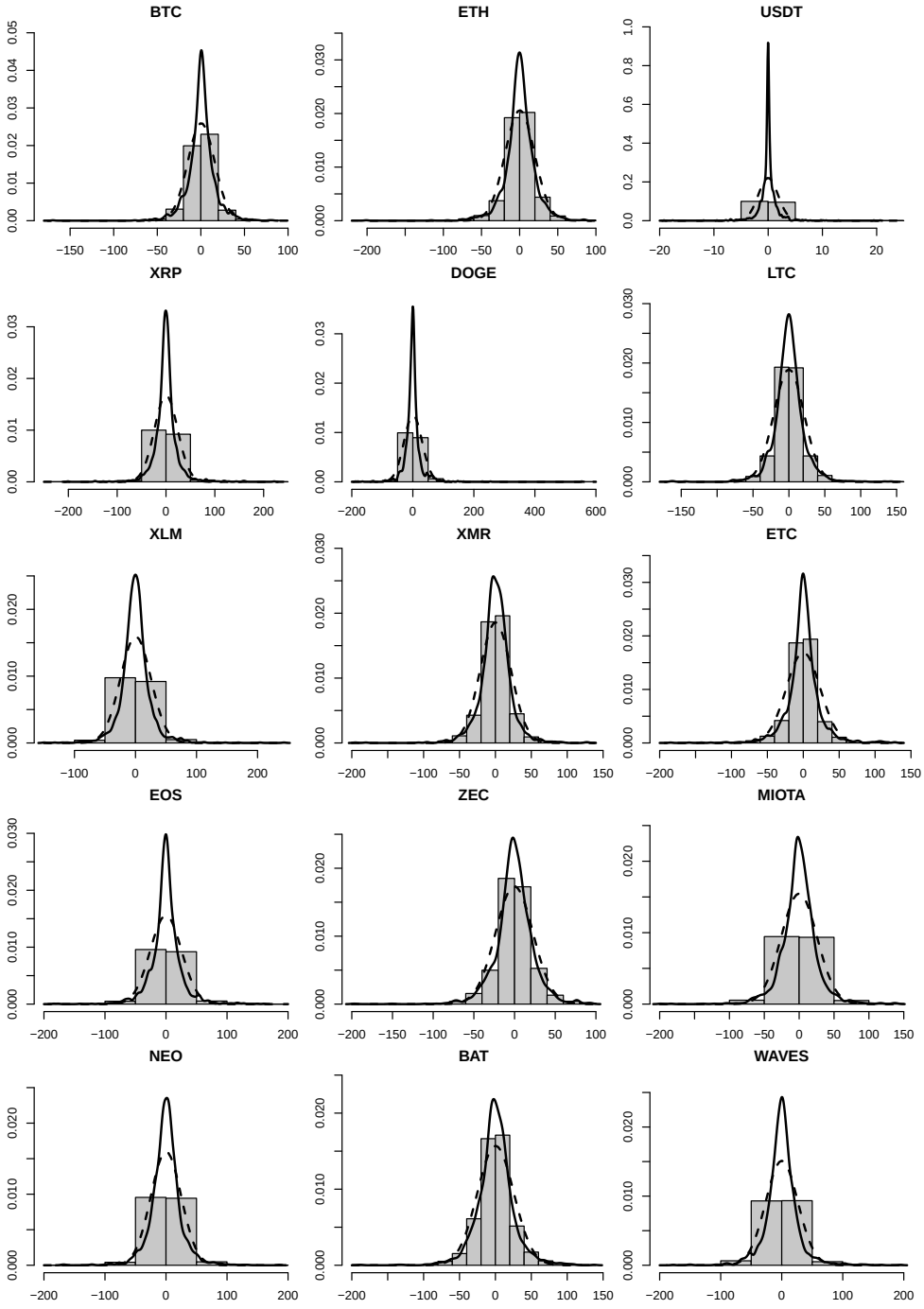

Figure C.9. Histogram of annualized daily log returns top 1-15. Lines indicate kernel density estimates (solid black) and the respective normal density (dashed black) for comparison.

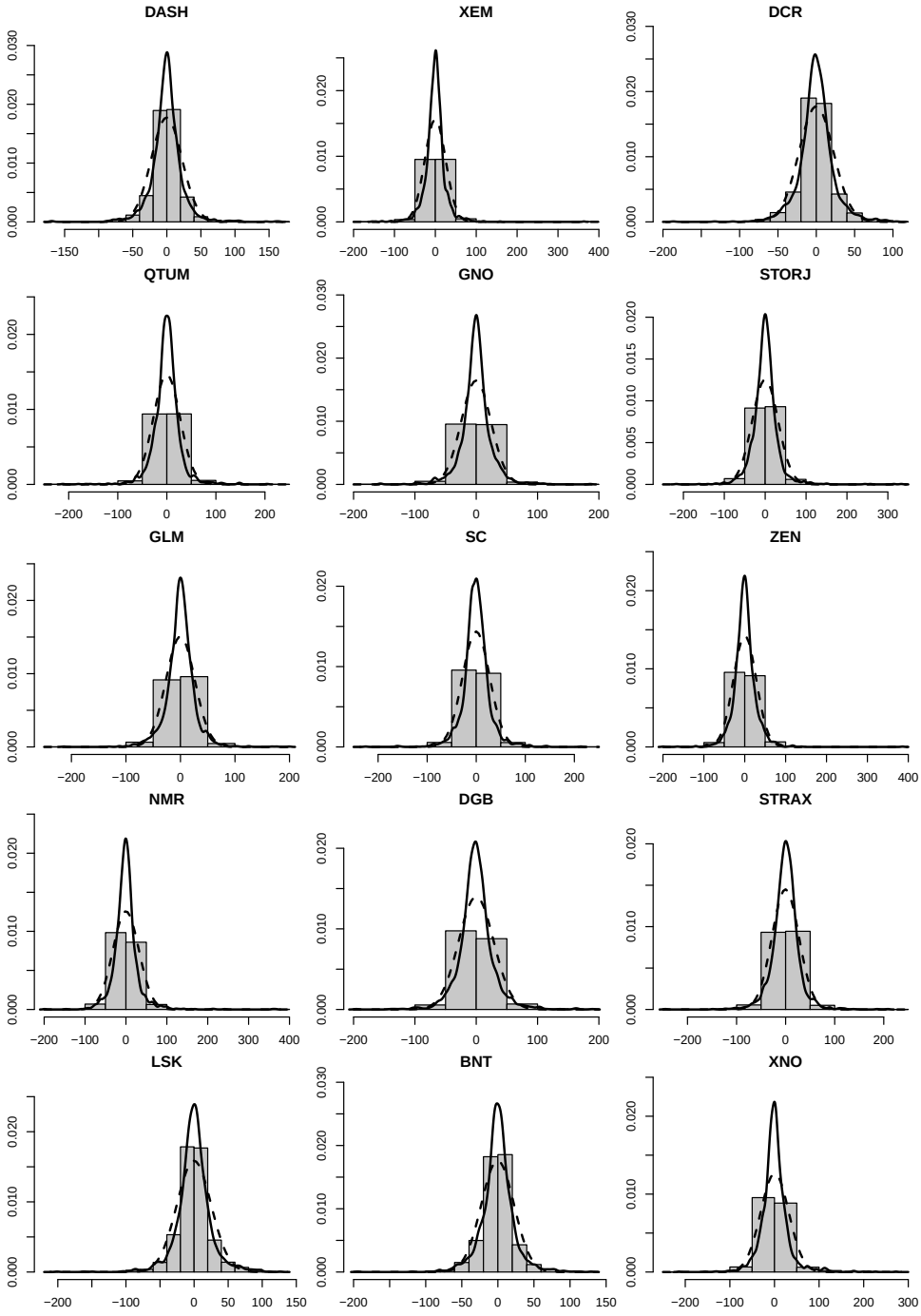

Figure C.10. Histogram of annualized daily log returns top 16-30. Lines indicate kernel density estimates (solid black) and the respective normal density (dashed black) for comparison.

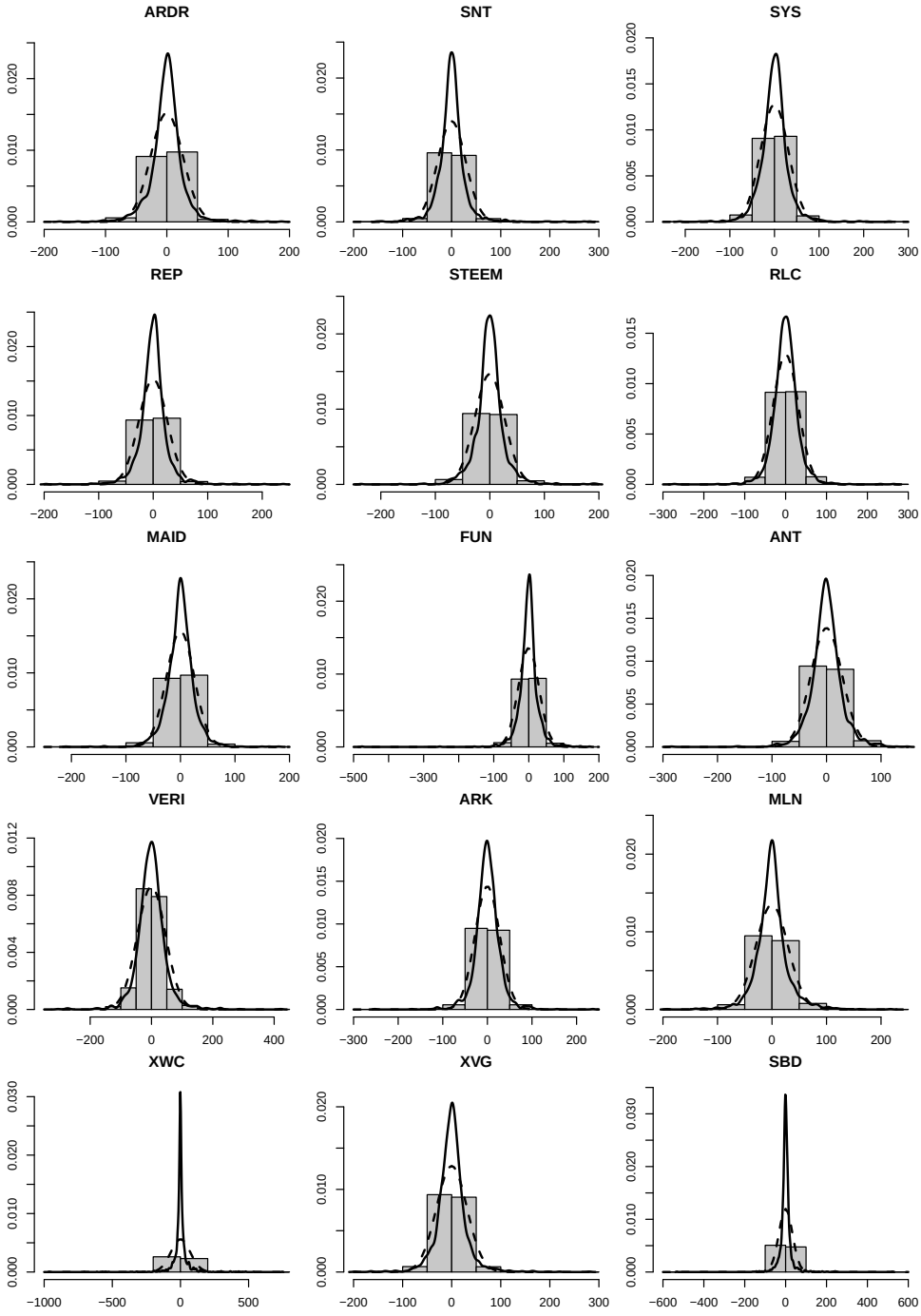

Figure C.11. Histogram of annualized daily log returns top 31-45. Lines indicate kernel density estimates (solid black) and the respective normal density (dashed black) for comparison.

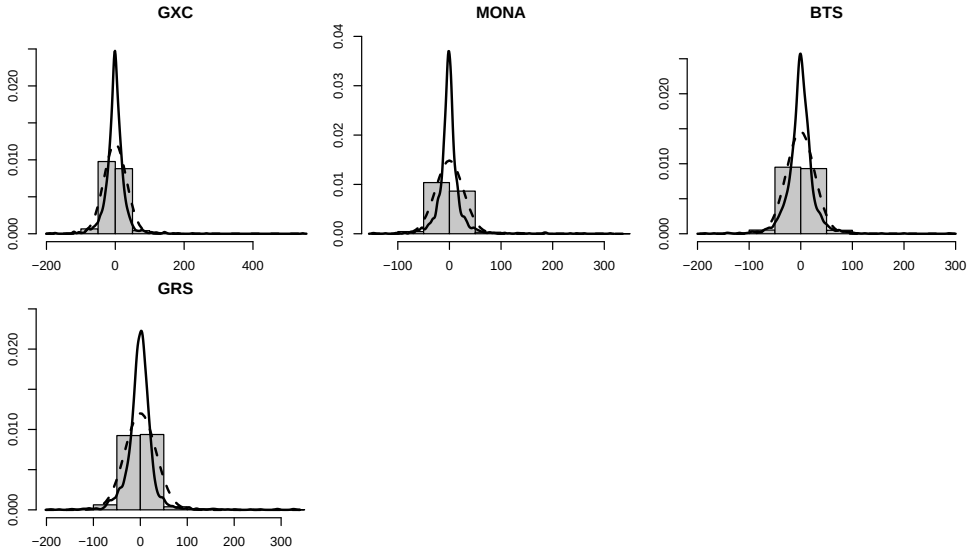

Figure C.12. Histogram of annualized daily log returns top 46-49. Lines indicate kernel density estimates (solid black) and the respective normal density (dashed black) for comparison.

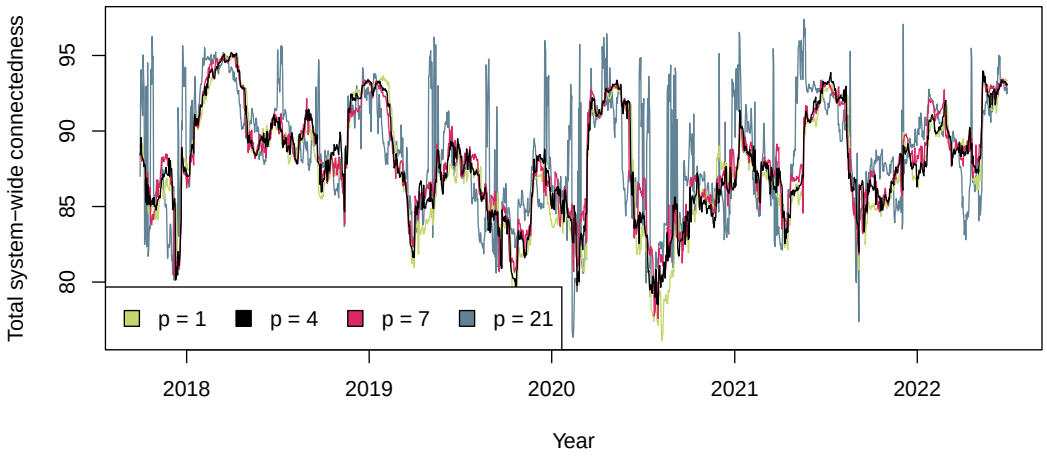

Figure C.13. Total system-wide connectedness robustness check: lag order. The figure shows the robustness of the total system-wide volatility connectedness for a rolling window estimation ($w = 90$, $H = 12$), for different lags $p = \{1, 4, 7, 21\}$.

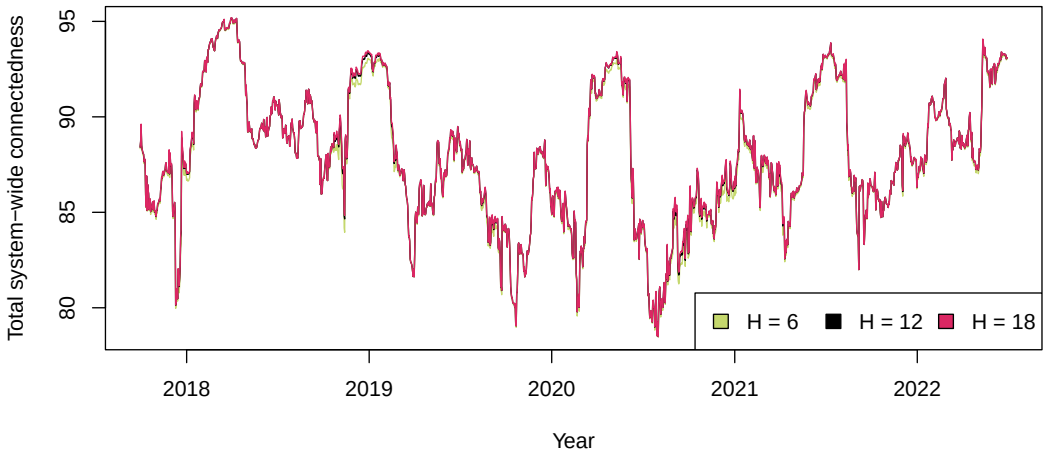

Figure C.14. Total system-wide connectedness robustness check: forecast horizon. The figure shows the robustness of the total system-wide volatility connectedness for a rolling window estimation ($w = 90$, $p = 4$), for different horizons $H = \{6, 12, 18\}$.

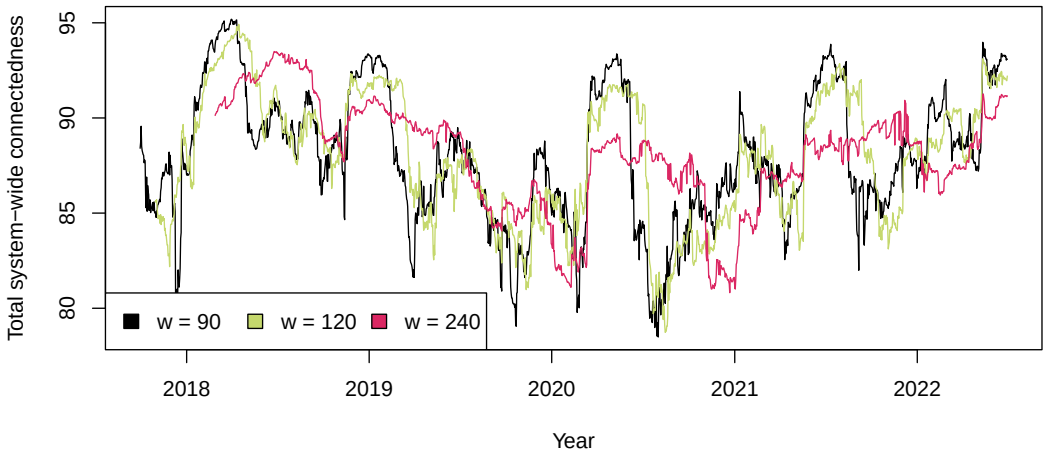

Figure C.15. Total system-wide connectedness robustness check: window size. The figure shows the robustness of the total system-wide volatility connectedness for a rolling window estimation ($p = 4$, $H = 12$), for different window sizes $w = \{90, 120, 240\}$.

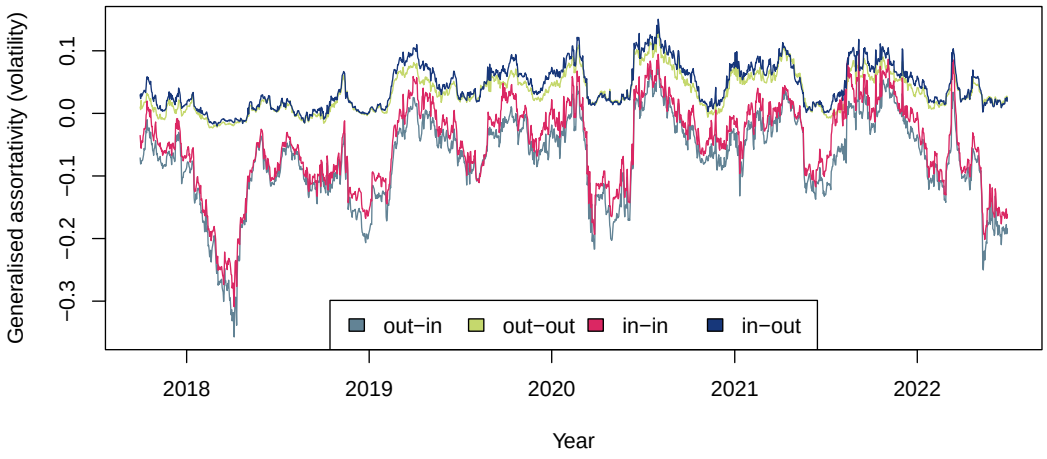

Figure C.16. Evolvement of generalized assortativity of the volatility connectedness network. Depicted is the evolvement of the generalized assortativity coefficient ($\alpha = 1, \beta = 1$) for a rolling window estimation of the volatility connectedness network ($w = 90$, $H = 12$, $p = 4$), for each mode of assortativity (*out–in*, *out–out*, *in–in* and *in–out*).

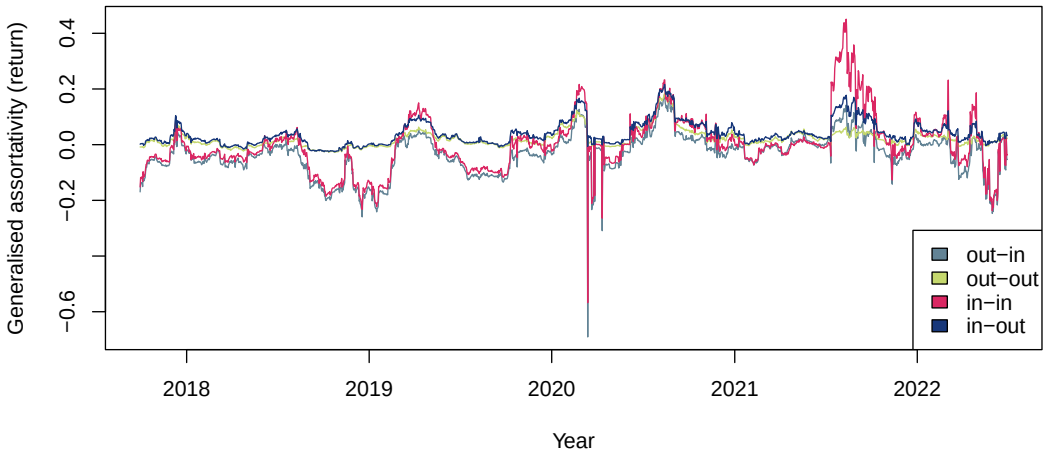

Figure C.17. Evolvement generalized assortativity of the return connectedness network. Depicted is the evolvement of the generalized assortativity coefficient ($\alpha = 1, \beta = 1$) for a rolling window estimation of the return connectedness network ($w = 90$, $H = 12$, $p = 4$), for each mode of assortativity (*out–in*, *out–out*, *in–in* and *in–out*).

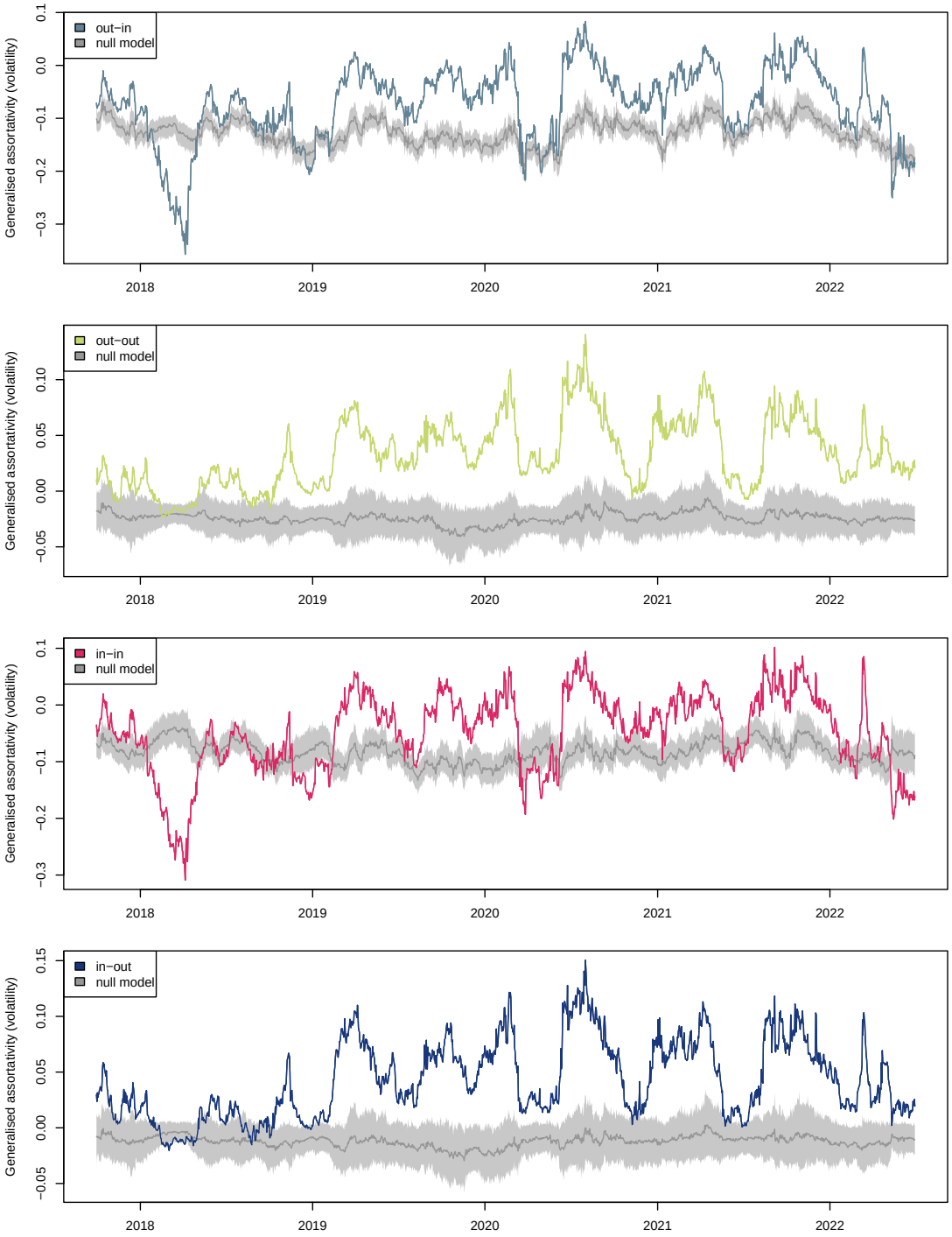

Figure C.18. Evolvement of generalized assortativity of the volatility connectedness network. Depicted is the evolvement of the generalized assortativity coefficient ($\alpha = 1, \beta = 1$) for a rolling window estimation of the volatility connectedness network ($w = 90$, $H = 12$, $p = 4$) and for each mode of generalized assortativity (*out–in*, *out–out*, *in–in* and *in–out*). The dark grey line and grey shaded area indicate the mean of the generalized assortativity of a respective null model together with a piecewise 95 percent confidence band, respectively.

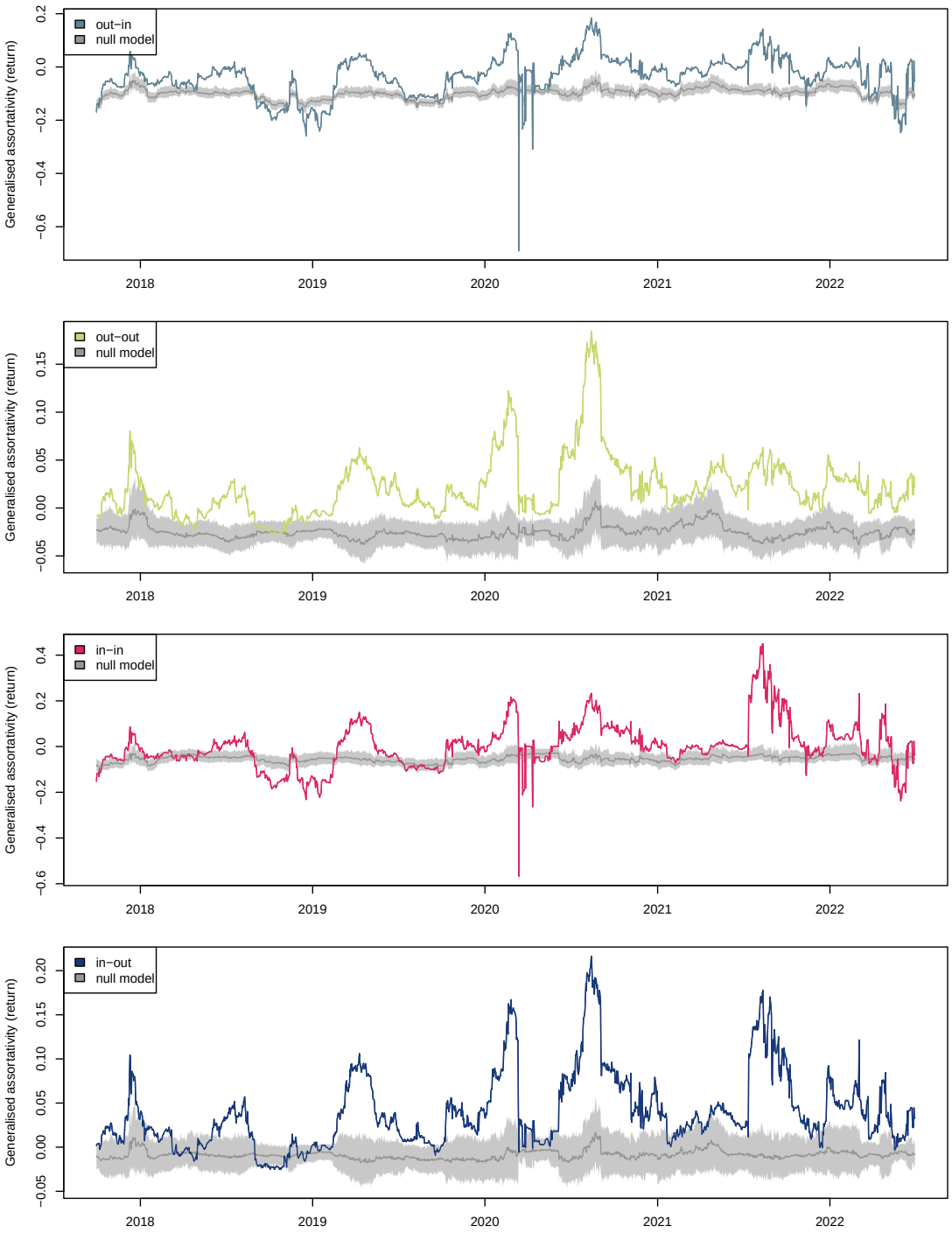

Figure C.19. Evolvement of generalized assortativity of the return connectedness network. Depicted is the evolvement of the generalized assortativity coefficient ($\alpha = 1, \beta = 1$) for a rolling window estimation of the return connectedness network ($w = 90$, $H = 12$, $p = 4$) and for each mode of generalized assortativity (*out–in*, *out–out*, *in–in* and *in–out*). The dark grey line and grey shaded area indicate the mean of the generalized assortativity of a respective null model together with a piecewise 95 percent confidence band, respectively.

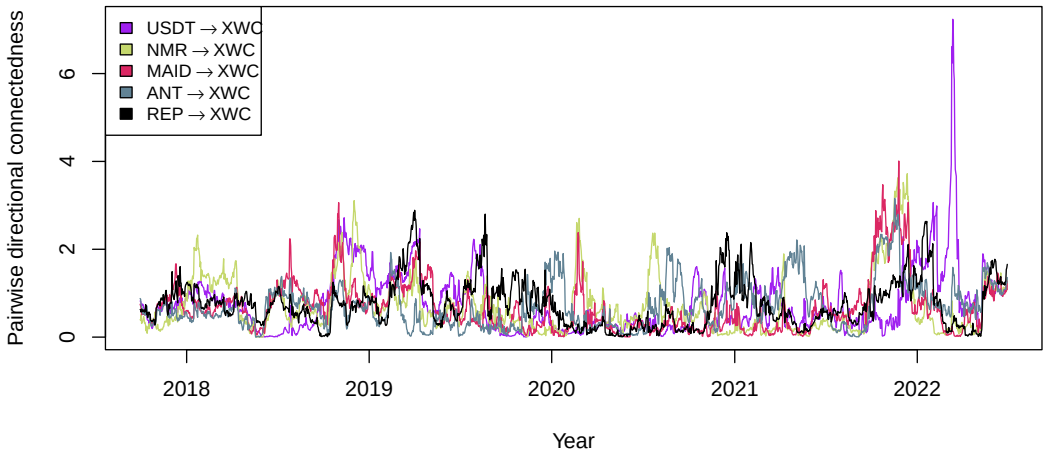

Figure C.20. Evolvement of pairwise directional connectedness (top assortative). Depicted is the evolvement of pairwise directional connectedness of the top 5 assortative connections between cryptocurrencies with respect to the generalized edge assortativeness values, ρ_e^ω, for the parameter combination ($\alpha = 1, \beta = 1, \text{mode} = \textit{out–in}$).

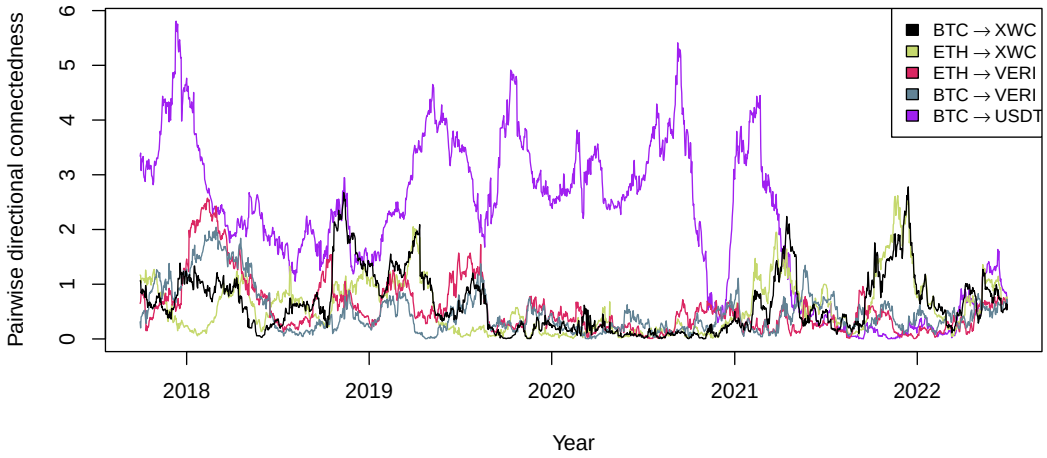

Figure C.21. Evolvement of pairwise directional connectedness (top disassortative). Depicted is the evolvement of pairwise directional connectedness of the top 5 disassortative connections between cryptocurrencies with respect to the generalized edge assortativeness values, ρ_e^ω, for the parameter combination ($\alpha = 1, \beta = 1, \text{mode} = \textit{out–in}$).

List of Symbols

α	tuning parameter of $r^{\omega}_{(\alpha,\beta)}$, $\beta \in \{0,1\}$, capturing amplification effect; tuning parameter of directed BA model; regularization parameter balancing between RR and LASSO penalty in the elastic net penalty
β	tuning parameter of $r^{\omega}_{(\alpha,\beta)}$, $\alpha \in \{0,1\}$, capturing connection effect; tuning parameter of directed BA model
$[\boldsymbol{A}(L)]^{-1}$	matrix lag polynomial
α_{ij}	for the disparity filter algorithm, probability that the normalized weight, p_{ij}, of an edge between vertices i and j is compatible with the null hypothesis
$\boldsymbol{A}$	adjacency matrix
A_h	moving average coefficient matrix at horizon h
A_i	moving average coefficient matrix at horizon i
a_{uv}	element of A
B	total number of bootstrap samples
BA	Barabási-Albert model
$c(G)$	number of connected components
C^H	total *system-wide* connectedness
$C^H_{\bullet \leftarrow i}$	total *to* connectedness of variable i
$C^H_{i \leftarrow \bullet}$	total *from* connectedness of variable i
$C^H_{i \leftarrow j}$	total directional connectedness between variables i and j
C_n	cycle on n vertices
$C_{i,t}$	log close price of variable i at time t
$c_{i,t}$	normalised close price of variable i at time t
$CI_{r^{\omega}_{(\alpha,\beta)},\mathrm{rnd},S}$	confidence interval of $r^{\omega}_{\mathrm{rnd}}(\alpha,\beta)$ for the confidence level S
$CI_{r^{\omega}_{(\alpha,\beta)},S,*}$	jackknife ($* = J$) or bootstrap ($* = B$) confidence interval of $r^{\omega}_{(\alpha,\beta)}$ for the confidence level S
CV	cross-validation
$\deg_G(v)$	degree of v

$\Delta(G)$	maximum degree
$\delta(G)$	minimum degree
δ_i^k	indicator if scientist i was co-author of paper k
δ_j	shock to the j-th element of $\boldsymbol{\varepsilon}_t$ at time t
δ_{in}	tuning parameter of directed BA model
δ_{out}	tuning parameter of directed BA model
$\text{dist}_G(u, v)$	distance (or shortest path) between vertices u and v in graph G
$\text{dist}_{G,f}(u, v)$	weighted distance (or weighted shortest path) between vertices u and v in graph G
$\deg_G^{\text{in}}(v)$	in-degree of v
$\deg_G^{\text{out}}(v)$	out-degree of v
Δ	difference operator, such that $\Delta\tilde{r}(e) = \tilde{r} - \tilde{r}_{(-e)}$
d	relative difference $d = \frac{\lvert x-y\rvert}{(x+y)}$; half the length of a confidence interval $d = z_{0.975} \cdot \hat{\sigma}_{r^{\omega}_{(\alpha,\beta)},*}$
$d_{i,t}$	normalised low price of variable i at time t
DY	Diebold and Yilmaz (2014) connectedness index methodology
$\boldsymbol{\varepsilon}_t$	N-dimensional white noise process at time T
$\boldsymbol{e}_j$	vector of which the j-th element equals one, and zero elsewhere
η_i	fitness parameter indicating the fitness of vertex i in the BA model
$\lvert E(G)\rvert$	cardinality of the edge set, i.e., the size m of a graph
$\tilde{e}_{uv}$	version of e_{uv} corrected for assigned weights
$\varepsilon_{i,t}$	i-th element of $\boldsymbol{\varepsilon}_t$ at time t
e	an edge
$E, E(G)$	edge set of a network
$E[X]$	expected value of random variable X
$e_{st}^{\text{out–in}}$	joint probability distribution of excess out- and in-strengths, i.e., the probability that an edge connects two vertices where one has excess out-strength s and the other has excess in-strength t
e_{jk}	joint probability distribution of excess degrees, i.e., the probability that an edge connects two vertices where one has excess degree j and the other has excess degree k
e_{uv}	expected weight of an edge connecting vertices u and v if edges had formed randomly

ER	Erdős-Rényi random graph model
f	weight function $f : E(G) \to \mathbb{R}$ assigning weights to edges of a graph
$\boldsymbol{GI}_x$	generalised impulse response function
γ	power law exponent; tuning parameter of directed BA model
$\text{Geo}(\tilde{q})$	geometric distribution, i.e., if $W_{ij} \sim \text{Geo}(\tilde{q})$, then $P(W_{ij} = \omega) = P(\omega) = (1-\tilde{q})^{\omega}\tilde{q}$
$\overline{G}$	complement graph of G
$G(n, m)$	arbitrary graph on n vertices with m edges
$G = (V, E)$	couple V and E, i.e., a graph or network
$G_{n,M}$	Gilbert (1959) model
$G_{n,p}$	Erdös and Rényi (1959, 1960) model
GUAC	generalised universal assortativity coefficient
H	total sum of edge weights of a network; number of forecast horizons, $h = 1, \ldots, H$
h	forecast horizon
$H_{i,t}$	log high price of variable i at time t
I_N	$(N \times N)$ dimensional identity matrix
J	variable of excess degree
j	end of an edge
j_e	excess degree of end j of edge e
j_i	excess degree of end j of edge i
$\bar{k}_u$	average excess degree of neighbors u of a vertex
$\bar{k}_A$	average excess degree of vertex A
$\overline{K}_n$	empty graph as the complement of a complete graph on n vertices
K	variable of excess degree
k	end of an edge; excess degree of a vertex
k'	total degree of a vertex
k_e	excess degree of end k of edge e
k_i	excess degree of end k of edge i
K_n	complete graph on n vertices
$K_{i,j}$	bipartite graph with $i = \lvert V_1 \rvert$ and $j = \lvert V_2 \rvert$

KPPS	Koop et al. (1996) and Pesaran and Shin (1998) generalised VAR framework
λ	regularization parameter controlling for the amount of shrinkage
$\lambda_{\max}$	maximum eigenvalue of a matrix
L	lag operator, i.e., $L^p \boldsymbol{x}_t = \boldsymbol{x}_{t-p}$
l	end of an edge
l_e^{out}	excess out-strength of end l of edge e
l_i	excess (in- or out-) strength of end l of edge i
$L_{i,t}$	log low price of variable i at time t
LASSO	least absolute shrinkage and selection operator
M	total number of edges in a network
m	end of an edge; total number of edges; number of new edges in every step t in the BA model
m_e^{in}	excess in-strength of end m of edge e
m_0	initial group of vertices in BA model
m_i	excess (in- or out-) strength of end m of edge i
$m_{\max}$	maximum size of a graph
MST	minimal spanning tree
$\|\cdot\|_p$	ℓ_p matrix norm
ν	sum of edge weights
N	total number of vertices; total number of variables $x_{i,t}$, $i = 1, \ldots, N$
n	total number of vertices
$N_G(v)$	open neighbourhood of v
$N_G[v]$	closed neighbourhood of v
$N_G^{\text{in}}(v)$	set of vertices that can reach v
$N_G^{\text{out}}(v)$	set of vertices that are reachable by v
n_k	total number of co-authors of a paper
Ω	sum of elements ω_e^{β}, $\Omega = H$ if $\beta = 1$, and $\Omega = M$ if $\beta = 0$
Ω_{t-1}	known history of the process $\boldsymbol{x}_t$ up to $t-1$
$O_{i,t}$	log open price of variable i at time t
OHLC	open, high, low, closing prices
$\boldsymbol{\Phi}(L)$	matrix lag polynomial

$\mathbf{\Phi}_i$	$(N \times N)$ coefficient matrix at lag i
$\Psi_j^{\mathrm{g}}(h)$	scaled generalised impulse response function
p	probability of two vertices being connected by an edge of any weight (nonzero), i.e., $p = 1 - P(0)$; probability for a new vertex to connect to an existing one based on its degree rather than its fitness in WSF model with stochastic weight assignment scheme
$P(0)$	probability that there is no edge between two vertices in the WRG model
$P(\omega)$	probability for W_{ij} to equal ω
$P(\rho_e > 0)$	proportion of assortative edges
$P(\rho_e^{\omega}(\alpha, \beta) > 0)$	proportion of generalised assortative edges
$P(\rho_v > 0)$	proportion of assortative vertices
$P(\rho_v^{\omega}(\alpha, \beta) > 0)$	proportion of generalised assortative vertices
$p(k)$	degree distribution, i.e., the probability that a vertex has degree k
$P(W_{ij} = \omega)$	probability for W_{ij} to equal ω
$p_{s'}^{\mathrm{in}}$	out-strength distribution, i.e., the probability that a vertex has in-strength s'
$p_{s'}^{\mathrm{out}}$	out-strength distribution, i.e., the probability that a vertex has out-strength s'
p_k	degree distribution, i.e., the probability that a vertex has degree k
P_n	a path
p_{ij}	for the disparity filter algorithm, the normalized weight of an edge between vertices i and j
$p_{s'}$	total strength distribution, i.e., the probability that a vertex has strength s'
$\tilde{q}$	parameter of the geometric distribution $\mathrm{Geo}(\tilde{q})$, where $\tilde{q} = 1 - p$
$q(k)$	excess degree distribution, i.e., the probability that a vertex has excess degree k
$q_s^{*\mathrm{in}}$	excess in-strength distribution (by backtracing an edge), i.e., the probability that a vertex that an edge leads out of has excess in-strength s
$q_s^{*\mathrm{out}}$	excess out-strength distribution (by following an edge), i.e., the probability that the vertex that an edge points to has excess out-strength s

q_s^{in}	excess in-strength distribution (by following an edge), i.e., the probability that a vertex that an edge points to has excess in-strength s
q_s^{out}	excess out-strength distribution (by backtracing an edge), i.e., the probability that a vertex that an edge leads out of has excess out-strength s
q_k	excess degree distribution, i.e., the probability that a vertex has excess degree k
q_s	excess strength distribution, i.e., the probability that a vertex has excess strength s
$\overline{(\rho_e)_+}$	mean absolute magnitude of assortative edges
$\overline{(\rho_e)_-}$	mean absolute magnitude of disassortative edges
$\overline{(\rho_e^\omega(\alpha,\beta))_+}$	mean absolute magnitude of generalised assortative edges
$\overline{(\rho_e^\omega(\alpha,\beta))_-}$	mean absolute magnitude of generalised disassortative edges
ρ	generalised assortativity coefficient based on total strengths
$\rho_v^\omega(\alpha,\beta,*)$	generalised vertex out- ($*=$ out) or in-assortativeness ($*=$ in) values
ρ^{GUAC}	generalised universal assortativity coefficient
ρ^{UAC}	universal assortativity coefficient by Zhang et al. (2012)
ρ_e	edge assortativeness values
ρ_e^ω	weighted edge assortativeness values
$\rho_e^\omega(\alpha,\beta)$	generalised edge assortativeness values
$\rho_e^\omega(\alpha,\beta,\text{mode})$	generalised edge assortativeness values (directed networks)
ρ_e^J	edge assortativeness values based on the jackknife method
ρ_v	vertex assortativeness values
$\rho_v^\omega(\alpha,\beta)$	generalised vertex assortativeness values
$\rho_{e_{uv}}$	edge assortativeness value of an edge e connecting vertices u and v
$\rho_{e_{uv}}^\omega$	generalised edge assortativeness value of an edge e connecting vertices u and v
$\tilde{\rho}$	generalised assortativity coefficient based on excess strengths
$\tilde{r}$	arbitrary assortativity coefficient
$\tilde{r}_{(-e)}$	arbitrary assortativity coefficient without the e-th edge
r	assortativity coefficient by Newman (2002)
r^ω	weighted version of r

$r^{\omega}_{(\alpha,\beta)}$	generalised assortativity coefficient
$r^{\omega}_{(\alpha,\beta),(-i)}$	generalised assortativity coefficient where the i-th edge of the network is omitted
$r^{\omega}_{\text{out–in}}$	directed version of r^{ω}
$r^{\omega}_{\text{rnd}}(\alpha,\beta)$	generalised assortativity coefficient of a randomized network
r^{LC}	assortativity coefficient by Leung and Chau (2007)
r^{N}	assortativity coefficient by Newman (2002)
r^{N}_{d}	assortativity coefficient by Newman (2003)
RR	ridge regression
$[\sigma_{ij}]$	element of matrix the $\mathbf{\Sigma}$
$\bar{s}_A$	average excess strength of vertex A
$\mathbf{\Sigma}$	covariance matrix of $\boldsymbol{\varepsilon}_t$
$\hat{\sigma}_{i,t}$	estimate of the return standard deviation of variable i at time t, i.e., volatility
$\hat{\sigma}^2_{i,t}$	estimate of the return variance of variable i at time t
$\hat{\sigma}^{\omega}_{q_s}$	weighted sample standard deviation of the excess strengths of the ends of an edge
$\hat{\sigma}_{r^{\omega}_{(\alpha,\beta)},*}$	jackknife ($*=J$) or bootstrap ($*=B$) standard error of $r^{\omega}_{(\alpha,\beta)}$
$\hat{\sigma}_{r^{\omega}_{\text{rnd}}}$	standard error of the generalised assortativity coefficient of a randomized network
$\sigma_{\max}$	maximum singular value of a matrix
$\sigma^2_{q_k}$	variance of the distribution q_k
$\sigma^2_{q_s}$	variance of the distribution q_s
$\tilde{s}^{\text{in}}_{(m,i)}$	excess in-strength of end m with respect to edge i
$\tilde{s}^{\text{out}}_{(l,i)}$	excess out-strength of end l with respect to edge i
S	confidence level; variable of excess strength
s^*_u	modified strength of vertex u
s'_u	modified strength of vertex u, $s'_u = s_u$ if $\alpha = 1$, and $s'_u = k'_u$ if $\alpha = 0$
s'_u	total strength of vertex u
s^{in}_m	in-strength of end m
s^{out}_l	out-strength of end l
S_n	star graph on $(n+1)$ vertices (one center)

s_u	strength of vertex u
$\bar{\hat{\theta}}^*$	mean of bootstrap statistics
$\boldsymbol{\theta}^{\mathrm{g}}(H)$	generalised forecast error variance decomposition matrix
$\hat{\theta}^*$	bootstrap statistic
$\mathrm{Tr}(A)$	trace of matrix A, i.e., the sum of its diagonal elements
$\theta_{ij}^{\mathrm{g}}(H)$	ij-th element of $\boldsymbol{\theta}^{\mathrm{g}}(H)$
$\tilde{\boldsymbol{\theta}}^{\mathrm{g}}(H)$	normalised generalised forecast error variance decomposition matrix
$\tilde{\theta}_{ij}^{\mathrm{g}}(H)$	ij-th element of $\tilde{\boldsymbol{\theta}}^{\mathrm{g}}(H)$
T	number of time steps in BA model; variable of excess strength; total number of points in time of $x_{i,t}$, $t = 1, \ldots, T$
t	particular point in time in BA model
$\bar{U}_{q_k}$	sample mean of excess degrees of the ends of an edge
$\bar{U}^{\omega}_{q_s^{\mathrm{out}}}(\alpha, \beta)$	weighted sample mean of the generalised excess out-strengths of the ends of an edge
$\bar{U}_{q_s}$	sample mean of excess strengths of the ends of an edge
$\bar{U}^{\omega}_{q_s}$	weighted sample mean of the excess strengths of the ends of an edge
$u \xrightarrow{*} v$	path between vertices u and v of unknown length
$u \xrightarrow{k} v$	path between vertices u and v of length k
u	a vertex
$U_{[0,1]}$	continuous uniform distribution on the interval $[0, 1]$
$u_{i,t}$	normalised high price of variable i at time t
U_{q_k}	expected value of the distribution q_k
U_{q_s}	expected value of the distribution q_s
UAC	universal assortativity coefficient by Zhang et al. (2012)
$\lvert V(G) \rvert$	cardinality of the vertex set, i.e., the order n of a graph
VAR(p)	vector autoregressive model with lag order p
v	a vertex
$V, V(G)$	vertex set of a network
$\boldsymbol{W}$	weighted adjacency matrix
$\boldsymbol{W}^*$	bootstrapped weighted adjacency matrix
ω_e	weight of edge e
$\tilde{w}_{uv}$	assigned weights

w	size of the rolling window
w^*_{hk}	element of $\boldsymbol{W}^*$
w_{ij}	element of $\boldsymbol{W}$; weight of an edge between vertices i and j
w_{uv}	weight of an edge between vertices u and v
WRG	weighted random graph model
WSF	weighted scale free model
$\boldsymbol{x}_t$	$(N \times 1)$ random vector at points in time t
$\boldsymbol{x}_{t+h}$	h-step ahead forecast of $\boldsymbol{x}_t$
X	a random variable
x	realization of random variable X
$x_{i,t}$	value of i-variable at time t
Y	a random variable
y	realization of random variable Y
$z_{0.975}$	standard normal quantile

References

Acharya, V., Engle, R., & Richardson, M. (2012). Capital shortfall: A new approach to ranking and regulating systemic risks. *American Economic Review*, *102*(3), 59–64. doi: 10.1257/aer.102.3.59

Acharya, V. V., Pedersen, L. H., Philippon, T., & Richardson, M. (2017). Measuring systemic risk. *Review of Financial Studies*, *30*(1), 2–47. doi: 10.1093/rfs/hhw088

Adrian, T., & Brunnermeier, M. K. (2016). Covar. *American Economic Review*, *106*(7), 1705–1741. doi: 10.1257/aer.20120555

Alizadeh, S., Brandt, M. W., & Diebold, F. X. (2002). Range-based estimation of stochastic volatility models. *The Journal of Finance*, *57*(3), 1047–1091. doi: 10.1111/1540-6261.00454

Anamika, Chakraborty, M., & Subramaniam, S. (2021). Does sentiment impact cryptocurrency? *Journal of Behavioral Finance*, 1–17. doi: 10.1080/15427560.2021.1950723

Andersen, T. G., Bollerslev, T., Christoffersen, P. F., & Diebold, F. X. (2006). Chapter 15 volatility and correlation forecasting. In G. Elliott, C. Granger, & A. Timmermann (Eds.), *Handbook of economic forecasting* (Vol. 1, pp. 777–878). Elsevier. doi: 10.1016/S1574-0706(05)01015-3

Andersen, T. G., Bollerslev, T., Christoffersen, P. F., & Diebold, F. X. (2013). Chapter 17 - financial risk measurement for financial risk management. In G. M. Constantinides, M. Harris, & R. M. Stulz (Eds.), *Handbook of the economics of finance* (Vol. 2, pp. 1127–1220). Elsevier. doi: 10.1016/B978-0-44-459406-8.00017-2

Arcagni, A., Grassi, R., Stefani, S., & Torriero, A. (2017). Higher order assortativity in complex networks. *European Journal of Operational Research*, *262*(2), 708–719. doi: 10.1016/j.ejor.2017.04.028

Arcagni, A., Grassi, R., Stefani, S., & Torriero, A. (2021). Extending assortativity: An application to weighted social networks. *Journal of Business Research*, *129*, 774–783. doi: 10.1016/j.jbusres.2019.10.008

Aswad, G. (2021). *El salvador's dangerous gamble on bitcoin.* Retrieved 2022-07-30, from `https://www.thelondonfinancial.com/uncategorized/economics-opinion/el-salvadors-dangerous-gamble-on-bitcoin`

Baker, M., & Wurgler, J. (2006). Investor sentiment and the cross-section of stock returns. *The Journal of Finance*, *61*(4), 1645–1680. doi: 10.1111/j.1540-6261.2006.00885.x

Barabási, A.-L. (2016). *Network science.* Cambridge: Cambridge University Press.

Barabási, A.-L., & Albert, R. (1999). Emergence of scaling in random networks. *Science (New York, N.Y.)*, *286*(5439), 509–512. doi: 10.1126/science.286.5439.509

Barabási, A.-L., Albert, R., & Jeong, H. (1999). Mean-field theory for scale-free random networks. *Physica A: Statistical Mechanics and its Applications*, *272*(1-2), 173–187. doi: 10.1016/S0378-4371(99)00291-5

Barrat, A., Barthélemy, M., Pastor-Satorras, R., & Vespignani, A. (2004). The architecture of complex weighted networks. *Proceedings of the National Academy of Sciences of the United States of America*, *101*(11), 3747–3752. doi: 10.1073/pnas.0400087101

Barthélemy, M., Barrat, A., Pastor-Satorras, R., & Vespignani, A. (2005). Characterization and modeling of weighted networks. *Physica A: Statistical Mechanics and its Applications*, *346*(1-2), 34–43. doi: 10.1016/j.physa.2004.08.047

Baruník, J., & Křehlík, T. (2018). Measuring the frequency dynamics of financial connectedness and systemic risk*. *Journal of Financial Econometrics*, *16*(2), 271–296. doi: 10.1093/jjfinec/nby001

Bech, M. L., & Atalay, E. (2010). The topology of the federal funds market. *Physica A: Statistical Mechanics and its Applications*, *389*(22), 5223–5246. doi: 10.1016/j.physa.2010.05.058

Beck, R. J., Fitzgerald, W. J., & Pauksztat, B. (2003). Individual behaviors and social structure in the development of communication networks of self-organizing online discussion groups. In B. Wasson, S. Ludvigsen, & U. Hoppe (Eds.), *Designing for change in networked learning environments: Proceedings of the international conference on computer support for collaborative learning 2003* (pp. 313–322). Dordrecht: Springer Netherlands. doi: 10.1007/978-94-017-0195-2_39

Benoit, S., Colliard, J.-E., Hurlin, C., & Pérignon, C. (2017). Where the risks lie: A survey on systemic risk*. *Review of Finance*, *21*(1), 109–152. doi: 10.1093/rof/rfw026

Berentsen, A., & Schar, F. (2018). A short introduction to the world of cryptocurrencies. *Review*, *100*(1), 1–19. doi: 10.20955/r.2018.1-16

Bianconi, G., & Barabási, A.-L. (2001). Competition and multiscaling in evolving networks. *Europhysics Letters (EPL)*, *54*(4), 436–442. doi: 10.1209/epl/i2001-00260-6

Blondel, V. D., Guillaume, J.-L., Lambiotte, R., & Lefebvre, E. (2008). Fast unfolding of communities in large networks. *Journal of Statistical Mechanics: Theory and Experiment*, *2008*(10), P10008. doi: 10.1088/1742-5468/2008/10/P10008

Boguñá, M., & Pastor-Satorras, R. (2002). Epidemic spreading in correlated complex networks. *Physical review. E, Statistical, nonlinear, and soft matter physics*, *66*(4 Pt 2), 047104. doi: 10.1103/PhysRevE.66.047104

Bollobás, B. (2008). *Random graphs* (2. ed., 5. print ed., Vol. 73). Cambridge: Cam-

bridge Univ. Press.

Bollobás, B., Borgs, C., Chayes, J., & Riordan, O. (2003). Directed scale-free graphs. In *Proceedings of the fourteenth annual acm-siam symposium on discrete algorithms* (pp. 132–139). USA: Society for Industrial and Applied Mathematics.

Bollobás, B., Riordan, O., Spencer, J., & Tusnády, G. (2001). The degree sequence of a scale-free random graph process. *Random Structures & Algorithms*, *18*(3), 279–290. doi: 10.1002/rsa.1009

Bonacich, P. (1987). Power and centrality: A family of measures. *American Journal of Sociology*, *92*(5), 1170–1182.

Bonanno, G., Caldarelli, G., Lillo, F., & Mantegna, R. N. (2003). Topology of correlation-based minimal spanning trees in real and model markets. *Physical review. E, Statistical, nonlinear, and soft matter physics*, *68*(4 Pt 2), 046130. doi: 10.1103/PhysRevE.68.046130

Borgs, C., Chayes, J. T., Daskalakis, C., & Roch, S. (2007). First to market is not everything: an analysis of preferential attachment with fitness. In *Stoc '07*.

Bostanci, G., & Yilmaz, K. (2020). How connected is the global sovereign credit risk network? *Journal of Banking & Finance*, *113*, 105761. doi: 10.1016/j.jbankfin.2020.105761

Bouri, E., Gabauer, D., Gupta, R., & Tiwari, A. K. (2021). Volatility connectedness of major cryptocurrencies: The role of investor happiness. *Journal of Behavioral and Experimental Finance*, *30*, 100463. doi: 10.1016/j.jbef.2021.100463

Boyd, J. P., Fitzgerald, W. J., & Beck, R. J. (2006). Computing core/periphery structures and permutation tests for social relations data. *Social Networks*, *28*(2), 165–178. doi: 10.1016/j.socnet.2005.06.003

Brede, M., & Sinha, S. (2005). Assortative mixing by degree makes a network more unstable. *arXiv:cond-mat/0507710v1*. doi: 10.48550/ARXIV.COND-MAT/0507710

Brey, A., LeBlanc, Z., & Deschamps, R. (2018). Temporal network analysis with r. *Programming Historian*(7). doi: 10.46430/phen0080

Brida, J. G., & Risso, W. A. (2010). Hierarchical structure of the german stock market. *Expert Systems with Applications*, *37*(5), 3846–3852. doi: 10.1016/j.eswa.2009.11.034

Brot, H., Honig, M., Muchnik, L., Goldenberg, J., & Louzoun, Y. (2013). Edge removal balances preferential attachment and triad closing. *Physical review. E, Statistical, nonlinear, and soft matter physics*, *88*(4), 042815. doi: 10.1103/PhysRevE.88.042815

Brownlees, C., & Engle, R. F. (2017). Srisk: A conditional capital shortfall measure of systemic risk. *Review of Financial Studies*, *30*(1), 48–79. doi: 10.1093/rfs/hhw060

Caldarelli, G. (2007). *Scale-free networks*. Oxford University Press. doi: 10.1093/acprof:oso/9780199211517.001.0001

Callaway, D. S., Hopcroft, J. E., Kleinberg, J. M., Newman, M. E. J., & Strogatz, S. H. (2001). Are randomly grown graphs really random? *Physical review. E, Statistical, nonlinear, and soft matter physics*, *64*(4 Pt 1), 041902. doi: 10.1103/PhysRevE.64.041902

Caloia, F. G., Cipollini, A., & Muzzioli, S. (2019). How do normalization schemes affect net spillovers? a replication of the diebold and yilmaz (2012) study. *Energy Economics*, *84*, 104536. doi: 10.1016/j.eneco.2019.104536

Cameron, A. C., & Trivedi, P. K. (2012). *Microeconometrics*. Cambridge University Press. doi: 10.1017/CBO9780511811241

Campbell, J. Y., Lo, A. W., & MacKinlay, A. C. (2012). *The econometrics of financial markets*. Princeton, NJ: Princeton University Press.

Chakrabarti, D., Wang, Y., Wang, C., Leskovec, J., & Faloutsos, C. (2008). Epidemic thresholds in real networks. *ACM Transactions on Information and System Security*, *10*(4), 1–26. doi: 10.1145/1284680.1284681

Chang, H., Su, B.-B., Zhou, Y.-P., & He, D.-R. (2007). Assortativity and act degree distribution of some collaboration networks. *Physica A: Statistical Mechanics and its Applications*, *383*(2), 687–702. doi: 10.1016/j.physa.2007.04.045

CoinMarketCap. (2022). *Listings and methodologies – metric methodologies – circulating supply*. Retrieved 2022-06-30, from `https://support.coinmarketcap.com/hc/en-us/sections/360008888252-Metric-Methodologies`

Coolen, A. C. C., Annibale, A., & Roberts, E. (2017). *Generating random networks and graphs* (First edition ed.). Oxford: Oxford University Press. doi: 10.1093/oso/9780198709893.001.0001

Corbet, S., Lucey, B., Urquhart, A., & Yarovaya, L. (2019). Cryptocurrencies as a financial asset: A systematic analysis. *International Review of Financial Analysis*, *62*, 182–199. doi: 10.1016/j.irfa.2018.09.003

Craig, B., & von Peter, G. (2014). Interbank tiering and money center banks. *Journal of Financial Intermediation*, *23*(3), 322–347. doi: 10.1016/j.jfi.2014.02.003

Da Costa, J. F. P. (2011). Weighted correlation. In M. Lovric (Ed.), *International encyclopedia of statistical science* (pp. 1653–1655). Berlin, Heidelberg: Springer Berlin Heidelberg. doi: 10.1007/978-3-642-04898-2

Dai, L., Derudder, B., & Liu, X. (2018). Transport network backbone extraction: A comparison of techniques. *Journal of Transport Geography*, *69*, 271–281. doi: 10.1016/j.jtrangeo.2018.05.012

Davidson, R., & MacKinnon, J. G. (2000). Bootstrap tests: how many bootstraps? *Econometric Reviews*, *19*(1), 55–68. doi: 10.1080/07474930008800459

Davison, A. C., & Hinkley, D. V. (2013). *Bootstrap methods and their application*.

Cambridge University Press. doi: 10.1017/CBO9780511802843

Deijfen, M., & Lindholm, M. (2009). Growing networks with preferential deletion and addition of edges. *Physica A: Statistical Mechanics and its Applications*, *388*(19), 4297–4303. doi: 10.1016/j.physa.2009.06.032

Demirer, M., Diebold, F. X., Liu, L., & Yilmaz, K. (2018). Estimating global bank network connectedness. *Journal of Applied Econometrics*, *33*(1), 1–15. doi: 10 .1002/jae.2585

Devroye, L. (1986). *Non-uniform random variate generation*. New York, NY: Springer New York. doi: 10.1007/978-1-4613-8643-8

DiCiccio, T. J., & Efron, B. (1996). Bootstrap confidence intervals. *Statistical Science*, *11*(3), 189–212. Retrieved from `http://www.jstor.org/stable/2246110`

Diebold, F. X., & Yilmaz, K. (2009). Measuring financial asset return and volatility spillovers, with application to global equity markets. *The Economic Journal*, *119*(534), 158–171. doi: 10.1111/j.1468-0297.2008.02208.x

Diebold, F. X., & Yilmaz, K. (2012). Better to give than to receive: Predictive directional measurement of volatility spillovers. *International Journal of Forecasting*, *28*(1), 57–66. doi: 10.1016/j.ijforecast.2011.02.006

Diebold, F. X., & Yilmaz, K. (2014). On the network topology of variance decompositions: Measuring the connectedness of financial firms. *Journal of Econometrics*, *182*(1), 119–134. doi: 10.1016/j.jeconom.2014.04.012

Diebold, F. X., & Yilmaz, K. (2015a). *Financial and macroeconomic connectedness*. Oxford University Press. doi: 10.1093/acprof:oso/9780199338290.001.0001

Diebold, F. X., & Yilmaz, K. (2015b). Trans-atlantic equity volatility connectedness: U.s. and european financial institutions, 2004–2014. *Journal of Financial Econometrics*, nbv021. doi: 10.1093/jjfinec/nbv021

Diestel, R. (2018). *Graph theory* (Fifth edition, first softcover printing ed., Vol. 173). Berlin: Springer.

Dorogovtsev, S. (2010). *Lectures on complex networks*. Oxford University Press. doi: 10.1093/acprof:oso/9780199548927.001.0001

Dorogovtsev, S., & Mendes, J. F. (2000). Evolution of networks with aging of sites. *Physical review. E, Statistical physics, plasmas, fluids, and related interdisciplinary topics*, *62*(2 Pt A), 1842–1845. doi: 10.1103/physreve.62.1842

Dugué, N., & Perez, A. (2015). Directed louvain : maximizing modularity in directed networks: Research report. *Université d'Orléans*. Retrieved from `https://hal .archives-ouvertes.fr/hal-01231784`

Efron, B. (1979). Bootstrap methods: Another look at the jackknife. *The Annals of Statistics*, *7*(1). doi: 10.1214/aos/1176344552

Efron, B. (1981). Nonparametric standard errors and confidence intervals. *Canadian Journal of Statistics*, *9*(2), 139–158. doi: 10.2307/3314608

Efron, B. (1982). *The jackknife, the bootstrap and other resampling plans.* Society for Industrial and Applied Mathematics. doi: 10.1137/1.9781611970319

Efron, B. (1987). Better bootstrap confidence intervals. *Journal of the American Statistical Association*, *82*(397), 171. doi: 10.2307/2289144

Engle, R. (2002). Dynamic conditional correlation. *Journal of Business & Economic Statistics*, *20*(3), 339–350. doi: 10.1198/073500102288618487

Erdös, P., & Rényi, A. (1959). On random graphs i. *Publicationes Mathematicae Debrecen*, *6*, 290–297.

Erdös, P., & Rényi, A. (1960). On the evolution of random graphs. *Publ. Math. Inst. Hungary. Acad. Sci.*, *5*, 17–61.

European Commission. (2019). *Regulation establishing a european framework for markets in crypto assets (mica): Proposal for a regulation of the european parliament and of the council on markets in crypto-assets, and amending directive (eu) 2019/1937.* Retrieved 2022-08-02, from `https://eur-lex.europa.eu/legal-content/EN/PIN/?uri=CELEX:52020PC0593`

Farine, D. R. (2014). Measuring phenotypic assortment in animal social networks: weighted associations are more robust than binary edges. *Animal Behaviour*, *89*, 141–153. doi: 10.1016/j.anbehav.2014.01.001

Faskowitz, J., Betzel, R. F., & Sporns, O. (2022). Edges in brain networks: Contributions to models of structure and function. *Network neuroscience (Cambridge, Mass.)*, *6*(1), 1–28.

Fornito, A., Zalesky, A., & Bullmore, E. T. (Eds.). (2016). *Fundamentals of brain network analysis.* San Diego: Academic Press.

Fortunato, S., & Hric, D. (2016). Community detection in networks: A user guide. *Physics Reports*, *659*, 1–44. doi: 10.1016/j.physrep.2016.09.002

Freeman, L. C. (1978). Centrality in social networks conceptual clarification. *Social Networks*, *1*(3), 215–239. doi: 10.1016/0378-8733(78)90021-7

Freeman, L. C., Freeman, S. C., & Michaelson, A. G. (1988). On human social intelligence. *Journal of Social and Biological Systems*, *11*(4), 415–425. doi: 10.1016/0140-1750(88)90080-2

Fricke, D., & Lux, T. (2015). Core–periphery structure in the overnight money market: Evidence from the e-mid trading platform. *Computational Economics*, *45*(3), 359–395. doi: 10.1007/s10614-014-9427-x

Gabauer, D. (2020). Volatility impulse response analysis for dcc–garch models: The role of volatility transmission mechanisms. *Journal of Forecasting*, *39*(5), 788–796. doi: 10.1002/for.2648

Gabor Csardi, & Tamas Nepusz. (2006). The igraph software package for complex network research. *InterJournal*, *Complex Systems*, 1695. Retrieved from `https://igraph.org`

Garcia-Domingo, J. L., Juher, D., & Saldaña, J. (2008). Degree correlations in growing networks with deletion of nodes. *Physica D: Nonlinear Phenomena*, *237*(5), 640–651. doi: 10.1016/j.physd.2007.10.012

Garlaschelli, D. (2009). The weighted random graph model. *New Journal of Physics*, *11*(7), 073005. doi: 10.1088/1367-2630/11/7/073005

Garlaschelli, D., & Loffredo, M. I. (2004). Patterns of link reciprocity in directed networks. *Physical review letters*, *93*(26 Pt 1), 268701. doi: 10.1103/PhysRevLett.93.268701

Garlaschelli, D., & Loffredo, M. I. (2008). Maximum likelihood: extracting unbiased information from complex networks. *Physical review. E, Statistical, nonlinear, and soft matter physics*, *78*(1 Pt 2), 015101. doi: 10.1103/PhysRevE.78.015101

Garlaschelli, D., & Loffredo, M. I. (2009). Generalized bose-fermi statistics and structural correlations in weighted networks. *Physical review letters*, *102*(3), 038701. doi: 10.1103/PhysRevLett.102.038701

Garman, M. B., & Klass, M. J. (1980). On the estimation of security price volatilities from historical data. *The Journal of Business*, *53*(1), 67. doi: 10.1086/296072

Gentle, J. E. (2017). *Matrix algebra*. Cham: Springer International Publishing. doi: 10.1007/978-3-319-64867-5

George G. Kaufman, & Kenneth E. Scott. (2003). What is systemic risk, and do bank regulators retard or contribute to it? *The Independent Review*, *7*, 371.

Ghimire, S., & Selvaraj, H. (2018). A survey on bitcoin cryptocurrency and its mining. In *2018 26th international conference on systems engineering (icseng)* (pp. 1–6). doi: 10.1109/ICSENG.2018.8638208

Gibbons, A., & Gibbons, A. M. (1999). *Algorithmic graph theory* (Reprinted, transferred to digital reprinting ed.). Cambridge: Cambridge Univ. Press.

Gilbert, E. N. (1959). Random graphs. *The Annals of Mathematical Statistics*, *30*(4), 1141–1144. doi: 10.1214/aoms/1177706098

Green, A., & Shalizi, C. R. (2022). Bootstrapping exchangeable random graphs. *Electronic Journal of Statistics*, *16*(1). doi: 10.1214/21-EJS1896

Hajra, K. B., & Sen, P. (2005). Aging in citation networks. *Physica A: Statistical Mechanics and its Applications*, *346*(1-2), 44–48. doi: 10.1016/j.physa.2004.08.048

Hamilton, J. D. (1994). *Time series analysis*. Princeton, NJ: Princeton Univ. Press.

Harary, F., Norman, R. Z., & Cartwright, D. (1966). *Structural models: An introduction to the theory of directed graphs* (2. printing ed.). New York: Wiley.

Hastie, T., Tibshirani, R., & Friedman, J. (2009). *The elements of statistical learning*. New York, NY: Springer New York. doi: 10.1007/978-0-387-84858-7

Hoerl, A. E., & Kennard, R. W. (1970a). Ridge regression: Applications to nonorthogonal problems. *Technometrics*, *12*(1), 69–82. doi: 10.1080/00401706.1970

.10488635

Hoerl, A. E., & Kennard, R. W. (1970b). Ridge regression: Biased estimation for nonorthogonal problems. *Technometrics*, *12*(1), 55–67. doi: 10.1080/00401706.1970.10488634

Holme, P. (2017). Temporal networks. In R. Alhajj & J. Rokne (Eds.), *Encyclopedia of social network analysis and mining* (pp. 1–10). New York, NY: Springer New York. doi: 10.1007/978-1-4614-7163-9_42-1

Holme, P., & Saramäki, J. (2012). Temporal networks. *Physics Reports*, *519*(3), 97–125. doi: 10.1016/j.physrep.2012.03.001

in 't Veld, D., & van Lelyveld, I. (2014). Finding the core: Network structure in interbank markets. *Journal of Banking & Finance*, *49*, 27–40. doi: 10.1016/j.jbankfin.2014.08.006

Jackson, M. O. (2011). *Social and economic networks.* Princeton, N.J. and Woodstock: Princeton University Press.

Jin, H., & Singh, K. (2021). *Tesla's musk halts use of bitcoin for car purchases.* Retrieved 2022-08-02, from `https://www.reuters.com/technology/tesla-stops-taking-bitcoin-cites-fossil-fuel-use-mining-cybercurrency-2021-05-12/`

John, A. (2022). *Stablecoin terra's broken dollar peg hits wider crypto markets.*

Kamada, T., & Kawai, S. (1989). An algorithm for drawing general undirected graphs. *Information Processing Letters*, *31*(1), 7–15. doi: 10.1016/0020-0190(89)90102-6

Kamisli, M., Kamisli, S., & Temizel, F. (2019). Empirical evidence of the relationships between bitcoin and stock exchanges: Case of return and volatility spillover. In U. Hacioglu (Ed.), *Blockchain economics and financial market innovation: Financial innovations in the digital age* (pp. 293–318). Cham: Springer International Publishing. doi: 10.1007/978-3-030-25275-5

Kim, A., Trimborn, S., & Härdle, W. K. (2021). Vcrix — a volatility index for cryptocurrencies. *International Review of Financial Analysis*, *78*, 101915. doi: 10.1016/j.irfa.2021.101915

Kim, C., & Kim, D. (2018a). *South korea plans to ban cryptocurrency trading, rattles market.* Retrieved 2022-08-01, from `https://www.investing.com/news/cryptocurrency-news/south-korea-plans-to-ban-cryptocurrency-trading-rattles-market-1090283`

Kim, C., & Kim, D. (2018b). *South korea says no plans to ban cryptocurrency exchanges, uncovers $600 million illegal trades.* Retrieved from `https://www.reuters.com/article/us-southkorea-bitcoin/south-korea-says-no-plans-to-ban-cryptocurrency-exchanges-uncovers-600-million-illegal-trades-idUSKBN1FK09J`

Kivela, M., Arenas, A., Barthelemy, M., Gleeson, J. P., Moreno, Y., & Porter, M. A. (2014). Multilayer networks. *Journal of Complex Networks*, *2*(3), 203–271. doi:

10.1093/comnet/cnu016

Koop, G., Pesaran, M., & Potter, S. M. (1996). Impulse response analysis in nonlinear multivariate models. *Journal of Econometrics*, *74*(1), 119–147. doi: 10.1016/0304-4076(95)01753-4

Koutmos, D. (2018). Return and volatility spillovers among cryptocurrencies. *Economics Letters*, *173*, 122–127. doi: 10.1016/j.econlet.2018.10.004

Krishnamoorthy, K. (2020). *Handbook of statistical distributions with applications*. CRC PRESS.

Kruskal, J. B. (1956). On the shortest spanning subtree of a graph and the traveling salesman problem. *Proceedings of the American Mathematical Society*, *7*(1), 48–50. doi: 10.1090/S0002-9939-1956-0078686-7

Kunegis, J. (2013). Konect: The koblenz network collection. In *Proceedings of the 22nd international conference on world wide web* (pp. 1343–1350). New York, NY, USA: Association for Computing Machinery. doi: 10.1145/2487788.2488173

Kyriazis, N. A. (2019). A survey on empirical findings about spillovers in cryptocurrency markets. *Journal of Risk and Financial Management*, *12*(4), 170. doi: 10.3390/jrfm12040170

Lastrapes, W. D., & Wiesen, T. F. (2021). The joint spillover index. *Economic Modelling*, *94*, 681–691. doi: 10.1016/j.econmod.2020.02.010

Leicht, E. A., & Newman, M. E. J. (2008). Community structure in directed networks. *Physical review letters*, *100*(11), 118703. doi: 10.1103/PhysRevLett.100.118703

Leung, C. C., & Chau, H. F. (2007). Weighted assortative and disassortative networks model. *Physica A: Statistical Mechanics and its Applications*, *378*(2), 591–602. doi: 10.1016/j.physa.2006.12.022

Lever, J., Krzywinski, M., & Altman, N. (2016). Regularization. *Nature Methods*, *13*(10), 803–804. doi: 10.1038/nmeth.4014

Lütkepohl, H. (2007). *New introduction to multiple time series analysis: With ... 36 tables* (1. ed., corr. 2. print ed.). Berlin and Heidelberg: Springer.

Magnani, M., & Marzolla, M. (2014). Path-based and whole-network measures. In R. Alhajj & J. Rokne (Eds.), *Encyclopedia of social network analysis and mining* (pp. 1256–1269). New York, NY: Springer New York. doi: 10.1007/978-1-4614-6170-8

Mahmoud, H. M. (2009). *Polya urn models*. Boca Raton: CRC PRESS.

Mantegna, R. N. (1999). Hierarchical structure in financial markets. *The European Physical Journal B*, *11*(1), 193–197. doi: 10.1007/s100510050929

Marcaccioli, R., & Livan, G. (2019). A pólya urn approach to information filtering in complex networks. *Nature communications*, *10*(1), 745. doi: 10.1038/s41467-019-08667-3

Maslov, S., & Sneppen, K. (2002). Specificity and stability in topology of protein

networks. *Science (New York, N.Y.)*, *296*(5569), 910–913. doi: 10.1126/science.1065103

Maslov, S., & Sneppen, K. (2004). Detection of topological patterns in protein networks. *Genetic engineering*, *26*, 33–47. doi: 10.1007/978-0-306-48573-2

Meghanathan, N. (2016). Assortativity analysis of real-world network graphs based on centrality metrics. *Computer and Information Science*, *9*(3), 7. doi: 10.5539/cis.v9n3p7

Meyer, C. D. (2008). *Matrix analysis and applied linear algebra*. Philadelphia: Society for Industrial and Applied Mathematics.

Milo, R., Kashtan, N., Itzkovitz, S., Newman, M. E. J., & Alon, U. (2003). On the uniform generation of random graphs with prescribed degree sequences. *arXiv:cond-mat/0312028v2*. doi: 10.48550/ARXIV.COND-MAT/0312028

Mochizuki, T., & Vigna, P. (2018). *Cryptocurrency worth $530 million missing from japanese exchange.* Retrieved 2022-08-01, from `https://www.wsj.com/articles/cryptocurrency-worth-530-million-missing-from-japanese-exchange-1516988190`

Mukhopadhyay, U., Skjellum, A., Hambolu, O., Oakley, J., Yu, L., & Brooks, R. (2016). A brief survey of cryptocurrency systems. In *2016 14th annual conference on privacy, security and trust (pst)* (pp. 745–752). doi: 10.1109/PST.2016.7906988

Nakamoto, S. (2008). *Bitcoin: A peer-to-peer electronic cash system [white paper].* Bitcoin Foundation. Retrieved 2022-06-04, from `https://bitcoin.org/bitcoin.pdf`

Newman, M. E. J. (2001). Scientific collaboration networks. ii. shortest paths, weighted networks, and centrality. *Physical review. E, Statistical, nonlinear, and soft matter physics*, *64*(1 Pt 2), 016132. doi: 10.1103/PhysRevE.64.016132

Newman, M. E. J. (2002). Assortative mixing in networks. *Physical review letters*, *89*(20), 208701. doi: 10.1103/PhysRevLett.89.208701

Newman, M. E. J. (2003). Mixing patterns in networks. *Physical review. E, Statistical, nonlinear, and soft matter physics*, *67*(2 Pt 2), 026126. doi: 10.1103/PhysRevE.67.026126

Newman, M. E. J. (2004). Analysis of weighted networks. *Physical review. E, Statistical, nonlinear, and soft matter physics*, *70*(5 Pt 2), 056131. doi: 10.1103/PhysRevE.70.056131

Newman, M. E. J. (2018). *Networks* (2nd ed. ed.). Oxford: Oxford University Press USA - OSO.

Newman, M. E. J., & Girvan, M. (2004). Finding and evaluating community structure in networks. *Physical review. E, Statistical, nonlinear, and soft matter physics*, *69*(2 Pt 2), 026113. doi: 10.1103/PhysRevE.69.026113

Newman, M. E. J., Strogatz, S. H., & Watts, D. J. (2001). Random graphs with

arbitrary degree distributions and their applications. *Physical review. E, Statistical, nonlinear, and soft matter physics*, *64*(2 Pt 2), 026118. doi: 10.1103/PhysRevE.64.026118

Nicholson, W. B., Matteson, D. S., & Bien, J. (2017). Varx-l: Structured regularization for large vector autoregressions with exogenous variables. *International Journal of Forecasting*, *33*(3), 627–651. doi: 10.1016/j.ijforecast.2017.01.003

Nicholson, W. B., Wilms, I., Bien, J., & Matteson, D. S. (2020). High dimensional forecasting via interpretable vector autoregression. *Journal of Machine Learning Research*, *21*(166), 1–52. Retrieved from `http://jmlr.org/papers/v21/19-777.html`

Nieminen, U. J. (1973). On the centrality in a directed graph. *Social Science Research*, *2*(4), 371–378. doi: 10.1016/0049-089X(73)90010-0

Nieminen, U. J. (1974). On the centrality in a graph. *Scandinavian journal of psychology*, *15*(4), 332–336. doi: 10.1111/j.1467-9450.1974.tb00598.x

Noldus, R., & van Mieghem, P. (2015). Assortativity in complex networks. *Journal of Complex Networks*, *3*(4), 507–542. doi: 10.1093/comnet/cnv005

Ohnesorge, J. (2018). A primer on blockchain technology and its potential for financial inclusion: Discussion paper. *Deutsches Institut für Entwicklungspolitik (DIE)*. Retrieved from `http://hdl.handle.net/10419/199522` doi: 10.23661/dp2.2018

Onnela, J.-P., Chakraborti, A., Kaski, K., Kertész, J., & Kanto, A. (2003). Dynamics of market correlations: taxonomy and portfolio analysis. *Physical review. E, Statistical, nonlinear, and soft matter physics*, *68*(5 Pt 2), 056110. doi: 10.1103/PhysRevE.68.056110

Onyeaka, H., Anumudu, C. K., Al-Sharify, Z. T., Egele-Godswill, E., & Mbaegbu, P. (2021). Covid-19 pandemic: A review of the global lockdown and its far-reaching effects. *Science progress*, *104*(2), 368504211019854. doi: 10.1177/00368504211019854

Ouimet, S. (2019). *Down more than 70% in 2018, bitcoin closes its worst year on record.* Retrieved 2022-08-02, from `https://www.coindesk.com/markets/2019/01/02/down-more-than-70-in-2018-bitcoin-closes-its-worst-year-on-record/`

Park, J., & Newman, M. E. J. (2003). Origin of degree correlations in the internet and other networks. *Physical review. E, Statistical, nonlinear, and soft matter physics*, *68*(2 Pt 2), 026112. doi: 10.1103/PhysRevE.68.026112

Patterson, M. (2018). *Crypto's 80% plunge is now worse than the dot-com crash.* Retrieved 2022-08-01, from `https://www.bloomberg.com/news/articles/2018-09-12/crypto-s-crash-just-surpassed-dot-com-levels-as-losses-reach-80`

Peng, C., Jin, X., & Shi, M. (2010). Epidemic threshold and immunization on generalized networks. *Physica A: Statistical Mechanics and its Applications*, *389*(3), 549–560. doi: 10.1016/j.physa.2009.09.047

Pesaran, H., & Shin, Y. (1998). Generalized impulse response analysis in linear multivariate models. *Economics Letters*, *58*(1), 17–29. doi: 10.1016/S0165-1765(97)00214-0

Piraveenan, M., Prokopenko, M., & Zomaya, A. Y. (2008). Local assortativeness in scale-free networks. *EPL (Europhysics Letters)*, *84*(2), 28002. doi: 10.1209/0295-5075/84/28002

Piraveenan, M., Prokopenko, M., & Zomaya, A. Y. (2009). Local assortativity and growth of internet. *The European Physical Journal B*, *70*(2), 275–285. doi: 10.1140/epjb/e2009-00219-y

Piraveenan, M., Prokopenko, M., & Zomaya, A. Y. (2010). Local assortativeness in scale-free networks. *EPL (Europhysics Letters)*, *89*(4), 49901. doi: 10.1209/0295-5075/89/49901

Piraveenan, M., Prokopenko, M., & Zomaya, A. Y. (2012). Assortative mixing in directed biological networks. *IEEE/ACM transactions on computational biology and bioinformatics*, *9*(1), 66–78. doi: 10.1109/TCBB.2010.80

Price, G. R. (1972). Extension of covariance selection mathematics. *Annals of human genetics*, *35*(4), 485–490. doi: 10.1111/j.1469-1809.1957.tb01874.x

Quenouille, M. H. (1956). Notes on bias estimation. *Biometrika*, *43*(3-4), 353–360. doi: 10.1093/biomet/43.3-4.353

R Core Team. (2021). *R: A language and environment for statistical computing.* Vienna, Austria. Retrieved from `https://www.R-project.org/`

Reingold, E. M., & Tilford, J. S. (1981). Tidier drawings of trees. *IEEE Transactions on Software Engineering*, *SE-7*(2), 223–228. doi: 10.1109/TSE.1981.234519

Reuters. (2022). *Central african republic adopts bitcoin as an official currency.* Retrieved 2022-07-30, from `https://www.reuters.com/world/africa/central-african-republic-adopts-bitcoin-an-official-currency-2022-04-27/`

Rosvall, M., & Bergstrom, C. T. (2010). Mapping change in large networks. *PloS one*, *5*(1), e8694. doi: 10.1371/journal.pone.0008694

Rubinov, M. (2016). Constraints and spandrels of interareal connectomes. *Nature communications*, *7*, 13812. doi: 10.1038/ncomms13812

Rubinov, M., & Sporns, O. (2011). Weight-conserving characterization of complex functional brain networks. *NeuroImage*, *56*(4), 2068–2079. doi: 10.1016/j.neuroimage.2011.03.069

Sabidussi, G. (1966). The centrality of a graph. *Psychometrika*, *31*(4), 581–603. doi: 10.1007/BF02289527

Sánchez García, J., & Cruz Rambaud, S. (2022). Machine learning regularization methods in high-dimensional monetary and financial vars. *Mathematics*, *10*(6), 877. doi: 10.3390/math10060877

Scala, A., & D'Agostino, G. (2013). The robustness of assortativity. In S. Bologna,

B. Hämmerli, D. Gritzalis, & S. Wolthusen (Eds.), *Critical information infrastructure security* (pp. 223–226). Berlin, Heidelberg: Springer Berlin Heidelberg.

Serrano, M. A., & Boguñá, M. (2003). Topology of the world trade web. *Physical review. E, Statistical, nonlinear, and soft matter physics*, *68*(1 Pt 2), 015101. doi: 10.1103/PhysRevE.68.015101

Serrano, M. A., Boguñá, M., & Pastor-Satorras, R. (2006). Correlations in weighted networks. *Physical review. E, Statistical, nonlinear, and soft matter physics*, *74*(5 Pt 2), 055101. doi: 10.1103/PhysRevE.74.055101

Serrano, M. A., Boguñá, M., & Vespignani, A. (2009). Extracting the multiscale backbone of complex weighted networks. *Proceedings of the National Academy of Sciences of the United States of America*, *106*(16), 6483–6488. doi: 10.1073/pnas.0808904106

Shen, S., & Siu, T. (2021). *China bans financial, payment institutions from cryptocurrency business.* Retrieved 2022-08-01, from `https://www.reuters.com/technology/chinese-financial-payment-bodies-barred-cryptocurrency-business-2021-05-18/`

Sims, C. A. (1980). Macroeconomics and reality. *Econometrica*, *48*(1), 1. doi: 10.2307/1912017

Snijders, T. A. B., & Borgatti, S. P. (1999). Non-parametric standard errors and tests for network statistics. *Connection Science*, *2*, 61–70.

Soramäki, K., Bech, M. L., Arnold, J., Glass, R. J., & Beyeler, W. E. (2007). The topology of interbank payment flows. *Physica A: Statistical Mechanics and its Applications*, *379*(1), 317–333. doi: 10.1016/j.physa.2006.11.093

Squartini, T., Picciolo, F., Ruzzenenti, F., & Garlaschelli, D. (2013). Reciprocity of weighted networks. *Scientific reports*, *3*, 2729. doi: 10.1038/srep02729

Stock, J. H., & Watson, M. W. (2001). Vector autoregressions. *Journal of Economic Perspectives*, *15*(4), 101–115. doi: 10.1257/jep.15.4.101

Takahata, Y. (1991). Diachronic changes in the dominance relations of adult female japanese monkeys of the arashiyama b troop. In Fedigan L. M. & Asquith P. J. (Eds.), *The monkeys of arashiyama* (pp. 123–139). State University of New York Press.

The World Bank Group. (2022). *Financial inclusion overview.* Retrieved 2022-07-30, from `https://www.worldbank.org/en/topic/financialinclusion/overview`

Thedchanamoorthy, G., Piraveenan, M., Kasthuriratna, D., & Senanayake, U. (2014). Node assortativity in complex networks: An alternative approach. *Procedia Computer Science*, *29*, 2449–2461. doi: 10.1016/j.procs.2014.05.229

Tibshirani, R. (1996). Regression shrinkage and selection via the lasso. *Journal of the Royal Statistical Society: Series B (Methodological)*, *58*(1), 267–288. doi: 10.1111/j.2517-6161.1996.tb02080.x

Torri, G., Giacometti, R., & Paterlini, S. (2018). Robust and sparse banking network estimation. *European Journal of Operational Research*, *270*(1), 51–65. doi: 10.1016/j.ejor.2018.03.041

Tretina, K. (2022a). *10 best cryptocurrencies of july 2022.* Retrieved 2022-07-30, from `https://www.forbes.com/advisor/investing/cryptocurrency/top-10-cryptocurrencies/`

Tretina, K. (2022b). *How to buy cryptocurrency.* Retrieved from `https://www.forbes.com/advisor/investing/cryptocurrency/how-to-buy-cryptocurrency/`

Tsay, R. S. (2014). *Multivariate time series analysis: With r and financial applications.* Hoboken, New Jersey: Wiley.

Tukey, J. W. (1958). Bias and confidence in not-quite large sample: Abstracts of papers. *The Annals of Mathematical Statistics*, *29*(2), 614–623. doi: 10.1214/aoms/1177706647

U. Pigorsch, & M. Sabek. (2022). Assortative mixing in weighted directed networks. *Physica A: Statistical Mechanics and its Applications*, *604*, 127850. doi: 10.1016/j.physa.2022.127850

Uluceviz, E., & Yilmaz, K. (2020). Real-financial connectedness in the swiss economy. *Swiss Journal of Economics and Statistics*, *156*(1). doi: 10.1186/s41937-019-0049-z

Vandewalle, N., Brisbois, F., & Tordoir, X. (2001). Non-random topology of stock markets. *Quantitative Finance*, *1*(3), 372–374. doi: 10.1088/1469-7688/1/3/308

Wang, W.-X., Hu, B., Wang, B.-H., & Yan, G. (2006). Mutual attraction model for both assortative and disassortative weighted networks. *Physical review. E, Statistical, nonlinear, and soft matter physics*, *73*(1 Pt 2), 016133. doi: 10.1103/PhysRevE.73.016133

Wasserman, S., & Faust, K. (1994). *Social network analysis: Methods and applications.* Cambridge University Press.

Watts, D. J., & Strogatz, S. H. (1998). Collective dynamics of 'small-world' networks. *Nature*, *393*(6684), 440–442. doi: 10.1038/30918

White, J. G., Southgate, E., Thomson, J. N., & Brenner, S. (1986). The structure of the nervous system of the nematode caenorhabditis elegans. *Philosophical transactions of the Royal Society of London. Series B, Biological sciences*, *314*(1165), 1–340. doi: 10.1098/rstb.1986.0056

Wiesen, T. F., Beaumont, P. M., Norrbin, S. C., & Srivastava, A. (2018). Are generalized spillover indices overstating connectedness? *Economics Letters*, *173*, 131–134. doi: 10.1016/j.econlet.2018.10.007

Wiesen, T. F., & Bharadwaj, L. (2021). Cryptocurrency connectedness: Does controlling for the cross-correlations matter? *SSRN Electronic Journal*. doi: 10.2139/ssrn.3894530

Wu, Z.-X., Xu, X.-J., & Wang, Y.-H. (2005). Properties of weighted structured scale-free networks. *The European Physical Journal B*, *45*(3), 385–390. doi: 10.1140/epjb/e2005-00188-1

Xu, X.-K., Zhang, J., Sun, J., & Small, M. (2009). Revising the simple measures of assortativity in complex networks. *Physical review. E, Statistical, nonlinear, and soft matter physics*, *80*(5 Pt 2), 056106. doi: 10.1103/PhysRevE.80.056106

Xulvi-Brunet, R., & Sokolov, I. M. (2004). Reshuffling scale-free networks: from random to assortative. *Physical review. E, Statistical, nonlinear, and soft matter physics*, *70*(6 Pt 2), 066102. doi: 10.1103/PhysRevE.70.066102

Yan, X., Jeub, L. G. S., Flammini, A., Radicchi, F., & Fortunato, S. (2018). Weight thresholding on complex networks. *Physical Review E*, *98*(4). doi: 10.1103/PhysRevE.98.042304

Yang, D., Pan, L., & Zhou, T. (2017). Lower bound of assortativity coefficient in scale-free networks. *Chaos (Woodbury, N.Y.)*, *27*(3), 033113. doi: 10.1063/1.4976030

Yang Wang, Chakrabarti, D., Chenxi Wang, & Faloutsos, C. (2003). Epidemic spreading in real networks: an eigenvalue viewpoint. In *22nd international symposium on reliable distributed systems, 2003. proceedings* (pp. 25–34). doi: 10.1109/RELDIS.2003.1238052

Yi, S., Xu, Z., & Wang, G.-J. (2018). Volatility connectedness in the cryptocurrency market: Is bitcoin a dominant cryptocurrency? *International Review of Financial Analysis*, *60*, 98–114. doi: 10.1016/j.irfa.2018.08.012

Ying, X., & Wu, X. (2009). Graph generation with prescribed feature constraints. In *Proceedings of the 2009 siam international conference on data mining* (pp. 966–977). SIAM.

Yook, S. H., Jeong, H., Barabási, A.-L., & Tu, Y. (2001). Weighted evolving networks. *Physical review letters*, *86*(25), 5835–5838. doi: 10.1103/PhysRevLett.86.5835

Yuan, Y., Yan, J., & Zhang, P. (2021). Assortativity measures for weighted and directed networks. *arXiv:2101.05389v1*. doi: 10.48550/ARXIV.2101.05389

Zhang, G.-Q., Cheng, S.-Q., & Zhang, G.-Q. (2012). A universal assortativity measure for network analysis. *arXiv:1212.6456v1*. doi: 10.48550/ARXIV.1212.6456

Zheng, D., Trimper, S., Zheng, B., & Hui, P. M. (2003). Weighted scale-free networks with stochastic weight assignments. *Physical review. E, Statistical, nonlinear, and soft matter physics*, *67*(4 Pt 1), 040102. doi: 10.1103/PhysRevE.67.040102

Zięba, D., Kokoszczyński, R., & Śledziewska, K. (2019). Shock transmission in the cryptocurrency market. is bitcoin the most influential? *International Review of Financial Analysis*, *64*, 102–125. doi: 10.1016/j.irfa.2019.04.009

Zou, H., & Hastie, T. (2005). Regularization and variable selection via the elastic net. *Journal of the Royal Statistical Society: Series B (Statistical Methodology)*, *67*(2), 301–320. doi: 10.1111/j.1467-9868.2005.00503.x

Zou, H., & Zhang, H. H. (2009). On the adaptive elastic-net with a diverging number of parameters. *Annals of statistics*, *37*(4), 1733–1751. doi: 10.1214/08-AOS625